

UNIVERSIDADE DE LISBOA  
FACULDADE DE FARMÁCIA



# **Novel particulate BCG-loaded delivery system for mucosal immunization against tuberculosis**

**Liliana Aranha Caetano**

Orientadores: Prof. Doutora Lídia Maria Diogo Gonçalves  
Prof. Doutor António José Leitão das Neves Almeida

Tese especialmente elaborada para obtenção do grau de Doutor em Farmácia,  
ramo Tecnologia Farmacêutica.

2016





## **Novel particulate BCG-loaded delivery system for mucosal immunization against tuberculosis**

**Liliana Aranha Caetano**

Orientadores: Prof. Doutora Lídia Maria Diogo Gonçalves  
Prof. Doutor António José Leitão das Neves Almeida

Tese especialmente elaborada para obtenção do grau de Doutor em Farmácia, ramo Tecnologia Farmacêutica.

Júri:

Presidente:

- Doutora Helena Maria Cabral Marques, Professora Associada com Agregação e membro do Conselho Científico da Faculdade de Farmácia da Universidade de Lisboa, Presidente do Júri, por subdelegação de competências;

Vogais:

- Doutora Carla Sofia Pinheiro Vitorino, Professora Auxiliar Convidada, Faculdade de Farmácia da Universidade de Coimbra;
- Doutor Bruno Filipe Carmelino Cardoso Sarmento, Professor Auxiliar, Instituto Universitário de Ciências da Saúde;
- Doutora Anita Raquel Quintal Gornes, Professora Adjunta, Escola Superior de Tecnologia da Saúde de Lisboa do Instituto Politécnico de Lisboa;
- Doutor António José Leitão das Neves Almeida, Professor Catedrático, Faculdade de Farmácia da Universidade de Lisboa, Coorientador;
- Doutora Elsa Maria Ribeiro Santos Anes, Professora Associada com Agregação, Faculdade de Farmácia da Universidade de Lisboa;
- Doutora Ana Francisca Campos Simão Bettencourt, Professora Auxiliar, Faculdade de Farmácia da Universidade de Lisboa;
- Doutora Lídia Maria Diogo Gonçalves, Professora Auxiliar Convidada, Faculdade de Farmácia da Universidade de Lisboa, Orientadora.

iMed.UlIsboa/Fundação para a Ciência e Tecnologia, Portugal  
Escola Superior de Tecnologia da Saúde de Lisboa/Caixa Geral de Depósitos, Portugal



Ao Ruben e à Matilde, pelo  
seu amor, compreensão e paciência

*To Ruben and Matilde, for all  
their love and patience*



## Acknowledgements

I would like to express my deepest gratitude to my main supervisor, Doctor Lúcia Maria Diogo Gonçalves, for the unwavering support and availability, as well as guidance through critical thinking and problem solving. A special thanks for your belief in my abilities when I found myself doubting them, your ever enthusiastic attitude towards science, and your friendship, which I greatly cherish and hope to be everlasting.

I am also extremely grateful to my supervisor Professor António José Leitão das Neves Almeida for all the trust, support and encouragement, as well as for the opportunity to integrate your research group and to participate in research projects and scientific forums. Your positive attitude towards life and science has made me realize how lucky I have been to pursue my endeavor in FFUL.

An acknowledgement to the Faculdade de Farmácia, Universidade de Lisboa, in particular to the Departamento de Farmácia Galénica e Tecnologia Farmacêutica, and the Research Institute for Medicines (iMed.Ulisboa) for the infrastructures and conditions that allowed me to develop the laboratory work in this study.

To the Portuguese government (Fundação para a Ciência e Tecnologia, FCT) for the research funding, namely as the strategic project PEst-OE/SAU/UI4013/2011).

To Escola Superior de Tecnologia da Saúde de Lisboa for financial support from merit scholarship for Ph.D. granted by Caixa Geral de Depósitos, Portugal (ESTeSL-IPL/CGD/2012).

To all my colleagues from the Nanostructured Systems for Overcoming Biological Barriers group (former Nanomedicine and Drug Delivery Systems group) for the pleasant working atmosphere and for letting I share a part of your lives with such unique camaraderie. I would like to single out Lara Figueiredo and Rita Amaral for the helpful and productive collaboration.

To my fellow colleagues at the Lisbon School of Health Technology, which have also embarked on this journey in pursuit of knowledge and share all the joys and frustrations of a scientific career.

To all my friends, for the understanding and steadfast friendship.

To my parents, brother, and parents-in-law, for the encouragement, support and for always being present.

To my daughter Matilde, without whom this thesis would have probably been written much faster, though certainly with much less laughs and joys.

Finally, to my husband Ruben, for the unconditional love and support, and for always inspiring me to do better. I have been truly blessed for sharing my life with you.

## Abstract

It has been well described that mucosal immune responses are of major importance for protection against pathogens invading the organism via mucosal surfaces, such as *Mycobacterium tuberculosis*. Current vaccine against tuberculosis, attenuated *Mycobacterium bovis* bacilli Calmette-Guérin (BCG), is commonly regarded as unsatisfactory due to its limited protection in adults against tuberculosis. The recognition that physicochemical properties, and route of administration, of vaccines influence their bioavailability and immunogenicity has led to intense research in the field of vaccine delivery. Several strategies can be employed in order to increase the immunogenicity of vaccines, namely by associating the antigens with suitable carriers and by choosing alternative vaccination routes. The aim of this thesis was to investigate the biocompatibility, cellular interaction, and immunogenicity of different types of surface modified BCG, such as BCG-loaded chitosan-alginate microparticles and BCG associated with chitosan.

Polymeric nano-/microparticles have emerged as promising vaccine carriers for mucosal immunization due to their ability to improve mucoadhesion and delivery of antigens to the mucosa, while acting as adjuvants. In this context, BCG was encapsulated into polymeric microparticles composed by chitosan, chitosan and alginate, or chitosan and alginate containing linoleic acid. All particles were prepared using an optimized ionic gelation method, presenting a spherical morphology within the micrometre size range, high drug encapsulation and yield of preparation. The addition of chitosan to BCG was found to reverse its surface charge, without compromising cell viability. Studies conducted on THP-1 cells have shown that, although some formulations induced a slight decrease in cell viability, all of them were considered biocompatible. In addition, the BCG-loaded microparticles were found to be quickly internalized by human macrophages. These results highlight the potential of BCG-loaded microparticles for whole live bacterial vaccine encapsulation.

Two independent *in vivo* experiments with BALB/c mice showed that the association of BCG with polymeric microparticles or chitosan endowed the vaccine with predominant Th1 type immunogenicity following intranasal vaccination, whereas the association of BCG with polymeric microparticles containing linoleic acid enabled a balanced Th1/Th2 profile, with a specific IgG2a/IgG1 ratio around the unity. The BCG-loaded polymeric microparticles containing linoleic acid were also found to increase the production of Th1 type cytokines, namely TNF- $\alpha$ , IL-2 and IFN- $\gamma$ , and to promote the secretion of specific IgA in the lung. These results constituted the first quantitative analysis of the immune responses elicited in mice by BCG-loaded chitosan-alginate microparticles containing linoleic acid administered by intranasal route, highlighting the potential of this carrier in improving cellular and mucosal immune responses as pre-exposure vaccine for tuberculosis.

In conclusion, polymeric microparticles proved to be a versatile platform for the delivery of attenuated vaccines, with high biocompatibility and easy surface modification, thus making them potential candidates as mucosal vaccine delivery systems. The results of this study also provide information on the adjuvant effects of the innovative association of BCG with polymeric microparticles, leading to the enhancement of cellular and mucosal immune responses following intranasal immunization, as well as on their interaction with macrophages.

## Resumo

A vacina contra a tuberculose consiste no bacilo atenuado de *Mycobacterium bovis* de Calmette-Guérin (BCG) formulado para administração subcutânea. Esta foi a primeira vacina viva atenuada a ser licenciada, em 1921, e mantém-se até aos dias de hoje como a única vacina profilática contra a tuberculose. A vacina BCG é administrada por via subcutânea a recém-nascidos, sendo efetiva na proteção de crianças contra as manifestações de tuberculose mais severas. Contudo, esta vacina tem gerado nos últimos anos alguma controvérsia relativamente à sua utilidade, uma vez que apresenta limitações no que concerne à proteção prolongada de indivíduos adultos contra a tuberculose pulmonar, a forma mais prevalente da doença. Por conseguinte, novas abordagens são necessárias para o desenvolvimento de vacinas mais eficazes contra a tuberculose.

Tem sido referido por vários investigadores que a proteção contra microrganismos patogénicos que infetam o organismo através das superfícies das mucosas, nomeadamente o *Mycobacterium tuberculosis*, é mais eficiente quando se verifica um aumento da secreção local de anticorpos, em comparação com a ação dos anticorpos presentes na circulação sistémica. Está também descrito que a veiculação de vacinas através das mucosas apresenta o potencial de ativar vários ramos da imunidade, inata e adquirida, bem como o potencial para ativar linhagens de linfócitos T de memória a nível local, cruciais para uma resposta imunitária eficaz e prolongada contra microrganismos patogénicos intracelulares. Por outro lado, tem sido constatado que a indução de anticorpos nas mucosas pelas vias da administração mais comumente utilizadas, subcutânea ou intramuscular, não parece ser possível. Nesse sentido, a administração dos antigénios através das mucosas (oral, nasal, pulmonar, geniturinária) parece constituir-se como a via de administração mais adequada para a próxima geração de vacinas, em particular contra microrganismos patogénicos colonizadores das mucosas.

Paralelamente ao crescente desenvolvimento de novas vacinas que se tem verificado nos últimos anos, assiste-se à intensificação da investigação de novas plataformas para

o aumento da biodisponibilidade e imunopotenciação de vacinas, através da descoberta de novos adjuvantes e associação de antígenos a sistemas de transporte (“*delivery*”) especializados. Os sistemas poliméricos nano / microparticulados têm revelado características promissoras para o direcionamento e libertação controlada de vacinas nas mucosas devido, por um lado, à sua capacidade de ultrapassar as barreiras biológicas através de vários mecanismos, de que são exemplos o prolongamento do tempo de residência nas mucosas por modulação da interação com a mucina, ou a capacidade de alguns polímeros mucoadesivos, como o quitosano, de promoverem a permeação dos tecidos epiteliais por ação ao nível das junções das células epiteliais (*tight junctions*); e, por outro lado, por possibilitarem o desenvolvimento de partículas com cinéticas específicas de erosão dos polímeros constituintes e consequente libertação controlada dos antígenos. De facto, a libertação controlada de antígenos na mucosa reveste-se de grande importância no contexto da evolução da resposta imune gerada pela vacinação. Alguns investigadores referem que a concentração de antígenos deve mimetizar, tanto quanto possível, os perfis antigénicos característicos do processo de infeção natural, ou seja, uma maior concentração de antígenos nos primeiros dias após administração e diminuição subsequente, com o objetivo de favorecer, numa primeira fase, a formação de memória dos linfócitos T, seguida da maturação de afinidade dos anticorpos. Nesse sentido, as micropartículas poliméricas têm emergido como uma estratégia válida para o transporte e libertação controlada de antígenos nas mucosas, com potencial para atuarem como adjuvantes e, em consequência, induzirem uma resposta imune mais eficaz e duradoura.

Assim, o presente trabalho teve como objetivo desenvolver e avaliar *in vitro* e *in vivo* um sistema microparticulado adequado para a encapsulação de vacinas atenuadas e sua administração através da mucosa nasal, com a finalidade de melhorar a apresentação de antígenos nos tecidos linfóides e gerar uma resposta imune eficaz. Para o efeito, foram desenvolvidas diferentes formulações contendo BCG microencapsulado em partículas poliméricas à base de quitosano e alginato, e ácido linoleico.

A administração da vacina por via nasal apresentou-se como a via mais natural para imunização contra a tuberculose em virtude de constituir a porta de entrada preferencial do agente patogénico. Para além deste aspeto, e em comparação com a atual via de administração subcutânea, a via nasal apresenta importantes vantagens referentes à eliminação dos inconvenientes associados ao uso de agulha, como risco de infeção por contaminação de agulhas ou dor no ato de administração, bem como à eliminação da necessidade de técnicos especializados para a administração da vacina, frequentemente escassos nos países com elevada prevalência da doença, contribuindo,

dessa forma, para uma maior capacidade de vacinação em larga escala em menor tempo.

Neste contexto, foram desenvolvidas micropartículas de quitosano e alginato em que, numa primeira fase, concentrações viáveis de BCG foram suspensas em quitosano, seguida da adição de alginato de sódio, na presença de um agente promotor da complexação iónica (TPP ou  $\text{CaCl}_2$ ), e, posteriormente, propôs-se a adição de ácido linoleico à formulação. O quitosano é um polímero biodegradável de natureza polissacarídea abundante na natureza, derivado por desacetilação da quitina, com diversas aplicações na indústria farmacêutica (como excipiente e suplemento de emagrecimento), alimentar, entre outras. As suas propriedades mucoadesivas, promotoras da permeabilidade de membranas e, segundo alguns autores, imunoestimulantes, conferem-lhe grande interesse para o desenvolvimento de micropartículas para veiculação de vacinas nas mucosas. O alginato de sódio é um polímero aniónico de origem natural que permite a formulação de micropartículas poliméricas com o quitosano através de ligações iónicas. Este polímero apresenta algumas particularidades interessantes para a formulação de vacinas vivas atenuadas e sua veiculação através da mucosa nasal, como sejam: biocompatibilidade, sendo por isso amplamente usado na imobilização de células; propriedades mucoadesivas, importantes para o aumento do tempo de contacto das partículas na árvore brônquica; e, finalmente, insolubilidade em meio ácido, conferindo, em teoria, uma maior resistência à degradação das partículas pelo conteúdo lisossomal das células apresentadoras de antigénio e, dessa forma, modificando o processamento celular dos antigénios e sua apresentação aos tecidos linfoides.

Os diversos métodos testados para obtenção das micropartículas tiveram por base a gelificação iónica entre os polímeros por agitação, tendo sido otimizados os respetivos parâmetros, como sejam as concentrações, valores de pH, volumes e *ratios* de polímeros a usar, ou os tempos e velocidades de agitação. O trabalho desenvolvido no âmbito da otimização da formulação das micropartículas permitiu obter partículas de quitosano e alginato com uma morfologia predominantemente esférica, com melhores rendimentos para razões de massa dos polímeros de 1:1, de carga superficial ajustável pela ordem de adição dos polímeros, e com tamanhos na ordem dos 10 a 15 micrómetros, tendo-se verificado um aumento da distribuição de tamanho das partículas para cerca de 20 a 25 micrómetros após encapsulação do BCG, sem prejuízo da viabilidade da vacina. É frequentemente descrito na literatura que os sistemas particulados se devem situar abaixo dos 5 micrómetros para que possam ser fagocitados. Contudo, vários estudos referem a internalização por macrófagos de partículas com tamanhos até 40 micrómetros. Por conseguinte, as partículas de

quitosano e alginato desenvolvidas mostraram ser adequadas para a encapsulação de vacinas vivas atenuadas, tendo *a priori* tamanho adequado à internalização pelos macrófagos alveolares.

Numa fase subsequente, a interação das partículas desenvolvidas com uma linha celular de macrófagos foi validada *in vitro*. Os ensaios efetuados com MTT (*tetrazolium assay*) em células THP-1 revelaram a ausência de citotoxicidade relevante nas concentrações testadas, quer dos polímeros isoladamente, quer das micropartículas poliméricas. Posteriormente, foi realizada uma avaliação semi-quantitativa da internalização das partículas por macrófagos, por análise microscópica com recurso a uma estirpe recombinante de BCG com expressão de uma proteína de fluorescência. Os resultados revelaram ligeiras diferenças entre formulações, tendo-se verificado para qualquer uma delas uma rápida internalização por macrófagos nas condições testadas. Estes resultados, embora com limitações, destacaram o potencial das micropartículas para estudos de vacinação *in vivo*.

Os estudos *in vivo* foram realizados com murganhos BALB/c para avaliação da capacidade das micropartículas atuarem como adjuvantes da vacina da BCG por administração por via intranasal, por comparação com a resposta imune gerada pela vacina em solução, por via intranasal e subcutânea (grupos de referência). Paralelamente, foi avaliado o efeito da associação às partículas de um ácido gordo polinsaturado, o ácido linoleico, o qual apresenta atividade pró-inflamatória e é descrito por alguns autores como promotor da permeabilidade ao nível das mucosas. A imunização foi feita com 10 microlitros da vacina em cada narina, correspondente a uma dose padrão de  $1 \times 10^7$  CFU BCG. Os parâmetros imunológicos foram avaliados em intervalos regulares durante os ensaios *in vivo*, com sacrifício dos murganhos no final para recolha de órgãos, avaliação da resposta imune local e do efeito da vacina no estímulo da produção de citocinas relevantes pelos esplenócitos.

Comparando a resposta imune observada nos murganhos dos grupos vacinados com as suspensões nasais de micropartículas contendo BCG ou com uma solução nasal de quitosano contendo BCG, com a resposta imune obtida com a formulação comercial pela via subcutânea, verificou-se que esta última apresentou níveis séricos muito inferiores de anticorpos específicos do tipo IgG2a, confirmando o esperado relativamente à formulação comercial da vacina administrada subcutaneamente, dado que esta via não favorece a produção de uma resposta imune do tipo Th1. Por outro lado, a resposta imune observada nos grupos de murganhos vacinados por via intranasal revelou a produção predominante de anticorpos específicos do tipo IgG2a, sendo que as micropartículas de quitosano, alginato e ácido linoleico, contendo BCG,

permitiram obter uma resposta imune mista do tipo Th1/Th2, traduzida pelo ratio unitário das concentrações séricas dos anticorpos específicos IgG2a e IgG1.

Através da determinação dos níveis de imunoglobulina A secretora, específica do antígeno derivado proteico purificado (PPD) de tuberculina bovina, nos extratos de pulmão e de intestino, foi possível comparar o efeito adjuvante para a indução de anticorpos nas mucosas entre os diferentes grupos. Verificou-se que as micropartículas de quitosano, alginato e ácido linoleico, contendo BCG, permitiram obter os níveis mais elevados de imunoglobulina A secretora no pulmão. Paralelamente, e contrariamente ao esperado, foram determinados níveis elevados de imunoglobulina A secretora também nos murganhos do grupo vacinado com as partículas vazias, sugerindo o efeito adjuvante das partículas em geral, com maior evidência para as partículas contendo ácido linoleico. Neste ensaio foi igualmente observado que a vacina constituída pela suspensão nasal de quitosano contendo BCG mostrou ser eficiente na indução de anticorpos na mucosa. Estes resultados evidenciaram diferenças entre as formulações, tendo demonstrado que para que ocorra a indução de anticorpos específicos nas mucosas não basta a libertação direta da vacina na mucosa, sendo favorável a associação a sistemas microparticulados com ação adjuvante.

Relativamente à resposta imune celular, a determinação da concentração de citocinas típicas de uma resposta do tipo Th1, nomeadamente IL-2, TNF- $\alpha$ , e IFN- $\gamma$ , segregadas pelos linfócitos do baço dos murganhos colocados em cultura, permitiu observar diferenças nos valores médios entre os grupos. O grupo de murganhos vacinados com as micropartículas de quitosano, alginato e ácido linoleico, contendo BCG, apresentou uma concentração média elevada de citocinas, com uma clara predominância de IL-2 e TNF- $\alpha$  relativamente aos restantes grupos.

Em suma, estes resultados constituíram a primeira análise quantitativa das respostas imunes induzidas em murganhos através da administração por via intranasal de micropartículas de quitosano, alginato, contendo BCG. A adição do ácido linoleico às partículas contendo BCG permitiu modificar o tipo de resposta imune de predominantemente Th1 para uma resposta mista do tipo Th1/Th2, mais adequada no caso da vacinação profilática contra o *Mycobacterium tuberculosis*, tendo sido também eficiente na indução de uma resposta imune ao nível da mucosa. Assim, as micropartículas poliméricas desenvolvidas revelaram-se promissoras para a veiculação de vacinas vivas atenuadas através da mucosa nasal e indução de resposta imune equilibrada tanto local como sistémica.



## Table of Contents

<i>Acknowledgements</i> .....	<i>i</i>
<i>Abstract</i> .....	<i>iii</i>
<i>Resumo</i> .....	<i>v</i>
<i>Table of Contents</i> .....	<i>xi</i>
<i>List of Figures</i> .....	<i>xv</i>
<i>List of Tables</i> .....	<i>xxi</i>
<i>Abbreviations</i> .....	<i>xxiii</i>
<i>Aims and organization of the thesis</i> .....	<i>xxv</i>
<b>Chapter I: General Introduction</b> .....	<b>1</b>
Abstract.....	5
1. Overview.....	7
2. Desired immune response for tuberculosis vaccines.....	9
2.1. Current BCG vaccine: successes and limitations.....	10
2.2. Tuberculosis vaccines in clinical trials.....	12
2.3. Designing better tuberculosis vaccines.....	16
3. Mucosal immunization: principles and hurdles.....	18
4. Particle-mediated vaccine delivery systems for mucosal immunization against tuberculosis.....	22
4.1. Adjuvants for mucosal vaccines.....	22
4.2. Particulate adjuvants for mucosal immunization.....	25
4.3. Chitosan for mucosal immunization .....	29
4.4. Other vaccine delivery systems and immunopotentiators for mucosal immunization.....	30
5. Rational for mucosal immunization against tuberculosis.....	30
6. Conclusions.....	33
7. References.....	35

---

<b>Chapter II: Effect of experimental parameters on microparticles formulation and BCG encapsulation.....</b>	<b>47</b>
Abstract.....	51
1. Introduction.....	53
2. Materials and methods.....	58
2.1. Materials.....	58
2.2. Preparation of polymeric microparticles.....	59
2.3. BCG studies.....	62
2.3.1. BCG single cell suspension.....	62
2.3.2. Surface charge characterization.....	63
2.3.3. Microencapsulation of BCG.....	63
2.3.4. BCG cell viability.....	63
2.4. Characterization of microparticles.....	64
2.4.1. Size distribution, surface charge and morphology.....	64
2.4.2. Production yield.....	64
2.4.3. Fourier transform infrared spectroscopy (FT-IR) analysis.....	65
2.4.4. Association efficiency.....	65
2.5. <i>In vitro</i> cell viability (MTT assay).....	65
2.6. Statistical analysis.....	66
3. Results and discussion.....	67
3.1. Characterization of polymeric microparticles.....	67
3.1.1. Size distribution and surface charge.....	68
3.1.2. Polymer-polymer interaction by FT-IR analysis.....	86
3.1.3. Surface morphology.....	87
3.1.4. Association efficiency.....	89
3.1.5. BCG cell viability.....	94
3.2. <i>In vitro</i> cell viability (MTT assay).....	95
4. Conclusions.....	96
5. Acknowledgements.....	97
6. References.....	98

**Chapter III: Interaction of BCG-loaded microparticles with macrophages and preliminary in vivo studies.....103**

Abstract.....	105
1. Introduction.....	107
2. Materials and Methods.....	110
2.1. Materials.....	110
2.2. Animals.....	110
2.3. Preparation of BCG-loaded microparticles.....	111
2.4. Evaluation of BCG cell viability (micro-CFU I).....	112
2.5. Characterization of microparticles.....	112
2.6. Interaction with antigen presenting cells.....	113
2.7. Intranasal immunization of BALB/c mice.....	114
2.8. Quantification of antigen-specific IgG subtypes and IgA.....	115
2.9. Statistical analysis.....	116
3. Results and discussion.....	116
3.1. Characterization of BCG-loaded microparticles.....	116
3.2. Association efficiency.....	119
3.3. BCG cell viability.....	120
3.4. Interaction with antigen presenting cells.....	121
3.5. Immune response in mice.....	127
4. Conclusions.....	132
5. Acknowledgements.....	133
6. References.....	134

**Chapter IV: Humoral and cellular immune responses in mice following intranasal immunization with BCG-loaded chitosan microparticles.....139**

Abstract.....	141
1. Introduction.....	143
2. Materials and Methods.....	145
2.1. Chemicals and strains.....	145
2.2. Mice.....	145
2.3. Microencapsulation of BCG in polymeric microparticles.....	146
2.4. Characterization of BCG-loaded microparticles.....	148
2.5. Assessment of specific immune responses in mice.....	149
2.5.1. Immunization schedule.....	149

2.5.2. Immunoglobulin IgG isotypes enzyme-linked immunosorbent assay (ELISA).....	150
2.5.3. Secretory IgA ELISA.....	151
2.5.4. Cytokines quantification by ELISA.....	151
2.6. Statistical analysis.....	151
3. Results.....	152
3.1. Characterization of BCG-loaded polymeric microparticles.....	152
3.2. Systemic PPD bovine-specific IgG immune response.....	154
3.3. IgG subtype profiling.....	156
3.4. Local PPD bovine-specific IgA immune response.....	158
3.5. Cytokines production by splenocytes.....	160
4. Discussion.....	162
5. Conclusions.....	164
6. Acknowledgements.....	164
7. References.....	165
<b>Chapter V: General conclusions and Future perspectives.....</b>	<b>169</b>
1. General conclusions.....	171
2. Future perspectives.....	177

## List of Figures

### **Chapter I: General introduction**

**Figure 1** – The development pipeline of new TB vaccines, July 2013. Global Tuberculosis report 2013 (2013). Reprinted, with permission from ref. 1 (Fig. 8.3, Page 95 [http://apps.who.int/iris/bitstream/10665/91355/1/9789241564656\\_eng.pdf?ua=1](http://apps.who.int/iris/bitstream/10665/91355/1/9789241564656_eng.pdf?ua=1), accessed 12 January 2014). Copyright@ Geneva, World Health Organization, 2013.

### **Chapter II: Effect of experimental parameters on microparticles formulation and BCG encapsulation**

**Figure 1** – Molecular structure of alginate. Monomers D-mannuronate (M) and L-guluronate (G) form polymer (A) (adapted from [http://archimede.bibl.ulaval.ca/archimede/fichiers/24237/24237\\_3.png](http://archimede.bibl.ulaval.ca/archimede/fichiers/24237/24237_3.png), accessed 10 October 2015).

**Figure 2** – Schematic crosslinking of alginate in the presence of calcium counter ions complexed with L-guluronic blocks (adapted from [http://www.scielo.org.mx/scielo.php?script=sci\\_arttext&pid=S1405-888X2014000100007&lng=es&tlng=en](http://www.scielo.org.mx/scielo.php?script=sci_arttext&pid=S1405-888X2014000100007&lng=es&tlng=en), accessed 10 October 2015).

**Figure 3** – Microparticles formation by alginate ionotropic pre-gelation with CaCl<sub>2</sub> followed by chitosan addition (adapted from<sup>34</sup>).

**Figure 4** – Microparticles formation by chitosan gel matrix formation with sodium alginate followed by TPP addition (adapted from<sup>31,33</sup>).

**Figure 5** – Microparticles formation by chitosan precipitation with TPP followed by alginate addition.

**Figure 6** – Effect of alginate to chitosan mass ratio on particle size distribution. (A) Particle size distribution of polymeric microparticles prepared with chitosan of low molecular weight chitosan (no fill), medium molecular weight (horizontal lines), and high molecular weight (angled lines). The d<sub>0.5</sub> particle size population is represented. (B) Size distribution span of microparticles prepared with chitosan of low molecular weight (□), medium molecular weight (○), and high molecular weight (▲). Results are presented as mean ± S.D. (n ≥3).

**Figure 7** – Microparticles domain formation using high, medium and low molecular weight chitosan. Three different systems were identified: clear solution (◆), opalescent/colloidal suspension (■), and aggregates (▲).

**Figure 8** – Effect of alginate to chitosan mass ratio on particle surface charge. Zeta potential of microparticles prepared with chitosan of low molecular weight (□), medium molecular weight (○), and high molecular weight (Δ). Results are presented as mean ± S.D. (n ≥3).

**Figure 9** – (A) Particle size distribution of plain chitosan-alginate microparticles prepared with ALG/CS mass ratio of 0.8:1 (solid) and 1:1 (dashed) and increasing homogenization times of the suspension using an ultrasound water bath. Two different chitosan molecular weight populations are represented: low molecular weight (white columns), and medium molecular weight (grey columns). (B) Particle size distribution span of plain chitosan-alginate microparticles prepared with increasing homogenization times of the suspension of microparticles of 0.8:1 (▲) and 1:1 (■) ALG/CS mass ratio. Results are presented as mean ± S.D. (n=3).

**Figure 10** – (A) Particle size distribution of plain chitosan-alginate microparticles of 1:1 ALG/CS mass ratio, prepared with chitosan of low molecular weight and alginates of decreasing G-content, according to Method (II) (solid) and Method (III) (dashed). (B) Zeta potential of plain chitosan-alginate microparticles of 1:1 ALG/CS mass ratio, prepared with chitosan of low molecular weight and alginates of decreasing G-content, according to Method (II) (□) and Method (III) (○). Results are presented as mean ± S.D. (n=3).

**Figure 11** – Characterization of plain chitosan-alginate microparticles of 1:1 ALG/CS mass ratio (“F14\_Low”) with increasing pH of alginate solution. (A) Particle size distribution, with four different pH populations represented for chitosan: pH 3.0 (white columns), pH 4.0 (light grey columns), pH 5.0 (dark grey columns), and pH 6.0 (dashed). (B) Zeta potential of microparticles, with four different pH populations represented for chitosan: pH 3.0 (□), pH 4.0 (○), pH 5.0 (▲), and pH 6.0 (x). Results are presented as mean ± S.D. (n=3).

**Figure 12** – Characterisation of particle mean diameter (d0.5) (□) and surface charge (zeta potential) (▽) with increasing final pH of the microparticles formulation.

**Figure 13** – Particle size distribution and span of “F14\_Low” particles without cryoprotectant (batch A), as well as of “F14\_Low” particles prepared with 5% or 10% sucrose (batches B and C), 5% or 10% glucose (batches D and E), or 5% or 10% trehalose (batches F and G). (A) Particle size distribution on production day (no fill) and after freeze-drying (horizontal lines). Three different particle size populations are represented: d0.1 (white columns), d0.5 (light grey columns) and d0.9 (dark grey columns). Results are presented as mean ± S.D. (n=3). (B) Size distribution span on production day (○) and after freeze-drying (▲). Results are presented as mean (n=3).

**Figure 14** – FT-IR spectra of plain chitosan-alginate “F14\_Low” microparticles (1:1 ALG/CS mass ratio) with increasing pH of the microparticles suspension. Bands wave numbers (cm<sup>-1</sup>) are as follows: 1641 (amide bond), 1613 (symmetric COO<sup>-</sup> stretching vibration), 1569 (strong protonated amino peak – from partial N-deacetylation of chitin), and 1415 (asymmetric COO<sup>-</sup> stretching vibration).

**Figure 15** – (A) Polarized light micrograph (100x) of “F13\_Medium” microparticles (0.8:1 ALG/CS) prepared according to Method (III) with chitosan of medium molecular weight. (B) Contrast phase micrograph (40x) of “F14\_Low” microparticles (1:1 ALG/CS) prepared according to Method (II) with chitosan of low molecular weight.

**Figure 16** – Particle size distribution of microparticles produced with alginate to chitosan ratio of 4.23:1 (F0), 0.8:1 (F13), and 1:1 (F14). F0 microparticles prepared according to Method (I) by alginate ionotropic pre-gelation with  $\text{CaCl}_2$  followed by chitosan coating; F13-F14 microparticles prepared according to Method (III) by chitosan pre-gelation with TPP followed by alginate coating; LMW, low molecular weight chitosan; MMW, medium molecular weight chitosan; HMW, high molecular weight chitosan.

**Figure 17** – Surface charge of inactivated BCG Pasteur (solid) and rBCG-GFP (dashed) following dispersion in different media. Results are presented as mean  $\pm$  S.D. (n=3).

**Figure 18** – Characterisation of “F14\_Low” microparticles with increasing BCG load. (A) Particle size (d0.5) of microparticles prepared according to Method (II) (solid) or Method (III) (dashed), and plain BCG (dotted). (B) Particle surface charge, and (C) encapsulation efficiency, of microparticles prepared according to Method (II) ( $\square$ ) or Method (III) ( $\odot$ ). Results are presented as mean  $\pm$  S.D. (n=3).

**Figure 19** – Cell viability of different strains of BCG (Pasteur and rBCG-GFP) following suspension in chitosan, maintained at 4°C for 15 weeks. Suspension of BCG in 0.9% NaCl was used as control. Results are expressed as mean  $\pm$  S.D.; n=3.

**Figure 20** – Relative cell viability of THP-1 cell line measured by the MTT reduction. Columns: black – control cells with culture medium; dark grey – BCG-GFP/0.9% NaCl; light grey – BCG-GFP/0.025% LMW chitosan; dotted white – BCG Pasteur/F13\_Medium microparticles; dotted grey – BCG Pasteur/F13\_High microparticles ( $1 \times 10^8$  CFU/mL). Results are expressed as mean  $\pm$  S.D. (n = 3). Statistical differences between the control group and formulations are reported as: \*\*\* $P < 0.001$ , \*\* $P < 0.01$ , \* $P < 0.05$ . Cell viability (% of control) = [A] test/[A] control x 100.

### ***Chapter III: Interaction of BCG-loaded microparticles with macrophages and preliminary in vivo studies***

**Figure 1** – Micro-Colony forming units assay. (A) Example of four dilution-points of two BCG suspensions (I and II) with technical duplicates; (B) (Micro-)photographs of BCG Pasteur CFU three weeks post-inoculation.

**Figure 2** – Immunization schedule for priming, blood sampling for specific IgGs subtypes quantification of by ELISA, and experimental endpoint with harvest of lungs for sIgA quantification.

**Figure 3** – Micrograph of rBCG-GFP-loaded chitosan-alginate microparticles (“F14\_Low”) following 10x dilution in 0.9% NaCl (Bar= 100  $\mu\text{m}$ ).

**Figure 4** – FT-IR spectra of solid (a) alginate, (b) chitosan, and (c) chitosan-alginate microparticles produced with alginate:chitosan mass ratio of 1:1 at pH 5.4. Bands wave numbers ( $\text{cm}^{-1}$ ) are as follows: 1641 (amide bond), 1613 (symmetric  $\text{COO}^-$  stretching vibration), 1526 (strong protonated amino peak – from partial N-deacetylation of chitin), and 1415 (asymmetric  $\text{COO}^-$  stretching vibration).

**Figure 5** – Cell number of BCG Pasteur following microencapsulation in “F14\_Low” chitosan-alginate microparticles (no fill), BCG suspension in 0.025% low molecular weight chitosan weight (horizontal lines), or BCG suspension in 0.9% NaCl (angled lines), after storage at 4°C. Results are expressed as mean  $\pm$  S.D.; n=3.

**Figure 6** – Microscopy images of THP-1 macrophage cultures infected with rBCG–GFP in a 24-well microplate at 1h (A and B) and 18h (C, D and E) after infection. (A) BCG-loaded F13\_Medium (ALG/CS mass ratio of 0.8:1) microparticles (MOI = 0.2; 1h pulse) (amp 100x). (B) BCG suspended in 0.9% NaCl (MOI = 0.2; 1h pulse) (amp 40x). (C) BCG suspended in 0.025% low molecular weight chitosan (MOI = 192; 18h pulse) (amp 100x). (D) BCG suspended in 0.025% low molecular weight chitosan (MOI = 38; 18h pulse) (amp 100x). (E) BCG suspended in 0.9% NaCl (MOI = 192; 18h pulse) (amp 100x). Blue: nucleus labelled using 4'-6'-diamidino-2-phenylindole (DAPI, Sigma); Red: lysosomal compartments visualised with Lysotrack™ red; Green: Green Fluorescent Protein (GFP) expressing bacteria.

**Figure 7** – Microscopy images of THP-1 macrophage cultures infected with rBCG-GFP in a 24-well microplate 24h after infection (amp 100x). (A) and (B) BCG suspended in 0.9% NaCl (MOI = 38). (C) BCG suspended in 0.9% NaCl (MOI = 192). (D) and (E) BCG suspended in 0.025% low molecular weight chitosan (MOI = 38). (F) BCG suspended in 0.025% low molecular weight chitosan (MOI = 192). (G) e (H) BCG-loaded L14 microparticles (ALG/CS mass ratio of 1:1) (MOI = 2). Blue: nucleus labelled using 4'-6'-diamidino-2-phenylindole (DAPI, Sigma); Red: lysosomal compartments visualized with Lysotrack™ red; Green: Green Fluorescent Protein (GFP) expressing bacteria.

**Figure 8** – Intracellular bacterial load in THP-1 macrophage cultures at 24 h after infection. (A) BCG-loaded ALG/CS microparticles (dark grey column); (B) BCG-loaded CS/ALG microparticles (light grey column); (C) BCG suspended in 0.025% LMW chitosan (dotted light grey column); (D) BCG suspended in 0.9% NaCl with 0.025% Tween™ 80 (no fill column). Results are expressed as mean  $\pm$  S.D; n=5. Multiplicity of Infection: MOI = n BCG-GFP cells /n THP-1 cells. Inset: BCG internalized by THP-1 cells observed with fluorescence microscopy.

**Figure 9** – Serum anti-*M. bovis* specific IgG, IgG1 and IgG2a titers after immunization by i.n. route of female BALB/c mice with BCG suspended in 0.9% NaCl (horizontal lines), BCG suspended in 0.025% low molecular weight chitosan (angled lines), BCG-loaded L14 chitosan-alginate microparticles (ALG/CS mass ratio 1:1) (dotted), and subcutaneously administrated BCG suspended in 0.9% NaCl (no fill). Titres reported are the reciprocal of serum dilutions that gave an optical density 2 x S.D. higher than the strongest negative control group (mean  $\pm$  S.D.; n=4).

**Figure 10** – Ratio of serum anti-*M. bovis* specific IgG2a and IgG1 titers after immunization by intranasal (i.n.) or subcutaneous (s.c.) route of female BALB/c mice with the BCG vaccine (mean

± S.D.; n=3). Titres reported are the reciprocal of serum dilutions that gave an optical density 2 x S.D. higher than the strongest negative control group, determined in 3 replicates per group.

**Figure 11** – Secretory IgA (sIgA) levels in lungs homogenates (normalized per gram) of mice immunized by intranasal route with BCG suspended in 0.9% NaCl (horizontal lines), BCG suspended in 0.025% low molecular weight chitosan (angled lines), BCG-loaded *L14* chitosan-alginate microparticles (ALG/CS mass ratio 1:1) (dotted), and subcutaneously administrated BCG suspended in 0.9% NaCl (no fill) (mean ± S.D.; n=4).

#### ***Chapter IV: Humoral and cellular immune responses in mice following intranasal immunization with BCG-loaded chitosan microparticles***

**Figure 1** – Preparation of BCG-loaded chitosan-alginate (CS/ALG) microparticles by ionotropic gelation of chitosan-suspended BCG with TPP, followed by alginate addition. Microparticles were obtained using the ultrasound bath (28 kHz). Samples were placed in the closed dark chamber containing cooled water.

**Figure 2** – Preparation of BCG-loaded chitosan/linoleic acid-alginate (CS-Linoleic acid/ALG) microparticles by ionotropic gelation of chitosan-suspended BCG with TPP containing 10 mg/mL linoleic acid, followed by alginate addition. Microparticles were obtained using the ultrasound bath (28 kHz). Samples were placed in the closed dark chamber containing cooled water.

**Figure 3** – Preparation of BCG-loaded alginate-chitosan (ALG/CS) microparticles by polymerization of alginate-suspended BCG with chitosan, followed by TPP addition. Microparticles were obtained using the ultrasound bath (28 kHz). Samples were placed in the closed dark chamber containing cooled water.

**Figure 4** – Immunization schedule for priming, blood sampling for specific IgGs subtypes quantification of by ELISA, and experimental endpoint with harvest of lungs, intestines and spleen for further immunogenicity studies.

**Figure 5** – Cell number of formulated BCG by micro-CFU assay after storage at 4°C. Columns: light grey – BCG suspended in 0.9% NaCl; dark grey – BCG suspended in 0.025% chitosan; dotted grey – BCG-loaded CS/ALG microparticles; dotted white – BCG-loaded ALG/CS microparticles; black – BCG-loaded CS-Linoleic acid/ALG microparticles. Results are expressed as mean ± S.D. (n = 3).

**Figure 6** – Systemic humoral (IgG) immune responses of immunized BALB/c mice. The production of PPD<sub>bov</sub> specific immunoglobulins IgG was assessed by ELISA in mice serum (mean ± S.D.; n≥4). (A) Global humoral immune responses; (B) Immune response in groups immunized by intranasal route. CS, chitosan; ALG, sodium alginate; MPs, microparticles; Linoleic, linoleic acid.

**Figure 7** – Serum anti-PPD<sub>bov</sub> specific IgG1 and IgG2a titres, and ratio of serum anti-PPD<sub>bov</sub> specific IgG2a and IgG1 titres, 26 weeks after priming immunization of female BALB/c mice with the BCG vaccines (mean ± S.D.; n≥4). Statistical analysis was performed by Dunnett's multiple comparison tests. \*  $P < 0.05$ ; \*\*\*  $P < 0.0001$ . CS, chitosan; ALG, sodium alginate; MPs, microparticles; LA, linoleic acid; s.c., subcutaneous.

**Figure 8** – Serum anti-PPD<sub>bov</sub> specific secretory IgA levels in mice lungs and intestines homogenates, 26 weeks after priming immunization of female BALB/c mice with the BCG vaccines (mean ± S.D.; n≥4). Statistical analysis was performed by Dunnett's multiple comparison tests, comparing i.n. vaccines with s.c. BCG. \*  $P < 0.05$ ; \*\*\*  $P < 0.0001$ . Intranasal BCG vaccines (grey). CS, chitosan; ALG, sodium alginate; MPs, microparticles; LA, linoleic acid; s.c., subcutaneous.

**Figure 9** – Concentration of cytokines IL-2, IFN- $\gamma$ , TNF- $\alpha$ , and IL-4 in supernatants of splenocytes after 72h stimulation with PPD bovine (mean ± S.D.; n≥4). Statistical analysis was performed by Dunnett's multiple comparison tests, comparing i.n. vaccines with s.c. BCG. \*  $P < 0.05$ ; \*\*  $P < 0.001$  \*\*\*  $P < 0.0001$ . CS, chitosan; ALG, sodium alginate; MPs, microparticles; LA, linoleic acid; s.c., subcutaneous.

## List of Tables

### **Chapter I: General introduction**

**Table 1** - Pros and cons of nasal and oral versus parenterally delivered vaccines (adapted from 67, 92, 96).

**Table 2** - Relative effects on polarization of immune response following parenteral immunization with foreign antigens formulated with adjuvants and delivery systems (adapted from 67, 96).

### **Chapter II: Effect of experimental parameters on microparticles formulation and BCG encapsulation**

**Table 1** - Values for the investigated variables during formulation studies.

**Table 2** – Particle size distribution (mean diameter and span) and surface charge (zeta potential) of microparticles on the preparation day.

**Table 3** – Size distribution of polymeric microparticles prepared by high-speed homogenization and ultrasonication, and yield of production.

**Table 4** - Size distribution and zeta potential of microparticles prepared by homogenization in an ultrasound water-bath, with increasing homogenization times.

**Table 5** – Effect of pH on particle size distribution, particle surface charge, and yield of production of microparticles prepared with alginate to chitosan mass ratio of 1:1 (F14\_Low).

**Table 6** - Characterization of batches of plain polymeric microparticles prepared with cryoprotectants sucrose, glucose, or trehalose.

**Table 7** - Characterization of chitosan-alginate microparticles (formulation “F14\_Low”) batches without (batch A) and with (batches B to H) cryoprotectants addition, on production day and following freeze-drying.

**Table 8** – Surface charge of inactivated *Mycobacterium bovis* BCG (strains Pasteur and rBCG-GFP) bacilli suspended in different media. Results are presented as mean  $\pm$  S.D. (n=3).

**Table 9** - Characterization of batches of BCG-loaded “F14\_Low” microparticles prepared with increasing concentrations of BCG.

**Table 10** – Particle size distribution, surface charge and encapsulation efficiency of BCG-loaded “F14\_Low” microparticles.

***Chapter III: Interaction of BCG-loaded microparticles with macrophages and preliminary in vivo studies***

**Table 1** – Summary of the formulations tested in mice and respective immunization route.

**Table 2** – Characteristics of BCG-loaded microparticles ( $1.4 \times 10^8$  CFU/mL) and BCG suspended in chitosan ( $2.5 \times 10^9$  CFU/mL) and NaCl ( $4.2 \times 10^8$  CFU/mL).

***Chapter IV: Humoral and cellular immune responses in mice following intranasal immunization with BCG-loaded chitosan microparticles***

**Table 1** – Summary of the formulations tested in mice and respective immunization route.

**Table 2** – Particle size distribution and surface charge of microparticle formulations used for intranasal immunization of mice with  $1 \times 10^8$  CFU/mL of BCG Pasteur (mean  $\pm$  S.D.;  $n \geq 3$ ).

## Abbreviations

Ad	Adenovirus
Ag	Antigen
ALG	Alginate
APC	Antigen presenting cell
ATCC,	American Type Cell Culture Collection
BALT	Bronchus-associated lymphoid tissue
BCG	Bacille Calmette-Guérin
CFP-10	Culture filtrate protein 10
CFU	Colony-forming unit
CI	Confidence interval
CS	Chitosan
CT	Cholera toxin
CTB	Cholera toxin B subunit
CTL	Cytotoxic T lymphocyte
DAPI	4',6-diamidino-2-phenylindole
DC	Dendritic cell
DMSO	Dimethylsulfoxide
E.E.	Encapsulation efficiency
ELISA	Enzyme-linked immunosorbent assay
ESAT-6	Secretory antigenic target 6
FT-IR	Fourier transform infrared spectroscopy
G	Guluronate
GALT	Gut-associated lymphoid tissue
GFP	Green fluorescent protein
HIV	Human immunodeficiency virus
HMW	High molecular weight
HV	High viscosity
Ig	Immunoglobulin
IL	Interleukin
INF	Interferon
ISCOM	Immunostimulating complex
LA	Linoleic acid
LMW	Low molecular weight
LT	<i>E. coli</i> heat labile toxin
LV	Low viscosity
M	Mannurate

MALT	Mucosa-associated lymphoid tissue
MHC	Major histocompatibility complex
MMW	Medium molecular weight
MOI	Multiplicity of infection
MPL	Monophosphoryl lipid A
MTT	3-(4,5-dimethyl-2-thiazolyl)-2,5-diphenyl-2H-tetrazolium bromide
MV	Medium viscosity
MVA	Modified Vaccinia Ankara
MW	Molecular weight
NALT	Nasal-associated lymphoid tissue
OADC	Oleic acid, albumin, dextrose and catalase supplement
OD	Optical density
OPD	O-phenylenediamine dihydrochloride
PBS	Phosphate-buffered saline buffer
PLA	Poly(L-lactide)
PLG	Poly(lactide-co-glycolide)
PLGA	Poly(D,L-lactide-co-glycolide)
PMA	Phorbol myristate acetate
PPD	Purified protein derivative
PRR	Pattern recognition receptor
QS21	Purified fraction of Quil A
Quil A	Immunostimulatory fraction from <i>Quillaja saponaria</i>
rBCG	Recombinant bacille Calmette-Guérin
S.D.	Standard deviation
SEM	Scanning electron microscopy
slgA	Secretory immunoglobulin A
TB	Tuberculosis
TGF	Transforming growth factor
Th	Helper T cells
THP-1	Human macrophage derived from monocyte cell line
TLR	Toll-like receptor
TNF	Tumour necrosis factor
TPP	Triphosphosphate
US	Ultrasonication
UT	Ultra-turrax
WHO	World Health Organization

## Aims and organization of the thesis

The work herein described aims at developing a live vaccine-loaded carrier as adjuvanted delivery system for mucosal immunization against tuberculosis. This will be achieved by the microencapsulation of BCG into polymeric microparticles, suitable for intranasal vaccination and for prolonging the residence time of the vaccine in the mucosa. This general aim is divided into the following specific objectives:

- (i) Optimization of BCG-loaded microparticles and characterization of the final formulations;
- (ii) Evaluation of the formulations cytotoxicity against a human monocyte cell line;
- (iii) Assessment of the interaction of the formulations with antigen presenting cells;
- (iv) Characterization of the adjuvant effect of microparticles by assessment of the specific immune responses elicited in a relevant animal model.

We expect to develop a biocompatible microparticulate formulation with an enhanced immunogenicity against *Mycobacterium tuberculosis*, and ultimately to identify the most promising formulations for mucosal immunization against infectious diseases.

Therefore this thesis is organized as follows:

**Chapter I** provides an overview on tuberculosis, current available vaccine and vaccine candidates in clinical trials, as well as the role of nano- and microencapsulation of antigens and adjuvants for improvement of immunization strategies, with special emphasis on mucosal immunization and polymeric carriers (published as an expert review paper).

**Chapter II** describes the optimization of the preparation method of BCG-loaded polymeric microparticles based on particle size and size distribution, encapsulation efficiency, yield of production, and assessment of BCG viability following microencapsulation, as well as their cytotoxicity (partially included in an article submitted for publication).

**Chapter III** describes the interaction of BCG-loaded polymeric microparticles with antigen presenting cells, assessed by *in vitro* studies with a human monocyte cell line, as a model for the interaction of microparticles with human macrophages, as well as preliminary results from *in vivo* studies.

**Chapter IV** describes the immunological adjuvant effect of BCG-loaded polymeric microparticles by assessment of the PPDbov-specific immune responses, systemic and local, elicited in mice following intranasal vaccination of BALB/c mice.

**Chapter V** summarizes the main general conclusions of this work as well as outlines the future work perspectives.

## ***Chapter I***

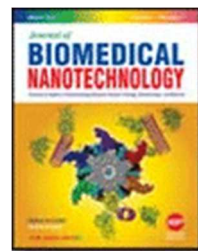
---

### ***General Introduction***



*This chapter was adapted from:*

*Liliana A. Caetano, António J. Almeida, Lídia M.D. Gonçalves. Approaches to tuberculosis mucosal vaccine development using nanoparticles and microparticles: a review. Invited expert opinion report to special issue of Journal of Biomedical Nanotechnology, 2014, 10: 2295-2316.*



## **Approaches to tuberculosis mucosal vaccine development using nanoparticles and microparticles: a review**

Liliana A. Caetano, António J. Almeida, Lídia M.D. Gonçalves

*ESTeSL-Lisbon School of Health Technology, Instituto Politécnico de Lisboa, Portugal.  
Research Institute for Medicines (iMed.U LISBOA), Faculty of Pharmacy, Universidade de Lisboa, Portugal.*



## Abstract

Next-generation vaccines for tuberculosis should be designed to prevent the infection and to achieve sterile eradication of *Mycobacterium tuberculosis*. Mucosal vaccination is a needle-free vaccine strategy that provides protective immunity against pathogenic bacteria and viruses in both mucosal and systemic compartments, being a promising alternative to current tuberculosis vaccines. Micro and nanoparticles have shown great potential as delivery systems for mucosal vaccines. In this review, the immunological principles underlying mucosal vaccine development will be discussed, and the application of mucosal adjuvants and delivery systems to the enhancement of protective immune responses at mucosal surfaces will be reviewed, in particular those envisioned for oral and nasal routes of administration. An overview of the essential vaccine candidates for tuberculosis in clinical trials will be provided, with special emphasis on the potential different antigens and immunization regimens.

**Keywords:** Tuberculosis vaccines; Mucosal immunity; Vaccine delivery systems; Microparticles; Nanoparticles; Adjuvants.



## 1. Overview

Primarily a disease of the lung, tuberculosis (TB) is a contagious and airborne infectious disease, and one of the leading causes of morbidity and mortality from infectious diseases throughout the world. The World Health Organization (WHO) estimates that one-third of the world population, i.e., around 2.2 billion individuals, is latently infected with bacteria belonging to the *Mycobacterium tuberculosis* (*M. tuberculosis*) complex.<sup>1</sup>

Tuberculosis is transmitted by untreated individuals suffering from open cavitory pulmonary infection through close contact, such as by sneezing or coughing. Upon aerosol exposure to *M. tuberculosis*, around 70% of immunocompetent individuals are able to prevent the establishment of infection, whereas the other 30% will become infected and develop acquired immunity to *M. tuberculosis*. Due to the late onset of the acquired cellular immune response within the lung, 5-10% of these infected persons will develop the active form of the disease, allowing the infection to become well established, whereas the other 90-95% will be asymptomatic. These remaining latently infected individuals maintain a reservoir of residual population of viable bacteria in the lungs, contained in the granuloma; if co-morbidity factors, such as malnutrition, stress or human immunodeficiency virus (HIV) co-infection, are present, they are potentially at risk to reactivate the infection and develop TB at some stage of their lives.<sup>2</sup>

Although tuberculosis can be cured in most cases by a cheap course of antibiotic treatment, the difficulty of a timely diagnosis, socioeconomic factors in endemic areas, and the fact that bacterial clearance requires many months of treatment, have combined to prevent successful global control of the disease by drug therapy. The resurgence of the disease is also being accelerated by the spread of HIV, while there is growing global concern about the emergence of drug resistant *M. tuberculosis* strains.<sup>3,4</sup> Vaccination of selected population groups to prevent serious complications of infection remains, therefore, as the most cost-effective strategy for control of tuberculosis.

Live attenuated *Mycobacterium bovis* bacille Calmette-Guérin (BCG) vaccine is the only available vaccine against tuberculosis. Developed by Albert Calmette and Camille Guerin, it was first administered to infants in 1921. Nowadays, the BCG vaccine is administered by parenteral route to around 100 million children each year, at or soon after birth, in over 100 countries to minimize the potential for serious forms of the tuberculosis disease, being the most widely used vaccine in the world.<sup>5</sup> Despite its efficacy against the most severe forms of tuberculosis in children, BCG is commonly regarded as unsatisfactory due to its variable efficacy in different parts of the globe, and

limited protection against pulmonary tuberculosis in adults, the most prevalent form of the disease. Therefore, there are great expectations for a new vaccine that will improve the protection provided against tuberculosis.<sup>6</sup>

An improved vaccine against TB should ideally be a pre-exposure vaccine able to elicit sterilizing immunity preferably at the time of initial infection. Since tuberculosis is highly prevalent in low-income countries and HIV co-epidemic regions, a needle-free vaccine would also be preferable, in order to be safer, easier to administrate, as well as suitable for high coverage mass vaccination campaigns. Other important issues to consider in the design of novel TB vaccines are the role of mucosal immunity against *M. tuberculosis*,<sup>7-9</sup> the current assumption that cellular immune responses are of crucial importance to prevent *M. tuberculosis* replications in the host,<sup>10, 11</sup> and the potential of intranasal routes of immunization to improve the efficacy of vaccination against pathogens entering the host through the respiratory mucosa.<sup>12-14</sup> Regarding the primary site of tuberculosis manifestation in the lungs, mucosal immunization strategies arise as a promising alternative to current intradermal administration route, for effective both local and systemic immune responses.<sup>15</sup>

Novel approaches are, therefore, required for a rational design of safe and effective vaccines against tuberculosis, either by (i) boosting current vaccine protection with the administration of critical mycobacterial antigens in suitable delivery vehicles – the subunit vaccine approach, or by (ii) the modification or replacement of current BCG vaccine by recombinant forms of more immunogenic mycobacteria, relying on multiple antigens and built-in adjuvanticity to modify antigens processing by antigen presenting cells (APC) - the whole bacterial vaccine approach.<sup>16</sup> Several new TB-vaccine candidates have also been evaluated for their protective efficacy in animal models using the mucosal route of immunization.<sup>17</sup> In formulating such vaccines, the adjuvants and delivery systems are crucially important.

This review focuses on the potential of nano and microparticles for the mucosal delivery of antigens as a rational vaccine design for tuberculosis. An overview of the immunological mechanisms involved in the development of effective immune responses against *M. tuberculosis* will be provided, as a starting point for the comprehension of rational vaccine design, and vaccine candidates currently under investigation will be highlighted. Critical aspects for the effective design of nano and microparticles as vaccine delivery systems, such as size, will be discussed, with special emphasis on the use of biodegradable polymers. Examples of vaccines intended for oral and intranasal administration will be provided.

## 2. Desired immune response for tuberculosis vaccines

The *M. tuberculosis* normally enters the host through the mucosal surfaces via the lung after inhalation of infectious droplets from an infected individual. Once in the lung, *M. tuberculosis* bacteria are uptake by antigen presenting cells (APC), including alveolar macrophages, the primary hosts for *M. tuberculosis* replication within the host, interstitial macrophages and local dendritic cells (DCs). Following uptake by alveolar macrophages, the bacilli enter the phagosome. During residence in phagosomes, *M. tuberculosis* secretes proteins, which can be loaded onto products of the major histocompatibility complex (MHC) class II, leading to CD4+ T-cell stimulation, whereas CD8+ T-cell stimulation requires peptide presentation by MHC I molecules. The uptake of bacteria by APC also leads to cytokine and chemokine release, prompting the accumulation and activation of monocyte/macrophages and lymphocytes, which surround the infected phagocytes in the granuloma.<sup>2, 18</sup>

In order to achieve sterile *M. tuberculosis* eradication with pre-exposure vaccination, both effector and memory T-cells must be stimulated through adequate antigen presentation. Although it remains uncertain which cell types are involved in *M. tuberculosis* antigen presentation to naïve T cells (either DCs that cross-present antigens from infected cells, or DCs migrating from the lungs), two pathways have been proposed: a) *M. tuberculosis* escapes to the cytosol of infected DCs, leading to direct loading of MHC I molecules; b) vesicles carrying mycobacterial antigens, as a result of infected cells apoptosis, are taken up by surrounding DCs, leading to antigenic peptides presentation by MHC II and MHC I molecules to CD4+ and CD8+ T-cells, respectively. The CD4+ T cells predominate as the major INF- $\gamma$  secreting cells during acute infection (INF- $\gamma$  being critical for macrophage activation and containment of *M. tuberculosis* within solid granulomas), whereas CD8+ T cells dominate during persistent infection.<sup>10, 19–21</sup>

The specific immune response against *M. tuberculosis* comprises a multitude of different cell types, including T-cells, neutrophils, B-cells, and natural killer cells. The importance of Th1 cell-mediated immune responses to elicit effective immunity against *M. tuberculosis*, as with other intracellular pathogens, is well known, with the role of CD4+ Th1-cells in tuberculosis being best understood. While the CD4+ Th1 cells produce IL-2, IFN- $\gamma$ , lymphotoxin, and tumour necrosis factor (TNF), which are cytokines critical for protection, the Th2 cells counter-regulate Th1 cells, thus, probably impairing protective immunity in TB.<sup>22–25</sup> This is best evidenced by the clinical association between HIV and TB, and also by the increased risk of latent *M. tuberculosis* infection reactivation in individuals treated with anti-TNF- $\alpha$  agents.<sup>26–28</sup>

The local immune response by CD4+ T-cells to *M. tuberculosis* in the lungs can be, however, significantly delayed, allowing the mycobacteria to persist within the host.<sup>19, 29, 30</sup> Studies in mice have shown that: (i) activation of specific T-cell responses against *M. tuberculosis* takes place only in the local draining lymph nodes of the lung; (ii) the transport of *M. tuberculosis*-infected cells from the lung parenchyma to the lymph nodes is significantly delayed for a period of at least 1–2 weeks; (iii) after initial proliferation in the lymph node, effector CD4+ T cells traffic rapidly to the lungs. Therefore, it is concluded that initiation of the adaptive immune response to *M. tuberculosis* depends on transport of live bacteria from the lungs to the lymph nodes. This *M. tuberculosis*' unique ability to delay the onset of an adaptive immune response by 2–3 weeks results in the bacterial population expansion in the lungs, leading the establishment of the infection, either as a reservoir of non-replicating bacteria in infected cells (latent infection), or with actively replicating bacteria, necessary for priming host' immune response, but also for TB pathology.<sup>29, 31, 32</sup>

Different mechanisms of *M. tuberculosis* evasion from the immune system appear to be critical in the deregulation of the immune response. The arrest of phagosome maturation pathway in host phagocytic cells by *M. tuberculosis*, inhibiting the phagosome-lysosome fusion, is well described,<sup>33, 34</sup> as it is the *M. tuberculosis* interference with IFN- $\gamma$  induced autophagy, which cells perform in order to decrease the viability of intracellular mycobacteria in mice and humans,<sup>35–38</sup> the inhibition of apoptosis by *M. tuberculosis*,<sup>20, 39, 40</sup> and *M. tuberculosis* egression into the cytosol.<sup>41, 42</sup> These evasion strategies compromise antigen presentation by inhibiting MHC class II processing (impairs CD4+ T-cell stimulation) and by modulating the lipoxygenase pathway (blocks cross-priming for CD8+ T-cells), allowing the pathogen intracellular survival.<sup>19, 22, 43, 44</sup> As consequence, the establishment of infection and progression to disease take place, even in immunocompetent individuals, which has been a significant barrier to effective vaccine development.

## 2.1. Current BCG vaccine: successes and limitations

The generic term BCG collectively refers to a family of approximately 13 daughter strains, following 13 years of serial passage *in vitro*, from a culture of an attenuated strain of living bovine tubercle bacillus. These strains provide protective immunity to challenge with virulent *M. tuberculosis*, although they have been shown to differ genetically and phenotypically, including their induction of immune responses and protection in animal models. The more representative strains (nearly 60% of the total number of BCG doses produced per year) are BCG Danish 1331, BCG Glaxo 1077, and BCG Pasteur 1173

(the BCG reference strain lyophilized at the Institute Pasteur in 1961). Although initially administered by oral route, the BCG vaccine is currently administered as a single intradermal injection, given at or soon after birth.<sup>45</sup>

Current BCG vaccine efficiently protects children against the early manifestations of TB. In newborns the protective effect of BCG vaccine against TB compared with that in unvaccinated children is estimated at 74% (95% confidence interval [CI] 62%-83%) and 64% (95% CI 30%-82%) for meningitis, and up to 78% (95% CI 58%-88%) for disseminated disease. However, it does not provide permanent or absolute protection against TB, as attested by a number of clinical trials where the efficacy of BCG vaccine against pulmonary TB showed to be highly variable in adults ranging from 0 to 80%.<sup>46-48</sup>

Many factors have been considered to explain the variable efficacy of BCG vaccine in adults, with particular relevance in regions where TB is most prevalent: a) co-infection with environmental mycobacteria;<sup>47, 48</sup> b) HIV impairment of CD4+ T cell;<sup>49</sup> c) impairment of adequate Th1 cell response settled by helminth infection;<sup>50</sup> d) unmet requirements for vaccine storage and handling and the resultant loss of vaccine viability;<sup>6</sup> and also e) methodology of studies conducted in different regions. Meta-analysis of prospective studies for the efficacy of BCG vaccine for preventing tuberculosis revealed that geographic latitude alone accounted for 41% of the between-study variance, as the declining of BCG-induced protection through childhood and young adult life coincided with the time frame for the gradual increase in TB incidence, which, in some highly TB-endemic regions, such as sub-Saharan Africa, reaches a peak of 4500 cases per 100 000 individuals in the 25–35 year-old age group.<sup>46</sup> Internal regulatory mechanisms in the host, induced to avoid collateral damage by the ongoing immune response after pathogen eradication, may also confound protective immunity, whereas BCG strain variability and loss of virulence genes due to the attenuation process also account for immune response variability.

On a global scale, widespread latent TB infection in adults is a significant barrier to attempts to boost immunity.<sup>18</sup> Although homologous boosting has often been effective for increasing humoral immune responses, it is an ineffective inducer of cellular immunity to target antigens. This has been demonstrated by the failure of attempts to boost protection in sensitized individuals with repeated administrations of BCG.<sup>51</sup> On the other hand, it has been shown that heterologous prime–boost immunization can be highly effective for enhancing humoral and cellular immunity, thus, reinforcing the urgent need not only for a new and improved vaccine for tuberculosis, but also optimization of immunization regimens.<sup>52</sup>

## 2.2. Tuberculosis vaccines in clinical trials

The vaccine candidates for tuberculosis under investigation in clinical trials are not only numerous but wide-ranged in used approaches and dosing strategies, somehow representative of the lack of full understanding about how *M. tuberculosis* interacts with the human immune system, thus, of the great challenge that is to develop an effective vaccine against pulmonary TB.

It is in general assumed that immune responses elicited by effective pre-exposure vaccines are capable to lower bacterial loads at an earlier time point than immune responses induced in unvaccinated individuals. Since clinical evolution of tuberculosis is correlated with bacterial load, the potential of such a reduction would be very significant to contain the initial stages of infection by *M. tuberculosis*, therefore, reducing the chance of evolution to active disease.<sup>53</sup> Although many novel TB vaccine candidates currently under development are designed to induce high levels of cellular immunity, generation of potent cell-mediated immune responses through vaccination is not a simple task. In fact, most of the successful vaccines in use today are based on humoral immunity, which mainly involves the production and secretion of antibodies into the extracellular fluid. Humoral immunity, however, is insufficient on its own, as it does not clear bacteria from cells, and no vaccination strategy so far has succeeded in the achievement of sterilizing immunity against TB infection.

Two main strategies have been followed in the past decade. The first, best envisioned for pre-exposure vaccination, aims to replace current BCG vaccine either by: a) genetically improved recombinant (r)BCG expressing critical immunodominant *M. tuberculosis*-specific antigens (such as RD1 locus-encoded antigens secretory antigenic target 6 (ESAT-6) and culture filtrate protein 10 (CFP-10), absent from BCG), or over-expressing BCG's own antigens involved in the infection (Ag85 complex); b) genetically attenuated *M. tuberculosis* following critical virulence genes deletion. This "whole bacterial vaccine" strategy relies on multiple antigens presentation and built-in adjuvanticity. The second major strategy has been the development of subunit vaccines. This approach greatly differs from the aforementioned, as it relies on the use of non-viable, non-replicating vaccines. Subunit vaccines consist mainly in mycobacterial antigens as fusion proteins in protein/adjuvant combinations and recombinant viral-vectored platforms. These vaccines are mainly considered for prime-boost' vaccination regimes, in which either current BCG-, rBCG-, or attenuated *M. tuberculosis*-priming vaccines continues to be given to neonates, and a new vaccine is given as a 'booster' dose to increase the efficacy and extend the duration of protection. Since the majority of

the global population has been exposed to BCG, heterologous boosting of BCG-primed immunity will likely be a key component of future multicomponent vaccine strategies.<sup>1, 16,</sup>

52

The status of the pipeline for new vaccine candidates in July 2013 is shown in Figure 1. Ten vaccine candidates are being evaluated in clinical trials for TB prevention, either designed for pre-exposure vaccination (to prevent infection) or for post-exposure purposes (to prevent primary progression of the disease or reactivation of latent TB); and two immunotherapeutic agents, meant to improve responsiveness to chemotherapy or to prevent relapse of re-infection.<sup>1, 54</sup>



**Figure 1** – The development pipeline of new TB vaccines, July 2013. Global Tuberculosis report 2013 (2013). Reprinted, with permission from ref. 1 (Fig. 8.3, Page 95 [http://apps.who.int/iris/bitstream/10665/91355/1/9789241564656\\_eng.pdf?ua=1](http://apps.who.int/iris/bitstream/10665/91355/1/9789241564656_eng.pdf?ua=1), accessed 12 January 2014). Copyright © Geneva, World Health Organization, 2013.

Two vaccines are in Phase IIb studies: (i) modified Vaccinia Ankara virus expressing antigen 85A of *M. tuberculosis* (MVA85A) vaccine, given to infants in South Africa from 2009 to 2012 as a booster following BCG immunization; and (ii) M72+AS01E, a fusion protein of the *M. tuberculosis* antigens 32A and 39A with the novel adjuvant AS01E, and tested for safety/immunogenicity in three different populations including infants, HIV positive individuals and adults with TB disease.

The MVA85A is a recombinant viral-vectored vaccine that was designed to stimulate immunity against *M. tuberculosis* by delivering Ag85A into cells, in order to trigger the immune response. It was the first candidate to reach efficacy trial of a TB vaccine in more

than four decades. Although pre-clinical studies demonstrated increased protection in mice and non-human primates over BCG alone, MVA85A failed to show efficacy in humans in early 2013, as the same rate of TB infection and clinical disease was observed in both immunized and non-immunized children. Despite the lack of success, it was demonstrated that a TB vaccine can be tested in infants according to ethical standards, and that researchers can develop the infrastructure and analytical methods needed to carry out a large clinical trial in a resource-poor country.<sup>55</sup>

The M72+AS01E is a subunit or protein-adjuvant vaccine, and the first candidate likely to enter efficacy trials. The used adjuvant AS01E is a chemical enhancer of immunogenicity that contains mono-phosphoryl lipid A (stimulates Toll-like receptor (TLR)4 and drives CD4+ Th1 as well as Th17 responses) mixed with QS21 (triggers CD8+ T-cell responses), and it is formulated in liposomes. As with MVA85A, M72+AS01E was envisioned as a booster vaccine for individuals who have already received BCG. Further efficacy trials are being planned to include young adults, the more affected population by pulmonary TB. So far, the vaccine has proven to be safe and to induce a good T-cell response when administered to adults in South Africa either without TB or with latent infection.<sup>16</sup>

Six additional vaccines are in Phase II trials, of which two are whole bacterial vaccines: (i) VPM 1002, a live rBCG-expressing listeriolysin and urease gene deletion to improve immunogenicity, with Phase IIa completed and waiting for a second Phase II trial to assess vaccine safety and immunogenicity in HIV exposed/unexposed newborns; and (ii) RUTI, a detoxified non-living vaccine based on fragmented *M. tuberculosis* bacteria formulated in liposomes as immunotherapeutic vaccine. Other three vaccines are protein subunit adjuvanted vaccines that combine two or more immunodominant antigens of *M. tuberculosis*, all being studied in Phase IIa clinical trials in Africa: (iii) Hybrid 1 + IC31, a fusion protein consisting of Ag85B and ESAT-6 formulated with adjuvant IC31, which was able to induce strong CD4+ Th1 IFN- $\gamma$  response in humans and to boost immunity in previously BCG immunized individuals;<sup>56</sup> (iv) Hybrid 56 + IC31 (containing Ag85B, ESAT-6 and AgRv2660, the latter being an antigen expressed during latency); (v) Hybrid 4 + IC31 (Ag85B and TB10.4, the latter being from ESAT-6 gene family, also expressed by BCG). These subunit vaccines are invariably admixed with potent Th1-activating adjuvants, IC31, which activates human TLR9 and facilitates antigen uptake by DCs, and liposome-based formulations. Finally, an adenovirus-vectored vaccine candidate (vi) AERAS-402/Crucell Ad35, an adenovirus vaccine expressing three *M. tuberculosis* antigens: Ag85A, Ag85B and TB10.4, and designed as a booster vaccine for infants, adolescents and adults.

Noteworthy, both VPM1002 and AERAS 422 have been engineered to overexpress immunogenic *M. tuberculosis* proteins in order to induce apoptosis of APC, thus, potentially enhancing cross-priming. Nevertheless, they follow different strategies: AERAS 422 consists in a viral-vectored vaccine containing only three antigens from *M. tuberculosis*, while VPM 1002 relies on *in vivo* replication, as it is a live attenuated vaccine, and multigenic presentation, as it contains BCG' whole antigen repertoire plus listeriolysin as immunogenic factor. Derived from *Listeria monocytogenes*, listeriolysin is required for phagosomal escape and translocation to the cytosol, being only active at acidic pH, while it also perforates the phagosomal membrane, allowing leakage of proteases and bacterial components into the cytoplasm of the infected cell. The reason why Urease C was deleted in VPM 1002 was to enable listeriolysin activity in acidic conditions, since it counteracts phagosomal acidification when normally expressed in BCG. VPM 1002 caused superior protection as compared to parental BCG, by inducing apoptosis of infected host cells, while facilitated cross-priming by DCs, inducing strong CD4+ and CD8+ T-cell responses.<sup>57–60</sup>

There are also three main vaccine candidates in Phase I clinical trials, namely: (i) Ad5 Ag85A, an adenovirus serotype 5 vector expressing Ag85A, recently evaluated in a Phase I trial that demonstrated no vaccine-related serious adverse events and showed greater immunogenicity in the study group primed with BCG; (ii) MTBVAC, the first live attenuated *M. tuberculosis* vaccine entering Phase I clinical trials, with deletions of the *phoP* and *fadD26* genes; and (iii) ID93, a recombinant fusion protein expressing three *M. tuberculosis* virulence antigens (Rv2608, Rv3619 and Rv3620) and the latency antigen Rv1813, formulated in the novel adjuvant GLA-SE. AERAS-402/Crucell Ad35 and MVA85A are also being tested in a combined Phase I/Phase II trial in adults in the United Kingdom for safety and immunogenicity, to try to drive a balanced CD4+/CD8+ immune response.

In addition to the candidates described above, a non-living vaccine based on the non-pathogenic bacterium *Mycobacterium vaccae* is also being studied as an adjuvant to standard antimicrobial therapy (Phase III efficacy studies in progress).

Although many of them look promising, none of the preventive vaccine candidates reached the Phase III of efficacy testing, thus, in none of these cases do we know with certainty whether they will confer robust protection against TB in humans. While conventional and recombinant forms of BCG are also increasingly being considered as priming vaccines in heterologous prime–boost vaccination strategies, finding a replacement for BCG for vaccination of HIV-infected populations will be a challenging

task. BCG-induced immune responses are impaired in HIV-infected infants, while there is a higher risk of developing disseminated BCG disease in HIV positive children. Therefore, some ongoing clinical trials are also evaluating the risk that BCG immunization poses for infants born to HIV-infected mother. The use of recombinant viral vectors or antigenic subunits for priming followed by BCG boosting has been suggested as a potentially safer alternative for vaccination of newborns.<sup>55, 61</sup>

So far, most TB vaccine strategies have focused on pre-exposure vaccination, in the quest for an improved vaccine capable of inducing strong and long-lasting memory T-cell responses that are promptly mobilized after infection with *M. tuberculosis*. Nevertheless, and as indicated by the results from the phase IIb trial of the MVA85A vaccine, the scenario is far more complex than simple assuming a direct relation between cellular immunity and protection against TB. In fact, the vaccine proved safe and induced modest cell-mediated immune responses, but failed to show significant efficacy.<sup>55</sup> Although it remains uncertain if the lack of efficacy in infants will be mirrored in the adult setting, as results from trials in adults are pending, it is clear that further studies in the field of biomarker research will be of crucial importance, to deepen our understanding of the immune correlates of protection in TB, as will be to continue fundamental and pre-clinical research in order to identify novel TB vaccine candidates of greater efficiency.<sup>38</sup>

### 2.3. Designing better tuberculosis vaccines

As aforementioned, *M. tuberculosis* is a master regulator of immune regulatory pathways: it induces strong CD4+ and CD8+ Treg activity, thus, suppressing Th1 and Th17 responses, while it down regulates apoptosis, autophagy, and IFN- $\gamma$  production. Bearing in mind the complex interaction of *M. tuberculosis* with the human host, and the role of cell-mediated immunity against *M. tuberculosis*, TB vaccines not only need to elicit optimal immune responses to *M. tuberculosis*, but also to induce a balanced response that avoids pathogenic mechanisms and favors protection against disseminating infection.

Three major factors are expected to impact the development of improved vaccines for tuberculosis: a) the use of rationally selected mycobacterial vaccine antigens; b) the development of effective delivery systems; and c) the optimization of vaccine routes of administration, in order to foster effective and protective immune responses both systemically and in the lung mucosa, in order to contain and minimize bacterial dissemination.

Considering the “whole bacterial vaccine” strategy, live attenuated bacteria seems to be the ideal antigen producers and vectors, since they mimic pathogens, being multigenic and normally surpassing natural barriers. The *M. bovis* BCG vaccine is the most widely used live attenuated vaccine, being a potent stimulator of CD4+ T cell, while should also induce CD1 restricted T-cells, since it consists of protein antigens, phospholipids and glycolipid antigens.<sup>62-64</sup> The rational modification of BCG for specific targeting of essential immune pathways, such as the cross-priming or the hinder of the arrest of phagosomal maturation, also appears to present high potential to improve TB vaccines efficacy. BCG features such as low production cost, possibility of administration at birth with very strong adjuvant activity, induction of immunity after a single dose, and low frequency of side effects, have also encouraged its use as a live carrier for recombinant antigens, whereas reduced coverage of vaccination campaigns in developing countries with peptide vaccines has fostered the investigation with live bacterial carriers for heterologous antigen presentation.<sup>6</sup>

The development of techniques for genetic manipulation of mycobacteria, completion of the genome sequence of *M. tuberculosis* in the 1990s, and recent advances in immunology provide remarkable opportunities for developing a new generation of TB vaccines with higher levels of impact. The immunodominant *M. tuberculosis*-specific antigens such as ESAT-6 and CFP-10, which are absent in current BCG vaccine strains and are required for the *M. tuberculosis* translocation to the host cytosol and MHC-based antigen presentation, have already been used in order to improve immunity generated by conventional or ‘improved’ recombinant BCG. This approach aims to lead to more immunogenic, and capable of inducing longer lasting protection, vaccine profile.<sup>38, 41, 65</sup> Recent work has also revealed that *M. tuberculosis* alters its metabolic state from active replication to slow or non-replication during infection, causing significant changes in *M. tuberculosis*'s gene expression profile.<sup>66</sup> Therefore, incorporation of starvation/latency antigens into alive or subunit vaccines may also, in principle, enhance the impact of these vaccines.

A rather shortcoming in the development of subunit vaccines might be the need of using adequate adjuvants and/or delivery systems, since the presence of novel adjuvants or delivery systems increases vaccine formulation complexity, thus, development costs, and it might also delay regulatory compliance for clinical development. Taking into consideration the costs of developing a new TB vaccine and the poor outcome of the recent clinical trial with MVA85A, one challenge for new subunit or viral-vectored TB vaccines in the future will be to match preferably low-cost strategies that could be affordably implemented in developing countries.

Because preventable diseases rarely become eradicated, vaccination programs – especially for childhood vaccination – tend to grow. The predominant use of invasive routes of administration can lead to decreased patient compliance as injections are perceived by the majority as painful, whereas new combination vaccines bear the risk of pharmaceutical and immunological interference. Injected vaccines have several other limitations and drawbacks, such as requirement of trained health care personal for administration, risk of infections or other injuries with needles, need for cold chain to maintain the stability of liquid based vaccines, while they are poor inducers of mucosal immunity and of limited use for mass vaccination purposes. Several of these disadvantages can be circumvented by the use of other vaccination routes, such as mucosal (e.g., oral, nasal and pulmonary) administration. Potentially, mucosal vaccination allows higher compliance, as it does not require the use of needles nor syringes, being minimally invasive, nor trained health care workers, hence, being suitable for mass vaccination programmes in under-developed countries, and in pandemic and bioterrorism situations.<sup>67</sup>

### **3. Mucosal immunization: principles and hurdles**

It is well known that local mucosal immune responses are of major important for protection against pathogens invading the organism via mucosal surfaces, such as *M. tuberculosis*.<sup>7–9, 15, 68, 69</sup> Mucosal surfaces are the major site of entry for most pathogens, comprising approximately 400 m<sup>2</sup> of surface area. They are associated with a large and highly specialized innate and adaptive mucosal immune system, representing almost 80% of all immune cells in a healthy human adult. These immune cells are present in the mucosae or circulate between various mucosa-associated lymphoid tissues (MALT), forming the largest mammalian lymphoid organ system and a common mucosal immune system. Mucosal-associated lymphoid tissue includes the gut-associated lymphoid tissue (GALT), bronchus-associated lymphoid tissue (BALT), nasopharynx-associated lymphoid tissue (NALT), the mammary and salivary glands, and the urogenital organs.<sup>70</sup>

The mucosal delivery of vaccines presents the potential to activate multiple arms of innate and adaptive immunity and to induce memory T cell responses at a local level. It has been demonstrated that effective immunity correlates better with the presence of specific antibodies in local secretions, such as secretory immunoglobulin A (sIgA), than with serum antibodies.<sup>8, 14, 15, 67, 69, 71–76</sup> Indeed, the production of secretory IgA is the hallmark of the mucosal immune system: it has been shown to be an important effector molecule to protect mucosal surfaces, and its role in immunity to mucosal pathogens is well documented in the gastrointestinal, respiratory and urogenital tracts. Secretory IgA

is able to bind and intercept invading pathogens during its secretion into mucosal fluids by transcytosis or in the mucosal fluids. The possible mechanisms involve the agglutination of microbes, inhibition of their motility, blocking of their attachment to the mucosal epithelium by targeting bacterial adhesins, clearance of microbial products and activation of phagocytic cells, leading to neutralisation of the infection.<sup>77-83</sup>

Despite mucosal vaccination attractive features, only few mucosal vaccines, mostly oral, are currently approved for human use, including the live attenuated oral polio vaccine, oral rotavirus vaccines, various oral cholera vaccines (killed whole-cell/cholera toxin (CT) B subunit or live-attenuated), nasal influenza vaccine and oral typhoid vaccine (live attenuated). In fact, due to the distinctiveness of the mucosal environment, to overcome the challenges of mucosal immunity is a relatively difficult task when compared to development of systemic vaccines. The main issues regarding delivery of antigens through mucosal vaccination are related with host defence barriers to pathogens, such as antigen dilution in mucosal secretions, detainment in mucus gels, proteases/nucleases attack, and the presence of epithelial barriers, which require large doses of antigen. Other reasons why mucosal vaccines aren't more widespread might arise from two major hurdles that mucosal immunization must overcome: difficult assessment of effectiveness and safety of new vaccines (as correlates of protection are often ill defined for mucosal vaccines); risk of inducing mucosal immune tolerance.<sup>84-86</sup>

Soluble non-adherent antigens present low ability to be taken up by the mucosal immune system, thus, might induce immunological tolerance. Mucosal immune tolerance occurs when exposure to antigen (through microbial colonization or vaccination) induces a state of both mucosal and systemic hypo-responsiveness, apparently related to immune homeostasis to limit inflammatory responses. The immune mechanisms involved in mucosal tolerance have been extensively studied in animal models with respect to both oral and nasal vaccines, mainly with antigens fused to cholera toxin B subunit (CTB).<sup>79, 87, 88</sup> In summary, antigen-specific regulatory T cells from immune induction sites are able to suppress effector T cells in the presence of IL-10 and TGF- $\beta$ , as well as to induce antigen specific apoptosis and deletion of these effector T cells. Factors which may contribute to the development of immune tolerance and hypo-responsiveness are: a) frequency and amount of antigen exposure and co-exposure to immune enhancing agents; b) previous antigen exposure, the later representing a major challenge for effective mucosal immunization against environmental and microbial antigens. This is particularly so for oral immunization, since there is significant and constant exposure to microbial and food antigen in the gastrointestinal tract.

Although little is known about how mucosal exposure to high doses of antigen impacts cell-mediated immunity, there is evidence that temporal sequence of antigen exposure (systemic priming and mucosal boosting), as well as the use of adjuvants to target antigens to APC, determine the quality of the resulting immune response. Therefore, optimization of immunization schedules and the use of mucosal adjuvants can be strategically pursued in order to influence the systemic and mucosal immune responses without compromising cell-mediated responses.<sup>77, 79, 89</sup> Targeting mucosal dendritic cells, for example, has proven to be an effective and safe strategy for inducing antigen-specific immunity.<sup>90</sup>

When compared to other non-invasive routes of administration, the nasal route of administration presents several advantages. Compared to oral delivery, nasal vaccine delivery elicits better mucosal and systemic immunity, whereas it appears to be less likely to induce mucosal tolerance in the airways, which may compromise local vaccination with soluble antigens (Table 1). Additional advantages of nasal vaccine delivery arise from the fact that nasal vaccine delivery can surpass antigen degradation by digestive enzymes, thus, requiring a smaller antigen dose, while it also enables cross-protective immunity in the gut through the common mucosal immune system. Nasal vaccine delivery has, therefore, the potential to address all the prerequisites for a successful needle-free vaccine for tuberculosis, while it may open the way to better vaccine efficacy.

Challenges in nasal delivery of vaccines are imposed by the high clearance and significant enzymatic activity in nasal mucosa, and also by the limited applicability if upper respiratory-tract infections are present. In order to overcome these barriers, vaccine formulations and delivery strategies have to be carefully designed to efficiently present the antigen to the mucosal immune system, stimulating an appropriate innate and adaptive immune response for the target pathogen.<sup>75, 91–93</sup>

In order to efficiently stimulate innate responses and to evoke adaptive immune responses, without disturbing mucosal homeostasis or inducing immunological tolerance, mucosal vaccines must be carefully designed.<sup>94</sup> Different strategies can be used to target the appropriate mucosal site. The development of improved antigen delivery systems, suitable for mucosal routes of immunization while protecting the antigen from degradation during delivery, should provide antigen access to APC at the induction site, therefore, facilitating mucosal vaccine development.<sup>67, 95</sup>

**Table 1** – Pros and cons of nasal and oral versus parenterally delivered vaccines (adapted from 67, 92, 96).

<b>Route</b>	<b>Pros</b>	<b>Cons</b>
<b>Parenteral</b>	<p><u>Formulation</u> Alum most widely used adjuvant - effectiveness Low antigen dose required</p> <p><u>Immune response and protection</u> Potent systemic antibody and T cell Protective efficacy against viral, bacterial and parasitic disease models in animals and humans</p> <p><u>Clinical use</u> Extensive</p> <p><u>Safety</u> No major problems with subunit vaccines</p>	<p><u>Formulation</u> Injection Requires medically trained personnel Possible transmission of infection by contaminated needles syringes Alum most widely used adjuvant – safety</p> <p><u>Immune response and protection</u> No mucosal immunity</p> <p><u>Safety</u> Mild to serious side effects with killed or attenuated vaccines</p>
<b>Nasal</b>	<p><u>Formulation</u> Needle-free administration Simple inhalation (spray or liquid drop formulations) Good patient compliance Minimal delivery risk (no syringes or needles required) Antigen efficiently transferred across nasal epithelium - favored by bioadhesive delivery systems Medium antigen dose required - less than required in oral administration</p> <p><u>Immune response and protection</u> Mucosal and systemic antibody and T cell responses Primary colonization and invasive site for airborne pathogens Easy access to mucosal inductive sites Protective efficacy against animal models of viral and bacterial diseases Consistent vaccine responses – lower cost</p>	<p><u>Formulation</u> Requires mucosal adjuvants or immunopotentiators Limited availability of adjuvants for human use Antigen degradation by proteases Difficult control of particulate and soluble antigens access to mucosal induction sites Administration in infants may be difficult</p> <p><u>Immune response and protection</u> Can induce tolerance</p> <p><u>Clinical use</u> Limited number of clinical trials</p> <p><u>Safety</u> Largely unknown (evidence of antigen transfer to neuronal tissue via olfactory bulb in mice) Live attenuated vaccines and live vectors can access central nervous system</p>
<b>Oral</b>	<p><u>Formulation</u> Needle-free administration Simple ingestion (liquid formulations, capsules, tablets) Most friendly approach (non-invasive) Minimal delivery risk (no syringes or needles required)</p> <p><u>Immune response and protection</u> Good induction of mucosal immune response Modest systemic antibody response</p> <p><u>Clinical use</u> Extensive use for live attenuated vaccines</p> <p><u>Safety</u> Considered the safest route of vaccine delivery</p>	<p><u>Formulation</u> Requires potent mucosal adjuvant Limited availability of adjuvants for human use Antigen degradation by proteases and inefficient uptake in the GI High antigen doses required Might require antigen encapsulation (liposomes, microspheres)</p> <p><u>Immune response and protection</u> Access to immune induction sites highly variable Low T cell immunity Variable duration and efficacy of immune responses Can induce tolerance Protective efficacy against small number of animal models of viral and bacterial diseases</p> <p><u>Clinical use</u> Limited clinical trials of subunit vaccines</p>

The development of mucosal vaccines should also take into account further immunization strategies, i.e., pre-exposure priming or boosting, and routes of administration, as this has implications for the delivery strategy feasible for the intended target group. For example, in the design of vaccines for small children, it should be addressed that infants are less capable to swallow tablets (limitation to orally delivered vaccines), there might be a risk that a suckling child will suffocate due to a congested nose (limitation to nasal delivery in this population), whereas the use of spacers (in combination with inhalers) is required for pulmonary delivery of aerosolized vaccines below the age of 9 years.<sup>67</sup>

#### **4. Particle-mediated vaccine delivery systems for mucosal immunization against tuberculosis**

As previously mentioned, mucosal vaccines, namely those intended for oral and nasal administration, have attracted significant interest in recent years. Due to its easier accessibility, the nasal cavity presents high potential among the mucosal sites as an alternative to the parenteral route for local and systemic immunization against tuberculosis. However, the delivery of antigens by mucosal path frequently results in a poor immune response, due to limited diffusion of antigens across the mucosal barriers, the rapid mucociliary clearance, and the presence of enzymatic degradation.

Important features in the design of mucosal vaccine formulations include: (i) protection of the antigen from enzymatic digestion; (ii) enhancement of antigen uptake by M cells or conventional epithelial cells in the GI and respiratory mucosae; (iii) stimulation of the innate immune system so that the appropriate adaptive immune response is triggered; and (iv) induction of immunological memory. In order to address these objectives, adjuvant or immunomodulatory molecules and particulate delivery systems can be used in vaccines' formulation meant for administration by mucosal routes.

##### **4.1. Adjuvants for mucosal vaccines**

The use of adjuvants or immunopotentiators in mucosal vaccines benefits especially non-replicating and non-particulate antigens, often only weakly immunogenic, towards productive immunity induction rather than tolerance. The potency of these adjuvants needs, however, to be carefully balanced with their potential to be toxic and induce tissue damage.<sup>83, 92, 96</sup>

Despite the broad range of pathogen etiology, many pathogens share invariant molecular structures that are the main targets of innate immune recognition. Examples of these

pathogen-associated molecular patterns (PAMPs) are: (i) lipopolysaccharide (LPS) present in Gram-negative bacteria; (ii) peptidoglycans of Gram-positive bacteria; (iii) unmethylated CpG motifs, characteristic of bacterial but not mammalian DNA; (iv) double-stranded RNA as structural signature of viruses; and (v) mannans as conserved components of yeast cell walls. Macrophages and dendritic cells, both antigen-presenting cells for T cells, have evolved a set of non-clonal pattern recognition receptors (PRRs) to bind these conserved structures. These receptors include collectins, CD14, Toll-like receptors, mannose-binding protein, serum amyloid P, complement receptors, C-reactive protein, Fc receptors, CD11b, c/CD18 and DEC 205, and they are strategically expressed on cells that first encounter pathogens during infection, such as surface epithelial cells and APC. The microbial ligation of PRRs on APC enhances the ability of the cells to present antigen and to stimulate T-cell activation, resulting in increased adaptive immune responses. Therefore, microbial pathogen-derived molecules can be used as immunomodulatory molecules.<sup>97–99</sup>

As the immediate interface between foreign pathogens and the immune system, epithelial cell also have a role in modulating the immune responses at mucosal surfaces. The expression of TLRs has been reported on respiratory and intestinal epithelial cells, whereas mucosal epithelial cells also express MHC class-I molecules, and low levels of MHC class-II molecules. When properly stimulated, mucosal epithelial cells secrete a range of antimicrobial peptides and proteins, as well as immunomodulatory cytokines, chemokines and colony-stimulating factors, and can also present antigens to CD4+ and CD8+ T cells, thus, also posing an interesting target for adjuvants and vaccine delivery systems.<sup>100, 101</sup>

The success of a vaccine can be highly dependent on the adjuvant and on the type of Th cells (Th1 or Th2) induced (Table 2). Depending on the mucosal site of infection and/or mucosal entry access of the infecting microbe, a number of different strategies can be used to promote antigen uptake at mucosal induction sites and targeting to specific cell receptors, in order to induce adequate type of immune response required both mucosally and systemically. In summary, Th1 cells mediate cellular immunity against intracellular bacteria and viruses through secretion of IL-2, IFN- $\gamma$  and TNF- $\beta$ . Th2 cells provide protection against extracellular infectious organisms through the secretion of cytokines IL-4, IL-5, IL-10 and IL-13, and also assist B cells in the production of IgA and neutralizing IgG antibodies against bacterial toxins. In this context, the choice of adjuvants for mucosal vaccines must consider which type of immune response is required, which administration route is best suited for antigen targeting into the relevant

mucosal induction site, and which APC targeting component to incorporate, if also relevant for the induction site and type of immune response required.<sup>96, 102</sup>

**Table 2** - Relative effects on polarization of immune response following parenteral immunization with foreign antigens formulated with adjuvants and delivery systems (adapted from <sup>67, 96</sup>).

<b>Adjuvant or delivery system</b>	<b>Th2 response</b>	<b>Th1 response</b>	<b>Mucosal delivery</b>
Solution	+	-	-
Aluminum	+++	+	-
Chitosan	+++	+	+
AB toxins (wild type)	+++	+	+
AB toxins (non-toxic mutant)	+++	+++	+
PLG microparticles	+++	+++	+
Quil A or QS21	++	+++	+
QS21 plus MPL	++	++++	+
IL-12	++	++++	+
Live attenuated vectors (virus/bacteria)	+	++++	+
Plasmid DNA	+	+++++	+
Synthetic oligonucleotide sequences	+	+++++	+

PLG, poly(lactide-co-glycolide); Quil A, immunostimulatory fraction from *Quillaja saponaria*; QS21, purified fraction of Quil A; MPL, monophosphoryl lipid A derived from lipopolysaccharide of Gram-negative bacteria.

Only two adjuvants – an aluminium salts-based adjuvant, and a lipid emulsion MF-59 stabilized with polysorbate - are currently licensed for mass vaccination. However, these adjuvants are only approved for subcutaneous administration, whereas the aluminium salts prompt parenteral toxic side effects and Th2-cell responses, thus, elucidating the urgent need for novel suitable adjuvants for a mucosal vaccines.<sup>103</sup> *E. coli* heat labile toxin (LT) and enterotoxigenic cholera toxin (CT) are the two most potent mucosal adjuvants. Both CT and LT help induce T-cell responses and have been successfully used for mucosal immunization of animals, but they remain too toxic to be used as such in human vaccines. Derivatives of CT and LT have been genetically modified to reduce their toxicity while retaining their adjuvanticity.<sup>104, 105</sup> The best known are CTB and CTA1 (co-administered or chemically linked to protein antigens to improve cell targeting and safe use in humans), and LTK63, LTR72 and LTR192G (LTK63 and LTR192G are potent mucosal and systemic adjuvants and are being assessed in human vaccine trials).<sup>106–109</sup>

Other adjuvants and targeting agents, such as immunopotentiators (compounds that directly activate immune cells through specific receptors or pathways) may be incorporated into the microparticles, providing a valuable platform for the construction of

potent immunostimulatory mucosal delivery systems. While adjuvants are able to stimulate the innate immune system and influence the profile of the elicited immune response, delivery systems insures optimal targeting and delivery of both antigen and adjuvant, for an effective activation of the immune system response, obviating Th2-dominant immune responses or tolerance phenomena towards the antigen. Together, delivery system and antigen determine the magnitude and quality of the innate immune response and the uptake and processing of the antigens by APC, whereas adjuvanted or delivery systems associated vaccines may, additionally, produce distinctive and profitable types of local and systemic immunity.<sup>70, 75, 96</sup>

## 4.2. Particulate adjuvants for mucosal immunization

Mucosal delivery and uptake of particulate systems is a subject which has recently started to be understood. In order to improve the efficiency of mucosal vaccines, much attention has been focused on finding particulate antigen-delivery systems that can be readily taken up at mucosal surfaces to induce better immune responses.<sup>110, 111</sup> Not only the entrapment of antigens in suitable particulate carriers protects the antigen against degradation on mucosal surfaces due to enzymes activity, it also acts as antigen depot. Moreover, the use of particulate delivery systems enhances antigen preferential uptake in the mucosa-associated lymphoid tissues (MALT), favouring antigen interaction with antigen presenting cells such as macrophages, thus, promoting the generation of memory B and T cells and increasing the immune response at the target site. Nasal administration of particulate antigens may produce effective vaccines both for protection of the upper respiratory tract and for induction of long lasting protective systemic immunity.<sup>112</sup>

Vaccine antigens may be incorporated into biodegradable particles that can protect them from enzymatic degradation (e.g., polymeric microparticles, microemulsions, immunostimulating complexes - ISCOMs, liposomes) and/or co-administered with particles containing antigens with various immunostimulatory or mucoadhesive properties (e.g., chitosan, alginate lectins, coatings of particles with positive charged peptides or other ligands) to enhance their uptake and immunogenicity at the mucosal site.<sup>113-120</sup> Intensive studies in the field of vaccine development during the last decades demonstrate the intensive research regarding the use of the biodegradable polyesters poly(lactide-co-glycolide)<sup>113, 121-127</sup> and poly- $\epsilon$ -caprolactone<sup>128, 129</sup>, polysaccharides such as alginate<sup>71, 72, 130-141</sup> and chitosan<sup>112, 118, 126, 142-153</sup>, and, more recently, solid lipid nanoparticles<sup>154</sup> in the pursuit of novel vaccines for a wide range of "old" pathogens.

Nanoparticles and microparticles are polymeric particulate delivery systems with a size which can vary from ~50 nm to the micrometre range. Although mainly studied for parenteral administration, they are suitable antigen carriers when mucosal immunization is pursued, since microfold epithelial cells (M-cells, present in mucosal membranes) are specialised in the uptake of particulate material and subsequent presentation to immune cells. They are also suitable for multimeric antigen presentation at the surface, thus they can mimic the natural presentation of antigens on viral or bacterial surfaces. Both micro- and nanoparticles facilitate antigen uptake in the gastrointestinal tract by intestinal epithelial cells in the mucosa, M cells and cells of the Peyer's patches following oral administration. As a result, they can enhance humoral and/or cellular immune reactions.<sup>155, 156</sup> Microparticle-delivered antigens are also effective by the intranasal route, where they can activate the NALT and draining lymph nodes.<sup>157</sup> Uptake of colloidal particles by dendritic cells can be further promoted by coupling targeting moieties, specifically recognising dendritic cell receptors, to their surface.<sup>114, 158, 159</sup>

It is well known that antigen presentation in MHC class I is important for generating cellular immunity during vaccination, in order to promote strong cytolytic and Th1 responses. However, antigen cross-presentation can be challenging, as most internalized exogenous antigens are more readily processed into the MHC class II pathway, which typically stimulates CD4+ T cell humoral responses. In order for cross-presentation to occur, antigen must escape from the endosomal compartment into the cytosolic and endoplasmic reticular space where MHC class I processing occurs. The particulate nature of micro- and nanoparticles intrinsically facilitates antigen cross-presentation. Moreover, particle features such as shape, size, composition, surface hydrophobicity and charge, can be manipulated to maximize interactions at the cellular level in order to direct a desired pattern of MHC presentation and acquired immunity, thus, improving the immune response. Several methods to enhance nanoparticle-mediated MHC class I antigen presentation have been explored, including: (i) specifically targeting nanoparticles to specialized dendritic cell populations that actively cross-present antigen; (ii) synthesizing nanoparticles with pH-responsive polymers that naturally facilitate antigen endosomal escape into the cytosol; and (iii) delivering plasmid DNA in nanoparticles to allow intracellular production of antigen for loading into MHC class I.<sup>160–162</sup>

One of the most popular particulate delivery systems that has been used in clinical studies for the formulation of vaccine antigens has been the biodegradable and biocompatible polymer poly(lactide-co-glycolide) (PLG). The biodegradable and biocompatible PLG polymers have been used in humans for many years as suture

material and as controlled release drug delivery systems, therefore, being the first candidates for the development of microparticles as vaccine delivery systems.<sup>155</sup> In these formulations, antigen can be entrapped or adsorbed to the surface of the PLG nanoparticle. Furthermore, by adjusting the rate of degradation of the particles, they can act as a depot from which the antigen can be gradually released. Entrapment in PLG microparticles polarizes immune responses induced with soluble antigens from predominantly antibody and Th2-type to the more protective type 1 T-cell subtype, and also facilitates the induction of CD8+ cytotoxic T lymphocytes (CTLs).

Mucosal oral immunization with microparticles induced protective immunity in several animal models of infection, including *Streptococcus pneumoniae* and *M.tuberculosis*.<sup>156, 163–166</sup> Oral immunization of adult volunteers with microencapsulated enterotoxigenic *Escherichia coli* CS6 antigen using PLG-microencapsulate purified CS6 was safe and well tolerated, inducing immune sIgA and serum IgA and IgG specific antibodies, but not adequately immunogenic as compared to non-encapsulated antigen, thus, further clinical development of the vaccine candidate was suspended.<sup>167</sup>

Despite considerable effort predominantly in pre-clinical studies, oral immunization with encapsulated antigens is still limited by several issues, such as: (i) difficult transposition of results from oral immunization from animals to humans; (ii) relatively low doses of antigen delivered; (iii) lack of particle size uniformity; and (iv) possibility of antigen denaturation due to exposure to organic solvents during microencapsulation process. The potency of microparticle-based oral vaccines might be improved by combining them with additional adjuvants such as CT.<sup>92</sup> The use of alginate micro and nano-particles as an antigen delivery system has also been described, indicating alginate has also presenting adjuvant properties, being able to induce a mucosal and systemic immune response in a variety of animal species by both oral and intranasal administration.<sup>71, 72,</sup>

136, 137, 140, 168

A recent study for aerosolized delivery of BCG vaccine was developed using a synthesized particle system with both micrometre and nanometre dimensions - so-called dried "nanomicroparticle". Interestingly, the non-uniform dimensions of the nanomicroparticles improved particulate aerosolization, dispersion, and trafficking of BCG- encapsulated nanomicroparticles in the respiratory tract of guinea pigs. Results have shown that aerosol delivery using this system was able to enhance their resistance to tuberculosis infection, and generated better immune protection than a standard parenteral BCG formulation.<sup>169</sup>

Not only particle's size strongly influences the immune recognition by APC, being crucial to elicit adequate immune response, it also determines particle traffic, as micro- and nanoparticles exhibit very different trafficking patterns. This size-dependent trafficking can greatly influence particulate strategies for vaccination, whether for mucosal or parenteral delivery. For example, it has been shown that nanoparticles' trafficking to the draining lymph nodes is size dependent, since 20–200 nm diameter nanoparticles injected intradermally in mice could readily migrate to the draining lymph nodes for uptake by lymph node resident DCs, whereas 500–2000 nm diameter nanoparticles were internalized by skin-resident DCs. These differences may compromise the immune response, as DCs in the lymph nodes can better prime cellular immune responses than skin resident Langerhans DCs.<sup>170</sup>

Depending on the used (bio)material, particle features such as size and erosion kinetics can be optimized in order to meet the required criteria for different delivery profiles and therapeutic applications. While the preservation of antigen stability, both during encapsulation and in the mucosal environment, is essential for antigen stability, thus, critical for the immune response, the kinetics of antigen availability also strongly influences the immune response elicited. Therefore, the development of successful controlled release vaccine delivery platform, through which release can be better controlled *in vivo*, may give new impulse to the development of controlled release vaccines.<sup>114, 158</sup>

Finally, taking into account that pre-exposure vaccination through mucosal routes should ideally be potent enough to require only a single or limited number of doses, have minimal toxicity, be inexpensive, and be easy to deliver and administer to patients, micro and nanoparticulate based solutions exhibit the inherent ability to address these requirements, due to their ability to release antigens over prolonged periods, as the ability to target relevant sites of pathogen infection and mucosal induction. Although most of current nanotechnology therapeutics has focused on the effective delivery of chemotherapeutic or antisense compounds to directly inhibit or kill pathogens that cause chronic infection, future developments in the research of particle-mediated vaccine delivery systems can potentially lead to overcome pathogen immune evasion by eliciting favorable immune defense mechanisms.<sup>171, 172</sup>

### 4.3. Chitosan for mucosal immunization

Different strategies have been developed to facilitate enhanced interaction of vaccines with particular regions of mucosal surfaces. Mucoadhesive properties are critical for effective mucosal immunization regarding oral and nasal vaccination.<sup>15, 173</sup> Mucoadhesion can be defined as the prolonged contact time between material (such as bioadhesive polymers) and biological mucus of different epithelia by interfacial forces.<sup>174</sup> Chitosan, being a cationic polysaccharide regarded as safe, is attracting increased attention as an agent for mucosal vaccine delivery, since it has mucoadhesive properties and it has been shown to promote transmucosal absorption. Ionic interactions between the cationic amino groups of chitosan and negative functional groups such as sialic acid of the mucus are considered to be responsible for mucoadhesion, promoting an increased residence time and opening of the tight junctions of the nasal epithelium.<sup>144, 152, 175–177</sup>

Due to chitosan immunostimulatory properties, chitosan-based particulate delivery systems can act both as carrier and as adjuvant, improving the elicited immune response via induction of serum IgG and secretory IgA levels, as previously demonstrated with different nasally administered vaccines (e.g., influenza, diphtheria, and pertussis). Nasal or pulmonary delivery of chitosan was able to enhance systemic and mucosal antibody responses to a number of antigens in mice,<sup>147, 178</sup> and there is also evidence that chitosan may be effective for oral delivery.<sup>120, 179</sup> Promising results have also been reported following nasal delivery of DNA vaccines with chitosan.<sup>122, 145</sup> More significantly, nasal delivery of an influenza vaccine with chitosan strongly enhanced serum haemagglutination inhibition titres in human subjects,<sup>150</sup> whereas nasal delivery of a diphtheria vaccine with chitosan effectively boosted toxin-neutralising antibodies in humans.<sup>180</sup>

Murine studies indicate that combination of chitosan with the non-toxic heat-labile enterotoxin (LT) of *Escherichia coli*, mutant LTK63 further enhanced antigen-specific serum IgG, sIgA, and local and systemic T-cell responses,<sup>181</sup> indicating that combinations of chitosan and other mucosal adjuvants may be beneficial. Recent evidence suggests that DCs were involved in the uptake of orally administered chitosan and that the polysaccharide induced local production of the cytokines IL-4, IL-10 and TGF- $\beta$ .<sup>182</sup> Chitosan-based nanoparticles as mucosal vaccine delivery system have also been used in our group in the last years showing promising capabilities.<sup>183–188</sup>

#### 4.4. Other vaccine delivery systems and immunopotentiators for mucosal immunization

The potential of liposomal formulations to increase the effectiveness of mucosally delivered vaccines has been described in recent studies: (i) liposomes protected antigen stability in acidic conditions following oral administration, thus, being suitable as oral vaccine delivery vehicles;<sup>189</sup> (ii) following intranasal immunization with liposome-formulated whole cell *Yersinia pestis* vaccine, both local IgA and IgG responses were enhanced, while the formulation protected against respiratory bacterial challenge, thus, being suitable as immunopotentiator;<sup>190</sup> (iii) nasal administration of the liposome-formulated *S. mutans* antigen enhanced local secretory IgA in human volunteers.<sup>191</sup> Liposomes association with immunomodulatory or targeting molecules, by co-formulation, entrapment or surface expression, are likely to present better results eliciting immune response, as demonstrated by the association of either recombinant CT<sup>192</sup> or monophosphoryl lipid A<sup>193</sup> to liposomes, which greatly enhanced the elicited immune responses following antigens' oral or oral/nasal delivery, respectively.

Immune-stimulating complexes (ISCOMs) have been used as adjuvants for many years in veterinary vaccines. They are constituted by immunostimulatory fractions from *Q. saponica* (QuilA) incorporated into lipid particles. Due to the presence of surface-active agents (saponins), they are able to interact with cholesterol from cell membranes, thereby, forming pores that can augment antigen transport across membranes. ISCOMs are effective at enhancing antigen uptake by APC, as well as inducing T-cell responses, particularly CD8+CTLs and Th1 cells, both locally and systemically following oral and nasal antigen administration. One disadvantage of ISCOMs is the potential risk of inducing red blood cells haemolysis.<sup>194–197</sup>

### 5. Rational for mucosal immunization against tuberculosis

The rational for fostering mucosal vaccines for TB vaccines takes into account that: a) local pulmonary immunity plays a major role in the control of TB infection; b) parenterally administered vaccines are generally poor inducers of mucosal immunity; c) non-invasive vaccine administration routes (per oral, nasal, or pulmonary) have shown to effectively induce mucosal immunity. Since TB infection is transmitted by the mucosal route (by inhalation of bacterial droplets into the alveoli in the lungs), it could be expected that sIgA antibodies can to some extent combat the infection. The contribution of the cellular immune system to mucosal protection should not, however, be underestimated, as antigenic exposure at mucosal sites activates both mucosal B and T-lymphocytes. The

advantage of cell-mediated versus antibody-mediated immune responses is that T cells can recognize peptides derived from core proteins of the pathogen, which are usually expressed and presented much earlier during infection than proteins targeted for neutralizing antibodies. Subsequently, cell-mediated immunity occurs before the induction of antibodies and forms an early line of defense.<sup>80, 91</sup>

Immunization strategies that generate potent immune responses locally in the lungs, i.e. at the site of primary infection, as well as in the circulation, represent a major opportunity to help both preventing and containing the infection, which is particularly critical in immunocompromised individuals. A vaccine able to induce both systemic and mucosal immune responses, by stimulating an adequate anti-mycobacterial T cell response in the lung mucosa, could prevent not only infectious disease in a more effective way but also colonization of mucosal surfaces.<sup>84, 85, 198, 199</sup>

Since the respiratory tract is a common site of entrance for pathogens, immune surveillance in the nasal mucosa is high. Nasopharynx-associated lymphoid tissue is a key component of MALT and contains the cells and tissues required for generation of antigen-specific immunity. Moreover, mucosal administration can lead to local production of antigen specific sIgA, which can prevent pathogens from colonising mucosal surfaces.<sup>91, 200</sup> In addition to the generation of sIgA, following mucosal antigen stimulation a chain of immune events is initiated, leading to the selection and potential deployment of other types of specific antibodies, helper T cells and cytotoxic T lymphocytes with the potential to attack host cells infected with *M. tuberculosis*.<sup>70, 102</sup>

Mucosal vaccination in general, and intranasal in particular, has been shown to yield as good, or even better, systemic immune responses against tuberculosis than the corresponding parenteral administration route.<sup>12, 13, 17, 67, 71, 72, 75, 105, 199, 201–205</sup> Studies of intranasal delivery of a recombinant adenovirus vaccine encoding Ag85A (MVA85A) in mice have shown significantly enhanced protection against *M. tuberculosis* challenge in mice compared with subcutaneous BCG immunization alone (1.5 log<sub>10</sub> greater reduction in bacterial burden in lungs), whereas the increased induction of strong polyfunctional Th1 cells in the lungs appeared to better correlate with protection than systemic observed immune response, by boosting CD4+ and CD8+ T cell responses in lung lymph nodes.<sup>73</sup>

A potential concern with nasal vaccines is access of gene delivery vehicles, live attenuated organisms, or potentially neurotoxic adjuvant molecules to the central nervous system via the olfactory region. The use of non-replicating gene delivery systems, such as DNA vaccines and highly attenuated viral vectors (including MVA) may help to address this potential problem. In fact, a number of viruses and bacteria present

intrinsic adjuvant properties, which include their ability to activate DCs through Toll-like receptors, induce pro-inflammatory cytokines and target intracellular MHC-processing compartments. The use of recombinant and replication-defective vectors, including adenoviruses and modified vaccinia virus Ankara strain (MVA), and also of subunit gene delivery systems, has been tested in the last decade for their capacity to boost BCG-primed immunity in experimental mucosal immunization strategies in a variety of disease models, showing that they can be used to generate localized pulmonary responses in both upper and lower airways and in the circulation.<sup>52, 75</sup>

Adenoviruses are natural mucosal immunogens and present a specific tropism for the respiratory tract, while presenting a good safety record in humans; as for MVA vectors, they are postulated as potentially safe for human use as they are non-replicative, non-integrating viruses and allow stable expression of encoded vaccine antigens. The interference of pre-existing human antibodies that could neutralize and negatively impact on adenoviral delivery needs further investigation.<sup>206, 207</sup>

The use of nontoxic adjuvants for mucosal delivery has also been under consideration for intranasal delivery, including the most commonly used Eurocine L3, *V. cholerae* cholera toxin and *Escherichia coli* heat-labile enterotoxin. These mucosal adjuvants have been tested in animal models in combination with novel TB vaccine candidates,<sup>94, 102, 105, 208, 209</sup> some of which have been evaluated by oral administration,<sup>201, 210–213</sup> or intranasally.<sup>13, 17, 203, 214–217</sup> Intranasal booster vaccination of mice with an Ag85B–ESAT-6 fusion protein administered with LTK63 adjuvant, a modified form of *E. coli* LT, generated strong and persistent Th1 responses and significant protection against *M. tuberculosis* challenge, reducing bacterial growth by nearly tenfold in lung and spleen tissues.<sup>13, 56</sup> These studies reveal that induction and regulation of mucosal immune responses can occur in the upper respiratory tract, while intranasal immunization can elicit both mucosal and circulating immunity.<sup>218</sup>

Oral vaccine delivery also represents a practical, cost-effective and relatively safe approach to TB immunization. Encouraging results have been achieved with oral administration of BCG in healthy adults, oral BCG delivery has demonstrated to be well tolerated, while immunogenic for T cell-mediated immunity.<sup>219</sup> Studies in laboratory animals have already demonstrated that oral vaccination with encapsulated BCG is highly effective for reducing TB incidence in both mice and wild brush-tail possums, a major reservoir of *M. bovis* TB,<sup>220</sup> while oral delivery of BCG also confers significant protection against respiratory *M. tuberculosis* challenge.<sup>211–213, 221, 222</sup> A Phase I placebo-controlled clinical study is currently underway in the USA to compare safety and

immunogenicity of BCG given via intradermal and/or oral routes, and will likely inform its future use as a component of single dose or prime–boost mucosal vaccine strategies.<sup>52</sup>

Recent studies in animal models have also focused on the potential of mucosal immunity in tuberculosis and its enhancement by pulmonary aerosol vaccine delivery, using BCG or subunit vaccines. Preliminary results showed an highly effective induction of prompt immune response at the infection site, with reduction of bacterial burden and lung pathology.<sup>169, 223, 224</sup> Although delivery to the lung represents an exciting opportunity in the development of newer and more effective TB vaccines, as it provides a non-invasive avenue for local and systemic defence against airborne pathogens, the respiratory tract provides substantial barriers that need to be overcome for successful pulmonary application.<sup>67, 225, 226</sup> In this regard, micro- and nano-sized particles offer novel concepts for the development of optimized therapeutic tools in pulmonary research. Polymeric nanoparticles seem to be especially promising as controlled delivery systems, due to prolonged retention in the lung.<sup>67, 174, 227–229</sup> The understanding of biological mechanisms, together with knowledge of the technology of vaccines, novel adjuvants and delivery systems, will provide guidance on important technical aspects of mucosal vaccine design, being as important as the investigation of new antigens.<sup>85, 230</sup>

## 6. Conclusions

Although the tuberculosis vaccines pipeline is filled with a number of high-profile candidates, in none of the cases do we know with certainty whether they will confer robust protection against tuberculosis in humans. Next-generation vaccines against tuberculosis should be designed aiming at preventing infection or achieving sterile eradication, either by redirecting immune responses at *Mycobacterium tuberculosis* critical antigens, or by using new antigen targeting and delivery platforms, and routes of immunization.

Mucosal vaccination is a needle- and medical waste-free vaccine strategy that provides protective immunity against pathogenic bacteria and viruses in both mucosal and systemic compartments, being suitable for mass vaccination programs in underdeveloped regions. However, mucosal routes of immunization have been rather neglected in the tuberculosis vaccines pipeline, possibly because of the obstacles that still have to be overcome in order for mucosal routes to become commercially viable alternatives. Nanotechnology solutions may address the need of improving the efficacy of immunization schedules, in order to reduce frequency and cost of vaccine

administration, to address the specific challenges of infectious disease in the developing world.

Both mucosal adjuvants and particulate antigen-delivery systems have demonstrated to be readily taken up at mucosal surfaces, being able to induce more effective mucosal immune responses against intracellular pathogens such as *Mycobacterium tuberculosis*. Among the several mucosal sites, the nasal cavity is a potential alternative to the parenteral route due to its easier accessibility. Antigens may be attached to a suitable particulate carrier for immunization purposes upon uptake at the nasal cavity, and several applications may be foreseen, such as immunization with protein antigens or whole bacterial vaccines, for both local and systemic immune responses against tuberculosis. Tuning particulate carriers' properties such as particle size, surface characteristics and the presence of specific adjuvants and permeation enhancers would allow selection of the translocation route and control the in vivo fate and efficacy of the vaccines. Particulate systems and immunomodulatory molecules present, therefore, very attractive features to be used in the development of new mucosal vaccines for tuberculosis and other infectious diseases.

## 7. References

1. World Health Organization. *Global Tuberculosis Report 2013*. (World Health Organization 2013, 2013). at <[http://apps.who.int/iris/bitstream/10665/91355/1/9789241564656\\_eng.pdf?ua=1](http://apps.who.int/iris/bitstream/10665/91355/1/9789241564656_eng.pdf?ua=1)>
2. Cooper, A. M. Cell-mediated immune responses in tuberculosis. *Annu. Rev. Immunol.* **27**, 393–422 (2009).
3. Lönnroth, K. *et al.* Tuberculosis control and elimination 2010–50: cure, care, and social development. *Lancet The* **375**, 1814–1829 (2010).
4. Jassal, M. & Bishai, W. R. Extensively drug-resistant tuberculosis. *Lancet Infect. Dis.* **9**, 19–30 (2009).
5. World Health Organization. *Tuberculosis global facts 2010/2011*. *Central European Journal of Public Health* **18**, (2010).
6. Kaufmann, S. H. E. Future vaccination strategies against tuberculosis: thinking outside the box. *Immunity* **33**, 567–577 (2010).
7. Foxwell, A. R., Kyd, J. M. & Cripps, A. W. Mucosal immunization against respiratory bacterial pathogens. *Expert Rev. Vaccines* **2**, 551–560 (2003).
8. Reljic, R., Williams, A. & Ivanyi, J. Mucosal immunotherapy of tuberculosis: is there a value in passive IgA? *Tuberculosis (Edinb)*. **86**, 179–90 (2006).
9. Li, W., Deng, G., Li, M., Liu, X. & Wang, Y. Roles of Mucosal Immunity against Mycobacterium tuberculosis Infection. *Tuberc. Res. Treat.* **2012**, 791–728 (2012).
10. Torrado, E., Robinson, R. T. & Cooper, A. M. Cellular response to mycobacteria: balancing protection and pathology. *Trends Immunol.* **32**, 66–72 (2011).
11. Sable, S. B. *et al.* Cellular immune responses to nine Mycobacterium tuberculosis vaccine candidates following intranasal vaccination. *PLoS One* **6**, e22718 (2011).
12. Giri, P. K., Verma, I. & Khuller, G. K. Protective efficacy of intranasal vaccination with Mycobacterium bovis BCG against airway Mycobacterium tuberculosis challenge in mice. *J. Infect.* **53**, 350–6 (2006).
13. Dietrich, J. *et al.* Mucosal administration of Ag85B-ESAT-6 protects against infection with Mycobacterium tuberculosis and boosts prior Bacillus Calmette-Guérin immunity. *J. Immunol.* **177**, 6353–6360 (2010).
14. Wang, J. *et al.* Single mucosal, but not parenteral, immunization with recombinant adenoviral-based vaccine provides potent protection from pulmonary tuberculosis. *J. Immunol.* **173**, 6357–6365 (2004).
15. Neutra, M. R. & Kozlowski, P. A. Mucosal vaccines: the promise and the challenge. *Nat. Rev. Immunol.* **6**, 148–58 (2006).
16. Ottenhoff, T. H. M. & Kaufmann, S. H. E. Vaccines against tuberculosis: where are we and where do we need to go? *PLoS Pathog.* **8**, e1002607 (2012).
17. Giri, P. K. & Khuller, G. K. Is intranasal vaccination a feasible solution for tuberculosis? *Expert Rev. Vaccines* **7**, 1341–56 (2008).
18. Stewart, G. R., Robertson, B. D. & Young, D. B. Tuberculosis: a problem with persistence. *Nat. Rev. Microbiol.* **1**, 97–105 (2003).
19. Flynn, J. L. Immunology of tuberculosis and implications in vaccine development. *Tuberculosis* **84**, 93–101 (2004).
20. Winau, F., Hegasy, G., Kaufmann, S. H. E. & Schaible, U. E. No life without death-apoptosis as prerequisite for T cell activation. *Apoptosis* **10**, 707–715 (2005).
21. Korbel, D. S., Schneider, B. E. & Schaible, U. E. Innate immunity in tuberculosis: myths and truth. *Microbes Infect.* **10**, 995–1004 (2008).
22. Divangahi, M., Desjardins, D., Nunes-Alves, C., Remold, H. G. & Behar, S. M. Eicosanoid pathways regulate adaptive immunity to Mycobacterium tuberculosis. *Nat. Immunol.* **11**, 751–758 (2010).
23. Flynn, J. L. *et al.* An essential role for interferon gamma in resistance to Mycobacterium tuberculosis infection. *J. Exp. Med.* **178**, 2249–2254 (1993).

24. Flynn, J. Tumor necrosis factor- $\gamma$  is required in the protective immune response against mycobacterium tuberculosis in mice. *Immunity* **2**, 561–572 (1995).
25. Cooper, A. M., Adams, L. B., Dalton, D. K., Appelberg, R. & Ehlers, S. IFN- $\gamma$  and NO in mycobacterial disease: new jobs for old hands. *Trends Microbiol.* **10**, 221–226 (2002).
26. Corbett, E. L. HIV and tuberculosis: surveillance revisited. *Int. J. Tuberc. Lung Dis.* **7**, 709 (2003).
27. Harris, J. & Keane, J. How tumour necrosis factor blockers interfere with tuberculosis immunity. *Clin. Exp. Immunol.* **161**, 1–9 (2010).
28. Tullius, M. V, Harth, G., Maslesa-Galic, S., Dillon, B. J. & Horwitz, M. A. A replication-limited recombinant Mycobacterium bovis BCG vaccine against tuberculosis designed for human immunodeficiency virus-positive persons is safer and more efficacious than BCG. *Infect. Immun.* **76**, 5200–5214 (2008).
29. Wolf, A. J. *et al.* Initiation of the adaptive immune response to Mycobacterium tuberculosis depends on antigen production in the local lymph node, not the lungs. *J. Exp. Med.* **205**, 105–15 (2008).
30. Lazarevic, V., Nolt, D. & Flynn, J. L. Long-term control of Mycobacterium tuberculosis infection is mediated by dynamic immune responses. *J. Immunol.* **175**, 1107–1117 (2005).
31. Reece, S. T. & Kaufmann, S. H. E. Floating between the poles of pathology and protection: can we pin down the granuloma in tuberculosis? *Curr. Opin. Microbiol.* **15**, 63–70 (2012).
32. Russell, D. G. Who puts the tubercle in tuberculosis? *Nat. Rev. Microbiol.* **5**, 39–47 (2007).
33. Jordao, L., Bleck, C. K. E., Mayorga, L., Griffiths, G. & Anes, E. On the killing of mycobacteria by macrophages. *Cell. Microbiol.* **10**, 529–48 (2008).
34. Gutierrez, M. G. *et al.* NF- $\kappa$ B activation controls phagolysosome fusion-mediated killing of mycobacteria by macrophages. *J. Immunol.* **181**, 2651–2663 (2008).
35. Gutierrez, M. G. *et al.* Autophagy is a defense mechanism inhibiting BCG and Mycobacterium tuberculosis survival in infected macrophages. *Cell* **119**, 753–66 (2004).
36. Singh, S. B., Davis, A. S., Taylor, G. A. & Deretic, V. Human IRGM induces autophagy to eliminate intracellular mycobacteria. *Science* (80-. ). **313**, 1438–1441 (2006).
37. Vergne, I., Chua, J., Singh, S. B. & Deretic, V. Cell biology of mycobacterium tuberculosis phagosome. *Annu. Rev. Cell Dev. Biol.* **20**, 367–94 (2004).
38. Kaufmann, S. H. How can immunology contribute to the control of tuberculosis? *Nat. Rev. Immunol.* **1**, 20–30 (2001).
39. Behar, S. M., Divangahi, M. & Remold, H. G. Evasion of innate immunity by Mycobacterium tuberculosis: is death an exit strategy? *Nat. Rev. Microbiol.* **8**, 668–74 (2010).
40. Behar, S. M. *et al.* Apoptosis is an innate defense function of macrophages against Mycobacterium tuberculosis. *Mucosal Immunol.* **4**, 279–87 (2011).
41. Van Der Wel, N. *et al.* M. tuberculosis and M. leprae translocate from the phagolysosome to the cytosol in myeloid cells. *Cell* **129**, 1287–98 (2007).
42. Jordao, L. & Vieira, O. V. Tuberculosis: New aspects of an old disease. *Int. J. Cell Biol.* **2011**, 403623 (2011).
43. Kaufmann, S. H. & Hess, J. Immune response against Mycobacterium tuberculosis: implications for vaccine development. *J. Biotechnol.* **83**, 13–7 (2000).
44. Russell, D. G., Mwandumba, H. C. & Rhoades, E. E. Mycobacterium and the coat of many lipids. *J. Cell Biol.* **158**, 421–426 (2002).
45. Aguirre-Blanco, A. M., Lukey, P. T., Cliff, J. M. & Dockrell, H. M. Strain-dependent variation in Mycobacterium bovis BCG-induced human T-cell activation and gamma interferon production in vitro. *Infect. Immun.* **75**, 3197–201 (2007).

46. Wilson, M. E., Fineberg, H. V & Colditz, G. A. Geographic latitude and the efficacy of bacillus Calmette-Guérin vaccine. *Clin. Infect. Dis.* **20**, 982–991 (1995).
47. Brandt, L. *et al.* Failure of the Mycobacterium bovis BCG vaccine: some species of environmental mycobacteria block multiplication of BCG and induction of protective immunity to tuberculosis. *Infect. Immun.* **70**, 672–678 (2002).
48. Weir, R. E. *et al.* The influence of previous exposure to environmental mycobacteria on the interferon-gamma response to bacille Calmette-Guérin vaccination in southern England and northern Malawi. *Clin. Exp. Immunol.* **146**, 390–399 (2006).
49. Azzopardi, P., Bennett, C. M., Graham, S. M. & Duke, T. Bacille Calmette-Guérin vaccine-related disease in HIV-infected children: a systematic review. *Int. J. Tuberc. Lung Dis.* **13**, 1331–1344(14) (2009).
50. Hatherill, M. *et al.* The potential impact of helminth infection on trials of novel tuberculosis vaccines. *Vaccine* **27**, 4743–4744 (2009).
51. Rodrigues, L. C. *et al.* Effect of BCG revaccination on incidence of tuberculosis in school-aged children in Brazil: the BCG-REVAC cluster-randomised trial. *Lancet* **366**, 1290–1295 (2005).
52. Dalmia, N. & Ramsay, A. J. Prime-boost approaches to tuberculosis vaccine development. *Expert Rev. Vaccines* **11**, 1221–33 (2012).
53. Russell, D. G., Barry, C. E. & Flynn, J. L. Tuberculosis: What we don't know can, and does, hurt us. *Science (80- )*. **328**, 852–856 (2010).
54. World Health Organization. *TUBERCULOSIS VACCINE Pipeline – 2010*. (2010). at <[http://www.stoptb.org/wg/new\\_vaccines/assets/documents/TB Vaccine Pipeline 10 - 03 21 11.pdf](http://www.stoptb.org/wg/new_vaccines/assets/documents/TB_Vaccine_Pipeline_10_-_03_21_11.pdf)>
55. Tameris, M. D. *et al.* Safety and efficacy of MVA85A, a new tuberculosis vaccine, in infants previously vaccinated with BCG: a randomised, placebo-controlled phase 2b trial. *Lancet* **381**, 1021–8 (2013).
56. van Dissel, J. T. *et al.* Ag85B-ESAT-6 adjuvanted with IC31 promotes strong and long-lived Mycobacterium tuberculosis specific T cell responses in naïve human volunteers. *Vaccine* **28**, 3571–81 (2010).
57. Rowland, R. & McShane, H. Tuberculosis vaccines in clinical trials. *Expert Rev. Vaccines* **10**, 645–58 (2011).
58. Hoft, D. F. *et al.* A new recombinant bacille Calmette-Guérin vaccine safely induces significantly enhanced tuberculosis-specific immunity in human volunteers. *J. Infect. Dis.* **198**, 1491–501 (2008).
59. Grode, L. *et al.* Increased vaccine efficacy against tuberculosis of recombinant Mycobacterium bovis bacille Calmette-Guérin mutants that secrete listeriolysin. *J. Clin. Invest.* **115**, 2472–2479 (2005).
60. Sadagopal, S. *et al.* Reducing the activity and secretion of microbial antioxidants enhances the immunogenicity of BCG. *PLoS One* **4**, e5531 (2009).
61. Hesseling, A. C. *et al.* Bacille Calmette-Guérin vaccine-induced disease in HIV-infected and HIV-uninfected children. *Clin. Infect. Dis.* **42**, 548–58 (2006).
62. Ota, M. O. C. *et al.* Influence of Mycobacterium bovis bacillus Calmette-Guérin on antibody and cytokine responses to human neonatal vaccination. *J. Immunol.* **168**, 919–25 (2002).
63. Dorer, D. E. *et al.* Lymphatic tracing and T cell responses following oral vaccination with live Mycobacterium bovis (BCG). *Cell. Microbiol.* **9**, 544–53 (2007).
64. Bishai, W., Sullivan, Z., Bloom, B. R. & Andersen, P. Bettering BCG: a tough task for a TB vaccine? *Nat. Med.* **19**, 410–1 (2013).
65. Fortune, S. M. & Rubin, E. J. The complex relationship between mycobacteria and macrophages: it's not all bliss. *Cell Host Microbe* **2**, 5–6 (2007).
66. Schuck, S. D. *et al.* Identification of T-cell antigens specific for latent mycobacterium tuberculosis infection. *PLoS One* **4**, e5590 (2009).
67. Amorij, J.-P. *et al.* Towards tailored vaccine delivery: Needs, challenges and

- perspectives. *J. Control. Release* **161**, 363–76 (2012).
68. Dietrich, G., Griot-Wenk, M., Metcalfe, I. C., Lang, A. B. & Viret, J.-F. Experience with registered mucosal vaccines. *Vaccine* **21**, 678–83 (2003).
  69. Holmgren, J. & Czerkinsky, C. Mucosal immunity and vaccines. *Nat. Med.* **11**, S45–S53 (2005).
  70. Brandtzaeg, P., Kiyono, H., Pabst, R. & Russell, M. W. Terminology: nomenclature of mucosa-associated lymphoid tissue. *Mucosal Immunol.* **1**, 31–7 (2008).
  71. Rebelatto, M. C., Guimond, P., Bowersock, T. L. & HogenEsch, H. Induction of systemic and mucosal immune response in cattle by intranasal administration of pig serum albumin in alginate microparticles. *Vet. Immunol. Immunopathol.* **83**, 93–105 (2001).
  72. Mutwiri, G. *et al.* Induction of mucosal immune responses following enteric immunization with antigen delivered in alginate microspheres. *Vet. Immunol. Immunopathol.* **87**, 269–276 (2002).
  73. Goonetilleke, N. P. *et al.* Enhanced immunogenicity and protective efficacy against Mycobacterium tuberculosis of bacille Calmette-Guerin vaccine using mucosal administration and boosting with a recombinant modified vaccinia virus Ankara. *J. Immunol.* **171**, 1602–1609 (2003).
  74. Borges, O., Lebre, F., Bento, D., Borchard, G. & Junginger, H. E. Mucosal vaccines: recent progress in understanding the natural barriers. *Pharm. Res.* **27**, 211–23 (2010).
  75. Källénus, G., Pawlowski, A., Brandtzaeg, P. & Svenson, S. Should a new tuberculosis vaccine be administered intranasally? *Tuberculosis* **87**, 257–66 (2007).
  76. Brandtzaeg, P. Mucosal immunity: induction, dissemination, and effector functions. *Scand. J. Immunol.* **70**, 505–15 (2009).
  77. McGhee, J. R. *et al.* The mucosal immune system: from fundamental concepts to vaccine development. *Vaccine* **10**, 75–88 (1992).
  78. Lamm, M. E. Interaction of antigens and antibodies at mucosal surfaces. *Annu. Rev. Microbiol.* **51**, 311–340 (1997).
  79. Czerkinsky, C. *et al.* Mucosal immunity and tolerance: relevance to vaccine development. *Immunol. Rev.* **170**, 197–222 (1999).
  80. van Ginkel, F. W., Nguyen, H. H. & McGhee, J. R. Vaccines for mucosal immunity to combat emerging infectious diseases. *Emerg. Infect. Dis.* **6**, 123–132 (2000).
  81. Brandtzaeg, P. Role of secretory antibodies in the defence against infections. *Int. J. Med. Microbiol.* **293**, 3–15 (2003).
  82. Corthésy, B. Role of secretory immunoglobulin A and secretory component in the protection of mucosal surfaces. *Future Microbiol.* **5**, 817–829 (2010).
  83. Pavot, V., Rochereau, N., Genin, C., Verrier, B. & Paul, S. New insights in mucosal vaccine development. *Vaccine* **30**, 142–54 (2012).
  84. Foo, S. Y. & Phipps, S. Regulation of inducible BALT formation and contribution to immunity and pathology. *Mucosal Immunol.* **3**, 537–44 (2010).
  85. Mitragotri, S. Immunization without needles. *Nat. Rev. Immunol.* **5**, 905–916 (2005).
  86. Brandtzaeg, P. Induction of secretory immunity and memory at mucosal surfaces. *Vaccine* **25**, 5467–84 (2007).
  87. Mann, J. F. S., Acevedo, R., Campo, J. Del, Pérez, O. & Ferro, V. A. Delivery systems: a vaccine strategy for overcoming mucosal tolerance? *Expert Rev. Vaccines* **8**, 103–12 (2009).
  88. Holmgren, J. Mucosal immunity and vaccination. *FEMS Immunol. Med. Microbiol.* **4**, 1–9 (1991).
  89. Mestecky, J., Russell, M. W. & Elson, C. O. Perspectives on mucosal vaccines: is mucosal tolerance a barrier? *J. Immunol.* **179**, 5633–8 (2007).
  90. Unger, W. W. J. & van Kooyk, Y. 'Dressed for success' C-type lectin receptors for

- the delivery of glyco-vaccines to dendritic cells. *Curr. Opin. Immunol.* **23**, 131–137 (2011).
91. Brandtzaeg, P. Function of mucosa-associated lymphoid tissue in antibody formation. *Immunol. Invest.* **39**, 303–55 (2010).
  92. Otczyk, D. C. & Cripps, A. W. Mucosal immunization: A realistic alternative. *Hum. Vaccin.* **6**, 978–1006 (2010).
  93. Almeida, A. J. & Alpar, H. O. Nasal delivery of vaccines. *J. Drug Target.* **3**, 455–467 (1996).
  94. Vajdy, M. & Singh, M. The role of adjuvants in the development of mucosal vaccines. *Expert Opin. Biol. Ther.* **5**, 953–65 (2005).
  95. Mohanan, D. *et al.* Administration routes affect the quality of immune responses: A cross-sectional evaluation of particulate antigen-delivery systems. *J. Control. Release* **147**, 342–349 (2010).
  96. Ryan, E. J., Daly, L. M. & Mills, K. H. Immunomodulators and delivery systems for vaccination by mucosal routes. *Trends Biotechnol.* **19**, 293–304 (2001).
  97. Medzhitov, R. & Janeway, C. a. Innate immunity: the virtues of a nonclonal system of recognition. *Cell* **91**, 295–8 (1997).
  98. Medzhitov, R. & Janeway, C. Innate immunity. *N. Engl. J. Med.* **343**, 338–344 (2000).
  99. Ozinsky, A. *et al.* The repertoire for pattern recognition of pathogens by the innate immune system is defined by cooperation between Toll-like receptors. *Proc. Natl. Acad. Sci. U. S. A.* **97**, 13766–71 (2000).
  100. Diamond, G., Legarda, D. & Ryan, L. K. The innate immune response of the respiratory epithelium. *Immunol. Rev.* **173**, 27–38 (2000).
  101. Parker, D. & Prince, A. Innate immunity in the respiratory epithelium. *Am. J. Respir. Cell Mol. Biol.* **45**, 189–201 (2011).
  102. Fujikuyama, Y. *et al.* Novel vaccine development strategies for inducing mucosal immunity. *Expert Rev. Vaccines* **11**, 367–379 (2012).
  103. Singh, M. *et al.* A preliminary evaluation of alternative adjuvants to alum using a range of established and new generation vaccine antigens. *Vaccine* **24**, 1680–6 (2006).
  104. Eriksson, K. & Holmgren, J. Recent advances in mucosal vaccines and adjuvants. *Curr. Opin. Immunol.* **14**, 666–672 (2002).
  105. Pizza, M. *et al.* Mucosal vaccines: non toxic derivatives of LT and CT as mucosal adjuvants. *Vaccine* **19**, 2534–2541 (2001).
  106. Kotloff, K. L. *et al.* Safety and immunogenicity of oral inactivated whole-cell *Helicobacter pylori* vaccine with adjuvant among volunteers with or without subclinical infection. *Infect. Immun.* **69**, 3581–3590 (2001).
  107. Lycke, N. From toxin to adjuvant: Basic mechanisms for the control of mucosal IgA immunity and tolerance. *Immunol. Lett.* **97**, 193–198 (2005).
  108. Stephenson, I. *et al.* Phase I evaluation of intranasal trivalent inactivated influenza vaccine with nontoxigenic *Escherichia coli* enterotoxin and novel biovector as mucosal adjuvants, using adult volunteers. *J. Virol.* **80**, 4962–4970 (2006).
  109. Lapa, J. A. *et al.* Randomized clinical trial assessing the safety and immunogenicity of oral microencapsulated enterotoxigenic *Escherichia coli* surface antigen 6 with or without heat-labile enterotoxin with mutation R192G. *Clin. Vaccine Immunol.* **15**, 1222–1228 (2008).
  110. Jain, S., Khomane, K., Jain, A. & Dani, P. Nanocarriers for transmucosal vaccine delivery. *Curr. Nanosci.* **7**, 160–177 (2011).
  111. Almeida, A. J. & Florindo, H. F. in *Nanostructured Biomaterials for Overcoming Biological Barriers* (eds. Alonso, M. J. & Csaba, N. S.) 117–133 (Royal Society of Chemistry, 2012).
  112. Bramwell, V. W. & Perrie, Y. Particulate delivery systems for vaccines: what can we expect? *J. Pharm. Pharmacol.* **58**, 717–28 (2006).
  113. Azevedo, A. F. *et al.* Microencapsulation of *Streptococcus equi* antigens in

- biodegradable microspheres and preliminary immunisation studies. *Eur. J. Pharm. Biopharm.* **64**, 131–7 (2006).
114. Storni, T., Kündig, T. M., Senti, G. & Johansen, P. Immunity in response to particulate antigen-delivery systems. *Adv. Drug Deliv. Rev.* **57**, 333–355 (2005).
  115. Hagan, D. T. O. Microparticles and polymers for the mucosal delivery of vaccines. *Adv. Drug Deliv. Rev.* **34**, 305–320 (1998).
  116. Vajdy, M. & O'Hagan, D. T. Microparticles for intranasal immunization. *Adv. Drug Deliv. Rev.* **51**, 127–41 (2001).
  117. Singh, M., Chakrapani, A. & O'Hagan, D. Nanoparticles and microparticles as vaccine-delivery systems. *Expert Rev. Vaccines* **6**, 797–808 (2007).
  118. Amidi, M., Mastrobattista, E., Jiskoot, W. & Hennink, W. E. Chitosan-based delivery systems for protein therapeutics and antigens. *Adv. Drug Deliv. Rev.* **62**, 59–82 (2010).
  119. O'Hagan, D. T. & Rappuoli, R. Novel approaches to pediatric vaccine delivery. *Adv. Drug Deliv. Rev.* **58**, 29–51 (2006).
  120. Van Der Lubben, I. M. *et al.* Chitosan microparticles for mucosal vaccination against diphtheria: oral and nasal efficacy studies in mice. *Vaccine* **21**, 1400–1408 (2003).
  121. Keijzer, C. *et al.* PLGA, PLGA-TMC and TMC-TPP nanoparticles differentially modulate the outcome of nasal vaccination by inducing tolerance or enhancing humoral immunity. *PLoS One* **6**, e26684 (2011).
  122. Bivas-Benita, M. *et al.* Pulmonary delivery of DNA encoding Mycobacterium tuberculosis latency antigen Rv1733c associated to PLGA-PEI nanoparticles enhances T cell responses in a DNA prime/protein boost vaccination regimen in mice. *Vaccine* **27**, 4010–7 (2009).
  123. Danhier, F. *et al.* PLGA-based nanoparticles: An overview of biomedical applications. *J. Control. Release* **161**, 505–22 (2012).
  124. Pawar, D. *et al.* Evaluation of mucoadhesive PLGA microparticles for nasal immunization. *AAPS J.* **12**, 130–7 (2010).
  125. Szłęk, J., Paclawski, A., Lau, R., Jachowicz, R. & Mendyk, A. Heuristic modeling of macromolecule release from PLGA microspheres. *Int. J. Nanomedicine* **8**, 4601–11 (2013).
  126. Slütter, B. *et al.* Nasal vaccination with N-trimethyl chitosan and PLGA based nanoparticles: Nanoparticle characteristics determine quality and strength of the antibody response in mice against the encapsulated antigen. *Vaccine* **28**, 6282–6291 (2010).
  127. Mata, E., Igartua, M., Patarroyo, M. E., Pedraz, J. L. & Hernández, R. M. Enhancing immunogenicity to PLGA microparticulate systems by incorporation of alginate and RGD-modified alginate. *Eur. J. Pharm. Sci.* **44**, 32–40 (2011).
  128. Da Costa Martins, R. *et al.* Evaluation of particulate acellular vaccines against *Brucella ovis* infection in rams. *Vaccine* **28**, 3038–46 (2010).
  129. Florindo, H. F. *et al.* The enhancement of the immune response against *S. equi* antigens through the intranasal administration of poly-epsilon-caprolactone-based nanoparticles. *Biomaterials* **30**, 879–91 (2009).
  130. Suckow, M. A. *et al.* in *Polysaccharide Applications* (eds. El-Nokaly, M. A. & Soini, H. A.) **737**, 1–14 (1999 American Chemical Society, 1999).
  131. Caetano, L. A., Figueiredo, L., Almeida, A. J. & Gonçalves, L. M. D. Alginate-chitosan particulate delivery systems for mucosal immunization against tuberculosis. in *Bioengineering (ENBENG), 2012 IEEE 2nd Portuguese Meeting in I.I.*, 2 (Xplore, IEEE, 2012). doi:10.1109/ENBENG.2012.6331346
  132. Gombotz, W. R. & Wee, S. F. Protein release from alginate matrices. *Adv. Drug Deliv. Rev.* **64**, 194–205 (2012).
  133. Dobakhti, F. *et al.* Immune response following oral immunization with BCG encapsulated in alginate microspheres. *Iran. J. Immunol.* **3**, 114–20 (2006).
  134. Ajdary, S. *et al.* Oral administration of BCG encapsulated in alginate microspheres

- induces strong Th1 response in BALB/c mice. *Vaccine* **25**, 4595–601 (2007).
135. Tafaghodi, M., Sajadi Tabassi, S. A. & Jaafari, M. R. Induction of systemic and mucosal immune responses by intranasal administration of alginate microspheres encapsulated with tetanus toxoid and CpG-ODN. *Int. J. Pharm.* **319**, 37–43 (2006).
  136. Li, X. *et al.* Preparation of alginate coated chitosan microparticles for vaccine delivery. *BMC Biotechnol.* **8**, 89 (2008).
  137. Dobakhti, F. *et al.* Adjuvanticity effect of sodium alginate on subcutaneously injected BCG in BALB/c mice. *Microbes Infect.* **11**, 296–301 (2009).
  138. Ghasemi, F. Study of oral BCG encapsulated in alginate microsphere to prepare DNA vaccine. *Clin. Biochem.* **44**, S163 (2011).
  139. Tafaghodi, M., Eskandari, M., Khamesipour, A. & Jaafari, M. R. Alginate microspheres encapsulated with autoclaved *Leishmania major* (ALM) and CpG-ODN induced partial protection and enhanced immune response against murine model of leishmaniasis. *Exp. Parasitol.* **129**, 107–14 (2011).
  140. Borges, O. *et al.* Alginate coated chitosan nanoparticles are an effective subcutaneous adjuvant for hepatitis B surface antigen. *Int. Immunopharmacol.* **8**, 1773–80 (2008).
  141. Florindo, H. F., Pandit, S., Gonçalves, L. M. D., Alpar, H. O. & Almeida, a J. Streptococcus equi antigens adsorbed onto surface modified poly-epsilon-caprolactone microspheres induce humoral and cellular specific immune responses. *Vaccine* **26**, 4168–77 (2008).
  142. Arca, H. C., Günbeyaz, M. & Senel, S. Chitosan-based systems for the delivery of vaccine antigens. *Expert Rev. Vaccines* **8**, 937–953 (2009).
  143. Esmaeili, F., Heuking, S., Junginger, H. E. & Borchard, G. Progress in chitosan-based vaccine delivery systems. *J. Drug Deliv. Sci. Technol.* **20**, 53–61 (2010).
  144. van der Lubben, I. M., Verhoef, J. C., Borchard, G. & Junginger, H. E. Chitosan and its derivatives in mucosal drug and vaccine delivery. *Eur. J. Pharm. Sci.* **14**, 201–7 (2001).
  145. Bivas-Benita, M. *et al.* Pulmonary delivery of chitosan-DNA nanoparticles enhances the immunogenicity of a DNA vaccine encoding HLA-A\*0201-restricted T-cell epitopes of *Mycobacterium tuberculosis*. *Vaccine* **22**, 1609–15 (2004).
  146. Caetano, L. A., Amaral, R., Figueiredo, L., Almeida, A. J. & Goncalves, L. M. D. Chitosan-alginate microparticulate delivery system for an alternative route of administration of BCG vaccine. in *Bioengineering (ENBENG), 2013 IEEE 3rd Portuguese Meeting in* 1–3 (2013). doi:10.1109/ENBENG.2013.6518391
  147. Bacon, A. *et al.* Carbohydrate biopolymers enhance antibody responses to mucosally delivered vaccine antigens. *Infect. Immun.* **68**, 5764–5770 (2000).
  148. Amidi, M. *et al.* N-Trimethyl chitosan (TMC) nanoparticles loaded with influenza subunit antigen for intranasal vaccination: Biological properties and immunogenicity in a mouse model. *Vaccine* **25**, 144–153 (2007).
  149. Bal, S. M., Slütter, B., Verheul, R., Bouwstra, J. A. & Jiskoot, W. Adjuvanted, antigen loaded N-trimethyl chitosan nanoparticles for nasal and intradermal vaccination: Adjuvant- and site-dependent immunogenicity in mice. *Eur. J. Pharm. Sci.* **45**, 475–481 (2012).
  150. Read, R. C. *et al.* Effective nasal influenza vaccine delivery using chitosan. *Vaccine* **23**, 4367–4374 (2005).
  151. Vila, A. *et al.* Low molecular weight chitosan nanoparticles as new carriers for nasal vaccine delivery in mice. *Eur. J. Pharm. Biopharm.* **57**, 123–131 (2004).
  152. Illum, L., Jabbal-Gill, I., Hinchcliffe, M., Fisher, a N. & Davis, S. S. Chitosan as a novel nasal delivery system for vaccines. *Adv. Drug Deliv. Rev.* **51**, 81–96 (2001).
  153. Calvo, P., Remuñán-López, C., Vila-Jato, J. L. & Alonso, M. J. Chitosan and Chitosan-Ethylene Oxide-Propylene oxide block copolymer nanoparticles as novel carriers for proteins and vaccines. *Pharm. Res.* **14**, 1431–1436 (1997).
  154. Almeida, A. J. & Souto, E. Solid lipid nanoparticles as a drug delivery system for

- peptides and proteins. *Adv. Drug Deliv. Rev.* **59**, 478–90 (2007).
155. Cleland, J. L. Single-administration vaccines: controlled-release technology to mimic repeated immunizations. *Trends Biotechnol.* **17**, 25–29 (1999).
  156. Eldridge, J. H., Meulbroek, J. A., Staas, J. K., Tice, T. R. & Gilley, R. M. Vaccine-containing biodegradable microspheres specifically enter the gut-associated lymphoid tissue following oral administration and induce a disseminated mucosal immune response. *Adv. Exp. Med. Biol.* **251**, 191–202 (1989).
  157. Heritage, P. L., Brook, M. A., Underdown, B. J. & McDermott, M. R. Intranasal immunization with polymer-grafted microparticles activates the nasal-associated lymphoid tissue and draining lymph nodes. *Immunology* **93**, 249–256 (1998).
  158. Bachmann, M. F. & Jennings, G. T. Vaccine delivery: a matter of size, geometry, kinetics and molecular patterns. *Nat. Rev. Immunol.* **10**, 787–96 (2010).
  159. Xiang, S. D. *et al.* Pathogen recognition and development of particulate vaccines: Does size matter? *Methods* **40**, 1–9 (2006).
  160. Kwon, Y. J., James, E., Shastri, N. & Fréchet, J. M. J. In vivo targeting of dendritic cells for activation of cellular immunity using vaccine carriers based on pH-responsive microparticles. *Proc. Natl. Acad. Sci. U. S. A.* **102**, 18264–18268 (2005).
  161. Flanary, S., Hoffman, A. S. & Stayton, P. S. Antigen delivery with poly(propylacrylic acid) conjugation enhances MHC-1 presentation and T-cell activation. *Bioconjug. Chem.* **20**, 241–248 (2009).
  162. Minigo, G. *et al.* Poly-L-lysine-coated nanoparticles: a potent delivery system to enhance DNA vaccine efficacy. *Vaccine* **25**, 1316–1327 (2007).
  163. Seong, S. Y., Cho, N. H., Kwon, I. C. & Jeong, S. Y. Protective immunity of microsphere-based mucosal vaccines against lethal intranasal challenge with *Streptococcus pneumoniae*. *Infect. Immun.* **67**, 3587–3592 (1999).
  164. Eldridge, J. H. *et al.* Controlled vaccine release in the gut-associated lymphoid tissues. I. Orally administered biodegradable microspheres target the Peyer's patches. *J. Control. Release* **11**, 205–214 (1990).
  165. Challacombe, S. J., Rahman, D., Jeffery, H., Davis, S. S. & O'Hagan, D. T. Enhanced secretory IgA and systemic IgG antibody responses after oral immunization with biodegradable microparticles containing antigen. *Immunology* **76**, 164–168 (1992).
  166. Yeboah, K. G. & D'souza, M. J. Evaluation of albumin microspheres as oral delivery system for *Mycobacterium tuberculosis* vaccines. *J. Microencapsul.* **26**, 166–79 (2009).
  167. Katz, D. E. *et al.* Oral immunization of adult volunteers with microencapsulated enterotoxigenic *Escherichia coli* (ETEC) CS6 antigen. *Vaccine* **21**, 341–346 (2003).
  168. Dobakhti, F. *et al.* Stabilizing effects of calcium alginate microspheres on *Mycobacterium bovis* BCG intended for oral vaccination. *J. Microencapsul.* **23**, 844–854 (2006).
  169. Garcia-Contreras, L. *et al.* Immunization by a bacterial aerosol. *Proc. Natl. Acad. Sci. U. S. A.* **105**, 4656–60 (2008).
  170. Manolova, V. *et al.* Nanoparticles target distinct dendritic cell populations according to their size. *Eur. J. Immunol.* **38**, 1404–13 (2008).
  171. Look, M., Bandyopadhyay, A., Blum, J. S. & Fahmy, T. M. Application of nanotechnologies for improved immune response against infectious diseases in the developing world. *Adv. Drug Deliv. Rev.* **62**, 378–93 (2010).
  172. Griffiths, G., Nyström, B., Sable, S. B. & Khuller, G. K. Nanobead-based interventions for the treatment and prevention of tuberculosis. *Nat. Rev. Microbiol.* **8**, 827–34 (2010).
  173. Baudner, B. C. & O'Hagan, D. T. Bioadhesive delivery systems for mucosal vaccine delivery. *J. Drug Target.* **18**, 752–770 (2010).
  174. Alpar, H. O., Somavarapu, S., Atuah, K. N. & Bramwell, V. W. Biodegradable

- mucoadhesive particulates for nasal and pulmonary antigen and DNA delivery. *Adv. Drug Deliv. Rev.* **57**, 411–30 (2005).
175. Lehr, C., Bouwstra, J., Schacht, E. & Junginger, H. In vitro evaluation of mucoadhesive properties of chitosan and some other natural polymers. *Int. J. Pharm.* **78**, 43–48 (1992).
  176. Haas, J. & Lehr, C.-M. Developments in the area of bioadhesive drug delivery systems. *Expert Opin. Biol. Ther.* **2**, 287–298 (2002).
  177. Leithner, K. & Bernkop-schn, A. in *Chitosan-Based Systems for Biopharmaceuticals* (eds. Sarmiento, B. & Neves, J.) 159–180 (2012 John Wiley & Sons, Ltd, 2012).
  178. McNeela, E. A. *et al.* A mucosal vaccine against diphtheria: formulation of cross reacting material (CRM(197)) of diphtheria toxin with chitosan enhances local and systemic antibody and Th2 responses following nasal delivery. *Vaccine* **19**, 1188–1198 (2000).
  179. Channarong, S., Chaicumpa, W., Sinchaipanid, N. & Mitrevej, A. Development and evaluation of chitosan-coated liposomes for oral DNA vaccine: the improvement of Peyer's patch targeting using a polyplex-loaded liposomes. *AAPS PharmSciTech* **12**, 192–200 (2011).
  180. McNeela, E. A. *et al.* Intranasal immunization with genetically detoxified diphtheria toxin induces T cell responses in humans: enhancement of Th2 responses and toxin-neutralizing antibodies by formulation with chitosan. *Vaccine* **22**, 909–14 (2004).
  181. Baudner, B. C. *et al.* Modulation of immune response to group C meningococcal conjugate vaccine given intranasally to mice together with the LTK63 mucosal adjuvant and the trimethyl chitosan delivery system. *J. Infect. Dis.* **189**, 828–832 (2004).
  182. Porporatto, C., Bianco, I. D. & Correa, S. G. Local and systemic activity of the polysaccharide chitosan at lymphoid tissues after oral administration. *J. Leukoc. Biol.* **78**, 62–69 (2005).
  183. Florindo, H. F., Pandit, S., Goncalves, L., Alpar, H. O. & Almeida, A. J. New approach on the development of a mucosal vaccine against strangles: Systemic and mucosal immune responses in a mouse model. *Vaccine* **27**, 1230–1241 (2009).
  184. Cadete, A. *et al.* Development and characterization of a new plasmid delivery system based on chitosan-sodium deoxycholate nanoparticles. *Eur. J. Pharm. Sci.* **45**, 451–8 (2012).
  185. Figueiredo, L., Calado, C. C. R., Almeida, A. J. & Gonçalves, L. M. D. Protein and DNA nanoparticulate multiantigenic vaccines against *H. pylori*: in vivo evaluation. in *2nd Portuguese BioEngineering Meeting* (ed. IEEE EMBS Portuguese Chapter) I.I, 1 (2012).
  186. Florindo, H. F. *et al.* Antibody and cytokine-associated immune responses to *S. equi* antigens entrapped in PLA nanospheres. *Biomaterials* **30**, 5161–9 (2009).
  187. Figueiredo, L., Cadete, A. & Gonçalves, L. M. D. Intranasal immunisation of mice against *Streptococcus equi* using positively charged nanoparticulate carrier systems. *Vaccine* **30**, 6551–6558 (2012).
  188. Rodrigues, M. A. *et al.* Development of a novel mucosal vaccine against strangles by supercritical enhanced atomization spray-drying of *Streptococcus equi* extracts and evaluation in a mouse model. *Eur. J. Pharm. Biopharm.* **82**, 392–400 (2012).
  189. Han, M., Watarai, S., Kobayashi, K. & Yasuda, T. Application of liposomes for development of oral vaccines: study of in vitro stability of liposomes and antibody response to antigen associated with liposomes after oral immunization. *J. Vet. Med. Sci.* **59**, 1109–1114 (1997).
  190. Baca-Estrada, M. E. *et al.* Intranasal immunization with liposome-formulated *Yersinia pestis* vaccine enhances mucosal immune responses. *Vaccine* **18**, 2203–2211 (2000).

191. Childers, N. K. *et al.* A controlled clinical study of the effect of nasal immunization with a *Streptococcus mutans* antigen alone or incorporated into liposomes on induction of immune responses. *Infect. Immun.* **67**, 618–623 (1999).
192. Harokopakis, E., Hajishengallis, G. & Michalek, S. M. Effectiveness of liposomes possessing surface-linked recombinant B subunit of cholera toxin as an oral antigen delivery system. *Infect. Immun.* **66**, 4299–4304 (1998).
193. Childers, N. K. *et al.* Adjuvant activity of monophosphoryl lipid A for nasal and oral immunization with soluble or liposome-associated antigen. *Infect. Immun.* **68**, 5509–5516 (2000).
194. Smith, R. E., Donachie, A. M. & Mowat, A. M. Immune stimulating complexes as mucosal vaccines. *Immunol. Cell Biol.* **76**, 263–269 (1998).
195. Hu, K. F. *et al.* The immunostimulating complex (ISCOM) is an efficient mucosal delivery system for respiratory syncytial virus (RSV) envelope antigens inducing high local and systemic antibody responses. *Clin. Exp. Immunol.* **113**, 235–243 (1998).
196. Rimmelzwaan, G. F. *et al.* Induction of protective immunity against influenza virus in a macaque model: comparison of conventional and iscom vaccines. *J. Gen. Virol.* **78 ( Pt 4)**, 757–765 (1997).
197. Mowat, A. M., Maloy, K. J. & Donachie, A. M. Immune-stimulating complexes as adjuvants for inducing local and systemic immunity after oral immunization with protein antigens. *Immunology* **80**, 527–534 (1993).
198. Chen, L., Wang, J., Zganiacz, A. & Xing, Z. Single intranasal mucosal *Mycobacterium bovis* BCG vaccination confers improved protection compared to subcutaneous vaccination against pulmonary tuberculosis. *Infect. Immun.* **72**, 238–246 (2004).
199. Santosuosso, M., McCormick, S., Zhang, X., Zganiacz, A. & Xing, Z. Intranasal boosting with an adenovirus-vectored vaccine markedly enhances protection by parenteral *Mycobacterium bovis* BCG immunization against pulmonary tuberculosis. *Infect. Immun.* **74**, 4634–43 (2006).
200. Ronan, E. O., Lee, L. N., Tchilian, E. Z. & Beverley, P. C. L. Nasal associated lymphoid tissue (NALT) contributes little to protection against aerosol challenge with *Mycobacterium tuberculosis* after immunisation with a recombinant adenoviral vaccine. *Vaccine* **28**, 5179–5184 (2010).
201. Doherty, T. M., Olsen, A. W., Van Pinxteren, L. & Andersen, P. Oral vaccination with subunit vaccines protects animals against aerosol infection with *Mycobacterium tuberculosis*. *Infect. Immun.* **70**, 3111–3121 (2002).
202. Dietrich, J., Billeskov, R., Doherty, T. M. & Andersen, P. Synergistic effect of bacillus Calmette Guerin and a Tuberculosis subunit vaccine in cationic liposomes: Increased immunogenicity and protection. *J. Immunol.* **178**, 3721–3730 (2007).
203. Haile, M. *et al.* Nasal boost with adjuvanted heat-killed BCG or arabinomannan-protein conjugate improves primary BCG-induced protection in C57BL/6 mice. *Tuberculosis* **85**, 107–14 (2005).
204. Stylianou, E. *et al.* Mucosal delivery of antigen-coated nanoparticles to lungs confers protective immunity against tuberculosis infection in mice. *Eur. J. Immunol.* **44**, 440–449 (2014).
205. Brennan, M. J. *et al.* Preclinical evidence for implementing a prime-boost vaccine strategy for tuberculosis. *Vaccine* **30**, 2811–23 (2012).
206. Xing, Z. & Lichty, B. D. Use of recombinant virus-vectored tuberculosis vaccines for respiratory mucosal immunization. *Tuberculosis* **86**, 211–7 (2006).
207. Hawkridge, T. & Mahomed, H. Prospects for a new, safer and more effective TB vaccine. *Paediatr. Respir. Rev.* **12**, 46–51 (2011).
208. Eyles, J. E., Sharp, G. J., Williamson, E. D., Spiers, I. D. & Alpar, H. O. Intra nasal administration of poly-lactic acid microsphere co-encapsulated *Yersinia pestis* subunits confers protection from pneumonic plague in the mouse. *Vaccine* **16**,

- 698–707 (1998).
209. Lagranderie, M., Chavarot, P., Balazuc, a M. & Marchal, G. Immunogenicity and protective capacity of *Mycobacterium bovis* BCG after oral or intragastric administration in mice. *Vaccine* **18**, 1186–95 (2000).
  210. Ancelet, L. R., Aldwell, F. E., Rich, F. J. & Kirman, J. R. Oral vaccination with lipid-formulated BCG induces a long-lived, multifunctional CD4(+) T cell memory immune response. *PLoS One* **7**, e45888 (2012).
  211. Clark, S. *et al.* Assessment of different formulations of oral *Mycobacterium bovis* Bacille Calmette-Guérin (BCG) vaccine in rodent models for immunogenicity and protection against aerosol challenge with *M. bovis*. *Vaccine* **26**, 5791–7 (2008).
  212. Aldwell, F. E. *et al.* Oral delivery of lipid-encapsulated *Mycobacterium bovis* BCG extends survival of the bacillus in vivo and induces a long-term protective immune response against tuberculosis. *Vaccine* **24**, 2071–8 (2006).
  213. Hamasur, B. *et al.* *Mycobacterium tuberculosis* arabinomannan–protein conjugates protect against tuberculosis. *Vaccine* **21**, 4081–4093 (2003).
  214. Baudner, B. C. *et al.* The concomitant use of the LTK63 mucosal adjuvant and of chitosan-based delivery system enhances the immunogenicity and efficacy of intranasally administered vaccines. *Vaccine* **21**, 3837–3844 (2003).
  215. Freytag, L. C. & Clements, J. D. Mucosal adjuvants. *Vaccine* **23**, 1804–13 (2005).
  216. Andersen, C. A. S. *et al.* Novel generation mycobacterial adjuvant based on liposome-encapsulated monomycoloyl glycerol from *Mycobacterium bovis* bacillus Calmette-Guérin. *J. Immunol.* **183**, 2294–302 (2009).
  217. Forbes, E. K. *et al.* Multifunctional, high level cytokine producing Th1 cells in the lung, but not spleen, correlate with protection against *Mycobacterium tuberculosis* aerosol challenge in mice. *J. Immunol.* **181**, 4955–4964 (2008).
  218. Cosgrove, C. A. *et al.* Boosting of cellular immunity against *Mycobacterium tuberculosis* and modulation of skin cytokine responses in healthy human volunteers by *Mycobacterium bovis* BCG substrain Moreau Rio de Janeiro oral vaccine. *Infect. Immun.* **74**, 2449–2452 (2006).
  219. Aldwell, F. E. *et al.* Oral vaccination with *Mycobacterium bovis* BCG in a lipid formulation induces resistance to pulmonary tuberculosis in brushtail possums. *Vaccine* **22**, 70–76 (2003).
  220. Buddle, B. M. *et al.* Effect of oral vaccination of cattle with lipid-formulated BCG on immune responses and protection against bovine tuberculosis. *Vaccine* **23**, 3581–9 (2005).
  221. Cross, M. L., Lambeth, M. R., Coughlan, Y. & Aldwell, F. E. Oral vaccination of mice with lipid-encapsulated *Mycobacterium bovis* BCG: Effect of reducing or eliminating BCG load on cell-mediated immunity. *Vaccine* **25**, 1297–303 (2007).
  222. Jeyanathan, M., Heriazon, A. & Xing, Z. Airway luminal T cells: a newcomer on the stage of TB vaccination strategies. *Trends Immunol.* **31**, 247–52 (2010).
  223. Jeyanathan, M. *et al.* Murine airway luminal antituberculosis memory CD8 T cells by mucosal immunization are maintained via antigen-driven in situ proliferation, independent of peripheral T cell recruitment. *Am. J. Respir. Crit. Care Med.* **181**, 862–72 (2010).
  224. Hokey, D. A. & Misra, A. Aerosol vaccines for tuberculosis: a fine line between protection and pathology. *Tuberculosis* **91**, 82–85 (2010).
  225. Labiris, N. R. & Dolovich, M. B. Pulmonary drug delivery. Part I: Physiological factors affecting therapeutic effectiveness of aerosolized medications. *Br. J. Clin. Pharmacol.* **56**, 588–599 (2003).
  226. Rytting, E., Nguyen, J., Wang, X. & Kissel, T. Biodegradable polymeric nanocarriers for pulmonary drug delivery. *Expert Opin. Drug Deliv.* **5**, 629–639 (2008).
  227. Beck-Broichsitter, M., Merkel, O. M. & Kissel, T. Controlled pulmonary drug and gene delivery using polymeric nano-carriers. *J. Control. Release* **161**, 214–24 (2012).

228. Bivas-Benita, M., Ottenhoff, T. H. M., Junginger, H. E. & Borchard, G. Pulmonary DNA vaccination: concepts, possibilities and perspectives. *J. Control. Release* **107**, 1–29 (2005).
229. Kunisawa, J., Fukuyama, S. & Kiyono, H. Mucosa-associated lymphoid tissues in the aerodigestive tract: their shared and divergent traits and their importance to the orchestration of the mucosal immune system. *Curr Mol Med* **5**, 557–572 (2005).

## ***Chapter II***

---

### ***Effect of experimental parameters on microparticles formulation and BCG encapsulation***



*This chapter was adapted from:*

*Liliana A. Caetano, António J. Almeida, Lídia M.D. Gonçalves. Effect of experimental parameters on alginate/chitosan microparticles for BCG encapsulation. Accepted for publication by Marine Drugs.*



## Abstract

The aim of the present study was to develop novel *Mycobacterium bovis* bacille Calmette-Guérin (BCG)-loaded polymeric microparticles with optimized particle surface characteristics and biocompatibility, so that whole live attenuated bacteria could be further used for pre-exposure vaccination against *Mycobacterium tuberculosis* by intranasal route.

BCG was encapsulated into chitosan and alginate microparticles by three different polyionic complexation methods by high speed stirring. For comparison purposes similar formulations were prepared with high shear homogenization and sonication. Additional optimization studies were conducted with polymers of different quality specifications in a wide range of pH values, and with three different cryoprotectants. Particle morphology, size distribution, association efficiency, surface charge, physicochemical properties and biocompatibility were assessed.

Particles exhibited a micrometer size and a spherical morphology. Chitosan addition to BCG shifted the bacilli surface charge from negative zeta potential values to strongly positive. Chitosan of low molecular weight originated particle suspensions of lower size distribution and higher stability, allowing efficient BCG microencapsulation and biocompatibility. Particle formulation consistency was improved when the availability of functional groups from alginate and chitosan was close to stoichiometric proportion. BCG-loaded microparticles presented biocompatibility profiles.

Thus, herein described microparticulate system arises as a promising strategy to deliver BCG vaccine by intranasal route.

**Keywords:** Alginate; Chitosan; BCG; Microencapsulation; Biocompatibility



## 1. Introduction

Enhanced immunization strategies must be urgently found for tuberculosis control.<sup>1,2</sup> The current available vaccine used for pre-exposure vaccination against tuberculosis is *Mycobacterium bovis* BCG. As most vaccines nowadays, BCG is parenterally administered by subcutaneous route. This implies a relatively high production cost, need for cold chain, and the need for trained personal for vaccine administration, while it also leads to lower patient compliance. Regarding the resulting immune response, parenterally delivered vaccines usually originate poor mucosal responses, which is critical to prevent tuberculosis, as *Mycobacterium tuberculosis* normally enters the host through the mucosal surfaces. Nasal route might arise, therefore, as an attractive and alternative administration route.<sup>3</sup>

Regarding tuberculosis, it is essential for a new vaccine to better target the lung while improving interaction with antigen presenting cells (APC) in the lung mucosa, such as alveolar macrophages.<sup>4</sup> It is also well described that the eradication of *Mycobacterium tuberculosis* with pre-exposure vaccination depends on adequate antigen presentation to amplify the elicited immune response, essentially of cellular Th1 type.<sup>5-8</sup> As such, whole live attenuated bacteria act as the ideal antigen producers and vectors, as they are multigenic and normally mimic pathogens and surpass natural barriers.

In the last decades, several studies have elucidated the pros and cons of nasal route for vaccine administration. It is well known that, for soluble antigens, limited absorption occurs at the nasal mucosa due to physiological barriers (i.e. mucosal epithelium, rapid mucociliary clearance, protease degradation).<sup>9</sup> Many strategies have been proposed in order to surpass these barriers and to increase the immunogenicity of intranasal delivered antigens, namely, the use of permeation enhancers, mucosal adjuvants and nano- and microparticulate delivery systems.<sup>10,11</sup> Some studies refer the boost of the immune response due to an adjuvant effect of particulate delivery systems, combined with the use of potent immunopotentiators, either present in the formulation or co-delivered with the antigens.<sup>12-19</sup>

Taking into consideration the aforementioned, we hypothesized that BCG bacilli modification through encapsulation in polymeric microparticulate delivery systems could be an alternative to the classical BCG vaccine, suitable for mucosal immunization. Our main goal was to encapsulate whole live BCG into polymers with biocompatible and mucoadhesive properties using only mild conditions, so that BCG viability was maintained and the biocompatibility of the developed microparticulate delivery system

was assured. Microencapsulation of BCG in chitosan-alginate microparticles will allow the following to take place *in vivo* in sequence: bacilli desorption from the particle surface; degradation and erosion of the polymer network; release of bacteria. Moreover, with the entrapment of BCG in polymeric microparticles, we expect to change BCG's recognition pattern by the immune system and to modulate the mechanism of cellular uptake by APC cells. The selection of the microsize range was related to the intrinsic length of BCG bacilli rod, which requires a minimum particle size of approximately 10 micron, whereas the preference for positively charged microparticles lies on their ability to better interact with negatively charged mucin.<sup>20-22</sup>

The use of biodegradable polymeric particles has been proposed as a promising approach to elicit adequate immune responses, while protecting antigens from degradation.<sup>19</sup> The preparation of polymeric particles can be achieved through a wide range of preparation methods, each one yielding particle formation within a determined size range. For instance, nanoprecipitation and supercritical fluid technology usually yield nanoparticles, whereas spray-drying and solvent evaporation may produce nano- or microparticles depending on the experimental conditions.<sup>23,24</sup> It is generally stated that, for nasal delivery of antigens, nanoparticles are more favorable than particles in the microsize range, as nanoparticles are better taken up by the M-cells present in the nasal associated lymphoid tissue (NALT), and better transported through the epithelial cells (by paracellular and transcellular transference), thus, leading to increased local and systemic immune responses. Nevertheless, microparticles sized up to 40 micron have also been described as successful in eliciting immune responses through nasal administration.<sup>11,25-28</sup>

Most commonly described biodegradable polymers are poly(D,L-lactide-co-glycolide) (PLGA) and poly(L-lactide) (PLA); however, particle formation with PLGA and PLA occurs only in the presence of organic solvents. This is a major drawback, for several reasons. Not only the use of organic solvents may lead to relevant toxicological effects, it can also prompt antigen denaturation or hamper cellular vaccine viability, while formulation methods are usually multi-steps and time consuming. In view of our aim of producing a live vaccine, the longer it takes the formulation steps, the greater the possibility of losing some of the vaccine or compromise cell viability, thereby reducing the encapsulation efficiency and potency of the vaccine.

In this context, chitosan (a deacetylated form of chitin extracted from crustaceans), and sodium alginate (a natural product extracted from algae belonging to the Phaeophyceae, mainly species of *Laminaria*) were chosen to prepare polymeric microparticles by ionic

cross-linking methods as described elsewhere.<sup>18,29–34</sup> Both chitosan and alginate have been extensively studied as biomaterials and pharmaceutical excipients due to their biodegradability and low toxicity, and have been included in the composition of several foods and dietary supplement.<sup>35,36</sup> With ionic gelation methods, particles are formed in a single step by a simple mechanism, usually involving two different polymers and one complexation agent, by adding one polymer solution to the other one with stirring. Most commonly described complexation agents used with chitosan and alginate are calcium chloride (calcium ions maintain alginate gel matrix during the reaction with chitosan, whereas it has been described that a mass ratio of calcium to alginate higher than 0.2 is necessary for microparticle formation) and tripolyphosphate (TPP) (it is described that with the lowest TPP concentrations minimum particle size can be achieved for chitosan microparticles).<sup>34,37</sup>

The widespread use of polyionic complexation methods might be explained due to their many advantages, such as their simplicity, versatility and flexibility, being applicable for virtually all polymers which can be polymerized in presence of a complexation agent, while easily adjusted by changing a number of experimental parameters. During optimization studies, the formulation conditions can be changed towards particle desired features, namely, particle size, association efficiency, surface charge, biocompatibility profile, and production yield. The type of used polymers (i.e. chemical nature, molecular weight, viscosity, purity, pH, and other relevant specifications), the polymer to polymer mass ratio, the type and concentration of complexation agent, the homogenization type (i.e. shear, speed and duration), the polymer to antigen ratio, are some of the variables which significantly influence the particle characteristics. Furthermore, the mild preparation conditions of these methods allow the encapsulation of antigens without degradation caused by high temperatures, oxidation or hydrolysis, as with other commonly used techniques.

As previously stated, both chitosan and alginate have been extensively used in the preparation of polymeric nano- and micro-particles for immunization purposes (Chapter 1, Section 4.2 and 4.3). Chitosan and its derivatives are described to increase the absorption of macromolecules through epithelial membranes, to improve paracellular transport (by opening the cellular tight junctions), and to increase both antigen residence time and uptake at the mucosal site (due to its intrinsic mucoadhesiveness).<sup>11,38–43</sup> Chitosan has been used to prepare nano- and microparticles intended for nasal and oral delivery of vaccines with great results, as chitosan particles were able to elicit strong systemic and local immune responses to different antigens.<sup>16,33,40,44–54</sup>

Alginates are block copolymers polysaccharides, composed of long homopolymeric regions of mannuronate (M) and guluronate (G) (Fig.1), as the result of the conversion of mannuronic and guluronic acid through neutralization during extraction from its natural source. The proportion, distribution and length of these blocks determine chemical and physical properties of the alginate molecules. While G-blocks provide gel-forming capacity, MM and MG units provide flexibility to the uronic acid chains, with flexibility increasing in the order  $GG < MM < MG$ .

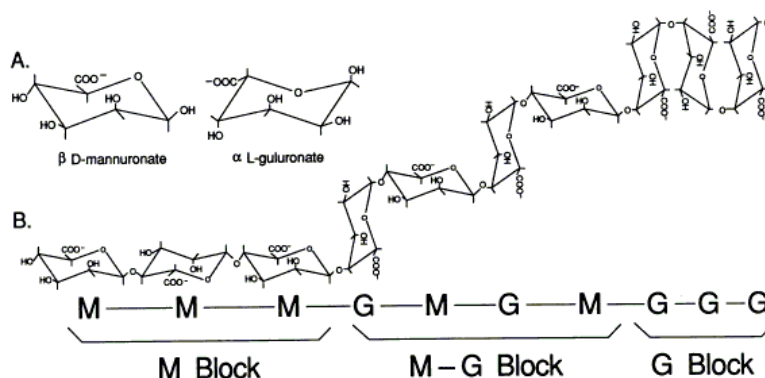


**Figure 1** – Molecular structure of alginate. Monomers D-mannuronate (M) and L-guluronate (G) form polymer (A) (adapted from [http://archimede.bibl.ulaval.ca/archimede/fichiers/24237/24237\\_3.png](http://archimede.bibl.ulaval.ca/archimede/fichiers/24237/24237_3.png), accessed 10 October 2015).

Alginates constitute a very versatile material, with numerous pharmaceutical applications due to their gelling, film-forming, thickening and stabilizing properties. Two other valuable properties of alginates are that they are water-soluble, allowing gel formation without heating or cooling, and also that the alginate matrix allows the entrapment of molecules by capillary forces, which remain free to migrate by diffusion, depending on the size. These features make alginates attractive gelling biopolymers for cell encapsulation purposes. Gel formation and gel structure are determined by alginate type and calcium salt ( $\text{Ca}^{2+}$ ) (Fig. 2), being influenced by pH, solubility and temperature. For instance, at lower pH values, alginate gel is shrunk and a reduction of the pore size of alginate matrix can be achieved, especially in the case of low G content alginate. As such, these components and factors must be matched in order to optimise overall formulation of alginate microparticles by ionotropic gelation.

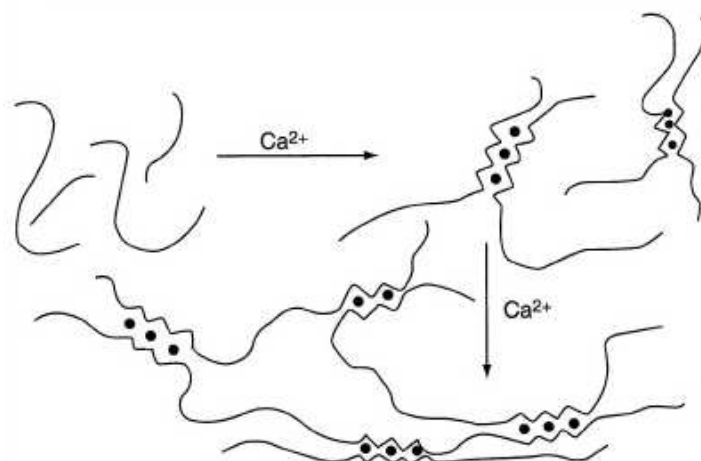


**Figure 2** – Schematic crosslinking of alginate in the presence of calcium counter ions complexed with L-guluronic blocks (adapted from [http://www.scielo.org.mx/scielo.php?script=sci\\_arttext&pid=S1405-888X2014000100007&lng=es&tlng=en](http://www.scielo.org.mx/scielo.php?script=sci_arttext&pid=S1405-888X2014000100007&lng=es&tlng=en), accessed 10 October 2015).

The formulation studies presented in this chapter aimed the optimization of the preparation conditions of BCG-loaded polymeric particles taking into consideration the final yield of production, association efficiency, particle size distribution and surface charge. Therefore, variables such as the type of polymer or of polymer blends, polymers' pH value, the polymer/polymer and BCG/polymers ratio, as well as the type and time of homogenization procedures and order of polymers and counter ions solutions incorporation were studied. Herein described effects of experimental conditions on critical features of microparticle formulations provide a processing window for manipulating and optimizing particles in the microsize range for intended applications.

The expected advantages of the herein described systems for vaccine delivery include the capacity of polymeric microparticulate systems to increase antigen residence time (due to differentiated release profile in the presence of alginate and chitosan) and to enhance antigen interaction with the cell surfaces (due to surface charge modulation). Moreover, due to chitosan's mucoadhesiveness, microparticles would be able to promote mucopenetration, thus, increasing antigen delivery.

## 2. Materials and methods

### 2.1. Materials

Most runs were performed using solutions containing low-molecular weight chitosan (<150 kDa) with degree of deacetylation 75–85% purchased from Sigma–Aldrich (UK). Medium MW chitosan ( $\approx$ 450 kDa) and high MW chitosan ( $\approx$ 600 kDa) with degree of deacetylation of 75-85% (as provided by suppliers), were also used for preliminary formulation studies. The chitosan solutions were prepared at 10 mg/mL in 1% v/v of acetic acid (Merck, Germany) using ultra-purified water and sterilized for 15 min at 121°C.

Sodium alginate polymers of high viscosity (14000 mPa.s, 20 mg/mL), medium viscosity (3000 mPa.s, 20 mg/mL) and low viscosity (20-40 mPa.s, 10mg/mL) (structural viscosity as provided by suppliers) were purchased from Sigma-Aldrich (UK). Other tested sodium alginates include: low G-content (40%) Keltone LVCR (218 mPa.s, 20 mg/mL), high G-content (63%) Manugel LBA (773 mPa.s, 100 mg/mL), and high G-content (65-75%) Protanal LF 10/60 (20-70 mPa.s, 10 mg/mL), which were a gift from FMC BioPolymer. All alginate solutions were prepared by dissolving 20 mg/mL of sodium alginate in filtered 0.20  $\mu$ m purified water and sterilized (15 min at 121°C). Sodium tripolyphosphate (TPP) and calcium chloride ( $\text{CaCl}_2$ ) were purchased from Sigma-Aldrich (UK), and solutions were prepared in ultra-purified water and sterilized for 15 min at 121°C.

The BCG strains - *M. bovis* BCG Pasteur strain 1173 (ATCC 35734<sup>TM</sup>) and a recombinant *M. bovis* BCG harboring a pMN437 plasmid for expression of Green Fluorescent Protein (rBCG-GFP),<sup>55</sup> were kindly supplied by Prof Elsa Anes (FFUL). Unless referred otherwise, all cell culture reagents were purchased from Difco, USA. Both *M. bovis* BCG Pasteur and rBCG-GFP cultures were grown on Middlebrook's 7H9 broth Medium supplemented with 5% (v/v) OADC (oleic acid, albumin, dextrose and catalase supplement) at 37°C / 5% CO<sub>2</sub>. In order to avoid the formation of residual bacterial aggregates, which are difficult to disperse as individual bacteria, 0.05 % (v/v) Tween 80 was also added. Media were supplemented with 50  $\mu$ g/mL hygromycin (Roche) for selection of recombinant mycobacteria. The THP-1 cells (ATCC TIB-202<sup>TM</sup>) a human monocyte cell line was obtained from (ATCC, USA). All animal cell culture reagents were purchased from Invitrogen (UK). Phorbol myristate acetate (PMA), 3-(4,5-dimethyl-2-thiazolyl)-2,5-diphenyl-2H-tetrazolium bromide (MTT), dimethylsulfoxide (DMSO) were all from Sigma-Aldrich (UK).

## 2.2. Preparation of polymeric microparticles

Polymeric microparticles were initially prepared using modifications of previously described ionic cross-linking methods,<sup>29–33</sup> by high speed stirring at room temperature and without organic solvents. In summary, three main formulation methods were defined – Methods (I), (II) and (III), to initiate the optimization studies.

In Method (I), polymeric microparticles were prepared via formation of an alginate ionotropic pre-gel, by allowing sodium alginate solution to react with calcium chloride prior to chitosan addition. (Fig.3). Briefly, a 7.5 mL aliquot of 18 mM calcium chloride solution was added drop wise into a beaker containing 117.5 mL of a 0.6 mg/mL sodium alginate solution, and stirred for 60 minutes under 600 rpm, to provide an alginate pre-gel. Then, 25.0 mL of a 0.7 mg/mL chitosan solution was added drop wise into the pre-gel and stirred over 90 min, giving a final alginate and chitosan concentration of 0.5 mg/mL and 0.1 mg/mL, respectively (alginate: chitosan mass ratio 4.23:1). A colloidal dispersion formed upon polycationic chitosan addition.

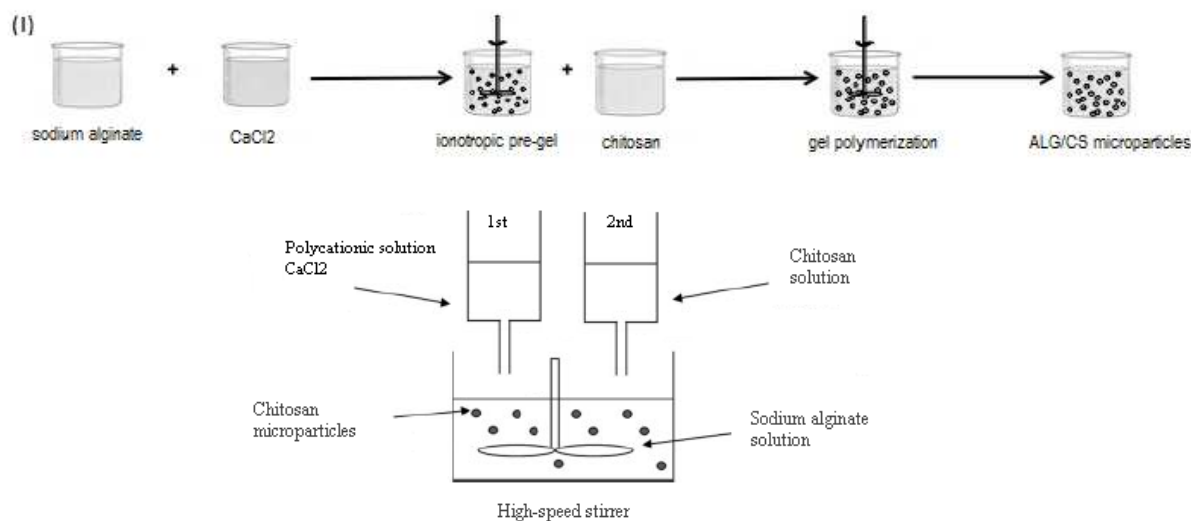


**Figure 3** – Microparticles formation by alginate ionotropic pre-gelation with  $\text{CaCl}_2$  followed by chitosan addition (adapted from<sup>34</sup>).

In formulation Methods II and III, ionic interaction between positively charged amine groups of chitosan and anionic cross-linkers, such as sodium tripolyphosphate (TPP) and sodium alginate led to microparticles formation. In Method (II), polymeric microparticles were prepared by allowing chitosan and alginate to polymerize prior to TPP addition. (Fig.4). Briefly, a 5.0 mL aliquot of 1.0 mg/mL chitosan were added drop wise into a beaker containing volume ranging from 0.1 to 5.0 mL of 1.0 mg/mL of sodium alginate solution, followed by dropwise addition of 1.0 mL of 1.0 mg/mL TPP under high-

speed stirring at 600 rpm for 120 to 150 minutes. Alginate: chitosan ratios ranged from 0.02:1 to 1:1 (w:w).

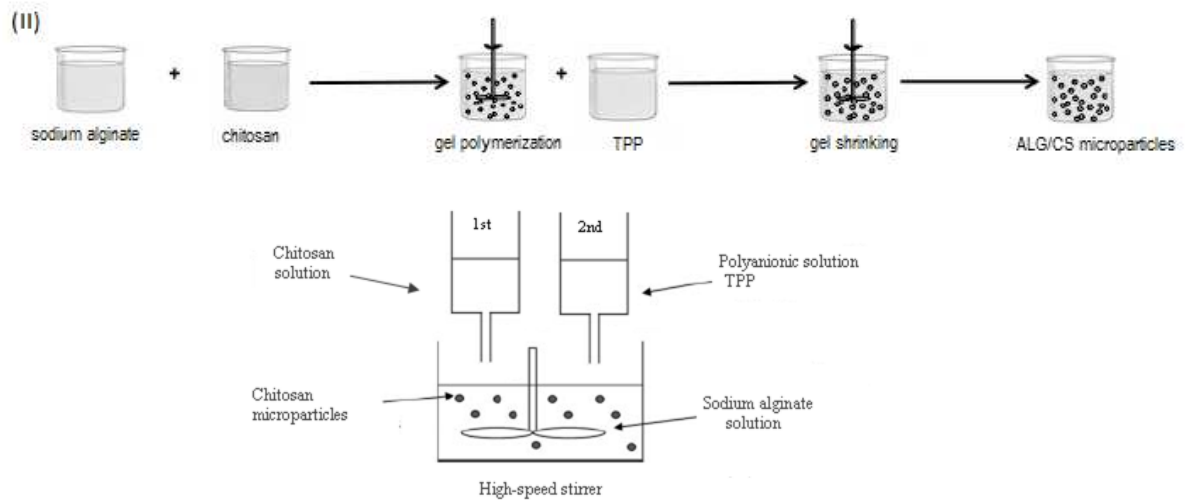


**Figure 4** – Microparticles formation by chitosan gel matrix formation with sodium alginate followed by TPP addition (adapted from<sup>31,33</sup>).

In Method (III), polymeric microparticles were prepared by inducing the pre-gelation of chitosan with TPP, followed by alginate coating (Fig. 5). Briefly, a 1.0 mL aliquot of 1.0 mg/mL TPP was dropped into a beaker containing 5.0 mL of 1.0 mg/mL chitosan solution, followed by polyanionic cross linking with volumes ranging from 0.1 mL to 5.0 mL of 1.0 mg/mL sodium alginate solution, also added drop wise, under high-speed stirring at 600 rpm for 120 to 150 minutes.

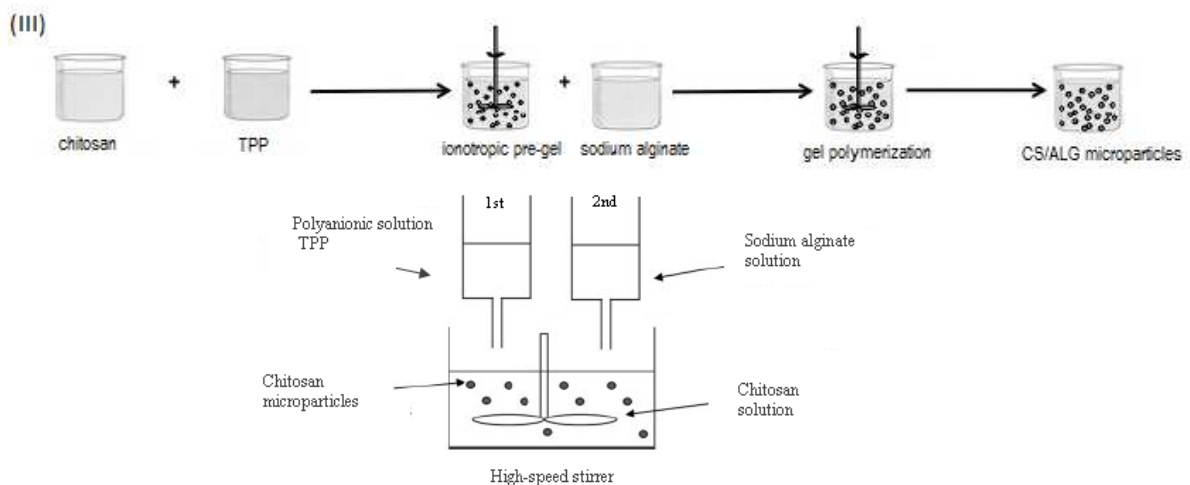


**Figure 5** – Microparticles formation by chitosan precipitation with TPP followed by alginate addition.

Preliminary experiments with three replicates were designed in order to investigate the appropriate concentration range for chitosan, alginate and sodium triphosphate,

according to a previously described method<sup>31</sup> with modifications. The purpose was to identify the impact of the key components of the polyelectrolyte matrix, such as different pH values and polymers mass ratio, on parameters such as particle size and zeta potential. Therefore, high, medium and low molecular weight chitosan, and TPP, were used and their volume was kept constant (5.0 mL and 2.0 mL, respectively), while high, medium and low viscosity alginate was used in increasing volumes.

**Table 1** – Values for the investigated variables during formulation studies.

Formulation	Chitosan (CS) (% w/v)	Alginate (ALG) (% w/v)	CaCl <sub>2</sub> * or TPP ** (% w/v)	ALG:CS mass ratio (w/w)
F0	0.010	0.050	0.010 *	4.23 : 1
F1	0.070	0.001	0.028 **	0.02 : 1
F2	0.069	0.003	0.028 **	0.04 : 1
F3	0.068	0.004	0.027 **	0.06 : 1
F4	0.068	0.005	0.027 **	0.08 : 1
F5	0.067	0.007	0.027 **	0.10 : 1
F6	0.066	0.008	0.026 **	0.12 : 1
F7	0.065	0.009	0.026 **	0.14 : 1
F8	0.064	0.010	0.026 **	0.16 : 1
F9	0.063	0.011	0.025 **	0.18 : 1
F10	0.063	0.013	0.025 **	0.20 : 1
F11	0.056	0.022	0.022 **	0.40 : 1
F12	0.050	0.030	0.020 **	0.60 : 1
F13	0.045	0.036	0.018 **	0.80 : 1
F14	0.042	0.042	0.017 **	1.00 : 1

F0 – Preparation Method (I); F1-F14 – Preparation Method (II) and (III).

High shear homogenization (ultra-turrax T10basic at 11400 rpm, IKA-Labortechnik, Germany) and sonication (Branson Sonifier 250, equipped with a 3 mm microtip probe, USA) were assessed as potential alternatives to high speed stirring to prepare microparticles. The techniques were evaluated considering physical stability of microparticle suspensions (general aspect, formation of aggregates) and microparticles characteristics, such as size distribution and surface charge. Microparticles preparation was in accordance with above described formulation Method (I) and Method (II), with modifications. Briefly, in accordance with previously described formulation Method (I), 0.75 mL of 18 mM calcium chloride were added to 11.75 mL of 0.6 mg/mL sodium alginate, and either homogenized for 3 min in ultra-turrax or sonicated for 3 min at 20% output intensity, prior to 2.5 mL of 0.7 mg/mL chitosan addition, and subsequent homogenization or sonication as described. As for Method (II), 5.0 mL of 1.0 mg/mL chitosan were added to 0.1 to 5.0 mL of 1.0 mg/mL of sodium alginate, followed by

addition of 1 mL of 1.0 mg/mL TPP, and either homogenized for 3 min in ultra-turrax or sonicated for 3 min at 20% output intensity.

Additional formulation optimization studies were conducted to identify best experimental conditions to obtain microparticles of intended size distribution and surface charge. In these studies, microparticles were prepared with sodium alginate of different quality specifications, namely, viscosity and guluronic acid monomers content (G-content, %), and the influence of pH value variations in microparticle size distribution and surface charge was determined. During pH value studies, a wide range of chitosan- and sodium alginate- solution's pH value was assessed (pH from 3.3 to 7.6), while alginate (Protanal™ LF 10/60) concentration was kept constant at 0.1%. Modifications to the formulation methods were introduced along the optimization process accordingly to the conclusions yielded by the obtained results during preliminary studies. Regarding future lyophilisation of microparticles, some preliminary studies using two concentrations (5% and 10% w/v) of three different cryoprotectants (sucrose, glucose, and trehalose) were also conducted.

## 2.3. BCG studies

### 2.3.1. BCG single cell suspension

Bacterial cultures in exponential growth phase (after 7 days) were pelleted at 4000 rpm (1559  $\times$ g) at 4°C for 15 min, washed twice in sterile 10mM PBS pH 7.4 and re-suspended in appropriate medium. The suspension was kept on the bench for 5 min, to allow the decantation of the large clumps of bacteria. Clumps of bacteria were removed by ultrasonic treatment of bacteria suspensions in an ultrasonic water bath for 15 min. For bacteria remaining in clumps, the complete volume of the suspension was collected and pressed through a 21 gauge needle against the syringe tube wall for 10 times, in order to get individualized bacilli.

Single cell suspension was confirmed by phase contrast microscopy or in a fluorescence microscope (for rBCG-GFP). In the absence of clumps, the OD of the suspension at  $\lambda = 600$  nm was adjusted to 0.1 (we assumed that 0.1 OD<sub>600</sub> corresponds to  $1 \times 10^7$  bacteria per mL<sup>56</sup>). This was later confirmed by methylene blue staining and haemocytometer count (for BCG Pasteur) and CFU counts after bacterial suspension plating, in order to more accurately determine the total viable number of bacteria, as this can vary immensely as a function of the growth medium composition of mycobacteria, and also due to a potential growth inhibition effect of chitosan. In fact, although the antimicrobial

potential of chitosan is documented for both Gram positive and Gram negative bacteria (*E. coli* and *S. aureus*), it is not documented specifically for mycobacteria.<sup>57-61</sup>

### 2.3.2. Surface charge characterization

In order to modify the physicochemical properties of BCG, monodispersed bacteria were suspended in different concentrations of chitosan and encapsulated or adsorbed into different formulations of microparticles. Then, size distribution and surface charge were determined. These studies were performed for both BCG Pasteur and rBCG-GFP strains.

Inactivation studies of both strains were also conducted to assess the effect of viability loss in BCG's surface characteristics, and to perform the further characterisation studies in safety. Mycobacteria were submitted to heat inactivation, by submersion of 15 mL falcon containing bacterial suspensions in a water bath preheated and maintained at 80°C for 15 minutes, in comparison with reference method of inactivation with 0.5 % (v/v) formaldehyde for 24 h at 37°C.<sup>62</sup> The efficacy of inactivation methods was determined by viability checks, as follows: 100 µL of the heat/formaldehyde killed suspension was used to inoculate each of two plates with solid agar Middlebrook's 7H10 medium supplemented with 5% OADC and incubated at 37°C in 5% CO<sub>2</sub> atmosphere for 3 weeks.

### 2.3.3. Microencapsulation of BCG

BCG-loaded microparticles were prepared as follows: 1.0 mL of whole live attenuated BCG bacillus monodispersed in NaCl 0.9% (range, 1-2 x 10<sup>8</sup> CFU/mL) was added to 5.0 mL of 1.0 mg/mL chitosan solution. Next, 1.0 mL of 1.0 mg/mL TPP was added drop wise to chitosan-suspended BCG, followed by drop wise addition of 5.0 mL of 1.0 mg/mL sodium alginate solution to the mixture. Final concentrations of prepared microparticles ranged 6-7 log<sub>10</sub> CFU/mL and 0.42 mg/mL of chitosan.

### 2.3.4. BCG cell viability

In order to determine the effect of chitosan on BCG cell viability, a colony-forming units (CFU) assay was performed. Briefly, aliquots of samples containing BCG of both strains (Pasteur and GFP) were seeded in agar inoculation medium (agar Middlebrook's 7H10 medium supplemented with OADC), widely used to cultivate and access the CFU in the case of slow growers such as *M. tuberculosis* and *M. bovis* BCG.<sup>56</sup> The samples were maintained at 4°C for approximately four months (15 weeks), and plates were inoculated

with samples for cell count at regular time points. After three weeks of incubation at 37°C and 5% CO<sub>2</sub>, colonies were counted to determine CFU.

## 2.4. Characterization of microparticles

### 2.4.1. Size distribution, surface charge and morphology

The microparticles were assessed according to size distribution and surface charge (zeta potential), by laser diffraction and electrophoretic mobility, using a Mastersizer 2000 and a Malvern Zetasizer, respectively (Malvern Instruments, UK). For particle size analysis, each sample was diluted with filtered purified water to the appropriate concentration to yield 10% obscuration limit. Each analysis was carried out in triplicate at 25°C. Results were expressed in terms of mean diameter and span ( $Span = [d(0.9) - d(0.1)] / d(0.5)$ ). Size distribution is characterized using the d0.5 parameter (diameter for which 50% of the distribution falls below) and the span parameter (width of particle size distribution). For the determination of the electrophoretic mobility, samples were diluted with filtered purified water. The mean values were obtained from the analysis of three different batches, each of them measured three times. Morphological examination of microparticles was performed by microscopy. The ImageJ software, 1.44p version (National Institutes of Health, USA) was used to perform image analysis.

### 2.4.2. Production yield

The production yield (YP) of the microparticles was determined using an indirect method based on the quantification of the chitosan concentration initially used in the formulation, and that found in the supernatant of the final microparticle suspension. The method of quantification is based on a colorimetric reaction between amine groups of chitosan and the dye Cibacron brilliant red 3B-A.<sup>29</sup> Briefly, 1 mL of microparticles suspension was centrifuged at 18 000×g for 15 min at 4°C (Alegria™64R Centrifuge, Beckman Coulter, USA), in order to separate the microparticles from free chitosan. After the addition of the dye to the solutions the absorbance values were measured at 575 nm at microplate spectrophotometer reader (Tecan Infinite M200, Austria). Chitosan concentrations were determined using a standard curve. Chitosan (CS) yield was determined using Equation 1, where  $[CS]_{total}$  is the concentration of chitosan used to prepare the microparticles, and  $[CS]_{supernatant}$  is the amount found in the supernatant.

#### EQ. 1. CHITOSAN YIELD

$$CS \text{ yield (\%)} = \frac{[CS]_{total} - [CS]_{supernatant}}{[CS]_{total}} \times 100$$

### 2.4.3. Fourier transform infrared spectroscopy (FT-IR) analysis

Preliminary information on chemical nature of the chitosan-alginate microparticles was collected using FT-IR analysis in an IRAffinity-1 (Shimadzu Corporation) spectrophotometer. The FT-IR measurements were made directly in the dried microparticles, which were previously lyophilized, gently mixed with approximately 300 mg of micronized KBr powder and compressed into discs at a force of 10 kN for 1 min using a manual tablet presser (Perkin Elmer, Norwalk, USA). All spectra were recorded at room temperature at the resolution of 4 cm<sup>-1</sup> and 50-times scanning, between 4000 and 500 cm<sup>-1</sup>.

### 2.4.4. Association efficiency

Association efficiency (A.E., %) was determined by cell count number using a haemocytometer (Neubauer chamber Bürker). The association efficiency is expressed as the percentage of BCG entrapped/adsorbed in microparticles reported to initial amount of cells in suspension (Eq. 2).

#### EQ. 2. ASSOCIATION EFFICIENCY

$$\text{Association efficiency (\%)} = \frac{\text{Total cells} - \text{Free cells}}{\text{Total cells}} \times 100$$

## 2.5. *In vitro* cell viability (MTT assay)

Animal cell viability was assessed using general cell viability endpoint MTT (3-(4,5-dimethyl-2-thiazolyl)-2,5-diphenyl-2H-tetrazolium bromide) as previously described with some modification.<sup>63</sup> Unless referred otherwise, all cell culture reagents were purchased from Invitrogen, UK. Briefly, the THP-1 cells (ATCC TIB-202™) a human monocyte cell line was used. THP-1 cells (grown in RPMI 1640 supplemented with 10 % FBS, penicillin and streptomycin,) were seeded onto 96 well cultures dishes at a density of 5x10<sup>5</sup> cells/mL and treated for 3 days with 20 nM phorbol myristate acetate (PMA; Sigma Aldrich, Spain) in order to differentiate into macrophage, and medium exchanged and incubated for one more day. Cells were then incubated for 72 h at 37°C with different concentrations of CS and ALG solutions and BCG loaded and empty formulations. Controls consisted of cells incubated with only culture medium. Each sample concentration was tested in triplicate in a single experiment, which was repeated at least 3 times.

After the incubation time, culture medium was replaced with culture medium containing 0.5 mg/mL of MTT and incubated for 3 h at 37°C. The MTT is converted, by living cells, into a dark, water insoluble, and blue formazan product. The medium was removed after 3 h and the intracellular formazan crystals were solubilised and extracted with dimethylsulfoxide (DMSO). After 15 min at room temperature, the absorbance of the extracted solution was measured at 570 nm in a microplate reader (Infinite M200, Tecan, Austria). The percentage of cell viability was determined for each concentration of tested sample according to Equation 3, where *Abs test* is the absorbance value obtained for cells treated with samples, and *Abs control* is the absorbance value obtained for cells incubated with culture medium.

**EQ. 3. RELATIVE CELL VIABILITY**

$$\text{Cell viability (\% of control)} = \frac{Abs\ test}{Abs\ control} \times 100$$

## 2.6. Statistical analysis

Data were subjected to ANOVA for analysis of statistical significance, and a *P* value of <0.05 was considered to be significant. Unless stated otherwise, results are expressed as mean values ± standard deviation (S.D.). The analysis was carried out using GraphPad Prism v. 5.02 (GraphPad Software, CA, USA).

### 3. Results and discussion

#### 3.1. Characterization of polymeric microparticles

The purpose of this study was to optimize the experimental parameters to prepare BCG-loaded polymeric microparticles intended for future intranasal immunization studies. The formation of microparticles with a particular size distribution or surface charge (critical aspects for vaccine delivery) may vary significantly depending on polymers' nature, polymer's concentration, purity, type of salt, MW of chitosan, and viscosity of alginate employed. Therefore, the conditions for the preparation of microparticles were optimized during preliminary formulation studies. Two polymers – chitosan and sodium alginate, with different quality specifications (molecular weight, viscosity, G-content, deacetylation degree, purity) were used to prepare, initially, plain polymeric microparticles, followed by BCG microencapsulation, by an ionotropic gelation method. In order to identify the effect of experimental parameters on particles' critical features, variations to the preparation method (such as alginate to chitosan mass ratio, stirring time, shear, polymers addition order, and solutions pH value) were studied.

Culture conditions for two different strains of BCG (BCG Pasteur and a recombinant strain expressing green fluorescent protein, rBCG-GFP) were determined. Prior to BCG's microencapsulation into polymeric microparticles, studies were conducted to evaluate BCG's bacilli surface charge following suspension in different media, or following inactivation by two different methods (heat or formaldehyde). A dispersion technique was also optimized, fostering the microencapsulation of whole live monodispersed single bacteria, instead of aggregated, clumped bacteria. Although BCG recombinant strain and killed bacteria were out of our main goal, which was to microencapsulate whole live BCG Pasteur bacteria for further immunization studies in mice, they played an important role on the microparticle characterization studies.

The prepared polymeric microparticles were characterized considering particle size distribution, surface charge, morphology, and the final yield of production. FT-IR studies were conducted in order to assess the interaction between chitosan and alginate ionic groups. Particle size was the leading assessed property during formulation optimization studies, oriented towards the obtaining of microparticles with a mean diameter of 5 – 10  $\mu\text{m}$ , within a narrow and reproducible size distribution. Another key aspect regarding the preparation of vaccine-loaded polymeric particles is association efficiency, which should be the highest possible. Biocompatibility of the prepared polymeric microparticles was determined in a cell viability (MTT reduction) assay, using a human monocyte cell line

(THP-1) differentiated into macrophage-like cells, as model for antigen presenting cells.<sup>64,65</sup>

### 3.1.1. Size distribution and surface charge

Previous studies showed that particle size distribution of plain polymeric microparticles prepared by ionic gelation was greatly influenced by the polymers' mass ratio and molecular weight.<sup>21,66,67</sup> Therefore, fourteen formulations were developed with alginate to chitosan mass ratio ranging from 0.02:1 to 4.23:1 (w/w), according to previously described Methods I, II and III. In addition, different combinations of low viscosity (LV) alginate and low molecular weight (LMW) chitosan, medium viscosity (MV) alginate and medium molecular weight (MMW) chitosan, and high viscosity (HV) alginate and high molecular weight (HMW) chitosan were used. Microparticles were characterised for size distribution (mean diameter and span) and surface charge (zeta potential) (Table 2).

The effect of polymer's molecular weight with increasing alginate to chitosan mass ratio on particle size distribution is presented in Figure 6. Regarding the use of low molecular weight chitosan, particles ranging from 18 to 34  $\mu\text{m}$  were obtained (Fig. 6A) with a narrow size distribution (span <2.5) (Fig. 6B). Using chitosan of medium molecular weight yielded a general increase in particle mean diameter, with formulation F13 (0.8:1 alginate to chitosan mass ratio, w/w) being the only exception. Using chitosan of high molecular weight led to an intermediate particle mean diameter, except also for F13 (Fig. 6A). Herein presented formulations were obtained with a relatively narrow size distribution (span  $\leq 5$ ), except for formulation F11 prepared with low molecular weight chitosan (span =9.5). The obtained span values suggest that particles are formed with better consistency when the availability of the functional groups is close to stoichiometric proportion.

Broad particle size distributions can be attributable to the presence of larger single particles, which in turn might prompt aggregate formation.<sup>68,69</sup> By visual inspection, we confirmed the presence of aggregates in formulations with the highest particle mean diameter (Fig. 7). Best formulations, defined as suitable to yield turbid solution without aggregation, were obtained with chitosan of medium molecular weight when ALG/CS mass ratio ranged from 0.6:1 to 0.12:1, and with chitosan of low molecular weight when ALG/CS mass ratio ranged from 0.4:1 to 1:1.

**Table 2** – Particle size distribution (mean diameter and span) and surface charge (zeta potential) of microparticles on the preparation day.

Formulation	ALG:CS mass ratio (w/w)	Chitosan MW	Particle size, d0.5 (µm)	Span	Zeta potential (mV)	Production yield (%)
F0	4.23:1	Low	18.5 ± 0.7	1.4 ± 0.0	-20.8 ± 7.9	n.d.
		Medium	260.5 ± 41.3	4.3 ± 0.6	-26.7 ± 4.9	n.d.
		High	68.1 ± 10.6	5.2 ± 2.9	-17.9 ± 6.8	n.d.
F11	0.4:1	Low	37.1 ± 0.7	9.5 ± 0.5	+34.0 ± 0.5	n.d.
		Medium	144.4 ± 5.1	3.0 ± 0.1	+47.1 ± 1.7	n.d.
		High	107.5 ± 10.1	4.1 ± 0.9	+30.4 ± 1.4	n.d.
F12	0.6:1	Low	39.3 ± 2.0	2.6 ± 0.1	+26.7 ± 1.1	n.d.
		Medium	94.7 ± 3.2	3.7 ± 0.2	+30.9 ± 1.1	n.d.
		High	65.9 ± 4.4	4.1 ± 0.7	+25.5 ± 0.5	n.d.
F13	0.8:1	Low	33.8 ± 0.9	2.6 ± 0.1	+22.7 ± 1.6	83.6 ± 0.0
		Medium	23.9 ± 0.6	2.7 ± 0.3	+25.6 ± 1.8	n.d.
		High	51.3 ± 1.8	3.3 ± 0.1	-0.2 ± 0.8	n.d.
F14	1:1	Low	25.9 ± 0.7	1.7 ± 0.1	+16.2 ± 0.6	36.8 ± 0.0
		Medium	139.0 ± 8.5	3.2 ± 0.1	-10.9 ± 1.6	n.d.
		High	80.6 ± 3.8	4.9 ± 0.2	-25.7 ± 3.3	n.d.

F0, microparticles obtained by Method (I) via alginate ionotropic pre-gelation with CaCl<sub>2</sub> followed by chitosan addition; F11-F14, microparticles, obtained by Method (II) via chitosan pre-gelation with alginate, followed by TPP addition. Microparticles' size is characterized using the size distribution parameters d0.1, d0.5 and d0.9 (diameter for which 10%, 50% and 90% of the size distribution falls below, respectively) and span (width of particle size distribution, according to the formula (d0.1-d0.9)/d0.5). Results are expressed as mean and standard deviation (n ≥ 3); n.d., not determined.

The obtained results show a greater influence of chitosan molecular weight than alginate to chitosan mass ratio on microparticles size distribution. Overall, the use of chitosan of low molecular weight led to the formation of smaller particles for the majority of ALG/CS mass ratios, resulting in fewer aggregates. This may stem from the ability of chitosan of low molecular weight to diffuse more promptly in the alginate gel matrix to form smaller, more homogeneous particles, whereas, in opposite, polymers of high molecular weight

or viscosity may bind to the surface of such matrices, forming an outer membrane and leading to incremental particle size.<sup>32,70</sup>

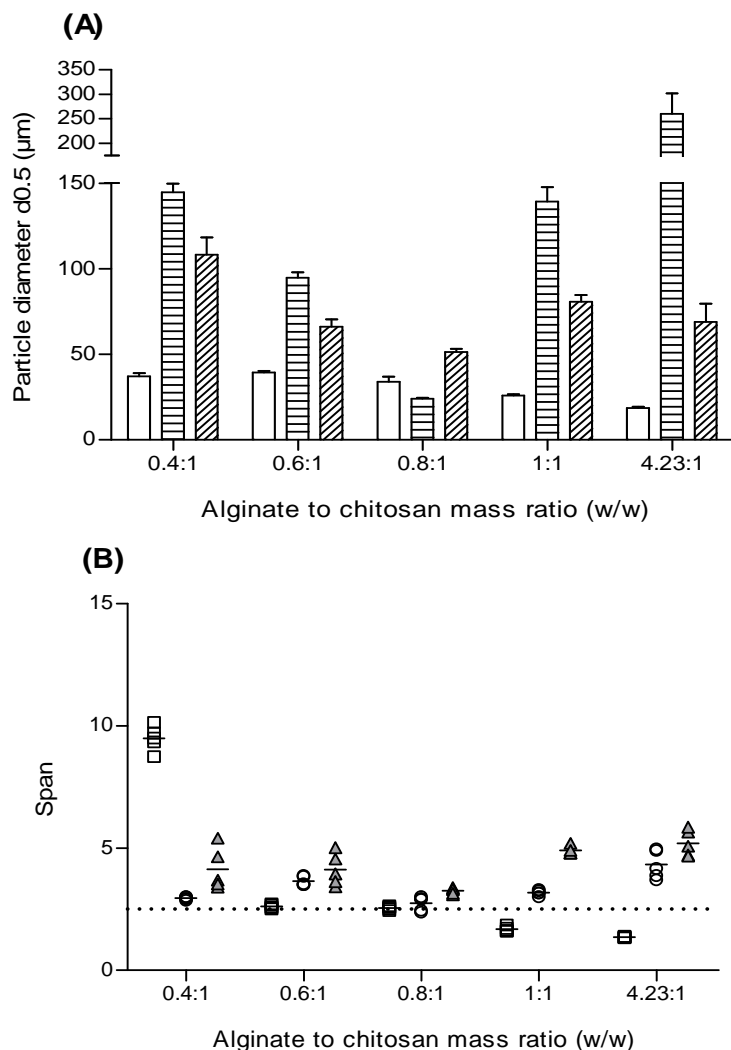


**Figure 6** – Effect of alginate to chitosan mass ratio on particle size distribution. (A) Particle size distribution of polymeric microparticles prepared with chitosan of low molecular weight chitosan (no fill), medium molecular weight (horizontal lines), and high molecular weight (angled lines). The d<sub>0.5</sub> particle size population is represented. (B) Size distribution span of microparticles prepared with chitosan of low molecular weight (□), medium molecular weight (○), and high molecular weight (▲). Results are presented as mean ± S.D. (n ≥ 3).

Regarding particle surface charge, the electrophoretic mobility of microparticles was measured and expressed as zeta potential values. The effect of polymer's molecular weight with increasing alginate to chitosan mass ratio on particle surface charge is presented in Figure 8. Alginate to chitosan mass ratios ranging from 0.4:1 to 0.8:1 led to the formation of microparticles with high positive zeta potential values ( $+22.7 \pm 1.6$  mV to  $+47.1 \pm 1.7$  mV), thus, being positively charged, except for one formulation (F13 prepared with chitosan of high molecular weight) ( $-0.2 \pm 0.8$  mV). Higher ALG/CS mass ratios (1:1 and 4.23:1) led to the formation of negatively charged microparticles, as zeta

potential reached negative values ( $-10.9 \pm 1.6$  mV to  $-26.7 \pm 4.9$  mV) with increasing polymer's molecular weight. Formulation F14 prepared with chitosan of low molecular weight was the exception ( $+16.2 \pm 0.6$  mV).

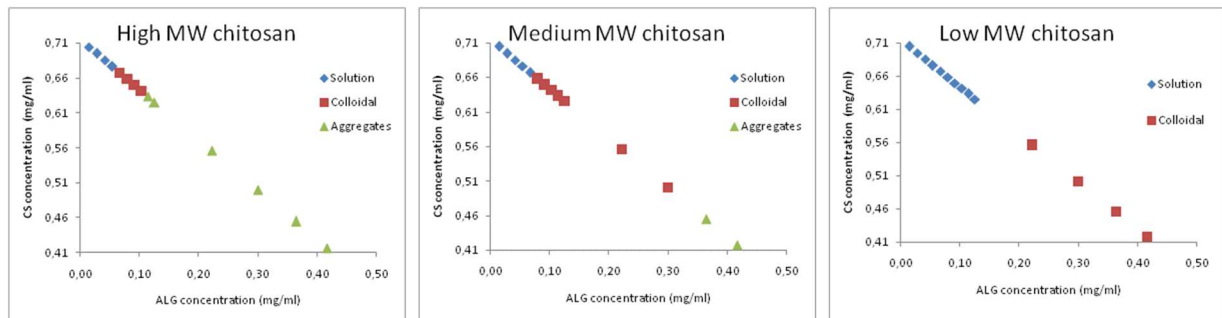


**Figure 7** – Microparticles domain formation using high, medium and low molecular weight chitosan. Three different systems were identified: clear solution ( $\diamond$ ), opalescent/colloidal suspension ( $\blacksquare$ ), and aggregates ( $\blacktriangle$ ).

Zeta potential values provide a quantitative measure of the charge on colloidal particles in liquid suspension. For chitosan-alginate microparticles, surface charge greatly depends on chitosan total protonated amino groups. Zeta potential profiles of  $\pm 30$  mV are described to prevent aggregation and stabilize particles in suspension.<sup>71</sup> This was also confirmed by visual inspection of the obtained colloidal suspensions, which remained stable without aggregation at room temperature for several days (data not shown).

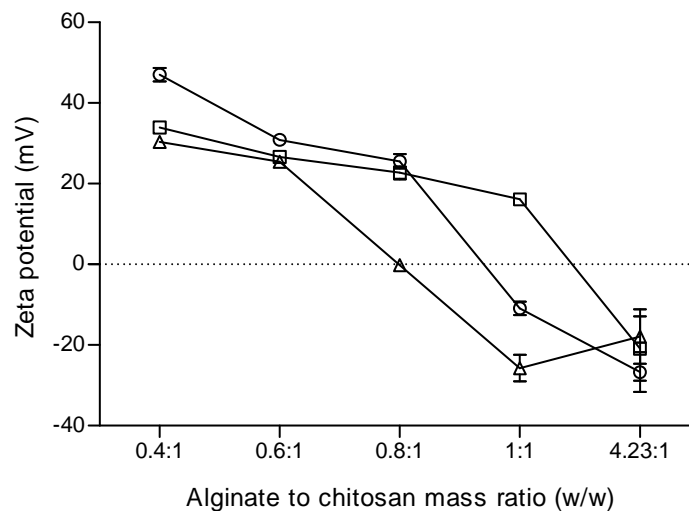


**Figure 8** – Effect of alginate to chitosan mass ratio on particle surface charge. Zeta potential of microparticles prepared with chitosan of low molecular weight ( $\square$ ), medium molecular weight ( $\circ$ ), and high molecular weight ( $\triangle$ ). Results are presented as mean  $\pm$  S.D. ( $n \geq 3$ ).

As for the formulation method, complexation with TPP performed best with 1:1 ALG/CS mass and chitosan of low molecular weight ("F14\_Low"), with microparticles presenting

a mean diameter of  $25.9 \pm 0.7 \mu\text{m}$ , span  $\leq 1.7$ , and positive surface charge ( $+22.7 \pm 1.6 \text{ mV}$ ). By using  $\text{CaCl}_2$  as complexation agent, in alternative to TPP, it was possible to improve particle size distribution with 4.23:1 ALG/CS mass ratio and chitosan of low molecular weight (“*F0\_Low*”), with microparticles presenting a reduced mean diameter of  $18.5 \pm 0.7 \mu\text{m}$  (span  $\leq 1.4$ ), and negative surface charge ( $-20.8 \pm 7.9 \text{ mV}$ ).

These results indicate that the molecular weight of the chitosan used to prepare the microparticles had a major impact in particle size distribution, whereas the alginate to chitosan mass ratio had an important role in modulating particle surface charge. It was also possible to identify the conditions which led to a greater heterogeneity in particle formation, evidenced as a broader particle size distribution revealed in increased span values. Overall, it was possible to observe, for microparticles prepared with a given ALG/CS mass ratio, a higher standard deviation of the span when chitosan of medium and high molecular weight were used (with formulation F11 being the exception), thus, indicating that particle size distribution varied considerably and was not completely reproducible. These results were important to put into evidence how to modulate the microparticles size distribution and surface charge profile according to the selected formulation method.

Particle size is determinant in intranasal delivery and mucosal uptake of particles,<sup>28</sup> and in the intracellular traffic of the particles.<sup>72,73</sup> Carriers sizing few microns have shown higher potential as intranasal delivery systems of antigens.<sup>74-76</sup> As size is increased, which can be partially due to the increase in the sample mass by weight of the microparticles, surface area decreases; this in turn might contribute to slowdown antigen release rate as depot effect. For this study purposes, particle size should be at least  $5 \mu\text{m}$ , in order to enable the entrapment of BCG bacilli, which are short to moderate long rods,  $0.3\text{-}0.6 \times 1\text{-}4 \mu\text{m}$ .<sup>77,78</sup> According to some authors, size must not overcome  $10 \mu\text{m}$  when phagocytosis is required, with  $200 \text{ nm}$  to  $5 \mu\text{m}$  being the ideal size.<sup>79</sup> Nevertheless, much larger particles ranging from  $1$  to  $40 \mu\text{m}$  have been successfully used for intranasal immunization, eliciting good systemic and mucosal responses in mice.<sup>9</sup>

Concomitantly with particle size distribution, zeta potential determination allows the estimation of particle suspension stability against subsequent aggregation, as  $\pm 30 \text{ mV}$  can be an indicator of particulate systems' stability.<sup>71</sup> Surface charge is a critical parameter that affects the mucoadhesion of chitosan/alginate microparticles to the nasal mucosa, which in turn will prolong the residence time of the vaccine at the site of action. The net positive charge indicates the presence of free surface amino groups in F11-F13 in addition to F14 obtained with chitosan of low molecular weight, which will help in initial

adhesion to nasal mucosa. Since mucoadhesive properties of chitosan are mainly explained by the electrostatic interaction and by hydrogen bond of amine groups of this cationic polymer with the negatively charged mucin,<sup>35</sup> one can expect positively charged particles to be preferable to negatively charged ones.

Taking into consideration the aforementioned results, it was possible to conclude that the association of 4.23:1 ALG/CS mass ratio (formulation F0) and low molecular weight chitosan provided the formulation optimal conditions to obtain polymeric microparticles with smaller mean diameter ( $+18.5 \pm 0.7 \mu\text{m}$ ) and narrower particle size distribution (span =1.4), with negative surface charge ( $-20.8 \pm 7.9 \text{ mV}$ ). However, considering that our proposed microparticulate delivery system must be suitable not only to encapsulate whole live BCG bacteria, but also to target the lung mucosa, positively charged particles are expected to be preferable. Therefore, particle size distribution and particle surface charge were considered altogether, and the 1:1 ALG/CS mass ratio formulation (F14) prepared with chitosan of low molecular weight, with a microparticles' size distribution of  $+25.9 \pm 0.7 \mu\text{m}$  (span =1.7) and positive surface charge ( $+16.2 \pm 0.6 \text{ mV}$ ), was chosen to proceed in formulation optimization studies.

#### 3.1.1.1. *Effect of homogenization method*

Preliminary formulation studies showed that particle size distribution of plain polymeric microparticles prepared with the ionic gelation methods was greatly influenced by the type and time of homogenization. Therefore, different homogenization methods were assessed within four different formulations (F0, F12, F13 and F14), in order to obtain microparticles of desired and consistent size distribution. The effect of high-speed homogenization (ultra-turrax, UT) and ultrasonication (US) used for particles preparation with increasing ALG/CS mass ratios of the final formulation is presented in Table 3.

The homogenization by ultrasonication led to the formation of microparticles within a narrower and smaller size range, with mean diameters between  $10.8 \mu\text{m}$  ("F13\_Low") and  $14.4 \mu\text{m}$  ("F14\_Low"), and high production yields (>80%) (Table 3). When high-speed homogenization was used, the overall mean diameter of the obtained microparticles greatly increased. The use of chitosan of low and high molecular weight resulted in more consistent and reproducible formulation methods, as the size distribution of microparticles with different ALG/CS mass ratios and within the same chitosan molecular weight presented with a narrower size distribution, represented by a lower span.

**Table 3** – Size distribution of polymeric microparticles prepared by high-speed homogenization and ultrasonication, and yield of production.

Formulation_ Chitosan MW	High-speed homogenization			Ultrasonication		
	Particle size, d0.5 (µm)	Span	Yield (%)	Particle size, d0.5 (µm)	Span	Yield (%)
F0_Low	34.5 ± 1.8	6.7 ± 0.5	n.d.	67.8 ± 10.6	5.6 ± 0.9	n.d.
F0_Medium	47.8 ± 2.2	4.1 ± 0.4	n.d.	11.5 ± 3.2	8.8 ± 1.3	n.d.
F0_High	91.8 ± 1.6	3.4 ± 0.1	n.d.	69.5 ± 9.9	6.5 ± 0.8	n.d.
F12_Low	30.2 ± 0.3	3.0 ± 0.0	n.d.	n.d.	n.d.	n.d.
F13_Low	20.4 ± 0.2	2.6 ± 0.0	n.d.	10.8 ± 0.6	6.7 ± 1.9	72.2 ± 0.0
F13_Medium	65.6 ± 1.7	3.5 ± 0.1	n.d.	11.8 ± 0.1	1.6 ± 0.0	97.3 ± 0.9
F13_High	52.9 ± 1.1	2.8 ± 0.0	n.d.	11.2 ± 0.4	4.7 ± 2.4	103.4 ± 2.6
F14_Low	25.2 ± 0.3	3.0 ± 0.0	53.8 ± 0.0	14.4 ± 0.3	1.2 ± 0.0	60.1 ± 10.7

F0, microparticles obtained by Method (I) with modifications, via alginate ionotropic pre-gelation with CaCl<sub>2</sub> followed by chitosan addition; F12-F14, microparticles obtained by Method (II) with modifications, via chitosan pre-gelation with alginate followed by precipitation with 1.0 mg/mL TPP, with ALG/CS mass ratios ranging from 0.6:1 to 1:1. MW, Molecular weight; n.d., not determined.

Taking into consideration the obtained results, and regarding particle size distribution, method consistency and production yield, we selected formulations “F13\_Medium MW chitosan” and “F14\_Low MW chitosan” for further optimization studies. In fact, although ultrasonication proved to be effective in the preparation of plain chitosan-alginate microparticles, our ultimate goal was to encapsulate whole live bacilli of BCG. Since both high shear and ultrasonication are described to compromise cell viability, due to the induced cell integrity loss, we investigated two alternative homogenization methods, namely, simple dispersion with a micropipette, or, alternatively, homogenization in an ultrasound water-bath. Increasing homogenization times were evaluated. The obtained microparticles were characterized in terms of particle size distribution (d0.5 and span) and surface charge (zeta potential) (Table 4).

Particle mean diameter obtained for both formulations was within 12.5 - 21.0 µm range (Table 4). The best results were achieved with simple dispersion (“0 min”) for formulation “F14\_Low” (12.5 ± 0.2 µm; -14.9 ± 0.2 mV) and “20 min” in ultrasound water-bath for formulation “F13\_Medium” (12.6 ± 0.1 µm; +12.1 ± 0.9 mV). The use of the ultrasound allowed to maintain particle size approximated to the desired particle size (10 µm).

Particles were overall negatively charged, as five formulations exhibited negative zeta potential values (-49.8 to -14.1 mV), with formulation “F13\_Medium” being the one exception.

**Table 4** – Size distribution and zeta potential of microparticles prepared by homogenization in an ultrasound water-bath, with increasing homogenization times.

Time (min)	F13_Medium			F14_Low		
	Particle size, d0.5 (µm)	Span	Zeta potential (mV)	Particle size, d0.5 (µm)	Span	Zeta potential (mV)
0	16.3 ± 0.1	2.0 ± 0.2	- 49.8 ± 0.7	12.5 ± 0.2	1.8 ± 0.4	- 14.9 ± 0.2
4	19.4 ± 0.6	2.4 ± 0.2	- 29.6 ± 1.2	15.7 ± 0.2	1.9 ± 0.2	- 19.5 ± 0.7
20	12.6 ± 0.1	2.0 ± 0.2	+12.1 ± 0.9	21.0 ± 0.3	1.6 ± 0.0	-14.1 ± 0.5

F13\_Medium, microparticles of 0.8:1 ALG/CS mass ratio prepared with medium molecular weight chitosan and medium viscosity alginate Protanal™; F14\_Low, microparticles of 1:1 ALG/CS mass ratio that were prepared with low molecular weight chitosan and low viscosity alginate Protanal™. All microparticles obtained via chitosan precipitation with TPP followed by addition of alginate (adapted from *Method III*); *Medium* and *Low* refers to chitosan molecular weight and to alginate viscosity.

Particle size increased with increasing homogenization times, as such: from 12.5 to 21.0 µm to “F14\_Low” (0 to 20 min); from 16.3 to 19.4 µm to “F13\_Medium” (0 to 4 min) (Fig. 9A). Size distribution of microparticles prepared with either 0.8:1 or 1:1 ALG/CS mass ratios, and different chitosan molecular weight, presented with a narrow size distribution (low span) (Fig. 9B), thus indicating a good consistency of the used preparation method. Smaller particle sizes were obtained for F14 formulation at 0 and 4 min, compared to F13, probably due to a more favorable ALG/CS mass ratio, as the 1:1 stoichiometric proportion of functional groups from alginate and chitosan might provide a better interaction and nucleation between polymers, leading to smaller sized particles.

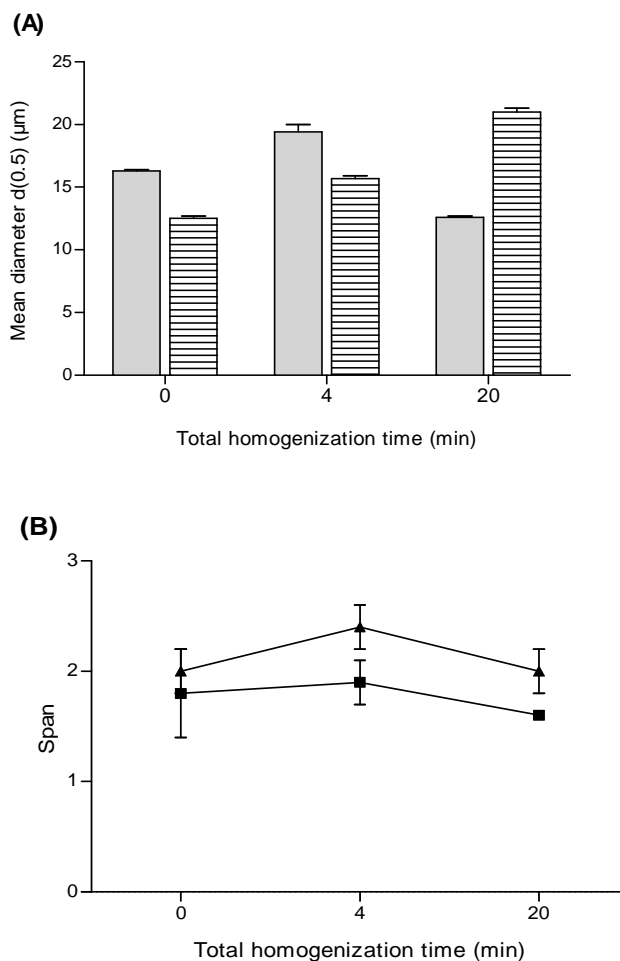


**Figure 9** – (A) Particle size distribution of plain chitosan-alginate microparticles prepared with ALG/CS mass ratio of 0.8:1 (solid) and 1:1 (dashed) and increasing homogenization times of the suspension using an ultrasound water bath. Two different chitosan molecular weight populations are represented: low molecular weight (white columns), and medium molecular weight (grey columns). (B) Particle size distribution span of plain chitosan-alginate microparticles prepared with increasing homogenization times of the suspension of microparticles of 0.8:1 (▲) and 1:1 (■) ALG/CS mass ratio. Results are presented as mean  $\pm$  S.D. (n=3).

### 3.1.1.2. *Effect of alginate type and polymers' addition order*

In order to evaluate the effect of polymers specifications in particle size distribution, three different sets of plain microparticles were prepared using three different commercial brands of low viscosity sodium alginate with distinct G-content, namely: low viscosity sodium alginate of high-G content (65-75%) Protanal™ LF 10/60; ultra-low viscosity sodium alginate of high-G content (63%) Manugel™ LBA; low viscosity sodium alginate of low-G content (40%) Keltone™ LVCR, all approved as pharmaceutical excipient. Chitosan quality specification was kept constant; we used low molecular weight chitosan with a deacetylation degree of 92%. We were also interested in understand whether, by

changing the polymers' addition order, it would be possible to modulate particle surface charge. Therefore, microparticles were prepared according to two different formulation methods - Methods (II) and (III), as previously described (Chapter 2, section 2.2) with modifications. The two methods differ in the addition order of the polymers.

Taking into consideration the aforementioned results obtained for particle size of "F14\_Low" prepared by simple dispersion ( $12.5 \pm 0.2 \mu\text{m}$ ), we decided to use the same homogenization method to prepare these microparticles, by simple dispersion with a micropipette for 1 minute following additions. In Method (II), chitosan and alginate were allowed to interact prior to TPP addition. Briefly, 5.0 mL of 1 mg/mL sodium alginate were dropwise added to 5.0 mL of 1.0 mg/mL chitosan and homogenized for 1 minute, prior to addition of 1.0 mL of 1.0 mg/mL TPP. In Method (III) microparticles were prepared by inducing the pre-gelation of chitosan with TPP, followed by alginate coating, as follows: 5.0 mL of 1.0 mg/mL TPP were dropwise added to 5.0 mL of 1.0 mg/mL chitosan and homogenized for 1 minute, prior to addition of 2.0 mL of 1.0 mg/mL sodium alginate.

The effect of formulation Methods (II) and (III) with decreasing G-content of the sodium alginate polymers used to prepare microparticles is presented in Figure 10. Regarding particle mean diameter (Fig. 10A), microparticles prepared with Method (II) presented a size distribution ( $d_{0.5}$ ) from  $60.9 \pm 5.5 \mu\text{m}$  (Protanal™) to  $89.4 \pm 6.7 \mu\text{m}$  (Manugel™). Changing the polymers' addition order by using Method (III) yielded a particle size distribution with a pronounced decrease in  $d_{0.5}$  values, ranging from  $14.7 \pm 0.6 \mu\text{m}$  (Manugel™) to  $24.0 \pm 1.4 \mu\text{m}$  (Keltone™). No significant differences were observed between alginates of different G-content within the same formulation method ( $P = 0.4634$ ). As for formulation Methods (II) and (III), it was possible to identify a bimodal particle size distribution depending on the used method.

Regarding particle surface charge (Fig. 10B), microparticles prepared with Method (II) presented zeta potential values from  $+14.1 \pm 0.6 \text{ mV}$  (Protanal™) to  $-16.3 \pm 1.3 \text{ mV}$  (Keltone™), whereas microparticles prepared with Method (III) presented lower zeta potential values reaching  $-29.6 \pm 0.9 \text{ mV}$  for Keltone™, thus, suggesting a different reorganization of the chitosan-alginate matrix when chitosan was allowed to form a pre-gel with TPP.

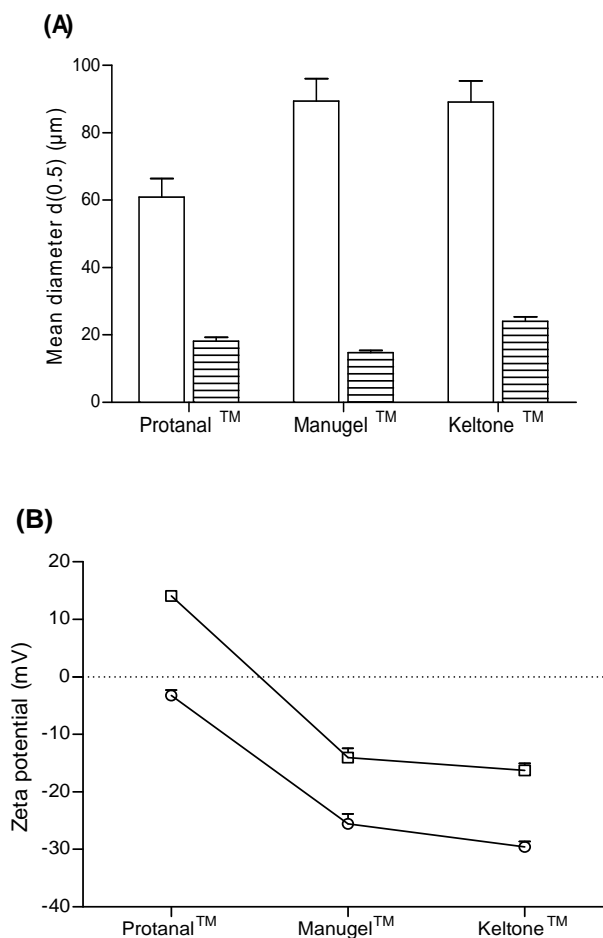


**Figure 10** – (A) Particle size distribution of plain chitosan-alginate microparticles of 1:1 ALG/CS mass ratio, prepared with chitosan of low molecular weight and alginates of decreasing G-content, according to Method (II) (solid) and Method (III) (dashed). (B) Zeta potential of plain chitosan-alginate microparticles of 1:1 ALG/CS mass ratio, prepared with chitosan of low molecular weight and alginates of decreasing G-content, according to Method (II) ( $\square$ ) and Method (III) ( $\circ$ ). Results are presented as mean  $\pm$  S.D. ( $n=3$ ).

These results were important to put into evidence that the addition order of the polymers plays an important role in the formation of chitosan-alginate microparticles. So far, it seems that ALG/CS mass ratio, homogenization method, and addition order of the polymers, have greater impact in particle size distribution and surface charge, than the herein assessed G-content of sodium alginate. Since Method (III) enabled the formation of microparticles with inferior mean diameter, within a more stable colloidal suspension (as  $\pm 30$  mV can be an indicator of particulate systems' stability), it was chosen as the formulation method for the following optimization studies.

### 3.1.1.3. *Effect of pH value*

It is well established that an ionic complex between alginate and chitosan is formed due to interactions between the carboxyl groups of alginate with the amino groups of chitosan.<sup>34,66,80,81</sup> The cationic nature of chitosan ( $pK_a \approx 6.5$ ) is conveyed by the positively charged  $-NH_3^+$  groups, whereas the anionic nature of alginate ( $pK_a \approx 3.4-3.7$ ) results from the presence of  $-COO^-$  groups. The cationic nature of chitosan leads to the protonation of the amino groups in acidic to neutral solution, with charge density depending on pH and chitosan deacetylation degree. These features contribute to the solubility of chitosan in aqueous acidic solutions. Furthermore, it is key for chitosan's bioadhesiveness, since chitosan's protonated amino groups readily bind to negatively charged surfaces such as mucosal membranes, and for the enhancement of polar drugs' transport across epithelial surfaces.

In order to assess the effect of pH value on microparticle formation, several sets of microparticles from formulation "F14\_Low" (ALG/CS mass ratio of 1:1, w/w) were prepared using 1.0 mg/mL solutions of low molecular weight 92% deacetylated chitosan, and low viscosity and high-G content sodium alginate (Protanal™ LF 10/60), with pH ranging from 3.0 to 7.0. Briefly, 2.0 mL of 1.0 mg/mL TPP were dropwise added to 5.0 mL of 1.0 mg/mL chitosan (pH 3.0 to 6.0) and homogenized for 10 minutes in an ultrasound water-bath, prior to addition of 5.0 mL of 1.0 mg/mL sodium alginate (pH 3.0 to 7.0). The obtained suspensions were characterized for particle size distribution, surface charge, and yield of production (Table 5).

The use of both alginate and chitosan solutions with a pH value below 5.0 resulted in increased particle size (15 to 44  $\mu m$ ) and particle aggregation (Table 5). Aggregation also occurred when chitosan solution pH was beyond 6.0 (data not shown), due to the loss of chitosan solubility, as chitosan has a  $pK_a$  value of  $\approx 6.5$ . Considering the desired particle size distribution (i.e. particle mean diameter of approximately 10  $\mu m$ , and narrow span), the optimal size distributions were obtained when chitosan solution pH was within 5.0 to 6.0, and alginate solution pH within 4.0 to 6.4, leading to the formation of 10-12  $\mu m$  sized ( $d_{0.5}$ ) microparticles. Within this pH range, the carboxyl groups of alginate are ionized, and the amine groups of chitosan are protonated, thus, favouring the optimum interaction for the polyionic complex formation. All these formulations presented a negative particle surface charge (Table 5).

**Table 5** – Effect of pH on particle size distribution, particle surface charge, and yield of production of microparticles prepared with alginate to chitosan mass ratio of 1:1 (F14\_Low).

ALG pH	CS pH	F14 pH	Particle size, d0.5 (µm)	Span	Zeta potential (mV)	Production yield* (w/w) (%)	Aggregates
3.0	3.0	3.3	44.2 ± 0.9	1.5 ± 0.0	+8.7 ± 0.1	6.4%	Yes
4.0	3.0	3.6	31.3 ± 0.3	31.0 ± 16.3	+3.7 ± 0.0	12.5%	Yes
5.0	3.0	3.9	16.1 ± 0.1	1.3 ± 0.0	-3.5 ± 0.0	11.7%	
6.4	3.0	4.0	15.2 ± 0.2	1.4 ± 0.1	-4.6 ± 0.0	17.8%	
7.0	3.0	4.0	18.0 ± 0.4	1.3 ± 0.0	-2.3 ± 0.0	n.d.	
3.0	4.0	4.1	43.8 ± 1.0	1.5 ± 0.0	+1.8 ± 0.0	16.9%	Yes
4.0	4.0	4.3	19.0 ± 0.8	1.7 ± 0.0	-4.9 ± 0.0	11.7%	Yes
5.0	4.0	4.5	13.0 ± 0.3	2.0 ± 0.1	-7.3 ± 0.1	13.6%	
6.4	4.0	4.6	13.2 ± 0.7	1.7 ± 0.0	-6.2 ± 0.1	11.9%	
7.0	4.0	4.6	15.8 ± 0.4	1.8 ± 0.0	-13.4 ± 0.1	18.3%	
3.0	5.0	4.9	12.9 ± 0.5	6.3 ± 1.2	-16.3 ± 0.0	10.4%	
4.0	5.0	5.0	12.1 ± 0.4	3.1 ± 0.5	-14.8 ± 0.0	11.4%	
5.0	5.0	5.3	11.4 ± 0.3	3.6 ± 0.5	-18.6 ± 0.1	6.7%	
6.4	5.0	5.4	10.9 ± 0.4	2.7 ± 0.4	-18.9 ± 0.1	11.4%	
7.0	5.0	5.4	11.8 ± 0.3	2.8 ± 0.4	-17.8 ± 0.1	10.6%	
3.0	6.0	5.7	11.5 ± 0.2	5.2 ± 0.3	-22.4 ± 0.1	8.3%	
4.0	6.0	6.3	10.0 ± 0.7	7.1 ± 0.8	-23.7 ± 0.2	14.2%	
5.0	6.0	7.2	11.9 ± 0.3	4.9 ± 0.3	-26.3 ± 0.1	14.6%	
6.4	6.0	7.5	11.4 ± 0.2	3.3 ± 0.4	-25.7 ± 0.1	n.d.	
7.0	6.0	7.6	13.8 ± 0.3	2.3 ± 0.0	-21.8 ± 0.2	n.d.	

F14, microparticles obtained using formulation Method (III) with low molecular weight / 92% deacetylation degree chitosan (CS), and low viscosity / high-G sodium alginate (ALG) (Protanal™ LF 10/60). Results are expressed as mean and standard deviation (n ≥ 3). \*Production yield was determined using gravimetric determination of particles' mass following lyophilisation, and it is expressed as mass percentage (w/w), referred to particles theoretical mass. n.d., not determined.

The best system was obtained with formulation's final pH value of 5.4, with particle mean diameter of  $10.9 \pm 0.4 \mu\text{m}$ , a 2.7 span, and negative surface charge (-18.9 mV) (Table 5). These particles were prepared with chitosan solution at pH=5.0 and alginate solution pH=6.4. Although it is well known that the pH-dependent interaction between alginate and chitosan leads to the formation of stronger complexes at pH value around 4.5–5.0, it is also described that the amine groups of chitosan ( $\text{pK}_a \approx 6.5$ ) have more affinity to alginate mannuronic acid (M) residues ( $\text{pK}_M \approx 3.38$ ) than to guluronic acid (G) residues ( $\text{pK}_G \approx 3.65$ ).<sup>35</sup> Since we used a high-G content ( $\approx 70\%$ ) alginate (Protanal LF™ 10/60), overall alginate  $\text{pK}_a$  is closer to 3.65. This might explain why microparticles of lower mean diameter ( $10.9 \pm 0.4 \mu\text{m}$ ) and narrower size distribution (span = 2.7) were obtained

with formulation's final pH of 5.4. In fact, at this pH range, the high protonation degree of chitosan's amino groups prompts a high extent reaction with alginate's carboxyl groups, leading to the formation of stable particles. We would expected that maximum ionic interaction occurs at a slightly inferior pH for high-M content alginates (such as  $\approx 60\%$  M-content Keltone™ alginate).

The production yield was very low ( $<17\%$ ) for all formulations when determined by gravimetry (Table 5). This is probably related to a low responsiveness of the gravimetric method for the determined mass range, as mass variations occurred within sub-milligram or micro-range. For that reason, the previously described method based on the quantification of chitosan concentration for the determination of the yield of production of microparticles (section 2.4.2) was selected for further studies. The results obtained were analysed from the comparison perspective between different pH conditions.

The effect of polymers' pH on particle size and surface charge is represented in Figure 11. Regarding zeta potential results, microparticles prepared with the majority of pH combinations were negatively charged (Fig. 11B). This is probably due to the contribution of alginate carboxyl groups to the negative net surface charge, therefore suggesting that Method (III) provides the arrangement of the polymeric matrix in such way that alginate somehow outers the chitosan particulate core.

The relation between particle size and surface charge with increasing formulation final pH is depicted in Figure 12. It can be observed that particle mean diameter is significantly higher for microparticle suspensions with final pH  $\leq 4.3$ . At this pH range alginate approaches its pKa values, and a significant part of alginate starts aggregating and precipitating, which might have contributed to the increased particle mean diameter.

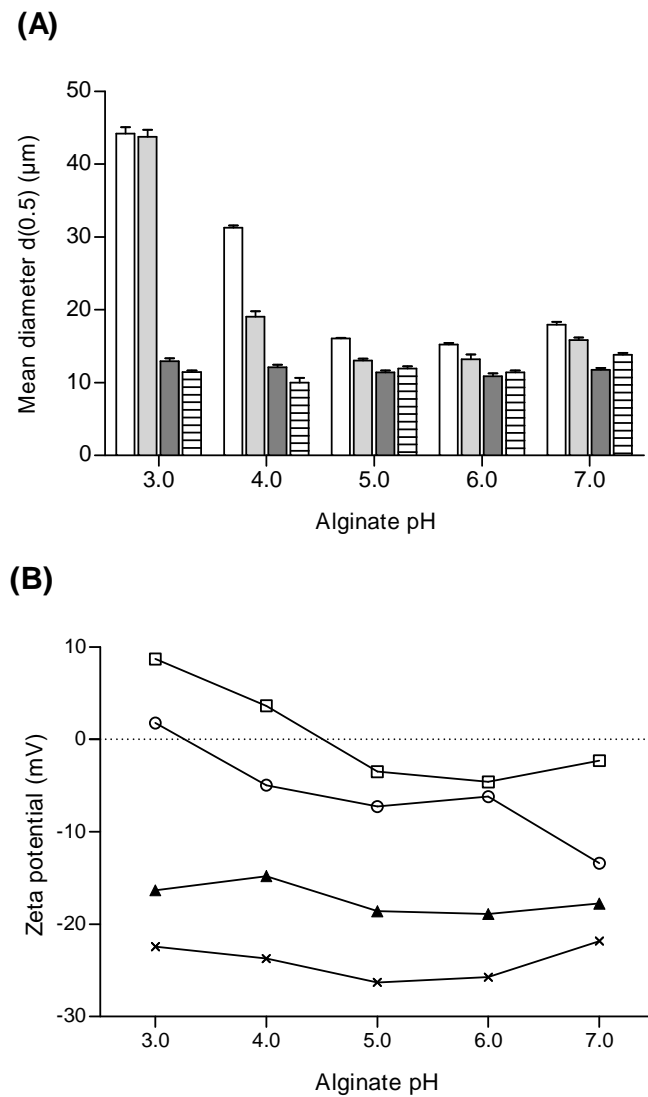


**Figure 11** – Characterization of plain chitosan-alginate microparticles of 1:1 ALG/CS mass ratio (“F14\_Low”) with increasing pH of alginate solution. (A) Particle size distribution, with four different pH populations represented for chitosan: pH 3.0 (white columns), pH 4.0 (light grey columns), pH 5.0 (dark grey columns), and pH 6.0 (dashed). (B) Zeta potential of microparticles, with four different pH populations represented for chitosan: pH 3.0 ( $\square$ ), pH 4.0 ( $\circ$ ), pH 5.0 ( $\blacktriangle$ ), and pH 6.0 ( $\times$ ). Results are presented as mean  $\pm$  S.D. (n=3).

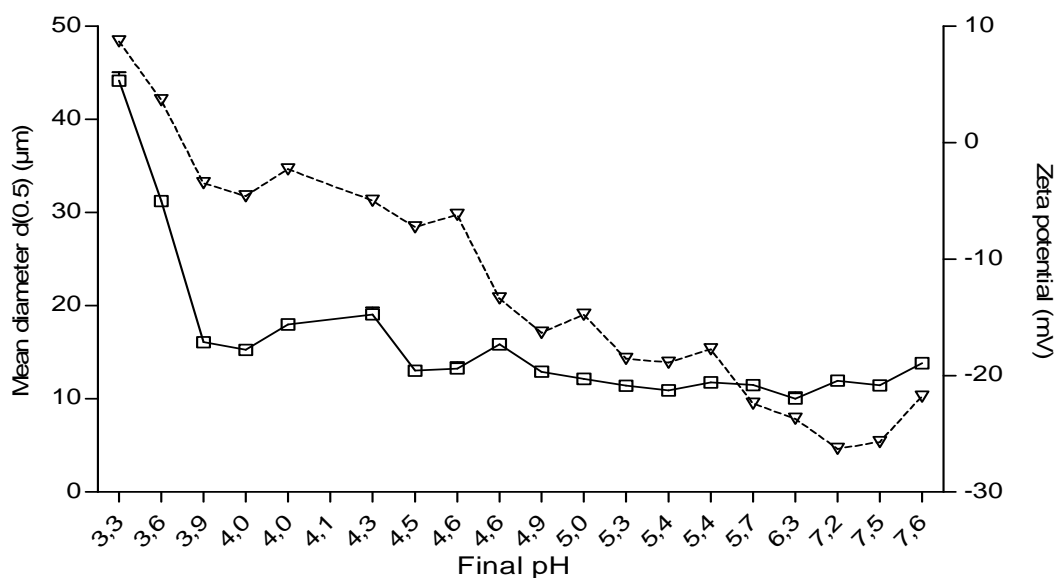


**Figure 12** – Characterisation of particle mean diameter (d0.5) (□) and surface charge (zeta potential) (▽) with increasing final pH of the microparticles formulation.

#### 3.1.1.4. Effect of the addition of cryoprotectants

Table 6 summarizes the different batches of plain “F14\_Low” microparticles prepared with two concentrations (5% and 10%, w/v) of three different cryoprotectants.

**Table 6** – Characterization of batches of plain polymeric microparticles prepared with cryoprotectants sucrose, glucose, or trehalose.

Batches	Cryoprotectant % (w/v)	ALG:CS:cryoprotectant mass ratio (w/w)
A	-	1:1:0
B	Sucrose 5%	1:1:120
C	Sucrose 10%	1:1:240
D	Glucose 5%	1:1:120
E	Glucose 10%	1:1:240
F	Trehalose 5%	1:1:120
G	Trehalose 10%	1:1:240

Microparticles were prepared according to Method III with modifications, as follows: 2.0 mL of 1.0 mg/mL TPP (pH=8.7) were dropwise added to 5.0 mL of 1.0 mg/mL low molecular weight and 92% deacetylation degree chitosan (pH=4.1) and homogenized for 2 minutes in an ultrasound water-bath, prior to addition of 5.0 mL of 1.0 mg/mL low viscosity / high-G sodium alginate (Protanal™ LF 10/60) (pH 6.7) and additional homogenization for 2 minutes in an ultrasound water-bath. Then, 0.6 or 1.2 mL of 1.0

g/mL of cryoprotectant solution, consisting of sucrose, glucose, or trehalose, were added to the microparticle suspension. Samples were prepared in triplicate.

Particle size distribution and zeta potential of samples were assessed as previously described, for samples without cryoprotectant (batch A) and samples with cryoprotectant (batches B to G), both prior to and after freeze-drying. The obtained results are summarized in Table 7 and Figure 13.

**Table 7** – Characterization of chitosan-alginate microparticles (formulation “F14\_Low”) batches without (batch A) and with (batches B to H) cryoprotectants addition, on production day and following freeze-drying.

Batches	Before freeze-drying			After freeze-drying	
	Particle size ( $\mu\text{m}$ )		Zeta potential (mV)	Particle size ( $\mu\text{m}$ )	
	d0.5	Span		d0.5	Span
A	13.3 $\pm$ 1.0	3.1 $\pm$ 2.3	-19.5 $\pm$ 0.7	170.6 $\pm$ 50.8	2.6 $\pm$ 0.3
B	13.6 $\pm$ 0.2	1.8 $\pm$ 0.5	+14.9 $\pm$ 0.3	93.5 $\pm$ 15.6	2.3 $\pm$ 0.1
C	13.2 $\pm$ 1.1	1.4 $\pm$ 0.1	n.d.	65.5 $\pm$ 7.3	2.0 $\pm$ 0.2
D	12.9 $\pm$ 0.0	1.8 $\pm$ 0.0	n.d.	54.1 $\pm$ 9.9	1.9 $\pm$ 0.3
E	13.5 $\pm$ 2.0	2.0 $\pm$ 0.7	+11.6 $\pm$ 1.2	47.1 $\pm$ 8.3	2.4 $\pm$ 0.2
F	13.2 $\pm$ 0.4	1.8 $\pm$ 0.3	+13.3 $\pm$ 0.5	81.9 $\pm$ 15.5	2.0 $\pm$ 0.1
G	12.1 $\pm$ 0.6	1.4 $\pm$ 0.1	n.d.	63.7 $\pm$ 4.5	2.0 $\pm$ 0.3

Results are presented as mean  $\pm$  S.D. (n=3); n.d., not determined.

The addition of cryoprotectants appears to have contributed to modify particle surface charge (Table 7), as microparticles with no cryoprotectant (batch A) presented negative zeta potential values (-19.5  $\pm$  0.7 mV), thus, being negatively charged, whereas microparticles prepared with cryoprotectants (batches B, E and F, for 5% sucrose, 10% glucose and 5% trehalose, respectively) presented a positive surface charge, with zeta potential values between +11.6  $\pm$  1.2 mV and +14.9  $\pm$  0.3 mV. This is probably due to the adsorption of the molecules to the surface. It has been described that slightly acidic sucrose and glucose generate a good isotonic medium (in terms of electrostatic stability) for negatively charged particles, but for positively charged particles, as in case of “F14\_Low”, these additives reverse zeta potential.<sup>82</sup>

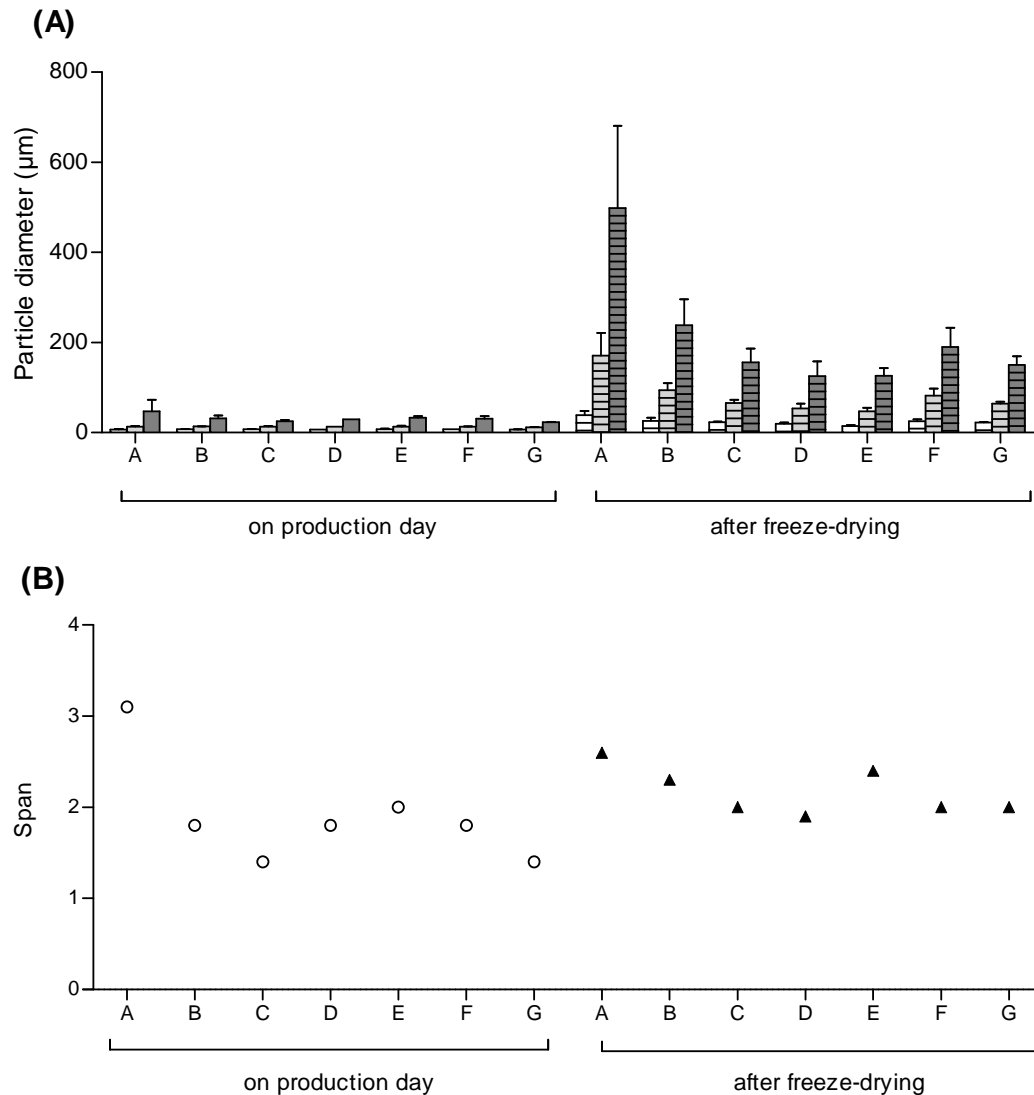


**Figure 13** – Particle size distribution and span of “F14\_Low” particles without cryoprotectant (batch A), as well as of “F14\_Low” particles prepared with 5% or 10% sucrose (batches B and C), 5% or 10% glucose (batches D and E), or 5% or 10% trehalose (batches F and G). (A) Particle size distribution on production day (no fill) and after freeze-drying (horizontal lines). Three different particle size populations are represented: d0.1 (white columns), d0.5 (light grey columns) and d0.9 (dark grey columns). Results are presented as mean  $\pm$  S.D. (n=3). (B) Size distribution span on production day ( $\circ$ ) and after freeze-drying ( $\blacktriangle$ ). Results are presented as mean (n=3).

Regarding particle mean diameter, it was within micrometer range for all prepared batches (Table 7). With samples analyzed before freeze-drying (on production day), it was possible to observe that there were no significant differences concerning particle size distribution (Fig. 13A). All batches presented similar size distributions, with average d0.5 values of  $13.1 \pm 0.5 \mu\text{m}$ , thus, suggesting that addition of cryoprotectants didn't influence particle size for batches prepared under the same conditions.

However, after freeze-drying, particle size distribution profile changed and all batches presented up to 10-fold increased  $d_{0.5}$  values (Fig. 13A), indicating a noteworthy increase of particle mean diameter, probably due to the formation of larger particles or particle aggregates. This could also be seen in the exacerbation of the  $d_{0.9}$  populations for all samples after freeze-drying. Nevertheless, the addition of cryoprotectants did prevent some aggregation following freeze-drying, as batch A (particles with no cryoprotectant) presented the highest particle mean diameter, with approximately 2-fold higher  $d_{0.5}$  values referred to batches where cryoprotectant had been added (batches B-G).

As for particle size distribution width, the obtained low span values ( $2.0 \pm 0.5 \mu\text{m}$ , in average) (Fig. 13B) revealed a high similitude in particle size distribution, thus, suggesting that microparticles preparation was reproducible. Microparticles prepared with 5% and 10% glucose (batches D and E, respectively) performed best, with lower  $d_{0.5}$  values and low span values, thus, corresponding to particles with a smaller, and narrow, particle size distribution.

It can be concluded that microparticle suspensions were affected by the nature and concentration of cryoprotectants, with 10% glucose cryoprotectant (batch E) showing better properties after freeze-drying, with smaller particle size, low span and average zeta potential positive value, compared to microparticles with no cryoprotectant (batch A). Future studies must be conducted with cryoprotectants in order to optimize particle size distribution and surface charge, so that physicochemical stability of microparticles after freeze-drying can be ensured.

### *3.1.2. Polymer-polymer interaction by FT-IR analysis*

Formation of microparticles of chitosan with alginate is a result of strong interactions by hydrogen bonds between the functional groups of the polymers in which amino and amide groups present in chitosan take part. As a result, there are changes in the FT-IR spectra in the absorption bands of the amino groups, carboxyl groups, and amide bonds.<sup>34</sup> Based on the identification of absorption bands concerned with the vibrations of functional groups present in CS and ALG macromolecules,<sup>83</sup> FT-IR analysis was able to illustrate changes in the wave number and absorbance in the region of amino and amide group vibrations with increasing pH of the microparticle suspension (Fig. 14).

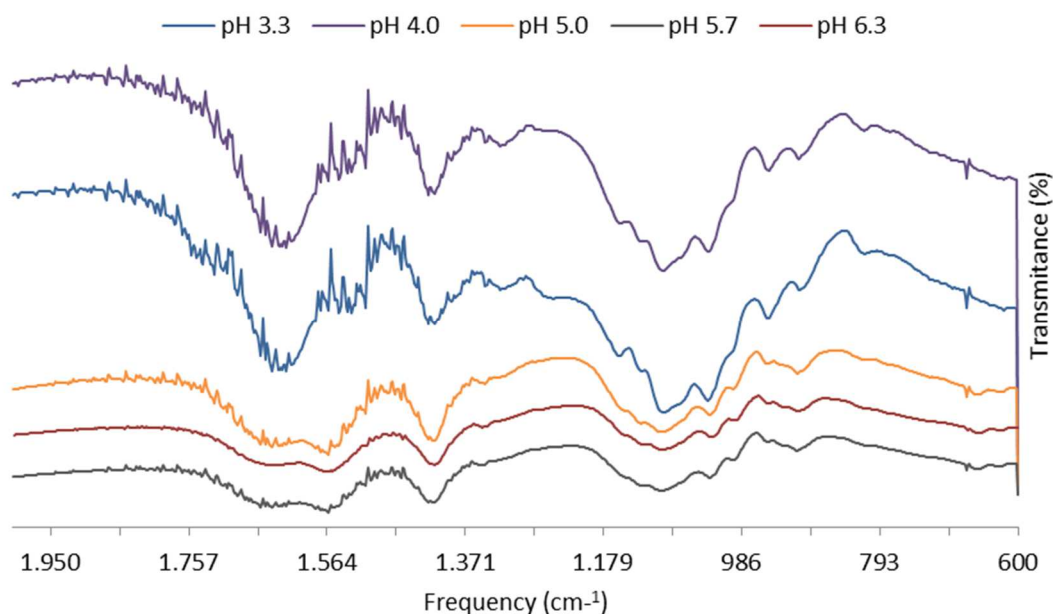


**Figure 14** – FT-IR spectra of plain chitosan-alginate “*F14\_Low*” microparticles (1:1 ALG/CS mass ratio) with increasing pH of the microparticles suspension. Bands wave numbers ( $\text{cm}^{-1}$ ) are as follows: 1641 (amide bond), 1613 (symmetric  $\text{COO}^-$  stretching vibration), 1569 (strong protonated amino peak – from partial N-deacetylation of chitin), and 1415 (asymmetric  $\text{COO}^-$  stretching vibration).

The FT-IR spectrum of microparticles produced with final pH of 4 and 5.7 reveals alginate carboxyl peaks slightly shift from of 1613 and 1415  $\text{cm}^{-1}$  to 1609 and 1414  $\text{cm}^{-1}$ , respectively, after complexation with chitosan. Chitosan both peaks were similarly shifted by few  $\text{cm}^{-1}$  after complexation with alginate, with the amide peak from 1641 into singlet band at 1609  $\text{cm}^{-1}$ , and the amino peak from 1559 to 1533  $\text{cm}^{-1}$  or 1560  $\text{cm}^{-1}$  at pH 4 and 5.7, respectively. The observed changes in the absorption bands of the amino groups, carboxyl groups, and amide bonds can be attributed to an ionic interaction between the carbonyl group of alginate and the amino group of chitosan. The peak absorbance of amino groups of chitosan at 1153  $\text{cm}^{-1}$  was also present after complexation, thus, suggesting an effective interaction between polymers at pH 4 and 5.7.

### 3.1.3. Surface morphology

Microparticle morphology was characterized by microscopy. Both F13 and F14 microparticles presented regular and smooth surfaces related to a generic spherical shape (Fig. 15). Additionally, particle size distribution observed in microscopic images was consistent with that obtained by laser diffraction, revealing homogeneous populations of narrow particle size distribution (Fig. 16).

Considering the results obtained during formulation optimization studies, *F14\_Low* formulation, produced with 1mg/mL low MW chitosan (pH=5.0) and 1 mg/mL Protanal™ sodium alginate (pH=6.4), and ‘simple dispersion’ method was chosen for further BCG encapsulation, so that a suitable formulation of BCG-loaded microparticles can be developed and further assessed in immunization studies. This formulation was chosen because it allowed the formation of microparticles of suitable mean diameter and surface charge without aggregation, under mild conditions and few steps, critical for future sterile production during vaccine production.

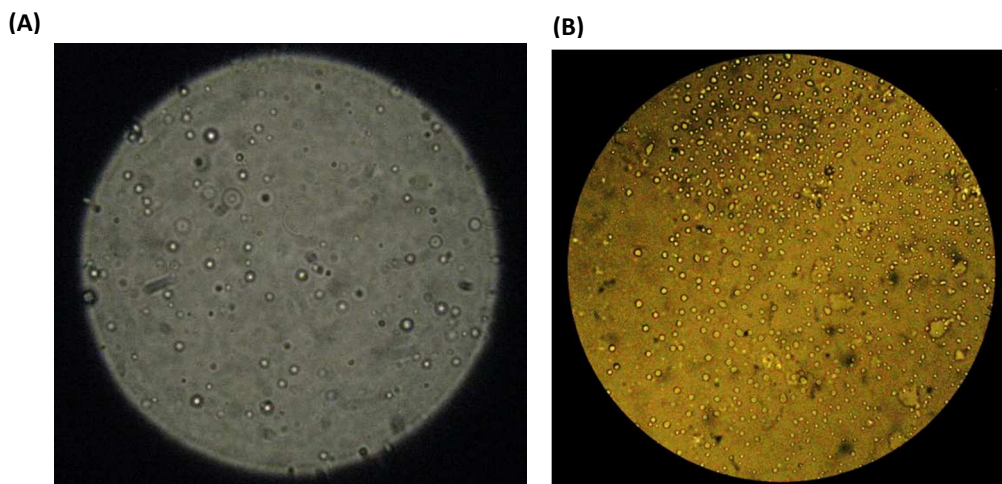


**Figure 15** – (A) Polarized light micrograph (100x) of “*F13\_Medium*” microparticles (0.8:1 ALG/CS) prepared according to Method (III) with chitosan of medium molecular weight. (B) Contrast phase micrograph (40x) of “*F14\_Low*” microparticles (1:1 ALG/CS) prepared according to Method (II) with chitosan of low molecular weight.

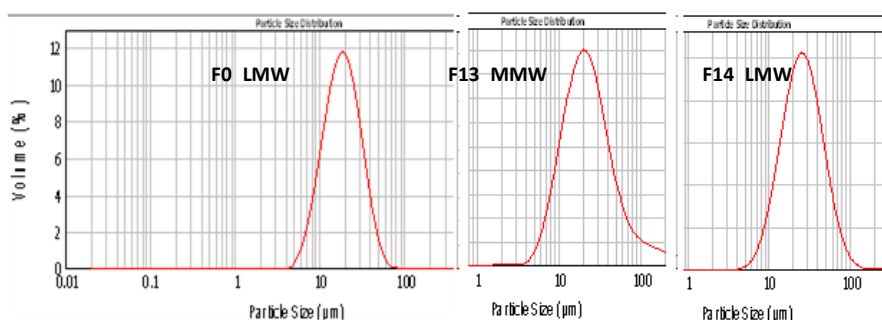


**Figure 16** – Particle size distribution of microparticles produced with alginate to chitosan ratio of 4.23:1 (F0), 0.8:1 (F13), and 1:1 (F14). F0 microparticles prepared according to Method (I) by alginate ionotropic pre-gelation with CaCl<sub>2</sub> followed by chitosan coating; F13-F14 microparticles prepared according to Method (III) by chitosan pre-gelation with TPP followed by alginate coating; LMW, low molecular weight chitosan; MMW, medium molecular weight chitosan; HMW, high molecular weight chitosan.

### 3.1.4. Association efficiency

The ability of chitosan/alginate microparticles to encapsulate/adsorb *Mycobacterium bovis* BCG depends to a great extent on bacteria surface charge. Therefore, zeta potential of heat inactivated *Mycobacterium bovis* BCG Pasteur and rBCG-GFP strains was measured at low electrolyte concentration following suspension in different media. An additional suspension of BCG in 0.9% NaCl was inactivated by formaldehyde exposition. The obtained results are summarized in Table 8 and Figure 17.

**Table 8** – Surface charge of inactivated *Mycobacterium bovis* BCG (strains Pasteur and rBCG-GFP) bacilli suspended in different media. Results are presented as mean  $\pm$  S.D. (n=3).

Inactivation method	Medium	Zeta potential (mV)	
		BCG Pasteur	rBCG-GFP
Temperature (80°C, 15')	H <sub>2</sub> O	-39.3 $\pm$ 1.0	-32.6 $\pm$ 1.0
	Cell culture medium	-27.9 $\pm$ 2.7	-21.2 $\pm$ 2.5
	10 mM PBS	-20.4 $\pm$ 1.5	-13.7 $\pm$ 1.4
	0.9% NaCl	-29.9 $\pm$ 11.5	-23.1 $\pm$ 11.0
	0.025% low MW chitosan	+83.9 $\pm$ 3.5	+90.6 $\pm$ 3.5
	0.1% low MW chitosan	+85.7 $\pm$ 12.1	+92.4 $\pm$ 11.9
Formaldehyde (0.5 %, 24h)	0.9% NaCl + formol	-12.5 $\pm$ 2.7	-5.8 $\pm$ 6.0

Both BCG Pasteur and rBCG-GFP bacilli presented predominantly negative zeta potential values, thus, indicating they have electronegative groups at their surface. Overall, the surface charge of BCG Pasteur appears to be only slightly more electro-negative than rBCG-GFP's for all tested conditions. A different macroscopic behavior of cell suspension was also distinguished - BCG Pasteur's suspension formed a fluffy surface layer, which originated partial and ephemeral aggregation; this phenomena was not observed for rBCG-GFP strain.

The nature of the adsorbing species on the cell surface of the two strains might explain the obtained variations. The negative surface charge for cells of all *Mycobacterium* BCG species arises from the phosphate groups of phosphodiester linkages between the peptidoglycan and the arabinogalactan of the basic cell wall structure which is common

to all species of Mycobacteria.<sup>84</sup> Some hydrophobic interaction involving lipid within the surface may also be involved, since the mycobacterial cell envelope is a lipid-rich complex structure that surrounds the bacillus and is thought to play a critical role in the pathogenicity of *Mycobacterium tuberculosis*. A large number of mycobacterial lipoproteins have been suggested to be important components for the synthesis of the mycobacterial cell envelope, as well as for sensing processes, protection from stressful factors and host-pathogen interactions.<sup>84</sup>

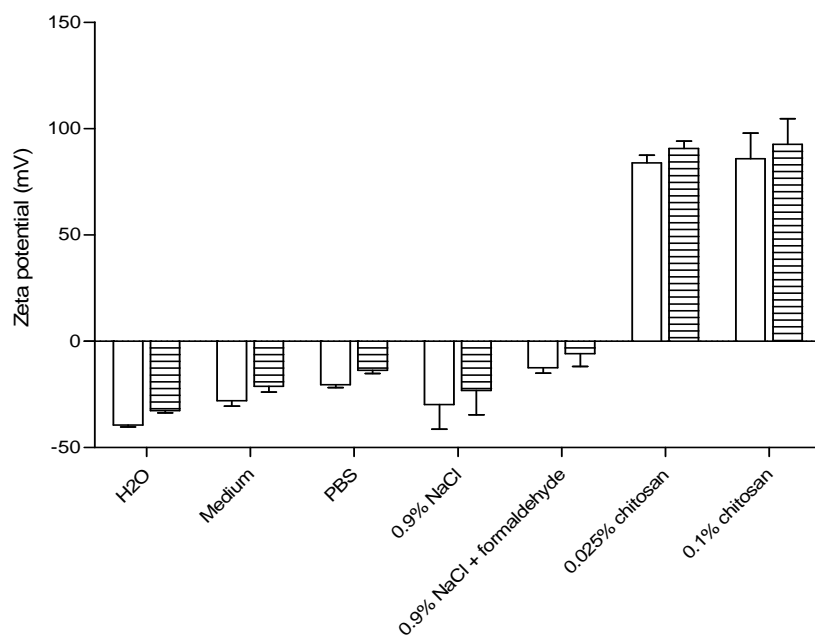


**Figure 17** – Surface charge of inactivated BCG Pasteur (solid) and rBCG-GFP (dashed) following dispersion in different media. Results are presented as mean ± S.D. (n=3).

Zeta potential profiles showed no major differences between bacilli suspension in either 0.9% NaCl, water, 10 mM PBS, or cell culture medium. However, when BCG bacilli from either strains were suspended in low molecular weight chitosan, an inversion of zeta potential values occurred, in a concentration dependent fashion, suggesting that the mechanism of association of the bacteria to chitosan is, at least partially, mediated by ionic interaction between bacilli and chitosan. Other mechanisms, such as hydrophobic interactions, might also be involved in bacteria microencapsulation.

As for the inactivation method, heat killed strains presented a marked electro-negative surface charge ( $-29.9 \pm 11.5$  mV for BCG Pasteur, and  $-23.1 \pm 11.0$  mV for rBCG-GFP), whereas formaldehyde-exposed strains exhibited an attenuated surface charge, with zeta potential values of  $-12.5 \pm 2.7$  mV for BCG Pasteur and  $-5.8 \pm 6.0$  mV for rBCG-GFP. This effect might be due to formaldehyde interaction with cell surface amino groups, inducing nonspecific crosslinkage that will decrease the number of available

ionisable groups, thus, slightly increasing zeta potential. Since bacilli of BCG Pasteur are negatively charged, we assumed it would be well suspended in chitosan.

Taking into consideration the abovementioned, we hypothesised that the greatest encapsulation/association efficiency for *M. bovis* BCG would be obtained by suspending BCG bacteria in chitosan at a pH below its pKa (e.g. pH=5), so that the polymer is predominantly positively charged. Additionally, we chose to entrap monodisperse bacteria in chitosan microparticles by means of controlled gelation of chitosan with TPP followed by alginate addition. This way we aimed to achieve good association efficiency.

As such, BCG-loaded “F14\_Low” microparticles (1:1 ALG/CS mass ratio) were prepared as previously described (section 2.3.3), by Method (II) or Method (III), with low viscosity sodium alginate Protanal™ LF 10/60 (high-G content) and low molecular weight chitosan (92% deacetylation degree). Table 9 summarizes the different batches of BCG-loaded “F14\_Low” microparticles that were prepared.

**Table 9** – Characterization of batches of BCG-loaded “F14\_Low” microparticles prepared with increasing concentrations of BCG.

Batches	Formulation method	BCG Pasteur load (CFU/mL)
A	II	-
B	II	1.7E+06
C	II	8.3E+06
D	II	1.7E+07
E	II	3.3E+07
F	III	-
G	III	1.7E+06
H	III	8.3E+06
I	III	1.7E+07
J	III	3.3E+07
K	--	7.1E+06

Preliminary formulation studies revealed that particle size distribution and surface charge were influenced by polymer to polymer mass ratio and formulation method. Whether BCG microencapsulation would have a great impact on microparticles features was uncertain, thus these parameters were investigated. The association efficiency was also determined. The obtained results are depicted in Table 10 and Figure 19.

**Table 10** – Particle size distribution, surface charge and association efficiency of BCG-loaded “F14\_Low” microparticles.

Batches	Particle size, d(0.5) (µm)	Span	Zeta potential (mV)	A.E. (%)
A	60.9 ± 5.5	3.0 ± 5.5	14.1 ± 0.6	--
B	35.3 ± 2.6	1.8 ± 0.1	10.5 ± 1.5	70.0 ± 1.6
C	39.3 ± 3.9	2.8 ± 1.8	12.9 ± 2.3	74.0 ± 3.9
D	41.0 ± 6.3	2.2 ± 0.1	11.8 ± 2.5	85.0 ± 4.8
E	36.8 ± 2.0	2.0 ± 0.2	13.0 ± 3.9	87.0 ± 3.4
F	18.2 ± 1.2	3.2 ± 0.7	-3.2 ± 0.9	--
G	22.2 ± 1.0	6.5 ± 2.6	-16.4 ± 2.1	--
H	28.3 ± 4.0	25.5 ± 12.3	-12.7 ± 2.4	76.0 ± 1.4
I	22.5 ± 2.7	4.0 ± 2.8	-13.7 ± 2.0	84.0 ± 3.4
J	21.4 ± 2.4	2.5 ± 0.4	-12.2 ± 2.6	83.0 ± 10.7
K	28.4 ± 1.9	3.2 ± 0.0	--	--

Regarding particle surface charge, two different patterns were obtained, depending on the formulation method (Fig. 18B). Method (II) originated microparticles (both plain and BCG-loaded) that were positively charged, with zeta potential values from  $+10.5 \pm 1.5$  mV to  $+14.1 \pm 0.6$  mV, whereas Method (III) originated negatively charged microparticles (both plain and BCG-loaded), with zeta potential values from  $-3.2 \pm 0.9$  mV to  $-16.4 \pm 2.1$  mV. In comparison to plain microparticles, BCG-loaded microparticles presented lower zeta potential values regardless of the used formulation method (Fig. 18B). These results indicate that negatively charged BCG bacilli is present, thus, indicating that encapsulation/adsorption occurred.

The association of BCG Pasteur to microparticles was efficient (70-87% A.E.) and in a concentration dependent fashion, regardless of the used formulation method (Fig. 18C). The association mechanism, however, is not determined. Due to the extremely high content of complex lipids present in the BCG's cell wall, it is extremely difficult and challenging to achieve efficient, uniform and reproducible microencapsulation experiments. Therefore, we accept that BCG bacilli are sometimes microencapsulated and other times just adsorbed due to partial and irregular adsorption onto the microparticle surface.

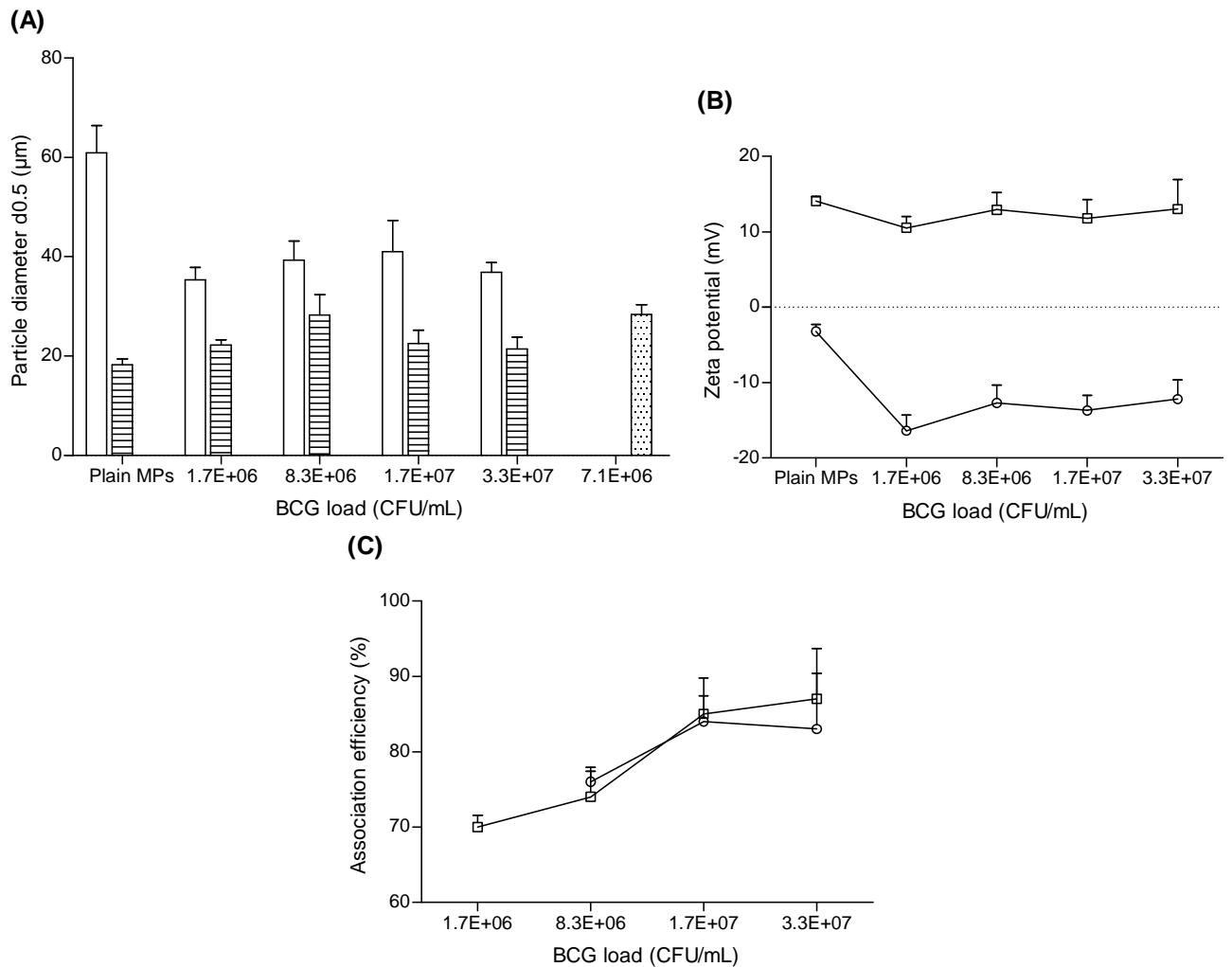


**Figure 18** – Characterisation of “F14\_Low” microparticles with increasing BCG load. (A) Particle size (d0.5) of microparticles prepared according to Method (II) (solid) or Method (III) (dashed), and plain BCG (dotted). (B) Particle surface charge, and (C) association efficiency, of microparticles prepared according to Method (II) (□) or Method (III) (○). Results are presented as mean ± S.D. (n=3).

Although these encouraging results, further studies are required to better understanding of how does the formulation method influences the microencapsulation of BCG. For instance, it is expected that the introduction of monodisperse bacilli into chitosan-alginate microparticles will originate small shifts on FT-IR spectra. As such, FT-IR analysis of BCG-loaded microparticles can be performed to elucidate how BCG interacts with the polymers and with the microparticles, as result of either bacilli entrapment or adsorption onto microparticles. Moreover, scanning electron microscopy (SEM) studies can also be performed in the future so that the interaction of BCG bacilli with the chitosan-alginate microparticles can be further elucidated.

### 3.1.5. BCG cell viability

Chitosan is described as having antimicrobial potential.<sup>57,58,60</sup> Whether BCG suspension in chitosan would compromise BCG cell viability was uncertain. Therefore, BCG cell viability following suspension in chitosan was investigated over time by a colony-forming units (CFU) assay, as previously described (section 2.3.4). Both strains BCG Pasteur and rBCG-GFP were assessed in this cell viability study. Results are presented in Figure 19.

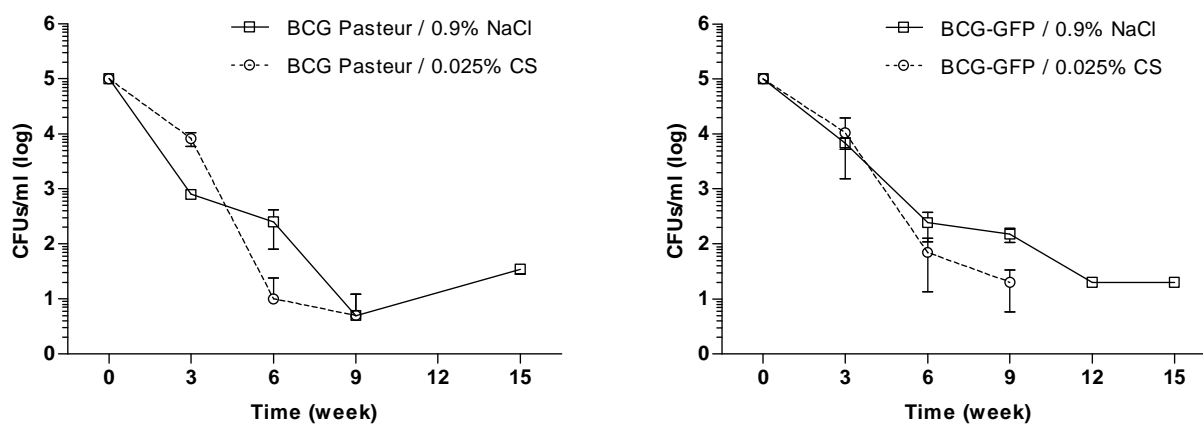


**Figure 19** – Cell viability of different strains of BCG (Pasteur and rBCG-GFP) following suspension in chitosan, maintained at 4°C for 15 weeks. Suspension of BCG in 0.9% NaCl was used as control. Results are expressed as mean  $\pm$  S.D.; n=3.

Results showed a significant reduction of BCG's cellular viability for both BCG strains, with small differences. For rBCG-GFP, viable cell density decreased 1 log on the 3<sup>rd</sup> week, and approximately 3 log on the 6<sup>th</sup> week. Regarding BCG Pasteur, cell viability was further reduced, with a viable cell density decrease of 1 to 2 log on the 3<sup>rd</sup> week, and approximately 2.5 to 4 log on the 6<sup>th</sup> week. These effects were observed for both strains regardless of the suspension media ( $P > 0.05$ ). Overall, although the suspension of BCG in 0.025% chitosan induced a decrease in BCG cell viability, the same effect was observed in the control groups of 0.9% NaCl-suspended BCG. Therefore, chitosan may not be considered cytotoxic at tested concentration.

### 3.2. *In vitro* cell viability (MTT assay)

The *in vitro* biocompatibility of the microparticles was evaluated with the MTT reduction assay using a PMA-differentiated THP-1 cell line (Fig. 20), which is recommended as a model for antigen presenting cells.<sup>65</sup>

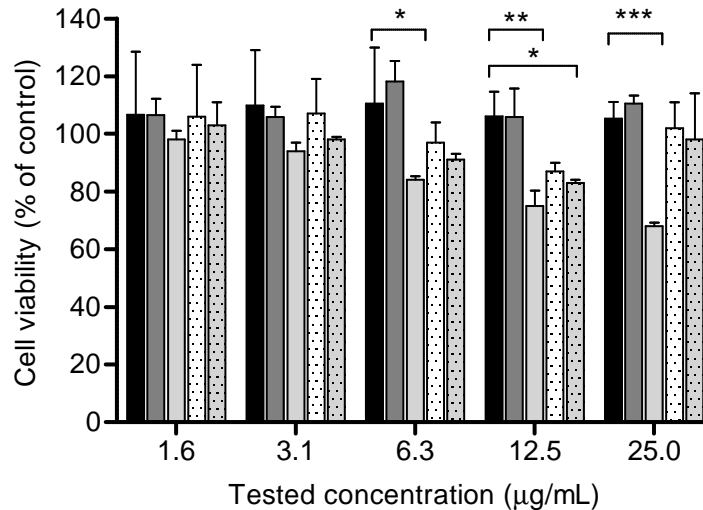


**Figure 20** – Relative cell viability of THP-1 cell line measured by the MTT reduction. Columns: black – control cells with culture medium; dark grey – BCG-GFP/0.9% NaCl; light grey – BCG-GFP/0.025% LMW chitosan; dotted white – BCG Pasteur/F13\_Medium microparticles; dotted grey – BCG Pasteur/F13\_High microparticles (1x10<sup>8</sup> CFU/mL). Results are expressed as mean  $\pm$  S.D. (n = 3). Statistical differences between the control group and formulations are reported as: \*\*\* $P < 0.001$ , \*\* $P < 0.01$ , \* $P < 0.05$ . Cell viability (% of control) = [A] test/[A] control x 100.

Results showed no significant reduction of cellular viability after 24h incubation with chitosan-suspended BCG and BCG-loaded microparticles, except for the highest concentrations of chitosan-suspended BCG, namely, 25  $\mu\text{g/mL}$  ( $P < 0.00001$ ), 12.5  $\mu\text{g/mL}$  ( $P = 0.0077$ ) and 6.3  $\mu\text{g/mL}$  ( $P < 0.05$ ), and a high concentration of BCG-loaded microparticles (12.5  $\mu\text{g/mL}$ ). These concentrations outrange concentrations intended for vaccination assays (e.g. 25  $\mu\text{g/mL}$  is about five times higher).

Overall, although some formulations induced a slight decrease in cell viability (15–20%), none of the BCG-loaded microparticles may be considered as cytotoxic according to the international definitions, since average values were not significantly different from the control group at tested concentrations. The obtained results are in conformity with other studies where chitosan did not interfere with cell viability.<sup>30</sup>

## 4. Conclusions

During these preliminary formulation studies, it was possible to optimize the preparation method for BCG-loaded chitosan-alginate microparticles with reproducible size distribution, association efficiency and production yield. Particle size and size distribution uniformity were considered to be critical aspects throughout the formulation studies. These parameters are influenced by several experimental conditions, such as properties of the used polymers; antigen type (whole live bacteria represent additional challenges regarding cell viability maintenance during formulation); type, speed and duration of homogenization; polymer/polymer and polymer/complexation agent mass ratios; relation between the pH of the different polymers.

In this study, biodegradable and biocompatible polymers (chitosan and sodium alginate), as well as two strains of *Mycobacterium bovis* BCG (BCG Pasteur, clinically available vaccine; and rBCG-GFP), were used. The number of variables that could be optimized was reduced throughout formulation development. Essentially, the optimization of the preparation method relied on the identification of best polymeric compositions, and identification of crucial steps in the ionic gelation methods that were determinant for particle size distribution and surface charge.

It was possible to observe that, for chitosan-alginate microparticles, size distribution was mainly influenced by the molecular weight of the used polymers and by the type of polymer blends. In opposition, particle surface charge was mainly influenced by polymer to polymer mass ratio due to the possibility of particle aggregation. By simple suspending BCG in chitosan, it was possible to tune BCG's physicochemical properties, namely surface charge.

Additionally, the association of monodispersed whole live BCG bacilli into microparticles was of paramount importance since it could directly influence BCG cell viability and particle size and surface charge. It was possible to develop a reproducible method for microencapsulation of whole live bacteria using only mild conditions, through ionic cross-linking, with good production yield and association efficiency, while maintaining cell viability and assuring the biocompatibility of the developed microparticulate delivery system.

The microencapsulation of BCG had no considerable effect on particles' key features (i.e. size distribution, surface charge, morphology). However, the formulation method and, to a minor extent, the concentrations of BCG used, proved to be crucial in achieving high association efficiency values. Regarding particle surface charge, it was possible to

demonstrate that the addition order of the polymers was crucial to obtain microparticles of either electronegative or electropositive surface charge.

In conclusion, a whole live attenuated cell-based particulate delivery system was developed for mucosal immunization purposes. Further characterization of these formulations in terms of *in vitro* cellular interaction with macrophages, and the *in vivo* study following intranasal immunization in mice are presented in the next chapters.

## **5. Acknowledgments**

The authors would like to thank Prof. Elsa Anes (FFUL) and her team (Dr. David Pires, Dr. Nuno Carmo) by supplying strains (Pasteur and GFP), for access to the laboratory as well for all advice and practical support. The authors thank iMed.Ulisboa for financial support (UID/DTP/04138/2013) from Fundação para a Ciência e Tecnologia (FCT), Portugal, and Escola Superior de Tecnologia da Saúde de Lisboa for financial support from merit scholarship for Ph.D. (ESTeSL-IPL/CGD/2012) granted by Caixa Geral de Depósitos, Portugal.

## 6. References

1. Kaufmann, S. H. E. Envisioning future strategies for vaccination against tuberculosis. *Nat. Rev. Immunol.* **6**, 699–704 (2006).
2. Kaufmann, S. H. E. Future vaccination strategies against tuberculosis: thinking outside the box. *Immunity* **33**, 567–577 (2010).
3. Mohanan, D. *et al.* Administration routes affect the quality of immune responses: A cross-sectional evaluation of particulate antigen-delivery systems. *J. Control. Release* **147**, 342–349 (2010).
4. Cooper, A. M. Cell-mediated immune responses in tuberculosis. *Annu. Rev. Immunol.* **27**, 393–422 (2009).
5. Bhatt, K. & Salgame, P. Host innate immune response to *Mycobacterium tuberculosis*. *J. Clin. Immunol.* **27**, 347–62 (2007).
6. Ota, M. O. C. *et al.* Influence of *Mycobacterium bovis* bacillus Calmette-Guérin on antibody and cytokine responses to human neonatal vaccination. *J. Immunol.* **168**, 919–25 (2002).
7. Dietrich, J., Billeskov, R., Doherty, T. M. & Andersen, P. Synergistic effect of bacillus Calmette Guerin and a Tuberculosis subunit vaccine in cationic liposomes: Increased immunogenicity and protection. *J. Immunol.* **178**, 3721–3730 (2007).
8. Ajdary, S. *et al.* Oral administration of BCG encapsulated in alginate microspheres induces strong Th1 response in BALB/c mice. *Vaccine* **25**, 4595–601 (2007).
9. Almeida, A. J. & Alpar, H. O. in *Antigen Delivery systems - Immunological and Technical Issues* 207–226 (Harwood Academic publishers, 1997).
10. Eyles, J. E., Sharp, G. J., Williamson, E. D., Spiers, I. D. & Alpar, H. O. Intra nasal administration of poly-lactic acid microsphere co-encapsulated *Yersinia pestis* subunits confers protection from pneumonic plague in the mouse. *Vaccine* **16**, 698–707 (1998).
11. Alpar, H. O., Somavarapu, S., Atuah, K. N. & Bramwell, V. W. Biodegradable mucoadhesive particulates for nasal and pulmonary antigen and DNA delivery. *Adv. Drug Deliv. Rev.* **57**, 411–30 (2005).
12. Tafaghodi, M., Sajadi Tabassi, S. A. & Jaafari, M. R. Induction of systemic and mucosal immune responses by intranasal administration of alginate microspheres encapsulated with tetanus toxoid and CpG-ODN. *Int. J. Pharm.* **319**, 37–43 (2006).
13. Singh, M. & O'Hagan, D. T. Recent advances in vaccine adjuvants. *Pharm. Res.* **19**, 715–28 (2002).
14. Slütter, B. & Jiskoot, W. Dual role of CpG as immune modulator and physical crosslinker in ovalbumin loaded N-trimethyl chitosan (TMC) nanoparticles for nasal vaccination. *J. Control. Release* **148**, 117–121 (2010).
15. Pichichero, M. E. Improving vaccine delivery using novel adjuvant systems. *Hum. Vaccin.* **4**, 262–270 (2008).
16. Bal, S. M., Slütter, B., Verheul, R., Bouwstra, J. A. & Jiskoot, W. Adjuvanted, antigen loaded N-trimethyl chitosan nanoparticles for nasal and intradermal vaccination: Adjuvant- and site-dependent immunogenicity in mice. *Eur. J. Pharm. Sci.* **45**, 475–481 (2012).
17. Kazzaz, J. *et al.* Encapsulation of the immune potentiators MPL and RC529 in PLG microparticles enhances their potency. *J. Control. Release* **110**, 566–73 (2006).
18. Borges, O. *et al.* Alginate coated chitosan nanoparticles are an effective subcutaneous adjuvant for hepatitis B surface antigen. *Int. Immunopharmacol.* **8**, 1773–80 (2008).
19. Caetano, L. A., Almeida, A. J. & Gonçalves, L. M. D. Approaches to Tuberculosis Mucosal Vaccine Development Using Nanoparticles and Microparticles: A

- Review. *J. Biomed. Nanotechnol.* **10**, 2295–2316 (2014).
20. Thiele, L. *et al.* Evaluation of particle uptake in human blood monocyte-derived cells in vitro. Does phagocytosis activity of dendritic cells measure up with macrophages? *J. Control. Release* **76**, 59–71 (2001).
  21. He, C., Hu, Y., Yin, L., Tang, C. & Yin, C. Effects of particle size and surface charge on cellular uptake and biodistribution of polymeric nanoparticles. *Biomaterials* **31**, 3657–66 (2010).
  22. Foged, C., Brodin, B., Frokjaer, S. & Sundblad, A. Particle size and surface charge affect particle uptake by human dendritic cells in an in vitro model. *Int. J. Pharm.* **298**, 315–22 (2005).
  23. Douglas, K. L. & Tabrizian, M. Effect of experimental parameters on the formation of alginate-chitosan nanoparticles and evaluation of their potential application as DNA carrier. *J. Biomater. Sci. Polym. Ed.* **16**, 43–56 (2005).
  24. Grabnar, P. A. & Kristl, J. The manufacturing techniques of drug-loaded polymeric nanoparticles from preformed polymers. *J. Microencapsul.* **28**, 323–35 (2011).
  25. Jenkins, P. G., Coombes, a G., Yeh, M. K., Thomas, N. W. & Davis, S. S. Aspects of the design and delivery of microparticles for vaccine applications. *J. Drug Target.* **3**, 79–81 (1995).
  26. Davis, S. S. Nasal vaccines. *Adv. Drug Deliv. Rev.* **51**, 21–42 (2001).
  27. Vajdy, M. & O'Hagan, D. T. Microparticles for intranasal immunization. *Adv. Drug Deliv. Rev.* **51**, 127–41 (2001).
  28. Almeida, A. J. & Alpar, H. O. Nasal delivery of vaccines. *J. Drug Target.* **3**, 455–467 (1996).
  29. Cadete, A. *et al.* Development and characterization of a new plasmid delivery system based on chitosan-sodium deoxycholate nanoparticles. *Eur. J. Pharm. Sci.* **45**, 451–8 (2012).
  30. Figueiredo, L., Calado, C. C. R., Almeida, A. J. & Gonçalves, L. M. D. Protein and DNA nanoparticulate multiantigenic vaccines against *H. pylori*: in vivo evaluation. in *2nd Portuguese BioEngineering Meeting* (ed. IEEE EMBS Portuguese Chapter) I.I, 1 (2012).
  31. Calvo, P., Remuñán-López, C., Vila-Jato, J. L. & Alonso, M. J. Chitosan and Chitosan-Ethylene Oxide-Propylene oxide block copolymer nanoparticles as novel carriers for proteins and vaccines. *Pharm. Res.* **14**, 1431–1436 (1997).
  32. Sarmento, B., Ribeiro, A. J., Veiga, F., Ferreira, D. C. & Neufeld, R. J. Insulin-loaded nanoparticles are prepared by alginate ionotropic pre-gelation followed by chitosan polyelectrolyte complexation. *J. Nanosci. Nanotechnol.* **7**, 2833–2841 (2007).
  33. Calvo, P., Remuñán-López, C., Vila-Jato, J. L. & Alonso, M. J. Novel hydrophilic chitosan-polyethylene oxide nanoparticles as protein carriers. *J. Appl. Polym. Sci.* **63**, 125–132 (1997).
  34. Sarmento, B., Ferreira, D., Veiga, F. & Ribeiro, a. Characterization of insulin-loaded alginate nanoparticles produced by ionotropic pre-gelation through DSC and FTIR studies. *Carbohydr. Polym.* **66**, 1–7 (2006).
  35. Sarmento, B. *Chitosan-Based Systems for Biopharmaceuticals*. *Polymer* (2012 John Wiley & Sons, Ltd, 2012).
  36. Tønnesen, H. H. & Karlsen, J. Alginate in drug delivery systems. *Drug Dev. Ind. Pharm.* **28**, 621–30 (2002).
  37. De, S. & Robinson, D. Polymer relationships during preparation of chitosan–alginate and poly-L-lysine–alginate nanospheres. *J. Control. Release* **89**, 101–112 (2003).
  38. Dodane, V., Amin Khan, M. & Merwin, J. R. Effect of chitosan on epithelial permeability and structure. *Int. J. Pharm.* **182**, 21–32 (1999).
  39. Amidi, M., Mastrobattista, E., Jiskoot, W. & Hennink, W. E. Chitosan-based delivery systems for protein therapeutics and antigens. *Adv. Drug Deliv. Rev.* **62**, 59–82 (2010).

40. Pawar, D. *et al.* Evaluation of mucoadhesive PLGA microparticles for nasal immunization. *AAPS J.* **12**, 130–7 (2010).
41. Lehr, C., Bouwstra, J., Schacht, E. & Junginger, H. *In vitro* evaluation of mucoadhesive properties of chitosan and some other natural polymers. *Int. J. Pharm.* **78**, 43–48 (1992).
42. Leithner, K. & Bernkop-schn, A. in *Chitosan-Based Systems for Biopharmaceuticals* (eds. Sarmento, B. & Neves, J.) 159–180 (2012 John Wiley & Sons, Ltd, 2012).
43. van der Lubben, I. M., Verhoef, J. C., Borchard, G. & Junginger, H. E. Chitosan and its derivatives in mucosal drug and vaccine delivery. *Eur. J. Pharm. Sci.* **14**, 201–7 (2001).
44. Baudner, B. C. *et al.* The concomitant use of the LTK63 mucosal adjuvant and of chitosan-based delivery system enhances the immunogenicity and efficacy of intranasally administered vaccines. *Vaccine* **21**, 3837–3844 (2003).
45. Tafaghodi, M. *et al.* Hepatitis B surface antigen nanoparticles coated with chitosan and trimethyl chitosan: Impact of formulation on physicochemical and immunological characteristics. *Vaccine* **30**, 5341–8 (2012).
46. McNeela, E. A. *et al.* Intranasal immunization with genetically detoxified diphtheria toxin induces T cell responses in humans: enhancement of Th2 responses and toxin-neutralizing antibodies by formulation with chitosan. *Vaccine* **22**, 909–14 (2004).
47. Amidi, M. *et al.* N-Trimethyl chitosan (TMC) nanoparticles loaded with influenza subunit antigen for intranasal vaccination: Biological properties and immunogenicity in a mouse model. *Vaccine* **25**, 144–153 (2007).
48. Jain, R. *et al.* Enhanced and enduring protection against tuberculosis by recombinant BCG-Ag85C and its association with modulation of cytokine profile in lung. *PLoS One* **3**, e3869 (2008).
49. Gupta, N. K., Tomar, P., Sharma, V. & Dixit, V. K. Development and characterization of chitosan coated poly-( $\epsilon$ -caprolactone) nanoparticulate system for effective immunization against influenza. *Vaccine* **29**, 9026–37 (2011).
50. Vila, A. *et al.* Low molecular weight chitosan nanoparticles as new carriers for nasal vaccine delivery in mice. *Eur. J. Pharm. Biopharm.* **57**, 123–131 (2004).
51. Kang, M. L., Cho, C. S. & Yoo, H. S. Application of chitosan microspheres for nasal delivery of vaccines. *Biotechnol. Adv.* **27**, 857–65 (2009).
52. Figueiredo, L., Cadete, A. & Gonçalves, L. M. D. Intranasal immunisation of mice against *Streptococcus equi* using positively charged nanoparticulate carrier systems. *Vaccine* **30**, 6551–6558 (2012).
53. Rodrigues, M. A. *et al.* Development of a novel mucosal vaccine against strangles by supercritical enhanced atomization spray-drying of *Streptococcus equi* extracts and evaluation in a mouse model. *Eur. J. Pharm. Biopharm.* **82**, 392–400 (2012).
54. Florindo, H. F. *et al.* The enhancement of the immune response against *S. equi* antigens through the intranasal administration of poly-epsilon-caprolactone-based nanoparticles. *Biomaterials* **30**, 879–91 (2009).
55. Jordao, L., Bleck, C. K. E., Mayorga, L., Griffiths, G. & Anes, E. On the killing of mycobacteria by macrophages. *Cell. Microbiol.* **10**, 529–48 (2008).
56. Bettencourt, P., Pires, D., Carmo, N. & Anes, E. in *Microscopy: Science, Technology, Applications and Education* (eds. Méndez-Vilas, A. & Díaz, J.) 614–621 (2010).
57. Zheng, L. Y. & Zhu, J. F. Study on antimicrobial activity of chitosan with different molecular weights. *Carbohydr. Polym.* **54**, 527–530 (2003).
58. Devlieghere, F., Vermeulen, a. & Debevere, J. Chitosan: Antimicrobial activity, interactions with food components and applicability as a coating on fruit and vegetables. *Food Microbiol.* **21**, 703–714 (2004).
59. Liu, N. *et al.* Effect of MW and concentration of chitosan on antibacterial activity of *Escherichia coli*. *Carbohydr. Polym.* **64**, 60–65 (2006).

60. Raafat, D. & Sahl, H.-G. Chitosan and its antimicrobial potential--a critical literature survey. *Microb. Biotechnol.* **2**, 186–201 (2009).
61. Goy, R. C., Britto, D. De & Assis, O. B. G. A Review of the Antimicrobial Activity of Chitosan. *Polímeros Ciência e Tecnol.* **19**, 241–247 (2009).
62. Doig, C., Seagar, a L., Watt, B. & Forbes, K. J. The efficacy of the heat killing of *Mycobacterium tuberculosis*. *J. Clin. Pathol.* **55**, 778–9 (2002).
63. Mosmann, T. Rapid colorimetric assay for cellular growth and survival: application to proliferation and cytotoxicity assays. *J. Immunol. Methods* **65**, 55–63 (1983).
64. Theus, S. A., Cave, M. D. & Eisenach, K. D. Activated THP-1 Cells : an Attractive Model for the Assessment of Intracellular Growth Rates of *Mycobacterium tuberculosis* Isolates. *Infect. Immun.* **72**, 1169–1173 (2004).
65. Chanput, W., Mes, J. J. & Wichers, H. J. THP-1 cell line: An in vitro cell model for immune modulation approach. *Int. Immunopharmacol.* **23**, 1–9 (2014).
66. Makraduli, L., Crcarevska, M. S., Geskovski, N., Dodov, M. G. & Goracinova, K. Factorial design analysis and optimisation of alginate-Ca-chitosan microspheres. *J. Microencapsul.* 1–12 (2012). doi:10.3109/02652048.2012.700957
67. Takka, S. & Gürel, A. Evaluation of chitosan/alginate beads using experimental design: formulation and in vitro characterization. *AAPS PharmSciTech* **11**, 460–6 (2010).
68. Kalkanidis, M. *et al.* Methods for nano-particle based vaccine formulation and evaluation of their immunogenicity. *Methods* **40**, 20–9 (2006).
69. Ruenraroengsak, P., Cook, J. M. & Florence, A. T. Nanosystem drug targeting: Facing up to complex realities. *J. Control. Release* **141**, 265–76 (2010).
70. Sarmiento, B. *et al.* Alginate/chitosan nanoparticles are effective for oral insulin delivery. *Pharm. Res.* **24**, 2198–206 (2007).
71. Dobakhti, F. *et al.* Stabilizing effects of calcium alginate microspheres on *Mycobacterium bovis* BCG intended for oral vaccination. *J. Microencapsul.* **23**, 844–854 (2006).
72. Bramwell, V. W. & Perrie, Y. Particulate delivery systems for vaccines: what can we expect? *J. Pharm. Pharmacol.* **58**, 717–28 (2006).
73. Griffiths, G., Nyström, B., Sable, S. B. & Khuller, G. K. Nanobead-based interventions for the treatment and prevention of tuberculosis. *Nat. Rev. Microbiol.* **8**, 827–34 (2010).
74. Storni, T., Kündig, T. M., Senti, G. & Johansen, P. Immunity in response to particulate antigen-delivery systems. *Adv. Drug Deliv. Rev.* **57**, 333–355 (2005).
75. Hagan, D. T. O. Microparticles and polymers for the mucosal delivery of vaccines. *Adv. Drug Deliv. Rev.* **34**, 305–320 (1998).
76. Van Der Lubben, I. M. *et al.* Chitosan microparticles for mucosal vaccination against diphtheria: oral and nasal efficacy studies in mice. *Vaccine* **21**, 1400–1408 (2003).
77. Garrity, G. M., Bell, J. A., Lilburn, T. G. & Lansing, E. in *Taxonomic outline of the prokaryotes Bergey's Manual of systematic bacteriology* (2004 Bergey's Manual Trust, 2004). doi:10.1007/bergeysoutline200405
78. Zhang, A. & Groves, M. J. Size characterization of *Mycobacterium bovis* BCG (Bacillus Calmette Guérin) Vaccine, Tice Substrain. *Pharm. Res.* **5**, 607–610 (1988).
79. Desjardins, M. & Griffiths, G. Phagocytosis: latex leads the way. *Curr. Opin. Cell Biol.* **15**, 498–503 (2003).
80. Simsek-Ege, F. a., Bond, G. M. & Stringer, J. Polyelectrolyte complex formation between alginate and Chitosan as a function of pH. *J. Appl. Polym. Sci.* **88**, 346–351 (2003).
81. Chen, S.-C. *et al.* A novel pH-sensitive hydrogel composed of N,O-carboxymethyl chitosan and alginate cross-linked by genipin for protein drug delivery. *J. Control. Release* **96**, 285–300 (2004).
82. Kaasalainen, M. *et al.* Effect of isotonic solutions and peptide adsorption on zeta

- potential of porous silicon nanoparticle drug delivery formulations. *Int. J. Pharm.* **431**, 230–236 (2012).
83. Pawlak, a & Mucha, M. Thermogravimetric and FTIR studies of chitosan blends. *Thermochim. Acta* **396**, 153–166 (2003).
84. Zhang, A., Groves, M. J. & Klegerman, M. E. The surface charge of cells of *Mycobacterium bovis* BCG vaccine, Tice substrain. *Microbios* **53**, 191–195 (1988).

## ***Chapter III***

---

### ***Interaction of BCG-loaded microparticles with macrophages and preliminary in vivo studies***



## Abstract

The aim of the present study was to assess *in vitro* the cellular uptake of BCG suspended in an aqueous chitosan solution and BCG-loaded microparticles by antigen presenting cells (APC), as well as the specific immune responses elicited against *Mycobacterium bovis* in a mice model following intranasal immunization.

The interaction of BCG-loaded microparticles with APC was assessed by fluorescence microscopy, using a human macrophage cell line and recombinant BCG expressing green fluorescence. The effect of plain and BCG-loaded microparticles, as well as BCG suspended in chitosan only, on immune response was assessed by ELISA quantification of specific IgG subtypes in mice serum and secretory IgA in mice lungs homogenates.

Cellular uptake by APC was approximately 2-fold higher for positively charged BCG suspended in chitosan than for negatively charged BCG-loaded chitosan-alginate microparticles. Increasing the number of BCG bacilli per macrophage caused a reduction of approximately 20% in the percentage of cellular uptake. Intranasal vaccination with BCG-loaded microparticles and BCG suspended in chitosan elicited higher levels of IgG1 and IgG2a than subcutaneous vaccine, and a predominant Th1 type response, whereas positively charged BCG suspended in chitosan originated the highest mucosal response in the lungs.

Thus, successful stimulation of specific humoral, cellular and mucosal immune responses against tuberculosis was achieved by using the herein proposed microparticulate delivery systems by intranasal immunization with whole live BCG.



## 1. Introduction

It is well known that mucosal immune responses are of major importance for protection against pathogens invading the organism via mucosal surfaces.<sup>1,2</sup> However, most currently available vaccines are parenterally administered, thus, poor inducers of mucosal immunity. The success of mucosal immunization has to some extent been hampered by host defense barriers such as mucosal secretions, proteases/nucleases attack, and epithelial barriers.<sup>3</sup> Tight epithelial cell layers present in the nasal mucosa and in the nasal associated lymphoid tissue (NALT), and short residence time for antigens due to mucociliary clearance, are great limitations to vaccine delivery in the upper respiratory tract. In order to overcome biological barriers and to colonize mucosal surfaces, adequate delivery systems can be used.<sup>4,5</sup>

Considering tuberculosis, there is a need for an improved vaccine.<sup>6-9</sup> It has been suggested that lack of efficacy of BCG in adulthood protection against tuberculosis may result from a limited release in the antigen presenting cells (APC), perhaps due to the strain attenuation process during vaccine production.<sup>10-12</sup> The entrapment of antigens into particulate delivery systems may increase the residence time of formulations at the site of administration, thus, intensifying the interaction of antigens with epithelial cells by a depot effect, which could extend antigen presentation in APC.<sup>13</sup>

Recent examples of effective vaccine strategies for antigen delivery to APC involves the formulation of acid-labile polymeric particles designed for a specific erosion kinetics and antigen release as function of pH value in endosomal compartments.<sup>14-16</sup> This type of particle is able to direct antigen presentation through either MHC class I or class II pathways, which is of particular interest considering the possibility to control antigen presentation by adjusting particles acid lability. Moreover, particle uptake by APC and intracellular trafficking may be modulated by particle size and surface charge, as well as particle composition and surface components, therefore, conferring particle features the ability to generate different immunological profiles.<sup>17</sup> Positively surface charged particles are described to efficiently bind to negatively charged cell membranes while promoting cellular uptake, thus, enabling a strong immune response after mucosal vaccination.<sup>18-21</sup>

The encapsulation of live organisms has been reported for different purposes, such as prolonging the storage time of *Mycobacterium tuberculosis* Bacillus Calmette-Guérin (BCG) using agarose microcapsules,<sup>22</sup> and, more recently, for vaccine delivery purposes.<sup>23,24</sup> Lipid microencapsulated BCG for oral immunization has been described as effective in eliciting cell-mediated immune responses and protection against aerosol

challenge with mycobacteria in mice.<sup>25–28</sup> However, to our knowledge, no studies were performed regarding the microencapsulation of whole live attenuated BCG for intranasal immunization purposes.

In this study, a novel polymeric delivery system for microencapsulation of whole live BCG was evaluated. We propose the use of live BCG because immunization with live vaccines remain an attractive immunization strategy, as live bacteria are multi-antigenic and normally mimic pathogens surpassing host's natural barriers, being the ideal antigen producers and vectors. The use of whole live bacterial vaccines relies on multiple antigens and built-in adjuvanticity, which provide several important advantages over other strategies, as they act like the natural infection, being readily taken up by specialized antigen presenting cells, thus, inducing strong humoral and cellular immune responses.<sup>29</sup> Through the formation of a stable polyionic system, we hope to modulate BCG's surface characteristics, such as size, surface charge and functional groups, in order to drive the immune system to BCG's recognition via MHC-II.

To maintain cell viability, it is necessary to avoid the use of cross-linking agents or chemically modified polymers during microencapsulation, using only biocompatible conditions. Polysaccharides and naturally occurring biopolymers present special interest due to their biocompatible, biodegradable, hydrophilic and protective properties.<sup>30–34</sup> The use of cationic and anionic polymers can lead to the formation of polyionic hydrogels and particles. Chitosan-alginate is one of the most interesting complexes studied so far for drug and vaccine delivery purposes.<sup>35–39</sup> Polyionic complexation of chitosan and alginate enables encapsulation and protection of the encapsulated (drug or vaccine), while enabling a more effective release control than the use of chitosan or alginate alone. Chitosan and alginate have been extensively investigated in recent years, including in our group, presenting favourable characteristics for vaccine entrapment and mucosal delivery.<sup>40–49</sup>

Chitosan is a cationic polysaccharide obtained by the N-deacetylation of chitin from crustaceans. Alginate is a polysaccharide of anionic nature, consisting of linear copolymers of  $\alpha$ -L-guluronate and  $\beta$ -D-mannuronate residues. In the presence of calcium ions, ionic interactions occur between the divalent calcium ions and the guluronic acid residues, leading to a gel formation. Most preparative methods for chitosan-based particles involve ionic gelation or polyelectrolyte cross-linking. The particles are formed by interaction between the carboxyl groups of the alginate and the amine groups of chitosan, or between the amine groups of chitosan with anionic molecules such as tripolyphosphate (TPP) or hyaluronic acid.<sup>50</sup> Chitosan's

mucoadhesive and mucopenetrating properties are described to be important to enhance antigen uptake across epithelial barriers.<sup>51,52</sup> Moreover, due to chitosan's immunostimulatory properties, chitosan-based particulate delivery systems can act both as carrier and as adjuvant, improving the elicited immune response via induction of serum IgG and secretory IgA levels, as previously demonstrated with different nasally administered vaccines (e.g., influenza, diphtheria, and pertussis).<sup>53,54</sup>

Regarding alginate, it has mucoadhesive properties and is resistant to acid degradation. This features make alginate an attractive polymer that might contribute to increase the residence time of microparticles in the lung mucosa, while increasing bacterial survival within the alveolar macrophages, thus, leading to a different antigen recognition pathway that can prompt a more balanced cellular/humoral immune response. The use of alginate beads coated with chitosan for mucosal immunization has also been described to improve the stability of DNA during storage and in biological fluids,<sup>55</sup> and to enhance the immune response elicited by hepatitis B antigen.<sup>56</sup> Both chitosan and alginate are non-toxic, thus, enable repeated administration if needed.

Taking into consideration the abovementioned, we propose a novel chitosan-alginate microparticulate delivery system prepared by polyionic complexation of chitosan and alginate while entrapping live attenuated monodispersed BCG intended for intranasal immunization purposes. Microparticles were characterized for particle size and morphology (by laser diffraction and optic microscopy), particle composition and polymers interaction (FT-IR), and particle surface charge (by electrophoretic mobility). Association efficiency and biocompatibility of BCG-loaded microparticles were also evaluated, the latter by commonly described MTT assay. Cellular uptake of BCG-loaded microparticles was assessed using a human macrophage THP-1 cell line. *In vivo* studies were conducted in a mice model by intranasal immunization with BCG-loaded chitosan-alginate microparticles, and the elicited immune response was assessed by ELISA quantification of specific serum levels of anti-mycobacterial IgG, IgG1 and IgG2a and secretory IgA levels in the lung.

## 2. Materials and methods

### 2.1. Materials

Chitosan, 75-85% deacetylated (as provided by suppliers), having molecular masses of <150 kDa (LMW), ( $\approx$  450 kDa (MMW), and >600 kDa (HMW), was purchased from Sigma-Aldrich (UK). Sodium alginate was purchased from Sigma-Aldrich (UK) in three different viscosities: high viscosity (HV), 3000 mPa.s, 20 mg/mL; medium viscosity (MV), 187 mPa.s, 20 mg/mL; and low viscosity (LV), 20-40 mPa.s, 10mg/mL (structural viscosity as provided by suppliers). We also used sodium alginate of different G-content, provided by FMC BioPolymer: low G-content (Keltone LVCR), 40% (218 mPa.s, 20 mg/mL), high G-content (Manugel LBA), 63% (773 mPa.s, 100 mg/mL); and high G-content (Protanal LF 10/60), 65-75% (20-70 mPa.s, 10 mg/mL). Sodium tripolyphosphate (TPP), calcium chloride ( $\text{CaCl}_2$ ) Phorbol myristate acetate (PMA), and Tween 80 were purchased from Sigma-Aldrich (UK). All other chemicals were of analytical grade or equivalent, and were used as received without further purification or modification.

All cells were obtained from American Type Cell Culture Collection (ATCC), unless referred otherwise. *Mycobacterium bovis* BCG cells (strain Pasteur 1173) were obtained from ATCC 35734<sup>TM</sup>. Human monocyte THP-1 cell line was obtained from ATCC TIB-202<sup>TM</sup>. Recombinant *M. bovis* BCG harbouring a pMN437 plasmid for expression of Green Fluorescent Protein (rBCG-GFP) were kindly supplied by Prof Elsa Anes.<sup>57</sup> The culture media used through all *in vitro* assays was obtained from Invitrogen (UK), unless referred otherwise. Middlebrook's 7H9 broth Medium supplemented with 5% (v/v) OADC (oleic acid, albumin, dextrose and catalase) was purchased from Difco (USA). The ProLong<sup>TM</sup> antifade reagent containing DAPI was obtained from Invitrogen (UK).

### 2.2. Animals

Female BALB/c mice (8- to 12 weeks old) were provided from Charles Rivers (Spain) and maintained under specific pathogen-free conditions. Animals were fed with standard laboratory food and water *ad libitum*. All *in vivo* studies using animals were carried out with the authorization of the local ethic committee and in strict accordance with the Declaration of Helsinki, the EEC Directive of 24th November 1986 (No. 86/609 EEC), the relevant Portuguese laws D.R. No. 31/92, D.R. 153 I-A 67/92, and all subsequent legislation.

### 2.3. Preparation of BCG-loaded microparticles

*Mycobacterium bovis* BCG cultures were grown for 7 days on Middlebrook's 7H9 broth Medium supplemented with 5% (v/v) OADC (oleic acid, albumin, dextrose and catalase) and 0.05 % (v/v) Tween 80 (at 37°C / 5% CO<sub>2</sub>). Briefly, *M. bovis* BCG cells were pelleted at 4000 rpm (1559 ×g) at 4°C for 15 min, washed with sterile 10mM phosphate buffered saline and resuspended in appropriate medium.

Whole live attenuated monodispersed BCG was suspended in chitosan and encapsulated into chitosan-alginate microparticles by means of previously described ionic gelation methods with modifications. Preliminary tests were carried out in order to assess the feasibility of produced microparticles as BCG bacilli carriers for increasing BCG concentrations (Chapter II, section 3.1.4, Table 9).

Two different approaches were used in order to modify BCG's properties. The first method aimed at microencapsulating whole live attenuated monodispersed BCG into chitosan-alginate microparticles. This was performed by monodispersing *M. bovis* BCG Pasteur ( $2.5 \times 10^9$  CFU/mL) in 0.1% (w/v) chitosan solution (pH=5.0) using a syringe, followed by dropwise addition of 0.2% (w/v) TPP solution (pH=9.0). Then, 0.1% (w/v) alginate solution (pH=6.0) were dropwise added to the BCG-chitosan suspension, in order to obtain BCG-loaded microparticles with a chitosan/alginate/TPP mass ratio of 5/5/2 (w/w/w). The second method consisted in simple monodispersing *M. bovis* BCG Pasteur ( $2.5 \times 10^9$  CFU/mL) in a 0.025% (w/v) chitosan solution (pH=5.0), followed by dropwise addition of 0.2% (w/v) TPP solution (pH=9.0). Alginate coating was not performed within this second method.

Particle morphology, size distribution, association efficiency, surface charge, physicochemical properties, *in vitro* interaction with macrophages, systemic and mucosal immune responses were assessed. For comparison purposes, similar formulations were prepared by simply suspending monodispersed BCG Pasteur bacilli in 0.9% NaCl, and administered either by intranasal or subcutaneous route to mice.

## 2.4. Evaluation of BCG cell viability (micro-CFU I)

In order to determine the effect of microparticle preparation conditions on the cell viability of microencapsulated BCG, a micro-CFU assay<sup>58</sup> was performed. The samples were maintained at 4°C for one month. Briefly, 1/10 dilutions of BCG-loaded microparticles, BCG suspended in 0.025% chitosan, and BCG suspended in 0.9% NaCl, were prepared in water on a 96-well plate to a final volume of 200  $\mu\text{L}$  (20  $\mu\text{L}$  + 180  $\mu\text{L}$ ). Then, solid agar plates (Middlebrook's 7H10 medium supplemented with OADC) were inoculated with 10  $\mu\text{L}$  of the  $10^{-1}$  to  $10^{-9}$  dilutions on each dot on the plate, as schematically represented in Figure 1A. The inoculated plates were maintained at 37°C and 5%  $\text{CO}_2$  for three weeks. After that period, formed micro-colonies were observed by microscopy and used to determine CFU (Fig. 1B).

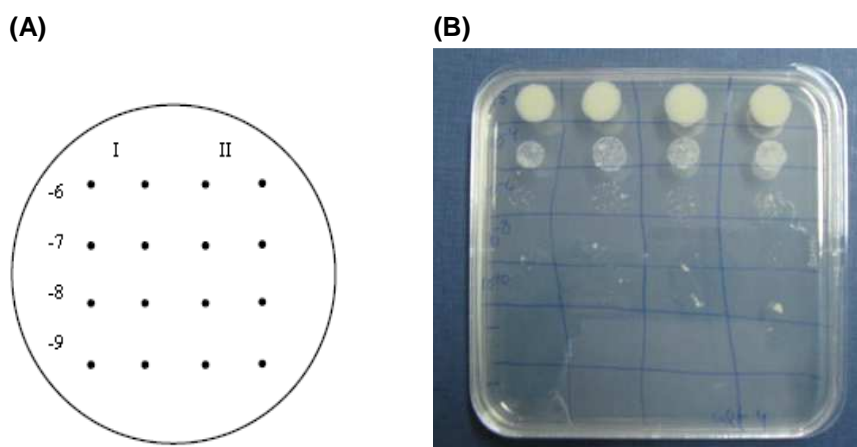


**Figure 1** – Micro-Colony forming units assay. (A) Example of four dilution-points of two BCG suspensions (I and II) with technical duplicates; (B) (Micro-)photographs of BCG Pasteur CFU three weeks post-inoculation.

## 2.5. Characterization of microparticles

Particle mean diameter and size distribution were determined by laser diffraction using a Mastersizer 2000 (Malvern Instruments, UK). Three measurements were performed on each sample. Particle size was quoted as  $d_{0.5}$  and span, for which the mean values and standard deviations were calculated. Zeta potential of microparticles was determined by electrophoretic mobility using a Zetasizer Nano Z (Malvern Instruments, UK). Six measurements were performed on each sample and the mean values and standard deviations calculated. Morphological examination of microparticles was performed by microscopy. The ImageJ software, 1.44p version (National Institutes of Health, USA) was used to perform image capture and analysis.

The FT-IR spectra of plain microparticles and employed polymers were obtained in solid state using an IRAffinity-1 (Shimadzu Corporation) FT-IR spectrophotometer. Samples of lyophilized microparticles or raw materials were gently mixed with approximately 300 mg of micronized KBr powder and compressed into discs at a force of 10 kN for 1 min using a manual tablet presser (Perkin Elmer, Norwalk, USA). All spectra were recorded at room temperature at the resolution of 4 cm<sup>-1</sup> and 50-times scanning, between 4000 and 500 cm<sup>-1</sup>, according to a double subtraction procedure.<sup>59,60</sup>

Association efficiency (A.E.) was determined by cell count number in a Neubauer chamber (Bürker haemocytometer). Briefly, 2.5 x 10<sup>9</sup> CFU/mL BCG Pasteur in 0.9% NaCl was combined with increasing amounts of chitosan, from 0 to 5 mL, and microparticles were prepared as previously described. The association efficiency was determined according to Equation 1.

#### EQ. 1. ASSOCIATION EFFICIENCY

$$\text{Association efficiency (\%)} = \frac{\text{Total cells} - \text{Free cells}}{\text{Total cells}} \times 100$$

## 2.6. Interaction with antigen presenting cells

For the evaluation of cellular uptake, chitosan-alginate microparticles loaded with rBCG-GFP were added to differentiated macrophage THP-1 cells (ATCC TIB-202™) grown on glass cover slips in 24 wells microplate (2x10<sup>5</sup> cells/mL). Cells were incubated with the microparticle formulations for 24h at 37°C in a humidified atmosphere of 5% CO<sub>2</sub>. After the incubation period, cells were washed with 10 mM PBS containing 10 mM glycine, prior to fixation with 4% (w/v) solution of paraformaldehyde in the dark for 15 minutes, followed by two washing steps with PBS. Glass cover slips containing cells were mounted with fluorescent mounting medium (ProLong Antifade, Invitrogen, UK) containing DAPI for nucleus labelling. Cells were observed and micro photographed in a Zeiss Axioskop 4.0 fluorescence microscope (Zeiss, Germany). Free imaging software ImageJ was used for microscopy data analysis. The quantitative analysis of intracellular uptake by macrophages was determined by cell associated green fluorescence count.<sup>58</sup>

## 2.7. Intranasal immunization of BALB/c mice

All vaccine formulations were freshly prepared under aseptic conditions in a biological safety cabinet, immediately prior dosing. Briefly, BCG was suspended in 0.025% low molecular weight chitosan (<150 kDa; DA 75–85%, Sigma–Aldrich (UK) at a target concentration of  $10^8$  CFU/mL. Aliquots of this chitosan-suspended BCG were used to prepare an alternative vaccine by ionotropic gelation with TPP, as follows: 0.5 mL of 2.0 mg/mL TPP were dropwise added to 3.0 mL of chitosan-suspended BCG, prior to dropwise addition of 1.0 mg/mL high G-content sodium alginate (Protanal LF 10/60, FMC). This BCG-loaded microparticle formulation (alginate to chitosan mass ratio of 1:1) was equivalent to  $8.3 \times 10^7$  CFU/mL BCG per dose, and 0.42 mg/mL of chitosan. Finally, BCG was suspended in 0.9% NaCl ( $10^8$  CFU/mL), and used as control.

Mice were intranasal immunized with BCG suspended in 0.9% NaCl (group 1), BCG suspended in 0.025% chitosan (group 2) or BCG-loaded microparticles (group 3) (Table 1). The intranasal vaccines were administered in volumes of 4–20  $\mu$ L (equivalent to  $1 \times 10^7$  CFU/dose BCG Pasteur per animal) using a micropipette tip, by slow delivery onto nostrils, so that the mice could inhale. Group 4 was immunized with BCG suspended in 0.9% NaCl as a single 100  $\mu$ L inoculum via subcutaneous injection at the nape of the neck ( $8.4 \times 10^6$  CFU, approximately 7 log, actual dose). All groups included four mice per group ( $25 \pm 2$  g).

**Table 1** – Summary of the formulations tested in mice and respective immunization route.

<b>Immunization groups</b>	<b>Immunization route</b>	<b>Formulations</b>	<b>Mice per group</b>
Group 1	Intranasal	BCG suspended in 0.9% NaCl	4
Group 2	Intranasal	BCG suspended in 0.25 mg/mL chitosan	4
Group 3	Intranasal	BCG-loaded in CS-ALG microparticles	4
Group 4	Subcutaneous	BCG suspended in 0.9% NaCl	4

Blood samples were collected from the tail vein every 15 days during 23 weeks (Figure 2), and sera separated by centrifugation (18,000g, 5 min at 4°C, Allegra 64R, Beckman, USA) and stored at –20°C until analysed by antigen specific enzyme-linked immunosorbent assay (ELISA) for IgG, IgG subclass 1 (IgG1) and IgG subclass 2a (IgG2a). In order to examine the mucosal immune response, lungs were collected from ethically sacrificed animals and IgA secretion levels were assessed by ELISA.

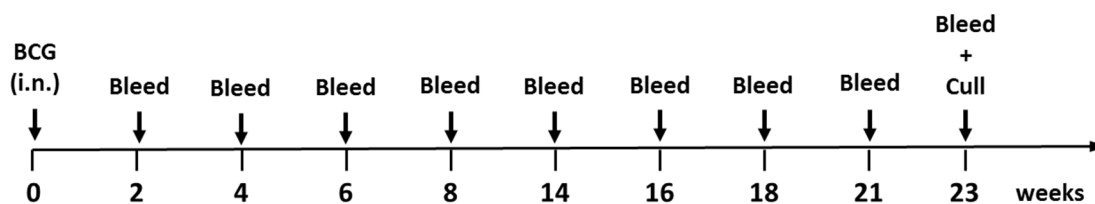


**Figure 2** – Immunization schedule for priming, blood sampling for specific IgGs subtypes quantification of by ELISA, and experimental endpoint with harvest of lungs for sIgA quantification.

## 2.8. Quantification of antigen-specific IgG subtypes and IgA

Purified protein derivative (PPD) bovine tuberculin-specific IgG titers were measured in blood samples at different stages of the immunization using an appropriate ELISA technique.<sup>61</sup> Briefly, ninety-six-well plates (Microolon™, High binding flat bottom plates, Greiner, Germany) were coated overnight at 37°C with 2.5 µg/mL of PPD bovine tuberculin (NIBSC, UK) in 100 mM sodium carbonate buffer (pH=9.6), and blocked with a 5% (w/v) skimmed milk powder (Merck KGaA, Germany) dissolved in 10 mM PBS (pH=7.4) containing 0.05% (v/v) of Tween™ 20 (PBST; Sigma–Aldrich, UK). Mice serum samples were added to plates in twofold serial dilutions, and plates were incubated for 2 h at 37°C. After the incubation time, plates were three times washed with PBST. Specific antibodies were detected after incubation for 2 h at 37°C with horseradish peroxidase-conjugated goat anti-mouse antibodies specific for IgG (1:1000, Sigma, Pool Dorset, UK), IgG1 and IgG2a (1:2000, Serotec, UK), and subsequent development of peroxidase reaction with o-phenylenediamine dihydrochloride (OPD) substrate (SigmaFAST™ OPD Kit, Sigma–Aldrich, UK). The development reaction was stopped after 15 min with the addition of 2.5 N H<sub>2</sub>SO<sub>4</sub>. Titers are reported as the reciprocal of serum dilutions that gave an optical density (490 nm) 5% higher than the strongest negative control reading.

For analysis of secretory IgA, the lungs collected at the end of the experiment were homogenized in buffer 0.9% sodium chloride with protease inhibitor PMSF 1 mM and 0.5% Tween™ 20. Tissue homogenization was performed with ultrasound probe for 3 times of 5 min intermittent pulsed for 30 s each in an ice bath. The homogenized tissues were centrifuged at 20,000 × g for 30 min at 4°C (Allegra 64R, Beckman, USA) and the supernatant was frozen at –80°C until freeze–drying. After freeze–drying, proteins were reconstituted with 500 µl of sterile water and directly added, in duplicates, to the plate wells. The mean OD (mean ± S.D., n≥3) was determined for

each treatment group, using IgA (1:1000; Serotec, UK) in the above described ELISA technique, and directly used to compare mucosal response.<sup>62</sup>

## 2.9. Statistical analysis

Results are expressed as mean values  $\pm$  standard deviation (S.D.). Statistical evaluation of data was carried out using GraphPad Prism v. 5.02 (GraphPad Software, CA, USA) by one-way analysis of variance (ANOVA), by the Tukey's comparison test in the in vivo studies, with significance set at P-values  $<0.05$ .

## 3. Results and discussion

The present study aimed at improving interaction of BCG with antigen presenting cells by modifying bacilli through microencapsulation in novel BCG-loaded chitosan-alginate microparticle formulations, and assessing the elicited specific immune response against *Mycobacterium tuberculosis* following intranasal immunization of mice.

### 3.1. Characterization of BCG-loaded microparticles

In this study, encapsulation of BCG into chitosan-alginate microparticles using an ionic gelation method with TPP and an alginate to chitosan mass ratio of 1:1 yielded a particle size distribution within the micrometer range. The average mycobacterial loading in BCG-loaded chitosan-alginate microparticles was  $1.4 \times 10^8$  CFU/mL. Table 2 summarizes the properties of BCG-loaded microparticles and of BCG suspended in different media.

**Table 2** – Characteristics of BCG-loaded microparticles ( $1.4 \times 10^8$  CFU/mL) and BCG suspended in chitosan ( $2.5 \times 10^9$  CFU/mL) and NaCl ( $4.2 \times 10^8$  CFU/mL).

Formulations	A.E.* (%)	Zeta potential (mV)	Particle size, d <sub>0.5</sub> (μm)	Span
BCG-loaded CS-ALG microparticles	61 $\pm$ 7	-10.7 $\pm$ 2.4	21.4 $\pm$ 2.4	2.5 $\pm$ 0.4
BCG suspended in 0.25 mg/mL LMW chitosan solution	--	+90.6 $\pm$ 3.5	--	--
BCG suspended in 0.9% NaCl	--	-23.1 $\pm$ 11.0	28.4 $\pm$ 1.9	3.2 $\pm$ 0.0

A.E., association efficiency, determined with BCG recombinant strain expressing green fluorescence; ZP, zeta potential; LMW, low molecular weight. Span expressed as  $[d(0.9) - d(0.1)] / d(0.5)$ . Results are represented as mean  $\pm$  S.D.;  $n \geq 3$ .

BCG-loaded microparticles presented a mean diameter of  $21.4 \pm 2.4 \mu\text{m}$ , showing a narrow size distribution with a span value of 2.5, and electronegative surface charge, with zeta potential values of  $-10.7 \pm 2.4 \text{ mV}$ . Particle size was confirmed by optical microscopy analysis, which also revealed that particles exhibited a spherical morphology, with a round shape and smooth surfaces (Fig. 3).

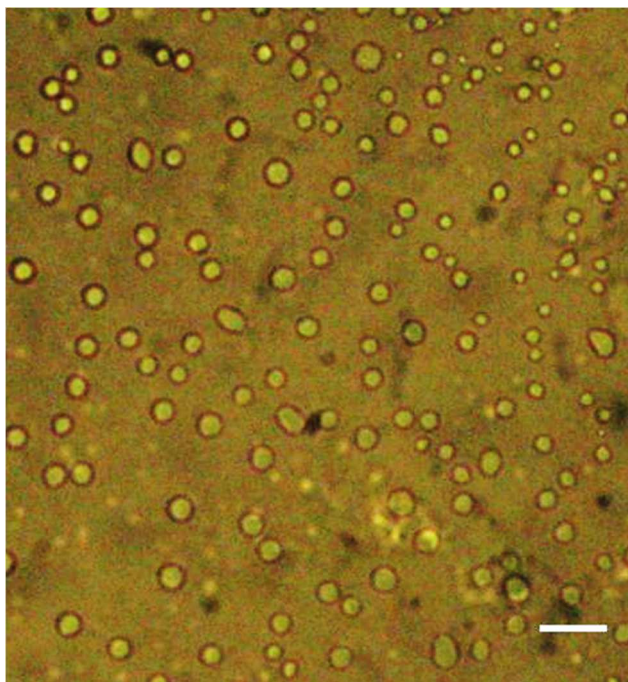


**Figure 3** – Micrograph of rBCG-GFP-loaded chitosan-alginate microparticles (“F14\_Low”) following 10x dilution in 0.9% NaCl (Bar= 100  $\mu\text{m}$ ).

Particle size and morphology are critical attributes for the intranasal delivery of vaccines.<sup>14,45,63–66</sup> It is generally accepted that 20–200 nm particles are taken up by receptor-mediated endocytosis, eliciting a cellular biased response, whereas particles of 0.2–5.0  $\mu\text{m}$  are predominantly phagocytosed, eliciting a humoral response.<sup>13,67,68</sup> Effective phagocytosis is also described for particles exceeding the 5  $\mu\text{m}$  threshold.<sup>69,70</sup> Besides particle size and morphology, other factors, such as particle surface charge and the mucoadhesion phenomena, influence the interactions between particles and the mucus.<sup>71</sup>

In this study, the obtained particles were below 30  $\mu\text{m}$ . The use of chitosan in the formulations markedly affected the surface charge of BCG, either by simple suspension or loaded into microparticles (Table 2). Chitosan is a cationic biodegradable polymer thoroughly studied for the preparation of both nano- and microparticulate drug and vaccine delivery systems. It has amine groups that are responsible for its overall electropositive charge and for its properties, such as permeability enhancement and mucoadhesiveness.<sup>50,72</sup> As a consequence of the strong positive charge of chitosan,

BCG suspended in chitosan presented a strongly positive surface charge, with zeta potential values of  $+90.6 \pm 3.5$  mV. Regarding BCG-loaded chitosan-alginate microparticles, the obtained zeta potential values were markedly inferior ( $-10.7 \pm 2.4$  mV). This is due to the ionic complexation between alginate and chitosan, which occurs due to interactions between carboxyl groups ( $-\text{COOH}$ ) of alginate and amine groups ( $-\text{NH}_2$ ) of chitosan.<sup>59,60,73</sup> As a result, there are also changes in the FT-IR spectra in the transmittance bands of the amino groups, carboxyl groups, and amide bonds (Fig. 4).

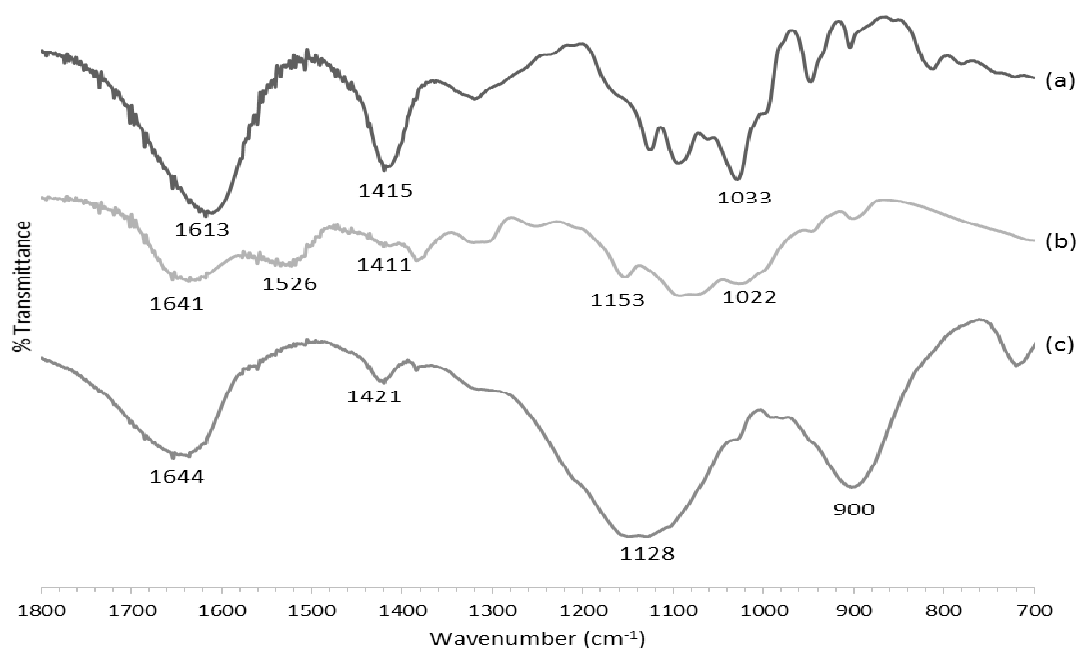


**Figure 4** – FT-IR spectra of solid (a) alginate, (b) chitosan, and (c) chitosan-alginate microparticles produced with alginate:chitosan mass ratio of 1:1 at pH 5.4. Bands wave numbers ( $\text{cm}^{-1}$ ) are as follows: 1641 (amide bond), 1613 (symmetric  $\text{COO}^-$  stretching vibration), 1526 (strong protonated amino peak – from partial N-deacetylation of chitin), and 1415 (asymmetric  $\text{COO}^-$  stretching vibration).

The FT-IR spectra of pure alginate (Fig. 4a) showed carboxyl peaks near  $1613 \text{ cm}^{-1}$  and  $1415 \text{ cm}^{-1}$ , which were broadened and slightly shifted from  $1613$  to  $1644 \text{ cm}^{-1}$  and from  $1415$  to  $1421 \text{ cm}^{-1}$  after complexation with chitosan, as seen in the FT-IR spectra of chitosan-alginate microparticles (Fig. 4c). The FT-IR spectra of pure chitosan (Fig. 4b) also showed a peak of amide bond at  $1641 \text{ cm}^{-1}$  and a protonated amino peak at  $1526 \text{ cm}^{-1}$ , which shifted by few  $\text{cm}^{-1}$  after complexation with alginate into a singlet band at  $1644 \text{ cm}^{-1}$ . Moreover, the peak of amino groups of chitosan at  $1153 \text{ cm}^{-1}$  (Fig. 4b) was slightly shifted to  $1128 \text{ cm}^{-1}$  after complexation with alginate (Fig. 4c), thus, suggesting an effective interaction between polymers. The observed shifts on maximum infrared peaks observed between individual polyelectrolytes and final

microparticle carriers were understood as ionic interactions, which led to the formation of new chemical entities with different absorption properties.

The singularity of the BCG vaccine here described lies on vaccine being composed by uniquely aqueous soluble substances. This will enable vaccine production by relatively straightforward ionic gelation procedures.

### 3.2. Association efficiency

In this study, the percentage of association efficiency (A.E.) was determined by cell count number using rBCG-GFP cells, being  $61 \pm 7\%$  for BCG-loaded chitosan-alginate microparticles (Table 2). Cell count allowed the determination of the ratio between microparticle-associated cells and total cells. This method was chosen because neither centrifugation nor microfiltration were optional in this situation, due to the unwanted compromise of cell viability and the microparticle size range, respectively.

The A.E. value was lower than the obtained before ( $76.0 \pm 1.4\%$  to  $84.0 \pm 3.4\%$ ) with the same formulation prepared by the same method (see Chapter 2, section 3.1.4, Table 10 and Fig. 19). These differences might be due to several reasons. In this study, we used a non-inactivated form of BCG instead of heat-killed BCG. Moreover, concentration of BCG used this time was approximately a 1-log higher. Although previous results indicated increasing A.E. in a concentration-dependent manner, a plateau might have been achieved within the herein used BCG concentration range. Also, in this study we have determined the initial concentration of BCG bacilli in suspension by two independent methods, namely, optical density and cell count, which led as to the conclusion that OD gave an upper estimative of CFU/mL, thus, a conversion factor was introduced in all calculations, leading to lower A.E. values. Finally, due to the high content of complex lipids present in the BCG's cell wall, uniform and reproducible microencapsulation results are difficult to achieve.

Results evidence that the use of polymer blend chitosan-alginate enabled efficient BCG microencapsulation while strongly affecting BCG surface charge. Taking into consideration our aim at microencapsulating BCG for immunization purposes, our target BCG concentration is  $10^7$  CFU/mL.<sup>27,74,75</sup> Thus, 61% A.E. is as a good result, as it corresponds in our formulation to  $8.6 \times 10^7$  CFU/mL.

### 3.3. BCG cell viability

BCG bacilli viability is an important factor in the development of an effective vaccine based on multigenicity and cell capability to be taken up by APC, namely, alveolar macrophages and dendritic cells, the cell host reservoirs for *Mycobacterium tuberculosis*. The protective efficacy of the BCG vaccine depends on bacilli access and replication in the host and consequent activation of CD4 and CD8 T lymphocyte populations capable of secreting IFN- $\gamma$ .<sup>76,77</sup> Many techniques used to prepare particulate systems, such as spray drying and solvent evaporation, can lead to the compromise of cell viability due to exposure to harsh conditions (i.e. heat, organic solvents, high shear) during formulation steps.<sup>78</sup>

As such, in this study we used only mild conditions and biocompatible polymers to encapsulate whole live attenuated BCG into chitosan-alginate microparticles by ionic gelation method. Cell viability was investigated during three weeks by a micro-CFU assay following standard procedure, as previously described (section 2.4). Based on the fact that activation of naïve T cells occurs in the presence of live bacteria, and that effector cells develop with expected kinetics within nine days, while cellular immune response takes 18 to 20 days to reach an effective level and stop bacterial growth,<sup>12</sup> we postulated that sufficient viable BCG should be maintained in vaccine formulation for three weeks so that suitable interaction with alveolar macrophages could take place and adequate immune responses elicited.

Figure 5 illustrates the obtained results, showing that viable cell number decreased approximately 1 log after 3 weeks for BCG-loaded chitosan-alginate microparticles and for BCG suspended in 0.025% chitosan, the latter being in accordance with previously obtained results for strains BCG Pasteur and rBCG-GFP suspended in chitosan, determined by cell count by regular plating (Chapter II, section 3.5.1, Fig. 19). Overall, the microencapsulation procedures preserved BCG integrity and viability, as there were no statistically significant differences ( $P=0.6314$ ) in cell viability losses between BCG-loaded microparticles and BCG suspended in 0.025% chitosan or in 0.9% NaCl.

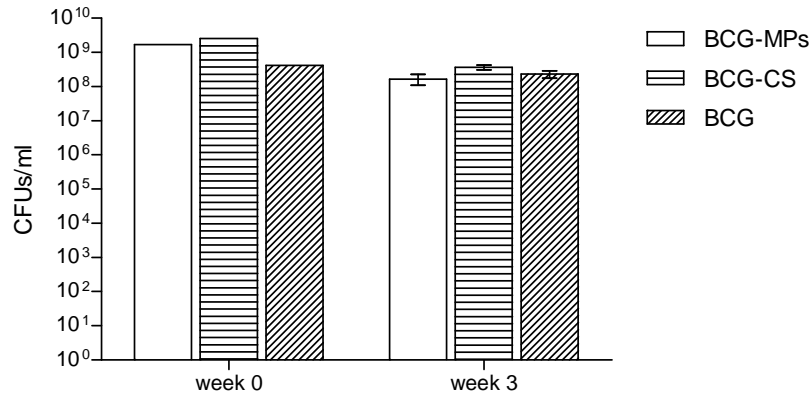


**Figure 5** – Cell number of BCG Pasteur following microencapsulation in “F14\_Low” chitosan-alginate microparticles (no fill), BCG suspension in 0.025% low molecular weight chitosan weight (horizontal lines), or BCG suspension in 0.9% NaCl (angled lines), after storage at 4°C. Results are expressed as mean  $\pm$  S.D.; n=3.

Although *in vitro* data do not always correlate with *in vivo* complex phenomena, this assay provided a deeper understanding of the expected behavior of our delivery systems. Since we aim at delivering 10<sup>7</sup> CFU/mL of BCG by intranasal immunization (as abovementioned), and taking into consideration the obtained A.E. value (61%), BCG concentration range that should be used in vaccine preparation was settled.

Regarding the micro-CFU method, it allowed maximizing the resources for counting CFU, since a single agar plate may hold several drops of the suspension, thus, reducing the number of plates needed, while enabling colonies count using a microscope, which reduces the time needed to form colonies visible by eye. This is a great advantage for slow growing bacteria, such as *Mycobacterium bovis*, as performing conventional CFU assays is both expensive and time consuming.<sup>58</sup> *M. bovis* require at least a month of incubation, since they take about 20-24 h to divide, and, on a plate, a single individualized bacterium takes 3-4 weeks to generate a visible colony.

### 3.4. Interaction with antigen presenting cells

Macrophage cell cultures *in vitro* are a suitable model to study mycobacteria-host interaction.<sup>57</sup> Generally, THP-1 humane derived macrophages are described to be less efficient than other macrophage cell lines (such as murine J774 macrophages) in bacteria internalization, whereas *M. bovis* BCG is described to be less internalized by macrophages than virulent strains of *M. bovis*.<sup>57,79</sup> As such, preliminary *in vitro* studies were performed for evaluation of BCG cellular uptake by human macrophages using a

differentiated THP-1 cell line and a recombinant BCG mycobacteria expressing Green Fluorescent Protein (rBCG-GFP).<sup>58</sup>

Three different formulation preparations containing BCG were evaluated within a multiplicity of infection (MOI) ranging from 0.2 to 192, i.e., bacterial load per macrophage. The infection of macrophages by BCG was evaluated at 1 hour and 18 hours after infection (pulse phase of the experiment). Fluorescence microscopy (Zeiss Axioskop 4.0 fluorescence microscope), and image analysis using free software ImageJ, allowed a reasonable evaluation of both quantitative and qualitative aspects of this model of interaction. The results are depicted in Fig. 6.

Individual rBCG-GFP bacilli are around 2  $\mu\text{m}$  long and 0.2  $\mu\text{m}$  of diameter.<sup>58</sup> Using 40x and 100x objectives (Zeiss) with a very high optical aperture and oil immersion, it was possible to observe individual GFP expressing bacteria inside THP-1 cells. In our experiments, high bacterial load was observed in macrophage cell cultures infected with BCG after 1 hour of pulse at estimated MOI of 0.2 for BCG-loaded microparticles (Fig. 6A), and after 18 hours of pulse at estimated MOI of 38 for BCG suspended in 0.025% low molecular weight chitosan (Fig. 6D). Lower bacterial loads were obtained when higher MOI was used (Fig. 6C and 6E). We attribute this to the observed clumped bacteria that were predominant at these higher bacterial loads.

Bacterial clumps are formed due to the presence of complex glycolipids in mycobacteria cell wall. The formation of bacteria clumps must be avoided because they are promptly degraded in phago-lysosomes within macrophages. In contrast, monodispersed bacteria persist in macrophage phagosomes, leading to distinct pro-inflammatory events and an improved antigen presentation.<sup>57</sup> BCG microencapsulation and BCG suspension in chitosan appear to have contributed in some extent for BCG monodispersion. Indeed, it was possible to distinguish macrophages containing mainly unicellular bacteria (Fig. 6A and 6D) and macrophages containing more aggregated/clumped bacteria, especially when a higher MOI was used (Fig. 6C and 6E).

Overall, our model showed to be adequate for the assessment of interaction of BCG with human macrophages and cellular uptake. One limitation of the used quantification method was the use of a single focal plan, which gives a biased result, as observed bacteria can be dispersed/adsorbed to the host cell, and not inside the cell, as apparent in Fig. 6B. In order to enhance image resolution, confocal microscopy can be used.<sup>58</sup>

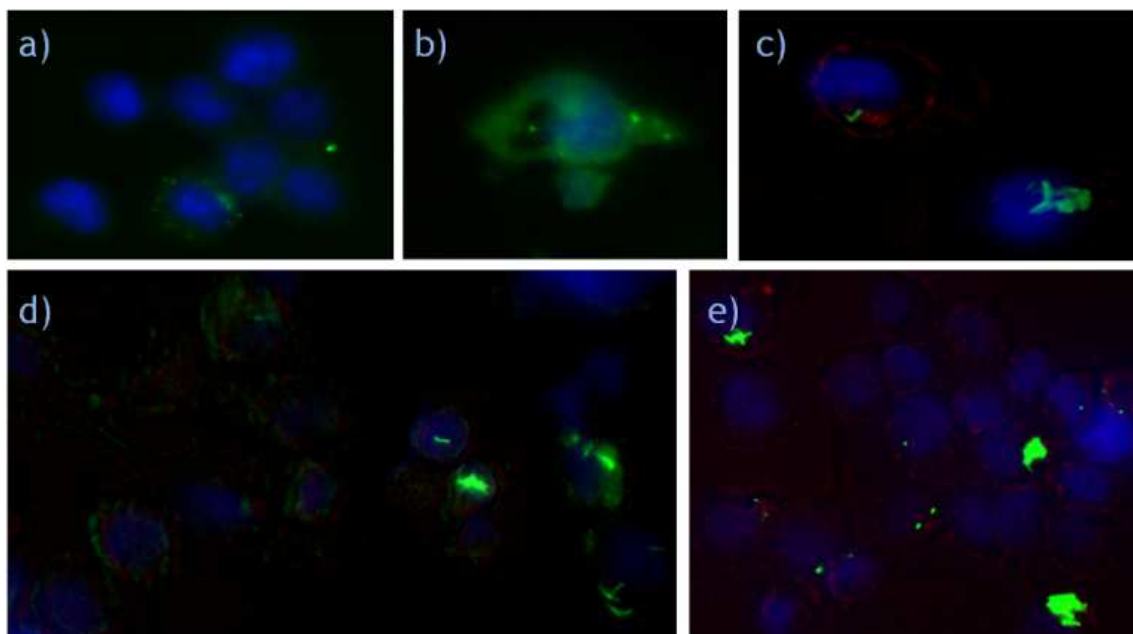


**Figure 6** – Microscopy images of THP-1 macrophage cultures infected with rBCG–GFP in a 24-well microplate at 1h (A and B) and 18h (C, D and E) after infection. (A) BCG-loaded *F13\_Medium* (ALG/CS mass ratio of 0.8:1) microparticles (MOI = 0.2; 1h pulse) (amp 100x). (B) BCG suspended in 0.9% NaCl (MOI = 0.2; 1h pulse) (amp 40x). (C) BCG suspended in 0.025% low molecular weight chitosan (MOI = 192; 18h pulse) (amp 100x). (D) BCG suspended in 0.025% low molecular weight chitosan (MOI = 38; 18h pulse) (amp 100x). (E) BCG suspended in 0.9% NaCl (MOI = 192; 18h pulse) (amp 100x). Blue: nucleus labelled using 4'-6'-diamidino-2-phenylindole (DAPI, Sigma); Red: lysosomal compartments visualised with Lysotracker™ red; Green: Green Fluorescent Protein (GFP) expressing bacteria.

Presence of bacterial clumps hampers the assessment of the real number of bacilli per macrophage, which is determinant for the signalling of innate immune responses. In order to avoid bacterial aggregation, Tween 80 was added to bacterial suspension prior to vaccine formulation, as previously described (section 2.3.). Persistent clumps of bacteria were then removed by ultrasonication and passage of the bacterial suspension through a 23 gauge needle, as adapted from previously described method.<sup>58</sup> In order to reassess the relations between particle size, surface charge and composition, and cellular uptake, three different formulation preparations containing BCG were evaluated (section 3.1, Table 2). The formulations were incubated with differentiated THP-1 macrophage cell cultures for 24 hours and intracellular bacterial load was determined by fluorescence microscopy. Manual cell count in a Neubauer chamber was used as confirmation method. The results are presented in Fig. 7 and Fig. 8.

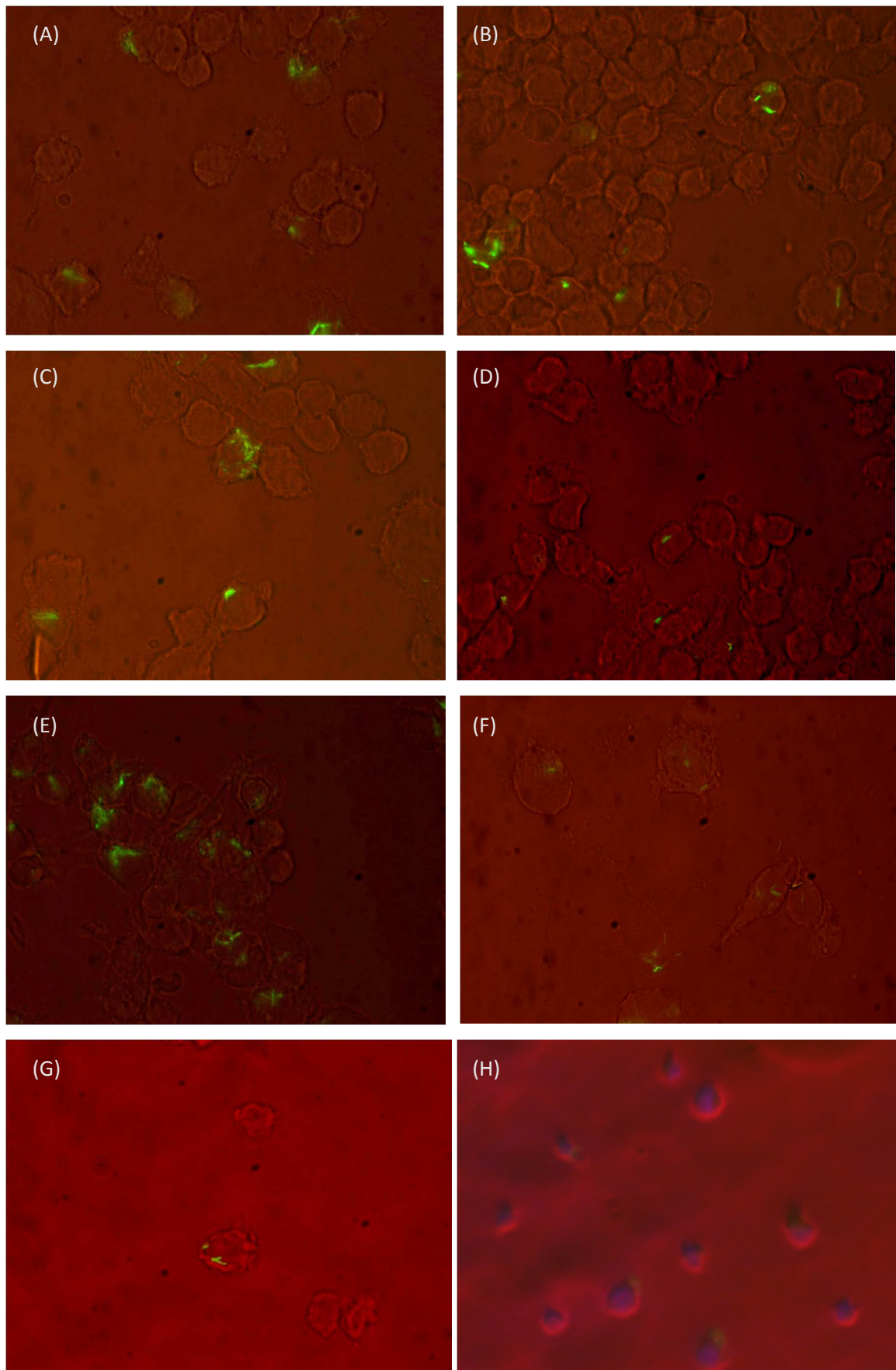


**Figure 7** – Microscopy images of THP-1 macrophage cultures infected with rBCG-GFP in a 24-well microplate 24h after infection (amp 100x). (A) and (B) BCG suspended in 0.9% NaCl (MOI

= 38). (C) BCG suspended in 0.9% NaCl (MOI = 192). (D) and (E) BCG suspended in 0.025% low molecular weight chitosan (MOI = 38). (F) BCG suspended in 0.025% low molecular weight chitosan (MOI = 192). (G) and (H) BCG-loaded *L14* microparticles (ALG/CS mass ratio of 1:1) (MOI = 2). Blue: nucleous labelled using 4'-6'-diamidino-2-phenylindole (DAPI, Sigma); Red: lysosomal compartments visualized with Lysotrack™ red; Green: Green Fluorescent Protein (GFP) expressing bacteria.

Overall, it was possible to distinguish macrophages containing mainly unicellular bacteria, thus, showing the adequacy of the used monodispersion techniques. Regarding the effect of the formulation on cellular uptake, microencapsulated BCG (Fig. 7G and 7H) accounted for an inferior intracellular bacterial load compared to BCG suspended in chitosan (Fig. 7D, 7E and 7F) or plain BCG (Fig. 7A, 7B and 7C). This is probably due to the increased microparticle mean diameter, which was 5-6 times superior to the length of single bacilli, thus, allowing the load of multiple bacteria per particle. The increased particle mean diameter results in inferior available surface area, leading to fewer BCG bacilli available for macrophages recognition. Moreover, the MOI used for BCG-loaded microparticles (MOI=2) was inferior to the lower MOI used for both BCG suspended in chitosan and BCG suspended in NaCl (MOI=38), which might have been sub-optimal. Future studies must be, therefore, conducted with harmonized MOI for each set of conditions.

Different particle surface charge may have also contributed for differences in cellular uptake among the BCG formulations. While most authors refer the potential of positively charged nano- and microparticles to foster cellular uptake,<sup>17,47,48,80</sup> Brandhonneur *et al.* showed up to two- to four-fold increased uptake by macrophages of negatively charged microparticles (-26 to -51 mV) in comparison to cationic PLL-grafted microspheres, greatly dependent on particle-to-cell ratio.<sup>81</sup> In our studies, cellular uptake was approximately 2-fold higher for positively charged BCG suspended in chitosan than for negatively charged BCG-loaded chitosan-alginate microparticles (Fig. 8).

BCG suspended in chitosan might enhance cellular uptake as a result of the ionic interactions established between positively charged particles and the negative charge of cell membrane. These results are in accordance with previous reports describing the advantages of using chitosan derivatives to manipulate particle surface charge to facilitate vaccine targeting.<sup>39,82</sup> Several authors have also described the ability of chitosan to enhance the immunogenicity of intranasal administered vaccines, such as influenza.<sup>37,53</sup>

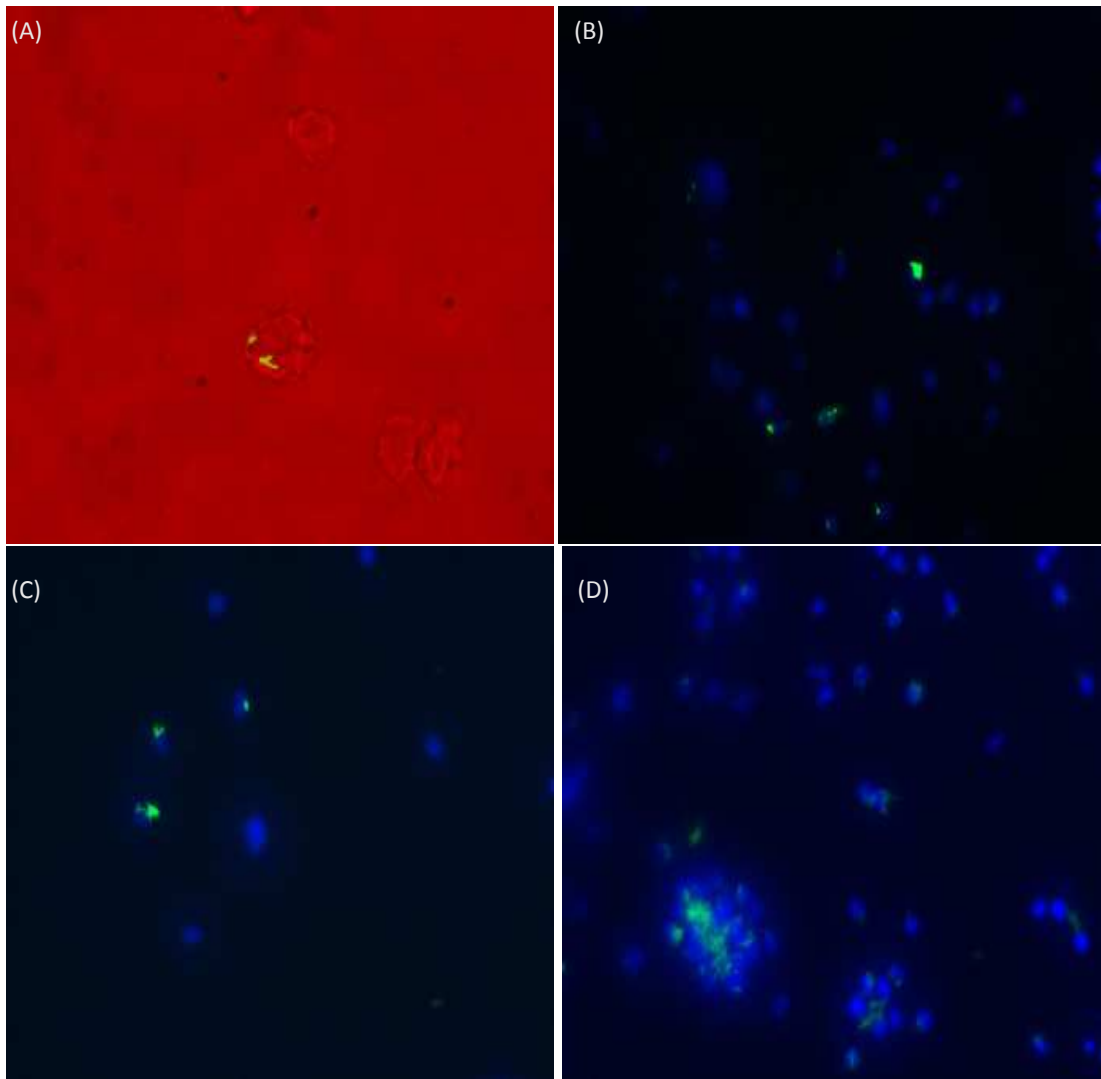
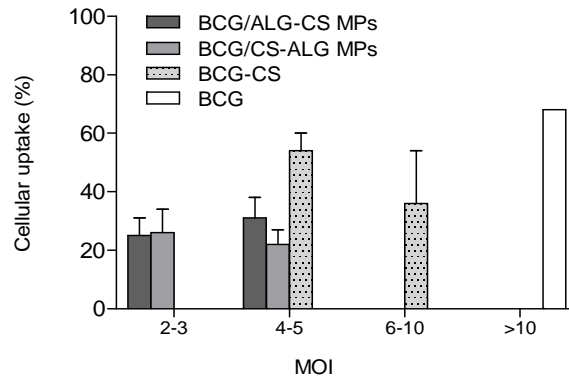


**Figure 8** – Intracellular bacterial load in THP-1 macrophage cultures 24h post-infection. (A) BCG-loaded ALG/CS microparticles (dark grey column); (B) BCG-loaded CS/ALG microparticles (light grey column); (C) BCG suspended in 0.025% LMW chitosan (dotted light grey column); (D) BCG suspended in 0.9% NaCl with 0.025% Tween™ 80 (no fill column). Results are expressed as mean  $\pm$  S.D; n=5. Multiplicity of Infection: MOI = n BCG-GFP cells / n THP-1 cells. Inset: BCG internalized by THP-1 cells observed with fluorescence microscopy.

Although BCG microencapsulation may not be as effective as BCG suspension in chitosan regarding cellular uptake, the use of BCG-loaded chitosan-alginate microparticles might contribute to an increased residence time of BCG antigens within intracellular environment, due to the modified erosion kinetics of chitosan-alginate microparticles, thus, leading to a prolonged immune response.

### 3.5. Immune response in mice

The mouse model has been widely used to proof-of-concept testing for immunogenicity studies, namely, level of antibody production, class and subclass characterization of antibodies, cell-mediated immunity, and duration of the immune response. Mice and rats are useful models for intranasal administration studies, with administration of the test article limited to droplets.<sup>83–85</sup>

In this preliminary *in vivo* study, two groups of female BALB/c mice were immunized by intranasal route with the BCG vaccine in order to assess the immunogenicity of the positively charged BCG (suspended in chitosan) and the negatively charged chitosan-alginate microparticles loaded with BCG. In order to determine the effect of immunization route on immune response, two additional groups of mice were immunized with plain BCG by either intranasal or subcutaneous route.

Both negatively and positively charged BCG stimulated the secretion of high and increasing levels of *M. bovis*-specific antibodies at all time points after 14 weeks of priming (Fig. 9). Intranasal vaccination with BCG vaccine resulted in a strong response for both IgG isotypes, IgG1 and IgG2a, being higher than responses elicited by BCG vaccine administered by subcutaneous route.

The IgG2a response was markedly higher after the 14th week for i.n. vaccines. The IgG2a response in BCG-loaded microparticles was lower in the first 14 weeks, but at the 16th week it reached similar levels to those of IgG1. This is shown clearer in the plot of the concentration ratio between the two isotypes (IgG2a/IgG1) of Fig. 10, where the concentration ratio is unitary or higher than unit beyond the 14th week for i.n. vaccines, whereas s.c. BCG vaccine resulted in a ratio  $<1$  due to a lower IgG2a response.

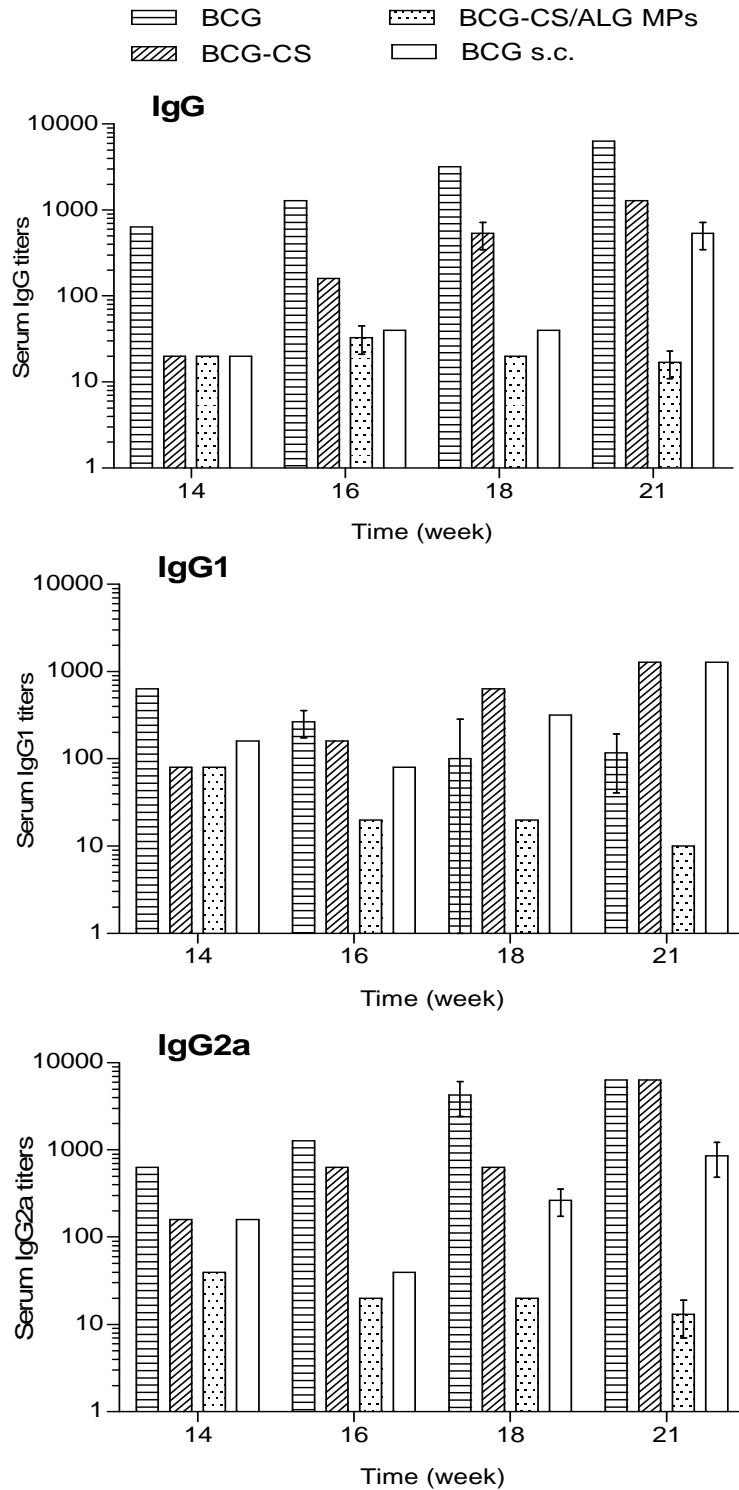


**Figure 9** – Serum anti-*M. bovis* specific IgG, IgG1 and IgG2a titers after immunization by i.n. route of female BALB/c mice with BCG suspended in 0.9% NaCl (horizontal lines), BCG suspended in 0.025% low molecular weight chitosan (angled lines), BCG-loaded *L14* chitosan-alginate microparticles (ALG/CS mass ratio 1:1) (dotted), and subcutaneously administrated BCG suspended in 0.9% NaCl (no fill). Titres reported are the reciprocal of serum dilutions that gave an optical density  $2 \times$  S.D. higher than the strongest negative control group (mean  $\pm$  S.D.;  $n=4$ ).

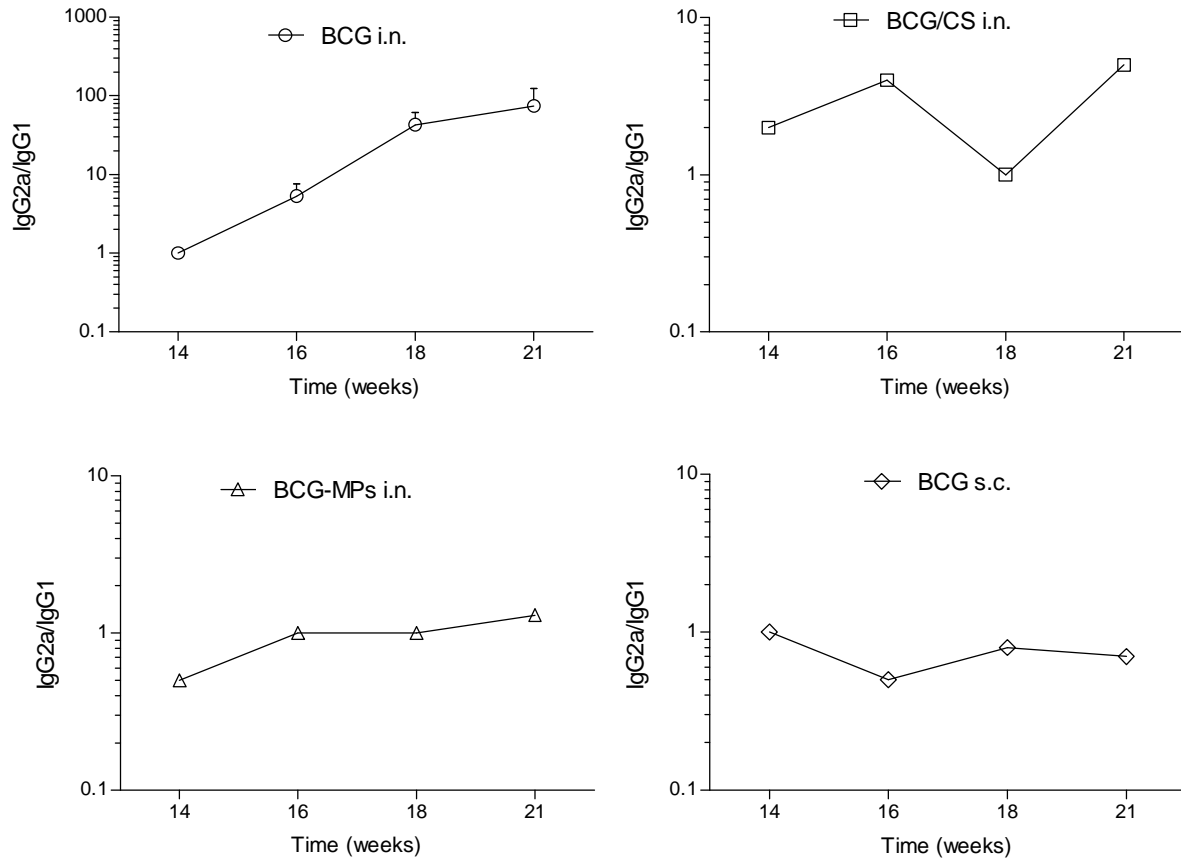


**Figure 10** – Ratio of serum anti-*M. bovis* specific IgG2a and IgG1 titers after immunization by intranasal (i.n.) or subcutaneous (s.c.) route of female BALB/c mice with the BCG vaccine (mean  $\pm$  S.D.; n=3). Titres reported are the reciprocal of serum dilutions that gave an optical density 2 x S.D. higher than the strongest negative control group, determined in 3 replicates per group.

In order to assess the success of the mucosal immunization, local sIgA levels in the lungs were evaluated. The secretory IgA concentration in lung extracts was higher for the positively charged BCG (suspended in chitosan), as Fig. 11 illustrates. Differences among all the vaccinated groups were not statistically different ( $P = 0.093$ ).

The results show that intranasal immunization with the BCG generated a sustained, well-balanced and broad immune response in mouse model, with a strong response for both IgG subtypes. The anti-*M. bovis* specific IgG secretion was high with a well-balanced ratio (IgG2a/IgG1) between both isotypes (approximately 1.0) for BCG-loaded microparticles. This reveals that microencapsulation of BCG enabled the stimulation of both Th1 and Th2 helper T cells, as IgG2a isotype is related to a Th1 response, whereas IgG1 isotype antibodies are predominant in a Th2 pathway. These results were important for considering microparticles effective for whole live bacterial vaccine encapsulation and intranasal delivery.

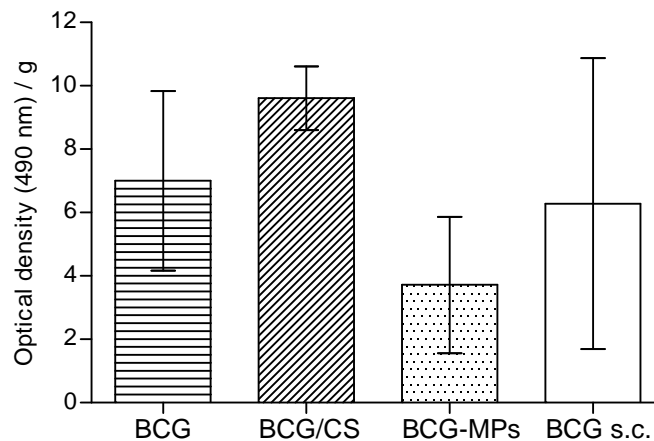


**Figure 11** – Secretory IgA (sIgA) levels in lungs homogenates (normalized per gram) of mice immunized by intranasal route with BCG suspended in 0.9% NaCl (horizontal lines), BCG suspended in 0.025% low molecular weight chitosan (angled lines), BCG-loaded *L14* chitosan-alginate microparticles (ALG/CS mass ratio 1:1) (dotted), and subcutaneously administrated BCG suspended in 0.9% NaCl (no fill) (mean  $\pm$  S.D.; n=4).

Positively charged BCG (suspended in chitosan) was able to evoke a more predominant cellular Th1 type immune response. The effective stimulation of Th1 was probably due to an adjuvant effect of chitosan, which is described to increase antigen bioavailability due to its mucoadhesion and capacity to promote the paracellular transport by opening tight junctions between cell.<sup>86,87</sup> These mechanisms are related to chitosan's positive charge, which favors the interaction with the negatively charged mucus layer. A strong interaction between mucus and positively charged particles will contribute to decrease the particle clearance from nasal mucosa, leading to a better uptake at the nasal epithelium and NALT and subsequent access of the vaccine to sub-mucosal lymphoid tissues. Particles composed of chitosan can, therefore, act as a strong immunostimulator for locally administered vaccines. This correlates with previously reported immunostimulatory properties of chitosan by our group, demonstrating that polymeric nanoparticles were able to stimulate humoral and also substantial cellular immune response when compared with soluble antigen.<sup>46,48</sup> The generation of a dominant Th1 profile as a consequence of pre-exposure immunization may facilitate the eradication of intracellular pathogens, contributing for a successful prevention against tuberculosis.<sup>88–90</sup>

The differences obtained for immune responses between positively charged BCG (suspended in chitosan) and microencapsulated BCG are probably due to not only differential surface charge, but also differences in particle size distribution between the two proposed delivery systems. As aforementioned, microencapsulation of BCG led to

the upload of multiple bacilli per particle, as monodispersion was not totally efficient in obtaining single bacilli in suspension. Therefore, the available surface area of BCG when microencapsulated is limited in comparison with BCG suspended in chitosan. Moreover, alginate-coated chitosan particles have been successfully used by intranasal route for delivery of hepatitis B surface antigen and CpG, ensuing a Th1 specific immune response, but a weak mucosal immune response compared to chitosan particles. This was speculated to be due to the weak mucoadhesive properties of alginate-coated chitosan particles.<sup>91</sup> In spite of the relative efficacy, i.n. administration of BCG, either suspended in chitosan or loaded into polymeric microparticles, resulted in a consistent immune response emerging as promising agents for the cellular immune response stimulation.

The local production of secretory IgA (sIgA) is believed to be very important against mucosal pathogens, establishing a first defence line at the mucosal surface blocking the pathogen adhesion. A well-established local immune response plays a very important role in immunization against intracellular pathogens, such as *M. tuberculosis*, being more effective in terms of protection than systemic antibodies. Here lies a major limitation of for most licensed vaccines, including current BCG vaccine, which are unable to stimulate local antibody secretion at the infection site.<sup>92-94</sup> Our results indicate that intranasal vaccination was effective at induction of local immunization, with sIgA levels higher for two of the three i.n. administered BCG formulations, in comparison to s.c. vaccine (Fig. 11).

Positively charged vaccine (BCG suspended in chitosan) was the most successful in stimulating IgA-secreting cells of the nasal-associated lymphoid tissue (NALT) and/or draining lymph nodes, in addition to their effective systemic stimulation. Chitosan properties of mucoadhesion might have a key role increasing the nasal residence time of the bacilli, due to resistance to mucociliary clearance in the nose. Ionic interaction, hydrogen bonds and Van der Waals interactions between the polymer and the mucosal layer promote the interpenetration phenomena,<sup>95</sup> whereas chitosan's immunostimulating activity leads to macrophage accumulation and activation, promoting resistance to infection and stimulating the cellular immune response, as previously demonstrated with different nasally administered vaccines using chitosan-based particulate carriers.<sup>48,62,96-98</sup> Therefore, the i.n. administration of positively charged BCG, herein described for the first time, appears to be a successful case regarding the elicited immune response in mouse model also for specific mucosal response.

One important limitation to consider regarding the intranasal delivery of BCG vaccine is the application method, as the gap between the mice nostril size and the applied volume will originate losses. Moreover, it is possible that during vaccine administration part of the dose is swallowed, leading to partial oral administration. Therefore, IgA levels should also be assessed on the intestines, in order to exclude oral administration effect.

## 4. Conclusions

In this study, the potential of BCG-loaded chitosan-alginate microparticles for the delivery of the vaccine to lung mucosa was investigated. The obtained results support chitosan-particulate system as a promising technological platform for i.n. vaccination. Live BCG was efficiently associated with chitosan and chitosan-alginate microparticles, with no compromise of cell viability, resulting in efficient cellular uptake by macrophages as model for antigen presenting cells, while performing with high biocompatibility.

Preliminary data from *in vivo* studies, obtained with the mouse model, confirmed a successful stimulation of both humoral and cellular immune responses. Both formulations, BCG suspended in chitosan and BCG-loaded chitosan-alginate microparticles, presented the ability to induce Th1-mediated immune responses characterized by high IgG2a antibody titers, as well as a Th2 immune response characterized mainly by IgG1 antibodies. Mucosal stimulation was confirmed by increased sIgA levels, particularly with positively charged BCG (prepared by BCG suspension in chitosan), probably due to the favorable combination of available surface area and mucoadhesive properties of this delivery system.

Our future strategy will be to combine polymeric microparticles with fatty acids as permeation enhancers. In order to boost mucopenetration of BCG-loaded microparticles and to promote inflammatory events within the macrophage, linoleic acid will be used.<sup>57,99</sup> Further *in vivo* studies should, therefore, include this new formulation, and also control groups with empty particles.

## **5. Acknowledgements**

The authors would like to thank Prof. Elsa Anes (FFUL) and her team (Dr. David Pires, Dr. Nuno Carmo) for BCG Pasteur strain supply and technical support. The authors thank iMed.Ulisboa for financial support (UID/DTP/04138/2013) from Fundação para a Ciência e Tecnologia (FCT), Portugal, and Escola Superior de Tecnologia da Saúde de Lisboa for financial support from merit scholarship for Ph.D. (ESTeSL-IPL/CGD/2012) granted by Caixa Geral de Depósitos, Portugal.

## 6. References

1. Bishai, W., Sullivan, Z., Bloom, B. R. & Andersen, P. Bettering BCG: a tough task for a TB vaccine? *Nat. Med.* **19**, 410–1 (2013).
2. Holmgren, J. & Czerkinsky, C. Mucosal immunity and vaccines. *Nat. Med.* **11**, S45–S53 (2005).
3. Pavot, V., Rochereau, N., Genin, C., Verrier, B. & Paul, S. New insights in mucosal vaccine development. *Vaccine* **30**, 142–54 (2012).
4. Baudner, B. C. & O'Hagan, D. T. Bioadhesive delivery systems for mucosal vaccine delivery. *J. Drug Target.* **18**, 752–770 (2010).
5. Caetano, L. A., Almeida, A. J. & Gonçalves, L. M. D. Approaches to Tuberculosis Mucosal Vaccine Development Using Nanoparticles and Microparticles: A Review. *J. Biomed. Nanotechnol.* **10**, 2295–2316 (2014).
6. Kaufmann, S. H. E., Hussey, G. & Lambert, P.-H. New vaccines for tuberculosis. *Lancet The* **375**, 2110–2119 (2010).
7. Kaufmann, S. H. E. Future vaccination strategies against tuberculosis: thinking outside the box. *Immunity* **33**, 567–577 (2010).
8. Ottenhoff, T. H. M. & Kaufmann, S. H. E. Vaccines against tuberculosis: where are we and where do we need to go? *PLoS Pathog.* **8**, e1002607 (2012).
9. World Health Organization. *WHO Global Tuberculosis Report 2013 Factsheet.* (2012).
10. Xing, Z. Importance of T-cell location rekindled: implication for tuberculosis vaccination strategies. *Expert Rev. Vaccines* **8**, 1465–8 (2009).
11. Källénus, G., Pawlowski, A., Brandtzaeg, P. & Svenson, S. Should a new tuberculosis vaccine be administered intranasally? *Tuberculosis* **87**, 257–66 (2007).
12. Cooper, A. M. Cell-mediated immune responses in tuberculosis. *Annu. Rev. Immunol.* **27**, 393–422 (2009).
13. Rice-Ficht, A. C., Arenas-Gamboa, A. M., Kahl-McDonagh, M. M. & Ficht, T. a. Polymeric particles in vaccine delivery. *Curr. Opin. Microbiol.* **13**, 106–12 (2010).
14. Bachmann, M. F. & Jennings, G. T. Vaccine delivery: a matter of size, geometry, kinetics and molecular patterns. *Nat. Rev. Immunol.* **10**, 787–96 (2010).
15. Mohanan, D. *et al.* Administration routes affect the quality of immune responses: A cross-sectional evaluation of particulate antigen-delivery systems. *J. Control. Release* **147**, 342–349 (2010).
16. Bhatt, K. & Salgame, P. Host innate immune response to *Mycobacterium tuberculosis*. *J. Clin. Immunol.* **27**, 347–62 (2007).
17. Thiele, L. *et al.* Evaluation of particle uptake in human blood monocyte-derived cells in vitro. Does phagocytosis activity of dendritic cells measure up with macrophages? *J. Control. Release* **76**, 59–71 (2001).
18. Borges, O. *et al.* Alginate coated chitosan nanoparticles are an effective subcutaneous adjuvant for hepatitis B surface antigen. *Int. Immunopharmacol.* **8**, 1773–80 (2008).
19. Lai, S. K., Wang, Y.-Y. & Hanes, J. Mucus-penetrating nanoparticles for drug and gene delivery to mucosal tissues. *Adv. Drug Deliv. Rev.* **61**, 158–71 (2009).
20. Woodrow, K. a, Bennett, K. M. & Lo, D. D. Mucosal vaccine design and delivery. *Annu. Rev. Biomed. Eng.* **14**, 17–46 (2012).
21. Caetano, L. A. Particulate delivery system for mucosal immunisation with *Mycobacterium bovis* bacille Calmette Guerin. (2013).
22. Esquisabel, A. *et al.* Preparation and stability of agarose microcapsules containing BCG. *J. Microencapsul.* **19**, 237–244 (2002).
23. Ouyang, W. *et al.* Artificial cell microcapsule for oral delivery of live bacterial cells for therapy: design, preparation, and in-vitro characterization. *J. Pharm. Pharm. Sci.* **7**, 315–24 (2004).

24. Arenas-Gamboa, A. M., Ficht, T. A., Kahl-McDonagh, M. M. & Rice-Ficht, A. C. Immunization with a Single Dose of a Microencapsulated *Brucella melitensis* Mutant Enhances Protection against Wild-Type Challenge. *Infect. Immun.* **76**, 2448–2455 (2008).
25. Aldwell, F. E. *et al.* Oral vaccination of mice with lipid-encapsulated *Mycobacterium bovis* BCG: anatomical sites of bacterial replication and immune activity. *Immunol. Cell Biol.* **83**, 549–53 (2005).
26. Aldwell, F. E. *et al.* Oral delivery of lipid-encapsulated *Mycobacterium bovis* BCG extends survival of the bacillus *in vivo* and induces a long-term protective immune response against tuberculosis. *Vaccine* **24**, 2071–8 (2006).
27. Clark, S. *et al.* Assessment of different formulations of oral *Mycobacterium bovis* Bacille Calmette-Guérin (BCG) vaccine in rodent models for immunogenicity and protection against aerosol challenge with *M. bovis*. *Vaccine* **26**, 5791–7 (2008).
28. Clark, S. O. *et al.* Oral delivery of BCG Moreau Rio de Janeiro gives equivalent protection against tuberculosis but with reduced pathology compared to parenteral BCG Danish vaccination. *Vaccine* **28**, 7109–16 (2010).
29. Kaufmann, S. H. & Hess, J. Immune response against *Mycobacterium tuberculosis*: implications for vaccine development. *J. Biotechnol.* **83**, 13–7 (2000).
30. Janes, K. A., Calvo, P. & Alonso, M. J. Polysaccharide colloidal particles as delivery systems for macromolecules. *Adv. Drug Deliv. Rev.* **47**, 83–97 (2001).
31. Love, R. J. & Jones, K. S. The recognition of biomaterials: Pattern recognition of medical polymers and their adsorbed biomolecules. *J. Biomed. Mater. Res. A* **101**, 2740–52 (2013).
32. Park, J. H., Saravanakumar, G., Kim, K. & Kwon, I. C. Targeted delivery of low molecular drugs using chitosan and its derivatives. *Adv. Drug Deliv. Rev.* **62**, 28–41 (2010).
33. Liu, Z., Jiao, Y., Wang, Y., Zhou, C. & Zhang, Z. Polysaccharides-based nanoparticles as drug delivery systems. *Adv. Drug Deliv. Rev.* **60**, 1650–62 (2008).
34. Costa, H. & Grenha, A. Natural carriers for application in tuberculosis treatment. *J. Microencapsul.* **30**, 295–306 (2013).
35. Suckow, M. A. *et al.* in *Polysaccharide Applications* (eds. El-Nokaly, M. A. & Soini, H. A.) **737**, 1–14 (1999 American Chemical Society, 1999).
36. van der Lubben, I. M., Verhoef, J. C., Borchard, G. & Junginger, H. E. Chitosan and its derivatives in mucosal drug and vaccine delivery. *Eur. J. Pharm. Sci.* **14**, 201–7 (2001).
37. Bacon, A. *et al.* Carbohydrate biopolymers enhance antibody responses to mucosally delivered vaccine antigens. *Infect. Immun.* **68**, 5764–5770 (2000).
38. Arca, H. C., Günbeyaz, M. & Senel, S. Chitosan-based systems for the delivery of vaccine antigens. *Expert Rev. Vaccines* **8**, 937–953 (2009).
39. Amidi, M., Mastrobattista, E., Jiskoot, W. & Hennink, W. E. Chitosan-based delivery systems for protein therapeutics and antigens. *Adv. Drug Deliv. Rev.* **62**, 59–82 (2010).
40. George, M. & Abraham, T. E. Polyionic hydrocolloids for the intestinal delivery of protein drugs: alginate and chitosan--a review. *J. Control. Release* **114**, 1–14 (2006).
41. Goycoolea, F. M., Lollo, G., Remuñán-López, C., Quaglia, F. & Alonso, M. J. Chitosan-alginate blended nanoparticles as carriers for the transmucosal delivery of macromolecules. *Biomacromolecules* **10**, 1736–43 (2009).
42. Anal, A. K., Bhopatkar, D., Tokura, S., Tamura, H. & Stevens, W. F. Chitosan-alginate multilayer beads for gastric passage and controlled intestinal release of protein. *Drug Dev. Ind. Pharm.* **29**, 713–24 (2003).
43. Caetano, L. A., Almeida, A. J. & Gonçalves, L. M. D. Modulation of *Mycobacterium bovis* Surface Properties using Alginate and Chitosan

- Microparticles for Mucosal Immunization. in *3rd Post-graduate iMed.UL Students Meeting* (ed. IpSC) 51 (PC51) (iMed.UL, 2011).
44. Caetano, L. A., Figueiredo, L., Almeida, A. J. & Gonçalves, L. M. D. Alginate-chitosan particulate delivery systems for mucosal immunization against tuberculosis. in *Bioengineering (ENBENG), 2012 IEEE 2nd Portuguese Meeting in I.I.*, 2 (Xplore, IEEE, 2012). doi:10.1109/ENBENG.2012.6331346
  45. Caetano, L. A., Amaral, R., Figueiredo, L., Almeida, A. J. & Goncalves, L. M. D. Chitosan-alginate microparticulate delivery system for an alternative route of administration of BCG vaccine. in *Bioengineering (ENBENG), 2013 IEEE 3rd Portuguese Meeting in 1–3* (2013). doi:10.1109/ENBENG.2013.6518391
  46. Rodrigues, M. A. *et al.* Development of a novel mucosal vaccine against strangles by supercritical enhanced atomization spray-drying of *Streptococcus equi* extracts and evaluation in a mouse model. *Eur. J. Pharm. Biopharm.* **82**, 392–400 (2012).
  47. Cadete, A. *et al.* Development and characterization of a new plasmid delivery system based on chitosan-sodium deoxycholate nanoparticles. *Eur. J. Pharm. Sci.* **45**, 451–8 (2012).
  48. Figueiredo, L., Cadete, A. & Gonçalves, L. M. D. Intranasal immunisation of mice against *Streptococcus equi* using positively charged nanoparticulate carrier systems. *Vaccine* **30**, 6551–6558 (2012).
  49. McNeela, E. A. *et al.* A mucosal vaccine against diphtheria: formulation of cross reacting material (CRM(197)) of diphtheria toxin with chitosan enhances local and systemic antibody and Th2 responses following nasal delivery. *Vaccine* **19**, 1188–1198 (2000).
  50. Sarmiento, B. *Chitosan-Based Systems for Biopharmaceuticals*. *Polymer* (2012 John Wiley & Sons, Ltd, 2012).
  51. Günbeyaz, M., Faraji, A., Ozkul, A., Puralı, N. & Senel, S. Chitosan based delivery systems for mucosal immunization against bovine herpesvirus 1 (BHV-1). *Eur. J. Pharm. Sci.* **41**, 531–45 (2010).
  52. Smith, J., Wood, E. & Dornish, M. Effect of chitosan on epithelial cell tight junctions. *Pharm. Res.* **21**, 43–9 (2004).
  53. Illum, L., Jabbal-Gill, I., Hinchcliffe, M., Fisher, a N. & Davis, S. S. Chitosan as a novel nasal delivery system for vaccines. *Adv. Drug Deliv. Rev.* **51**, 81–96 (2001).
  54. Vicente, S., Prego, C., Csaba, N. & Alonso, M. J. From single-dose vaccine delivery systems to nanovaccines. **20**, 267–276 (2010).
  55. Douglas, K. L. & Tabrizian, M. Effect of experimental parameters on the formation of alginate-chitosan nanoparticles and evaluation of their potential application as DNA carrier. *J. Biomater. Sci. Polym. Ed.* **16**, 43–56 (2005).
  56. Borges, O. *et al.* Immune response by nasal delivery of hepatitis B surface antigen and codelivery of a CpG ODN in alginate coated chitosan nanoparticles. *Eur. J. Pharm. Biopharm.* **69**, 405–16 (2008).
  57. Jordao, L., Bleck, C. K. E., Mayorga, L., Griffiths, G. & Anes, E. On the killing of mycobacteria by macrophages. *Cell. Microbiol.* **10**, 529–48 (2008).
  58. Bettencourt, P., Pires, D., Carmo, N. & Anes, E. in *Microscopy: Science, Technology, Applications and Education* (eds. Méndez-Vilas, A. & Díaz, J.) 614–621 (2010).
  59. Sarmiento, B., Ferreira, D., Veiga, F. & Ribeiro, a. Characterization of insulin-loaded alginate nanoparticles produced by ionotropic pre-gelation through DSC and FTIR studies. *Carbohydr. Polym.* **66**, 1–7 (2006).
  60. Pawlak, a & Mucha, M. Thermogravimetric and FTIR studies of chitosan blends. *Thermochim. Acta* **396**, 153–166 (2003).
  61. Dobakhti, F. *et al.* Adjuvanticity effect of sodium alginate on subcutaneously injected BCG in BALB/c mice. *Microbes Infect.* **11**, 296–301 (2009).
  62. Figueiredo, L., Calado, C. C. R., Almeida, A. J. & Gonçalves, L. M. D. Protein

- and DNA nanoparticulate multiantigenic vaccines against *H. pylori*: *in vivo* evaluation. in *2nd Portuguese BioEngineering Meeting* (ed. IEEE EMBS Portuguese Chapter) I.I, 1 (2012).
63. Almeida, A. J. & Alpar, H. O. Nasal delivery of vaccines. *J. Drug Target.* **3**, 455–467 (1996).
  64. Vajdy, M. & O'Hagan, D. T. Microparticles for intranasal immunization. *Adv. Drug Deliv. Rev.* **51**, 127–41 (2001).
  65. Vila, a. *et al.* PLA-PEG particles as nasal protein carriers: The influence of the particle size. *Int. J. Pharm.* **292**, 43–52 (2005).
  66. Slütter, B., Hagenaars, N. & Jiskoot, W. Rational design of nasal vaccines. *J. Drug Target.* **16**, 1–17 (2008).
  67. Ahsan, F., Rivas, I. P., Khan, M. A. & Torres Suárez, A. I. Targeting to macrophages: Role of physicochemical properties of particulate carriers - Liposomes and microspheres - On the phagocytosis by macrophages. *J. Control. Release* **79**, 29–40 (2002).
  68. Moghimi, S. M. *et al.* Particulate systems for targeting of macrophages: Basic and therapeutic concepts. *J. Innate Immun.* **4**, 509–528 (2012).
  69. Cannon, G. J. & Swanson, J. a. The macrophage capacity for phagocytosis. *J. Cell Sci.* **101** ( Pt 4, 907–913 (1992).
  70. Champion, J., Walker, A. & Mitragotri, S. Role of particle size in phagocytosis of polymeric microspheres. *Pharm. Res.* **25**, 1815–1821 (2008).
  71. Almeida, A. J. & Florindo, H. F. in *Nanostructured Biomaterials for Overcoming Biological Barriers* (eds. Alonso, M. J. & Csaba, N. S.) 117–133 (The Charlesworth Group, 2012).
  72. Leithner, K. & Bernkop-schn, A. in *Chitosan-Based Systems for Biopharmaceuticals* (eds. Sarmiento, B. & Neves, J.) 159–180 (2012 John Wiley & Sons, Ltd, 2012).
  73. Simsek-Ege, F. a., Bond, G. M. & Stringer, J. Polyelectrolyte complex formation between alginate and Chitosan as a function of pH. *J. Appl. Polym. Sci.* **88**, 346–351 (2003).
  74. Aldwell, F. E. *et al.* Oral vaccination with *Mycobacterium bovis* BCG in a lipid formulation induces resistance to pulmonary tuberculosis in brushtail possums. *Vaccine* **22**, 70–76 (2003).
  75. Dorer, D. E. *et al.* Lymphatic tracing and T cell responses following oral vaccination with live *Mycobacterium bovis* (BCG). *Cell. Microbiol.* **9**, 544–53 (2007).
  76. Olsen, a. W., Brandt, L., Agger, E. M., Van Pinxteren, L. a H. & Andersen, P. The influence of remaining live BCG organisms in vaccinated mice on the maintenance of immunity to tuberculosis. *Scand. J. Immunol.* **60**, 273–277 (2004).
  77. Kaveh, D. a, Carmen Garcia-Pelayo, M. & Hogarth, P. J. Persistent BCG bacilli perpetuate CD4 T effector memory and optimal protection against tuberculosis. *Vaccine* **32**, 6911–6918 (2014).
  78. Agnihotri, S. a, Mallikarjuna, N. N. & Aminabhavi, T. M. Recent advances on chitosan-based micro- and nanoparticles in drug delivery. *J. Control. Release* **100**, 5–28 (2004).
  79. Anes, E. *et al.* Dynamic life and death interactions between *Mycobacterium smegmatis* and J774 macrophages. *Cell. Microbiol.* **8**, 939–60 (2006).
  80. Foged, C., Brodin, B., Frokjaer, S. & Sundblad, A. Particle size and surface charge affect particle uptake by human dendritic cells in an *in vitro* model. *Int. J. Pharm.* **298**, 315–22 (2005).
  81. Brandhonneur, N. *et al.* Specific and non-specific phagocytosis of ligand-grafted PLGA microspheres by macrophages. *Eur. J. Pharm. Sci.* **36**, 474–485 (2009).
  82. Jabbal-Gill, I., Watts, P. & Smith, A. Chitosan-based delivery systems for mucosal vaccines. *Expert Opin. Drug Deliv.* **9**, 1051–67 (2012).

83. European Medicines Agency. *Note for guidance on preclinical pharmacological and toxicological testing of vaccines*. London: EMEA (1997). at <[http://www.ema.europa.eu/docs/en\\_GB/document\\_library/Scientific\\_guideline/2009/10/WC500004004.pdf](http://www.ema.europa.eu/docs/en_GB/document_library/Scientific_guideline/2009/10/WC500004004.pdf)>
84. WHO Expert Committee on Biological Standardization. *Guidelines on the nonclinical evaluation of vaccine adjuvants and adjuvanted vaccines* ©. (2014).
85. Babiuk, V. G. S. van D. L. den H. P. J. G. L. A. Use of animal models in the development of human vaccines. *Future Microbiol.* **2**, 667–675 (2007).
86. Baudner, B. C. *et al.* The concomitant use of the LTK63 mucosal adjuvant and of chitosan-based delivery system enhances the immunogenicity and efficacy of intranasally administered vaccines. *Vaccine* **21**, 3837–3844 (2003).
87. Dodane, V., Amin Khan, M. & Merwin, J. R. Effect of chitosan on epithelial permeability and structure. *Int. J. Pharm.* **182**, 21–32 (1999).
88. Abebe, F. & Bjune, G. The protective role of antibody responses during *Mycobacterium tuberculosis* infection. *Clin. Exp. Immunol.* **157**, 235–43 (2009).
89. Forbes, E. K. *et al.* Multifunctional, high level cytokine producing Th1 cells in the lung, but not spleen, correlate with protection against *Mycobacterium tuberculosis* aerosol challenge in mice. *J. Immunol.* **181**, 4955–4964 (2008).
90. Igietseme, J. U., Eko, F. O., He, Q. & Black, C. M. Antibody regulation of Tcell immunity: implications for vaccine strategies against intracellular pathogens. *Expert Rev. Vaccines* **3**, 23–34 (2003).
91. Borges, O. Alginate coated chitosan nanoparticles as adjuvant for mucosal vaccination with hepatitis B antigen. (Coimbra University, 2007).
92. Corthésy, B. Role of secretory immunoglobulin A and secretory component in the protection of mucosal surfaces. *Future Microbiol.* **5**, 817–829 (2010).
93. Brandtzaeg, P. Induction of secretory immunity and memory at mucosal surfaces. *Vaccine* **25**, 5467–84 (2007).
94. Reljic, R., Williams, A. & Ivanyi, J. Mucosal immunotherapy of tuberculosis: is there a value in passive IgA? *Tuberculosis (Edinb)*. **86**, 179–90 (2006).
95. Khutoryanskiy, V. V. Advances in mucoadhesion and mucoadhesive polymers. *Macromol. Biosci.* **11**, 748–764 (2011).
96. Read, R. C. *et al.* Effective nasal influenza vaccine delivery using chitosan. *Vaccine* **23**, 4367–4374 (2005).
97. Porporatto, C., Bianco, I. D. & Correa, S. G. Local and systemic activity of the polysaccharide chitosan at lymphoid tissues after oral administration. *J. Leukoc. Biol.* **78**, 62–69 (2005).
98. Florindo, H. F., Pandit, S., Goncalves, L., Alpar, H. O. & Almeida, A. J. New approach on the development of a mucosal vaccine against strangles: Systemic and mucosal immune responses in a mouse model. *Vaccine* **27**, 1230–1241 (2009).
99. Vicente, S. *et al.* A polymer/oil based nanovaccine as a single-dose immunization approach. *PLoS One* **8**, e62500 (2013).

## ***Chapter IV***

---

***Humoral and cellular immune responses in mice following intranasal immunization with BCG-loaded chitosan microparticles***



## Abstract

The aim of the present study was to develop a novel microparticulate delivery system containing whole live *Mycobacterium bovis* bacillus Calmette-Guérin (BCG) with enhanced physicochemical properties for an increased activity in eliciting a specific immune response against tuberculosis by intranasal immunization. The BCG was encapsulated in polymeric microparticles or suspended in chitosan by a polyionic gelation method, as previously described. For comparison purposes formulations containing empty particles were also prepared. Particle size distribution, association efficiency, surface charge, and cell viability were assessed. The specific immune responses were assessed in a BALB/c mice model by ELISA quantification of specific IgG subtypes in serum at several time points, and by ELISA quantification of secretory IgA (sIgA) levels in lungs and intestine homogenates at the end of the *in vivo* study. The production of specific cytokines was also assessed by ELISA quantification in spleen extracts. Intranasal immunization with BCG-loaded microparticles and BCG suspended in chitosan elicited higher levels of IgG1 and IgG2a than subcutaneous vaccine, with a predominant Th1-type response. The specific mucosal response was higher in the lungs than in the intestine, with significant differences among vaccine formulations. Finally, a predominant Th1-type response was elicited by intranasal immunization with BCG, with higher levels of IL-2, TNF- $\alpha$ , IFN- $\gamma$  in comparison with the subcutaneous vaccine.



## 1. Introduction

Live attenuated *Mycobacterium bovis* bacille Calmette–Guérin (BCG) is the currently used vaccine against tuberculosis (TB), being administered to neonates by subcutaneous route. However, BCG vaccine elicits unsatisfactory levels of protection in adults. It is well known that revaccination is not the answer, and WHO discourages the use of BCG booster doses. Therefore, there is an urgent need to develop an improved vaccine against TB.

Regarding TB epidemics, future vaccine candidates should follow low cost strategies that could be affordably implemented in developing countries. Ten new vaccine candidates are currently under assessment in clinical trials; so far, none has proven satisfactory efficacy in eliciting adequate immune responses. Followed strategies comprise mainly viral-vectored vaccines (e.g. MVA85A, a modified vaccinia Ankara-Ag85A-vectored vaccine), and adjuvanted proteins (e.g. M72+AS01, a fusion protein of *Mycobacterium tuberculosis* antigens 32A and 39A with adjuvant AS01E).<sup>1</sup> Disappointingly, early 2013 results for MVA85A following a phase-2b trial showed no significant increased protection against TB. Major drawbacks of these strategies rely on safety concerns and regulatory issues, which might increase development costs and delay regulatory compliance, such as the potential risk of viral replication within the host with viral-vectored vaccines, or the lack of adequate licensed adjuvants for human use (namely, aluminium hydroxide, AS03/04 and MF59, none of them efficient to induce strong Th1 responses).

A promising alternative is immunization with live vaccines. Live bacteria are multigenic and normally mimic pathogens surpassing host's natural barriers, being the ideal antigen producers and vectors. Taking into consideration BCG's heavy use worldwide, its low production cost, possibility of administration at birth, induction of immunity after a single dose, strong adjuvanticity, low frequency side effects, and recent progress with BCG as a live bacterial carrier for recombinant antigens,<sup>2</sup> BCG remains a strong candidate for an improved vaccine against TB. As BCG is not sufficiently effective against TB, adjuvants can be used to improve its immunogenicity.

It is well known that local mucosal immune responses are of major important for protection against pathogens invading the organism via mucosal surfaces<sup>2,3</sup>. Since *M. tuberculosis* causes infection mainly via the respiratory mucosa, it is expected that a strong mucosal response will be important for protection.<sup>4-6</sup>

The most effective way to induce mucosal immunity in the upper respiratory tract is intranasal immunization.<sup>4,7</sup> However, most currently available vaccines are parenterally administered, thus poor inducers of mucosal immunity. The success of mucosal immunization has somewhat been hampered because of host defence barriers such as mucosal secretions, proteases/nucleases attack, and epithelial barriers.<sup>8</sup> There is also limited applicability if upper respiratory-tract infections are present. Therefore, mucosal adjuvants capable to induce robust cellular immune responses while avoiding immune tolerance are required,<sup>9</sup> while adequate delivery systems can be used in order to overcome biological barriers and to colonize mucosal surfaces.<sup>10,11</sup>

A large number of micro- and nano-vaccine delivery systems, of different structures and compositions, have been under investigation in recent years as vaccine candidates, in order to amplify local and systemic immune responses, as well as to boost cellular immunity.<sup>11-21</sup> Several polymers of biodegradable and biocompatible nature, such as chitosan and alginate, have been used for the preparation of nanoparticles for nasal immunization purposes.

Chitosan has been used in surface modification of nanoparticles and liposomes for nasal immunization with promising results. Due to chitosan immunostimulatory properties, chitosan-based particulate delivery systems can act both as carrier and as adjuvant, improving the elicited immune response via induction of serum IgG and secretory IgA levels, as previously demonstrated with different nasally administered vaccines (e.g., influenza, diphtheria, and pertussis). Nasal or pulmonary delivery of chitosan was able to enhance systemic and mucosal antibody responses to a number of antigens in mice.<sup>22,23</sup> Regarding alginates, they can be used effectively to encapsulate cells by formation of a biocompatible gel matrix.<sup>24</sup> Moreover, alginates are mucoadhesive and are likely to increase the residence time of antigens at mucosal sites.<sup>25-28</sup> Finally, alginates are acid-resistant<sup>29,30</sup> and might contribute to increase the survival of BCG in the alveolar macrophages, thus, leading to a different antigen recognition pathway that can prompt a more balanced cellular/humoral immune response.

The use of alginate beads coated with chitosan for mucosal immunization has been described to improve the stability of DNA during storage and in biological fluids,<sup>31</sup> and to enhance the immune response elicited by hepatitis B antigen.<sup>32</sup> Chitosan-based nanoparticles as mucosal vaccine delivery system have also being used in our group in the last years showing promising capabilities.<sup>33-37</sup> However, to our knowledge, no chitosan-alginate microparticulate system has so far been tested for nasal immunization with BCG.

In this study, a novel microparticulate delivery system containing whole live BCG was tested for mucosal immunization against tuberculosis purposes. Our formulation approach is founded on the premise that BCG must maintain its viability and multigenicity, in order to elicit an adequate immune response against *M. tuberculosis*, by mimicking pathogens surpassing host's natural barriers. The targeting of microparticles to the nasal mucosa offers the possibility of uptake by APC and also antigen's cross-presentation, so that the cellular immune response can be enhanced.<sup>10</sup> Chitosan was the selected biopolymer for formulation development, based on its biodegradable, mucoadhesive and immunostimulant properties.<sup>27,35,37,38</sup> Immune responses generated in mouse lung, spleen and intestine were examined following intranasal immunization with *M. bovis* bacillus Calmette-Guérin (BCG), using a chitosan/alginate microparticulate delivery system.

## 2. Materials and methods

### 2.1. Chemicals and strains

Low molecular weight ultra-pure chitosan Protasan UP CL 113 with degree of deacetylation 75-90% and low viscosity sodium alginate Protanal LF 10/60 with L-guluronic acid 65-75% were obtained from FMC BioPolymer A.S (Norway). Sodium tripolyphosphate (TPP) and linoleic acid were obtained from Sigma-Aldrich (UK). Purified Protein Derivative (PPD) of *Mycobacterium bovis* Tuberculin was obtained from NIBSC (UK).

*Mycobacterium bovis* BCG (strain Pasteur 1173) was obtained from American Type Cell Culture Collection (ATCC 35734). BCG cultures were grown for seven days on Middlebrook's 7H9 broth Medium supplemented with 5% (v/v) OADC (oleic acid, albumin, dextrose and catalase) (Difco, USA) and 0.05 % (v/v) Tween 80 (Sigma-Aldrich, UK), at 37°C / 5% CO<sub>2</sub>. After that period, BCG cells were pelleted at 4000 rpm (1559 ×g) at 4°C for 15 min, washed with phosphate buffered saline and resuspended in appropriate medium. Unless referred otherwise, all cell culture reagents were obtained from Difco (USA).

### 2.2. Mice

Female BALB/c mice (6- to 8 weeks old) were provided from Charles Rivers (Spain) and maintained under specific pathogen-free conditions. Animals were fed with standard laboratory food and water ad libitum. All *in vivo* studies using animals were carried out in

accordance with relevant Portuguese and European Community regulations and guidelines.

### 2.3. Microencapsulation of BCG in polymeric microparticles

BCG-loaded microparticles were prepared by mild ionotropic gelation using the droplet technique according to previously described Method (III) (Chapter 2, section 2.2) with modifications.<sup>39</sup> BCG was formulated in Protasan UP CL 113, an ultra-pure low molecular weight, high deacetylation degree chitosan, at a target concentration of  $10^7$  CFU/ml. Briefly,  $2.5 \times 10^9$  CFU/mL *M. bovis* BCG Pasteur suspension was dispersed in 1.0 mg/mL chitosan solution (pH 5.0) using a syringe with a 23 gauge needle, in order to monodisperse the bacteria. Portions of the BCG-chitosan matrix were further formulated to produce BCG-loaded microparticles as follows. BCG-chitosan matrix was cross-linked by drop-wise addition of 2.0 mg/mL TPP (pH 9.0) using a micropipette tip. The BCG-loaded pre-gel was then put into an ultrasonic water bath (Branson Ultrasonics, USA) at room temperature. The mixture was removed from the ultrasounds after 10 minutes and 1.0 mg/mL Protanal LF 10/60 (pH 6.0), a pharmaceutical grade, low viscosity and high G-content sodium alginate, was dropped in using a micropipette tip. In order to allow the polymerization of the gel, the mixture was ultrasonicated for additional 10 minutes at room temperature. BCG-chitosan matrix was used as core-forming phase and sodium alginate as shell-forming phase, with a final mass ratio of 5:5:40 (w:w) (chitosan/alginate/TPP) (Fig. 1).

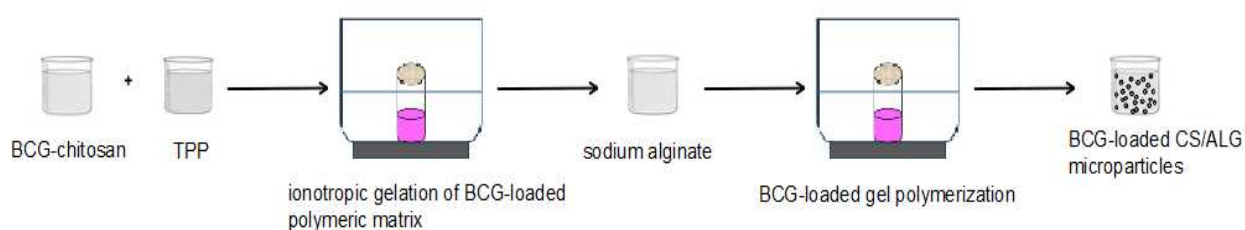


**Figure 1** – Preparation of BCG-loaded chitosan-alginate (CS/ALG) microparticles by ionotropic gelation of chitosan-suspended BCG with TPP, followed by alginate addition. Microparticles were obtained using the ultrasound bath (28 kHz). Samples were placed in the closed dark chamber containing cooled water.

To facilitate the nasal delivery of the chitosan-alginate formulation in mice mucopenetration is required. To achieve this, a variant of the above described formulation was developed using linoleic acid, a fatty acid with pro-inflammatory effects, as permeation enhancer.<sup>40,41</sup> Briefly, 1% (v/v) linoleic acid (LA) was prepared by dilution in ethanol, prior to its dispersion into 2.0 mg/mL TPP solution (pH 9.0) in a 1:4 ratio. The

linoleic acid-TPP solution was drop-wise added to initially prepared BCG-chitosan matrix using a micropipette tip. This mixture was ultrasonicated for 10 minutes at room temperature. Then, 1.0 mg/mL alginate (Protanal LF 10/60) (pH 6.0) was dropped in and the mixture was ultrasonicated for additional 10 minutes. The final mass ratio of the formulation was 5:5:5:40 (w:w) (chitosan/alginate/linoleic acid/TPP) (Fig. 2).

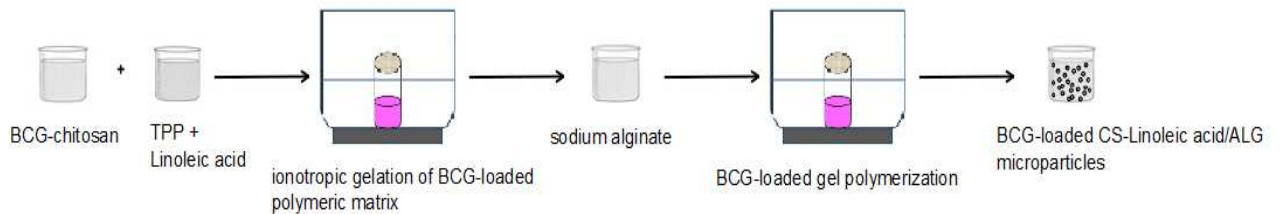


**Figure 2** – Preparation of BCG-loaded chitosan/linoleic acid-alginate (CS-Linoleic acid/ALG) microparticles by ionotropic gelation of chitosan-suspended BCG with TPP containing 10 mg/mL linoleic acid, followed by alginate addition. Microparticles were obtained using the ultrasound bath (28 kHz). Samples were placed in the closed dark chamber containing cooled water.

BCG was also formulated in alginate beads by external gelation using the droplet technique. BCG suspension was mixed with 1.0 mg/mL high G alginate solution (Protanal LF 10/60) (pH 6.0) in a 1:5 ratio, using a 23 gauge needle to produce monodispersed bacteria. The BCG-alginate matrix was then drop-wise added into a solution of 1.0 mg/mL high deacetylation degree chitosan (Protasan UP CL 113) (pH 5.0) using a micropipette tip. This mixture was then ultrasonicated (28 kHz) at room temperature allowing the gel to polymerize. The BCG-loaded gel matrix was removed from the ultrasonic water bath after 10 minutes. To facilitate the nasal delivery of the alginate-chitosan formulation in mice small particle size is required. To achieve this, 2.0 mg/ml TPP (pH 9.0) were drop-wise added to the mixture promoting the cross-linkage and gel structure reorganization, prior to final ultrasonication for 10 minutes at room temperature (Fig. 3).

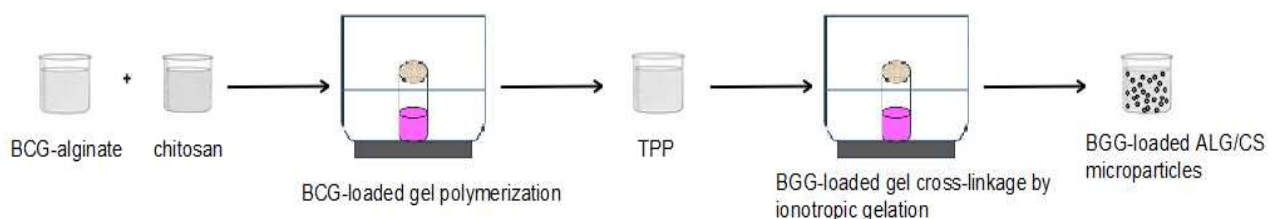


**Figure 3** – Preparation of BCG-loaded alginate-chitosan (ALG/CS) microparticles by polymerization of alginate-suspended BCG with chitosan, followed by TPP addition. Microparticles were obtained using the ultrasound bath (28 kHz). Samples were placed in the closed dark chamber containing cooled water.

## 2.4. Characterization of BCG-loaded microparticles

Particle size and size distribution were determined by laser diffraction using a Malvern Mastersizer 2000 (Malvern Instruments, UK). Five measurements were performed on each sample and three replicates were measured for each formulation. Particle size was quoted as  $d(0.5)$  diameter for which mean values and standard deviations were calculated. The surface charge of microparticles was determined by electrophoretic mobility using a Malvern Nanosizer Z (Malvern Instruments, UK). The microparticles were dispersed in filtered purified water. Six measurements were performed on each sample and three replicates were measured for each formulation.

Since neither centrifugation nor indirect determination by microfiltration could be used to determine the association efficiency (A.E.) of microparticles, due to the unwanted compromise of BCG cell viability, and due to the size of microparticles, respectively, the ratio of microparticle-associated cells among total cells was determined by cell count number, using a haemocytometer. A.E. is expressed as the percentage of BCG cells associated/encapsulated in microparticles reported to the initial amount of cells used for particle preparation. This result was confirmed by cell viability measurement by a micro-colony-forming units (CFU) assay.

The viability of formulated BCG, either by suspension in chitosan or encapsulation/adsorption in/to polymeric microparticles was assessed for one month at 4°C storage, by comparison with BCG suspended in 0.9% NaCl, by a micro-colony-forming units (CFU) assay as previously described<sup>42</sup> (Chapter III, section 2.4) with some modifications. Briefly, 1/10 dilutions of samples of all BCG-containing formulations, as used in the immunization assay, were grown in appropriate medium (agar Middlebrook's 7H10 supplemented with OADC). After 10- to 17 days of incubation at 37°C, colonies were observed through a microscope and used to determine CFU.

Plain microparticles were also prepared as described, without BCG, for further immunization study as negative controls. All procedures were performed under sterile conditions, and vaccine formulations were freshly prepared immediately prior immunization.

## 2.5. Assessment of specific immune responses in mice

### 2.5.1. Immunization schedule

For all immunizations, female BALB/c mice were maintained under specific pathogen-free conditions. Mice were randomly divided into 9 groups of 4- to 7 mice per group (Table 1). Mice were immunized by intranasal route with either BCG suspended in chitosan (Group 1), BCG-loaded microparticles (Groups 6, 7 and 8), or BCG suspended in 0.9% NaCl (Group 2). Plain microparticles (Groups 3, 4 and 5) were also administered by intranasal route (negative controls). Positive control (Group 9) was established with BCG suspended in 0.9% NaCl administered by subcutaneous route. The subcutaneously administered BCG is referential to current practice within immunization regimens with BCG.

**Table 1** – Summary of the formulations tested in mice and respective immunization route.

<b>Immunization groups</b>	<b>Immunization route</b>	<b>Formulations</b>	<b>Mice per group</b>
Group 1	Intranasal	BCG suspended in 0.025 mg/mL LMW chitosan	5
Group 2	Intranasal	BCG suspended in 0.9% NaCl	5
Group 3	Intranasal	Plain CS-ALG microparticles	5
Group 4	Intranasal	Plain ALG-CS microparticles	5
Group 5	Intranasal	Plain CS-ALG-Linoleic acid microparticles	5
Group 6	Intranasal	BCG-loaded CS-ALG microparticles	7
Group 7	Intranasal	BCG-loaded ALG-CS microparticles	7
Group 8	Intranasal	BCG-loaded CS-ALG-Linoleic acid microparticles	7
Group 9	Subcutaneous	BCG suspended in 0.9% NaCl	4

LMW, low molecular weight. CS, chitosan. ALG, sodium alginate.

All vaccine formulations were aseptically prepared immediately prior dosing. Mice were immunized by intranasal route on day 1 (priming) using a micropipette tip to administer 20 µl of sample (10 µl in each nostril) containing a standardised dose of  $1 \times 10^7$  CFU per animal. Intranasal vaccine formulations were slowly delivered onto nostrils so that the mice could inhale. Subcutaneous vaccine was administered at the base of the neck (50 µl of sample, equivalent to  $1 \times 10^7$  CFU). This dose was considered relevant in other studies where BCG strains Pasteur 1173 and Danish 1331 have been used for oral immunization purposes.<sup>43,44</sup>

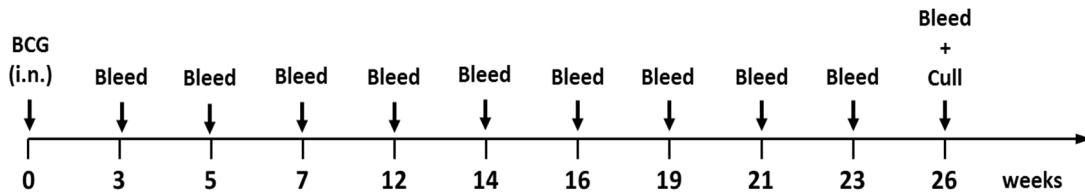


**Figure 4** – Immunization schedule for priming, blood sampling for specific IgGs subtypes quantification of by ELISA, and experimental endpoint with harvest of lungs, intestines and spleen for further immunogenicity studies.

Blood samples from animals from each group were collected approximately every 15 days (Fig. 4) from the tail vein and sera separated by centrifugation (10,000g, 5 min at 4°C, Allegra 64R, Beckman, USA) and stored at –20°C until tested by antigen specific enzyme-linked immunosorbent assay (ELISA). Twenty six weeks after the immunization, mice were culled and tested by antigen specific enzyme-linked immunosorbent assay (ELISA) for systemic production of IgG and IgG subtypes (IgG1 and IgG2a) and for local secretory IgA, and the IFN- $\gamma$  TNF- $\alpha$ , IL-2 and IL-4 levels of splenocytes cultures were quantified.

### 2.5.2. Immunoglobulin IgG isotypes enzyme-linked immunosorbent assay (ELISA)

Purified protein derivative (PPD) bovine tuberculin-specific IgG titres were measured in blood samples at different stages of the immunization using an appropriate ELISA technique. Briefly, ninety-six-well plates (Microlon™, High binding flat bottom plates, Greiner, Germany) were coated with PPD bovine tuberculin in PBS (at 2.5  $\mu$ g/mL dose per well) 2 h at 37°C. After blocking with 5% (w/v) skimmed milk powder (Merck KGaA, Germany) in 10 mM PBS (pH 7.4) containing 0.05% (v/v) of Tween™ 20 (PBST; Sigma–Aldrich, UK), mouse serum samples in twofold serial dilutions were added. Plates were incubated for 2 h at 37°C, followed by washing three times with PBS with 0.05% (v/v) Tween 20. Specific antibodies were detected after incubation for 2 h at 37°C with horseradish peroxidase-conjugated goat anti-mouse antibodies specific for IgG, (1:1000, Sigma, Pool Dorset, UK), IgG1 and IgG2a (1:2000, Serotec, UK), and subsequent development of peroxidase reaction with substrate OPD (SigmaFAST™ OPD Kit, Sigma–Aldrich, UK). Titres are reported as the reciprocal of serum dilutions that gave an optical density 5% higher than the strongest negative control reading.

### 2.5.3. Secretory IgA ELISA

For analysis of secretory IgA, the lungs and the intestines collected at the end of the experiment were homogenized in buffer 0.9% sodium chloride with protease inhibitor PMSF 1 mM and 0.5% Tween™ 20. The homogenization was done with ultrasound probe for 3 times of 5 min intermittent pulsed for 30 s each in an ice bath. The homogenized tissues were centrifuged at 20,000 × g for 30 min at 4°C (Allegra 64R, Beckman, USA) and the supernatant was frozen at –80°C until freeze–drying. After freeze–drying, proteins were reconstituted with 500 µl of sterile water and directly added, in triplicate, to the plate wells. The mean OD (mean ± SD, n≥3) was determined for each treatment group, using horseradish peroxidase-conjugated goat anti-mouse IgA (1:1000; Serotec, UK) in the above described ELISA technique, and directly used to compare mucosal response.

### 2.5.4. Cytokines quantification by ELISA

For the analysis of PPD bovine specific cytokines, spleens from mice were aseptically removed 26 weeks after immunization and cells were prepared as previously reported.<sup>27,45</sup> Supernatants obtained 72 h after mouse splenocyte stimulation with and without 5.0 µg/mL of PPD bovine tuberculin were used for IFN-γ TNF-α, IL-2 and IL-4 quantification by ELISA, using a commercially available RayBio™ kit (RayBiotech, Inc., USA). The concentrations, expressed as pg/mL, were determined by reference to different cytokines standard.

## 2.6. Statistical analysis

Results are expressed as mean values ± standard deviation (S.D.). Statistical analysis was performed on the data obtained in the *in vivo* studies by the Dunnett's multiple comparison test, with significance set at *P*-values <0.05.

### 3. Results

#### 3.1. Characterization of BCG-loaded polymeric microparticles

In order to elicit both humoral and cellular immune responses, we entrapped whole live attenuated BCG Pasteur in polymeric microparticles, prepared by ionotropic gelation with chitosan and alginate, so that cell viability was maintained.<sup>39</sup> The BCG-loaded polymeric microparticles were compared in the *in vivo* studies with positively charged BCG (suspended in chitosan), or negatively charged BCG only. Since particles alone are described to have immunogenic effects,<sup>46</sup> empty polymeric microparticles were also evaluated. The characterization of prepared microparticles is depicted on Table 2.

**Table 2** – Particle size distribution and surface charge of microparticle formulations used for intranasal immunization of mice with  $1 \times 10^8$  CFU/mL of BCG Pasteur (mean  $\pm$  S.D.;  $n \geq 3$ ).

Formulation	Particle size distribution ( $\mu\text{m}$ )		Zeta potential (mV)	A.E. (%)
	d(0.5)	span *		
BCG suspended in 0.025 mg/mL LMW chitosan	--	--	+85.7 $\pm$ 12.1	--
BCG suspended in 0.9% NaCl	28.4 $\pm$ 0.0	3.2 $\pm$ 0.0	-29.9 $\pm$ 11.5	--
Plain CS/ALG microparticles	7.4 $\pm$ 2.0	1.7 $\pm$ 0.5	-40.2 $\pm$ 1.3	--
Plain ALG/CS microparticles	23.9 $\pm$ 0.0	2.3 $\pm$ 0.0	+14.1 $\pm$ 0.6	--
Plain CS-Linoleic acid/ALG microparticles	8.5 $\pm$ 3.0	2.9 $\pm$ 2.3	-34.3 $\pm$ 3.6	--
BCG-loaded CS/ALG microparticles	37.8 $\pm$ 0.0	2.3 $\pm$ 0.5	-32.8 $\pm$ 0.0	61
BCG-loaded ALG/CS microparticles	96.9 $\pm$ 0.0	2.0 $\pm$ 0.0	-47.4 $\pm$ 9.2	64
BCG-loaded CS-Linoleic acid/ALG microparticles	61.4 $\pm$ 23.3	2.4 $\pm$ 0.2	-32.2 $\pm$ 14.1	64

A.E., association efficiency; LMW, low molecular weight. Span expressed as  $[d(0.9) - d(0.1)] / d(0.5)$ .

The size of the BCG-loaded polymeric microparticles (ALG/CS mass ratio 1:1) was determined by laser diffraction to be of an average diameter of  $65.4 \pm 29.7 \mu\text{m}$ , whereas the size of monodispersed BCG (suspended only) was approximately 2.5-fold lower ( $25.9 \pm 3.5 \mu\text{m}$ ). Approximately 4.2-fold increase in particle diameter was observed for all polymeric microparticle preparations after BCG microencapsulation. The observed difference in particle size distribution is due to the reorganization of the chitosan gel matrix in presence of carboxylic groups from alginate and BCG negatively charged bacilli. The effect of the preparation method on particle size distribution was discussed in detail in chapters II (section 3.1.1.1.) and III (sections 2.3 and 3.1). Further, we measured the span. The span gives an estimation of the robustness of the preparation method, as a lower span correlates with a more homogeneous distribution of particle

mean diameter. The use of consistent and reproducible preparation methods is important regarding the future upscale of vaccine manufacture. Overall, a more reproducible preparation method was achieved with microparticle preparation by ultrasound homogenization than by BCG simple suspension.

The particle surface charge of the BCG-loaded chitosan-alginate microparticles (ALG/CS mass ratio 1:1) was determined by electrophoretic mobility to be of an average zeta potential of  $-37.5 \pm 8.6$  mV, whereas the surface charge of plain microparticles was approximately 3-fold higher, although negatively charged. It is important to note the significant differences observed in particle surface charge between BCG suspended in NaCl ( $-29.9 \pm 11.5$  mV) and BCG suspended in chitosan ( $+85.7 \pm 12.1$  mV). As previously described (Chapter II, section 3.1.4.), the negative surface charge of BCG bacilli arises from phosphate groups present in the *Mycobacteria* cell wall.<sup>47</sup> The overall electropositive charge of BCG suspended in chitosan is due to the presence of free amine groups from chitosan, which are, in turn, partially unavailable in composite polymeric microparticles by interaction with alginate carboxylic groups. Particles of different size distribution and surface charge are expected to propitiate distinct immunological outcomes *in vivo*.

The shape of the microparticles was spherical, as determined by optical microscopy (data not shown). The association efficiency was approximately 64%, as verified by cell count by a haemocytometer and confirmed by cell viability measurement using a micro-colony-forming units (CFU) assay.

The inoculation of freshly prepared vaccines and vaccines maintained at 4°C storage in appropriate medium showed that BCG was viable independently of the formulation (Fig. 5). No significant differences ( $P = 0.7922$ ) in cell number were observed between the control group (BCG suspended in 0.9% NaCl) and BCG-formulated groups (either chitosan-suspended or microencapsulated into polymeric microparticles).

The obtained results demonstrated that no significant cell viability loss occurred during one month, which is described as the relevant time to establish the immune response within antigen presenting cells.<sup>48</sup> Since no relevant differences were observed amongst formulations, we exclude the hypothesis that differences in immune responses between the groups might rely on variations of BCG viability. These preparations were used in the prime vaccination study by intranasal route with BCG.

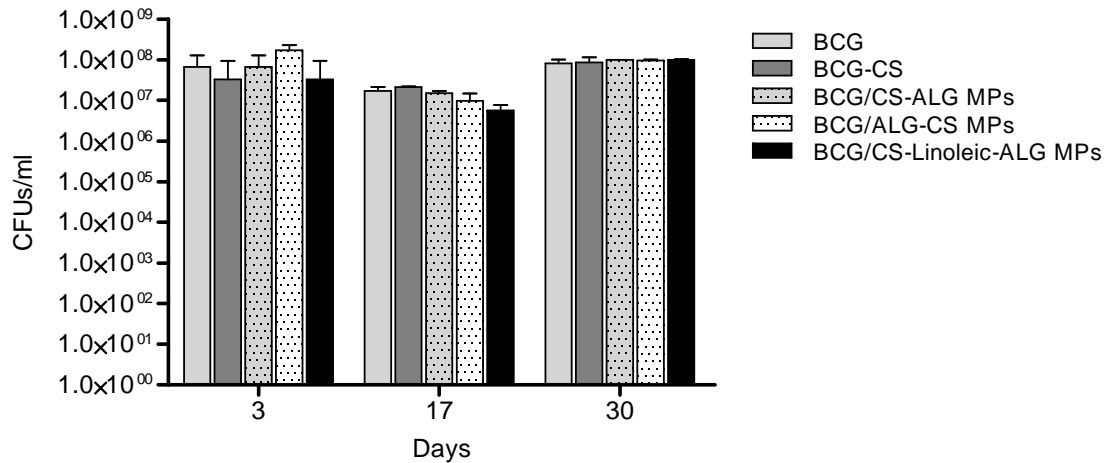


**Figure 5** – Cell number of formulated BCG by micro-CFU assay after storage at 4°C. Columns: light grey – BCG suspended in 0.9% NaCl; dark grey – BCG suspended in 0.025% chitosan; dotted grey – BCG-loaded CS/ALG microparticles; dotted white – BCG-loaded ALG/CS microparticles; black – BCG-loaded CS-Linoleic acid/ALG microparticles. Results are expressed as mean  $\pm$  S.D. (n = 3).

### 3.2. Systemic PPD bovine-specific IgG immune response

Mice were immunized with a single administration of BCG preparations by intranasal route corresponding to a standardized dose of  $1 \times 10^7$  CFU per animal. Sera of immunized animals were tested for the presence of *M. bovis*-specific IgG antibodies and subtypes at all time points after the third week post-immunization. The animals were followed up for 26 weeks (182 days) to generate a proper memory T cell response. Later, the animals were sacrificed and the *M. tuberculosis*-specific T cell response was monitored. The obtained results are depicted in Fig. 6.

Mice immunized with plain microparticles produced very little or no specific anti PPDbov-IgG in their sera (data not shown). Five weeks after priming, a high anti-PPDbov-IgG response was observed for all BCG immunized groups, which was approximately 2-fold intensified after the 12<sup>th</sup> week for both intranasal and subcutaneously immunized groups. Compared to the subcutaneous route of administration, intranasal immunization elicited the production of inferior levels of specific IgG (Fig. 6A). Amongst BCG preparations administered by intranasal route, it was possible to observe slight differences in the elicited humoral response (Fig. 6B). Compared to BCG, BCG suspended in chitosan and BCG-loaded microparticles exhibited higher levels of specific total IgG by ELISA quantification with PPDbov.

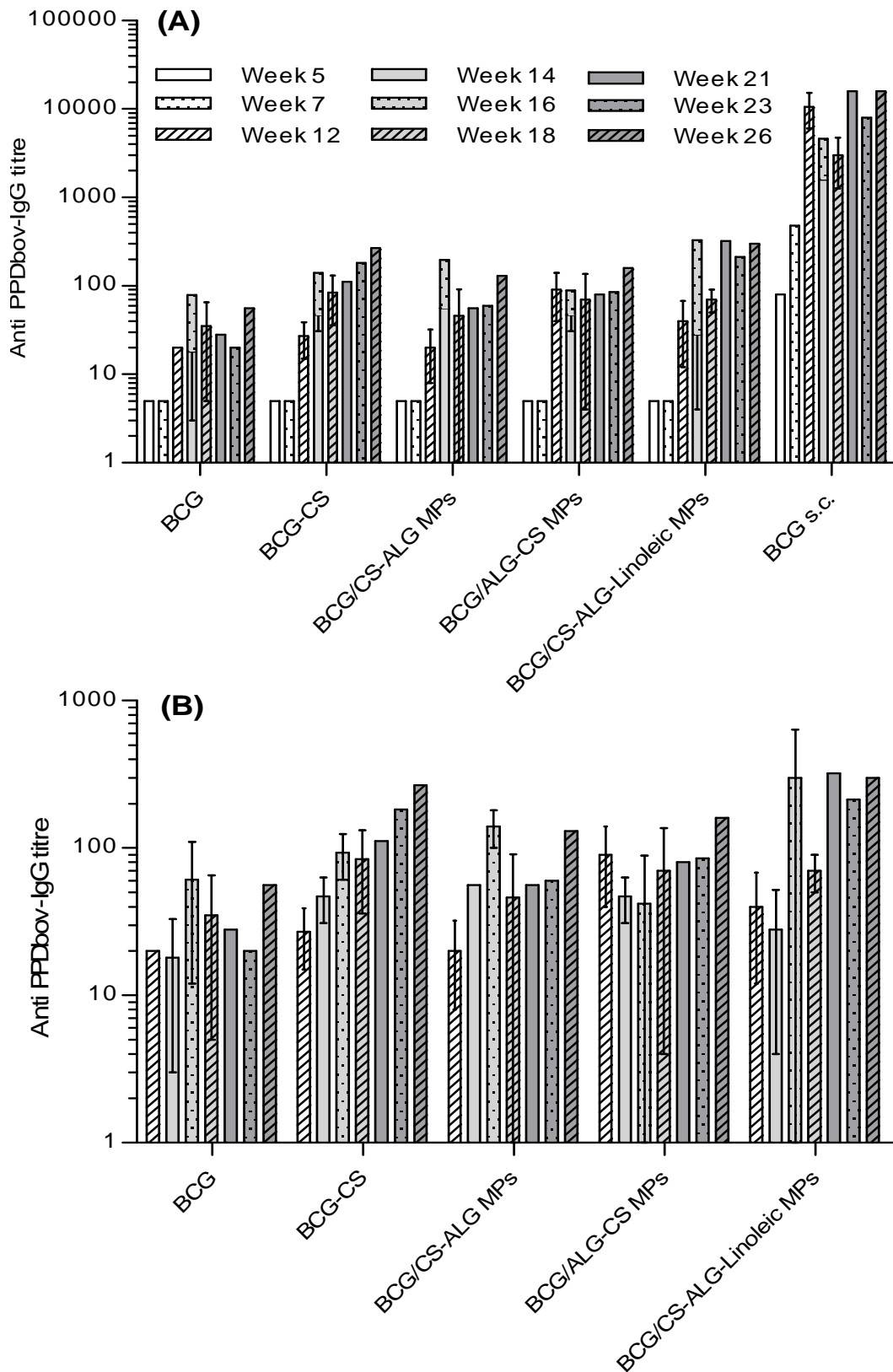


**Figure 6** – Systemic humoral (IgG) immune responses of immunized BALB/c mice. The production of PPDbov specific immunoglobulins IgG was assessed by ELISA in mice serum (mean  $\pm$  S.D.;  $n \geq 4$ ). (A) Global humoral immune responses; (B) Immune response in groups immunized by intranasal route. CS, chitosan; ALG, sodium alginate; MPs, microparticles; Linoleic, linoleic acid.

### 3.3. IgG subtype profiling

It has been well established that when B cells interact with Th1 cells they produce mainly IgG2a, while Th2 cells secrete primarily IgG1. The generation of a dominant Th1 immune responses following intranasal immunization of animals is described to impart an important role for the eradication of intracellular pathogens, thus, contributing for effective prevention against *M. tuberculosis* infection.<sup>49,50</sup> The ideal profile is a balanced Th1/Th2 response, in order to avoid either immunological hyporesponsiveness due to mucosal tolerance or an hyperreactivity leading to autoimmune disturbances.<sup>50,51</sup>

In this study, the *PPD**bov*-specific IgG1 isotype titres were higher for s.c. BCG (Fig. 7), indicating that BCG administration by subcutaneous route elicited mainly a Th2-type response. As for *PPD**bov*-specific IgG2a isotype, the highest titres were obtained after intranasal immunization with BCG alone and positively charged BCG (suspended in chitosan) (Fig. 7), indicative of Th1-type immune response.

Higher ratios of *PPD**bov*-specific IgG2a/IgG1 substantiated the occurrence of predominant Th1-type responses upon intranasal immunization with BCG alone (17.9 ratio;  $P < 0.0001$ ), BCG-loaded chitosan-alginate microparticles (2.8 ratio;  $P < 0.0001$ ), and positively charged BCG (suspended in chitosan) (2.0 ratio;  $P < 0.05$ ), in comparison to subcutaneous route (Fig. 7). A balanced Th1/Th2 response (1.0 ratio) was obtained with “BCG-loaded chitosan-alginate-linoleic acid” particulate vaccine. Overall, the Th1/Th2 profile was more balanced for the abovementioned polymeric vaccines (2.0; 2.8; 1.0) than for BCG alone (17.9) at the end of the trial period, with i.n. immunization performing noticeably better than s.c. route.

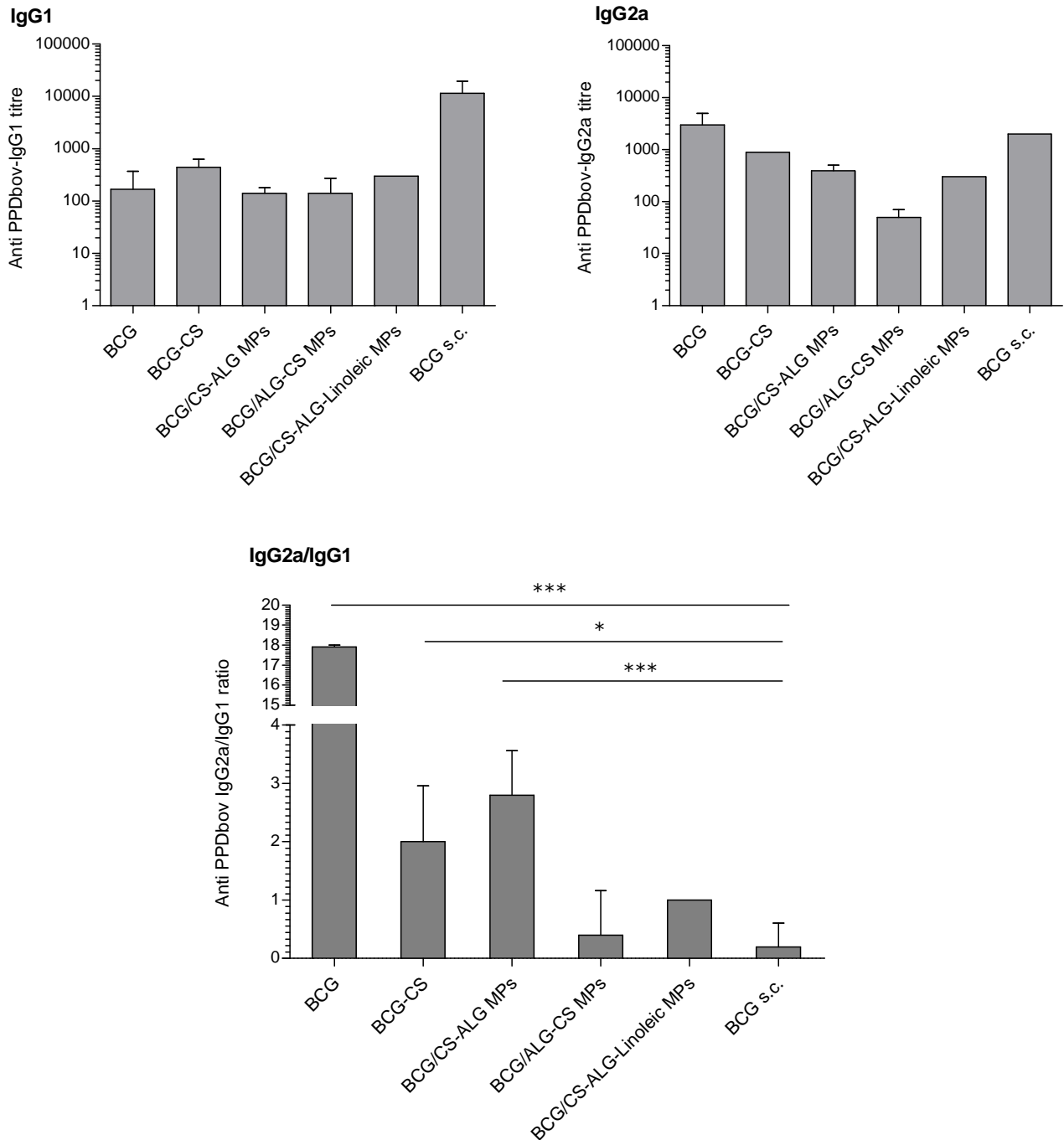


**Figure 7** – Serum anti-*PPDbov* specific IgG1 and IgG2a titres, and ratio of serum anti-*PPDbov* specific IgG2a and IgG1 titres, 26 weeks after priming immunization of female BALB/c mice with the BCG vaccines (mean  $\pm$  S.D.;  $n \geq 4$ ). Statistical analysis was performed by Dunnett's multiple comparison tests. \*  $P < 0.05$ ; \*\*\*  $P < 0.0001$ . CS, chitosan; ALG, sodium alginate; MPs, microparticles; Linoleic, linoleic acid; s.c., subcutaneous.

### 3.4. Local PPD bovine-specific IgA immune response

The local secretion of specific IgA antibodies plays a major role in establishing a first defence line at the mucosal surfaces against the adhesion and colonization of pathogens such as *M. tuberculosis*.<sup>49</sup> It is also well established that immunization of mucosal inductive sites, such as nasopharyngeal-associated lymphoreticular tissue (NALT), contributes for the secretion of antigen-specific mucosal IgA antibodies in diverse mucosal effector sites other than the inductive sites,<sup>50</sup> such as gut-associated lymphoreticular tissue (GALT). In order to evaluate the mucosal responses following intranasal immunization, secretory IgA levels were determined in mice lungs and intestines homogenates. The results are depicted in Fig. 8. Statistically differences were determined among i.n. vaccines and s.c. BCG.

Overall, the specific anti-PPD<sub>bov</sub> mucosal response was more pronounced in the lung than in the intestine (Fig. 8). Regarding the mucosal response in the lung elicited following intranasal administration of BCG vaccines, “BCG-loaded chitosan-alginate-linoleic acid microparticle” formulation prompted higher sIgA levels ( $P < 0.0001$ ) than BCG alone. Differences observed might be due to presence of linoleic acid in the formulation, which might be involved in mucosal immunity. Globally, however, higher sIgA levels were obtained in the lung with s.c. BCG vaccine and empty microparticles. Regarding the mucosal immune response in the intestine, higher sIgA levels were obtained following i.n. administration of BCG alone ( $P < 0.0001$ ), positively charged BCG (BCG-CS) ( $P < 0.0001$ ), and BCG-loaded alginate-chitosan microparticles ( $P < 0.0001$ ), in comparison to s.c. BCG.

The obtained results suggest that i.n. immunization was effective in stimulating specific mucosal responses in both mucosal effector sites, NALT and GALT, whereas s.c. immunization with BCG led to a major response in the NALT only. The sIgA profile observed in the lung suggests that particle mean diameter partially hampers the uptake of BCG by the NALT. Among the i.n. vaccines, “BCG-loaded chitosan-alginate-linoleic acid microparticle” formulation exhibited adequate responses in both mucosae and elicited the highest IgG levels, as previously demonstrated (Fig. 6B), thus, suggesting that this vaccine formulation was capable of inducing both systemic and mucosal antibody responses.

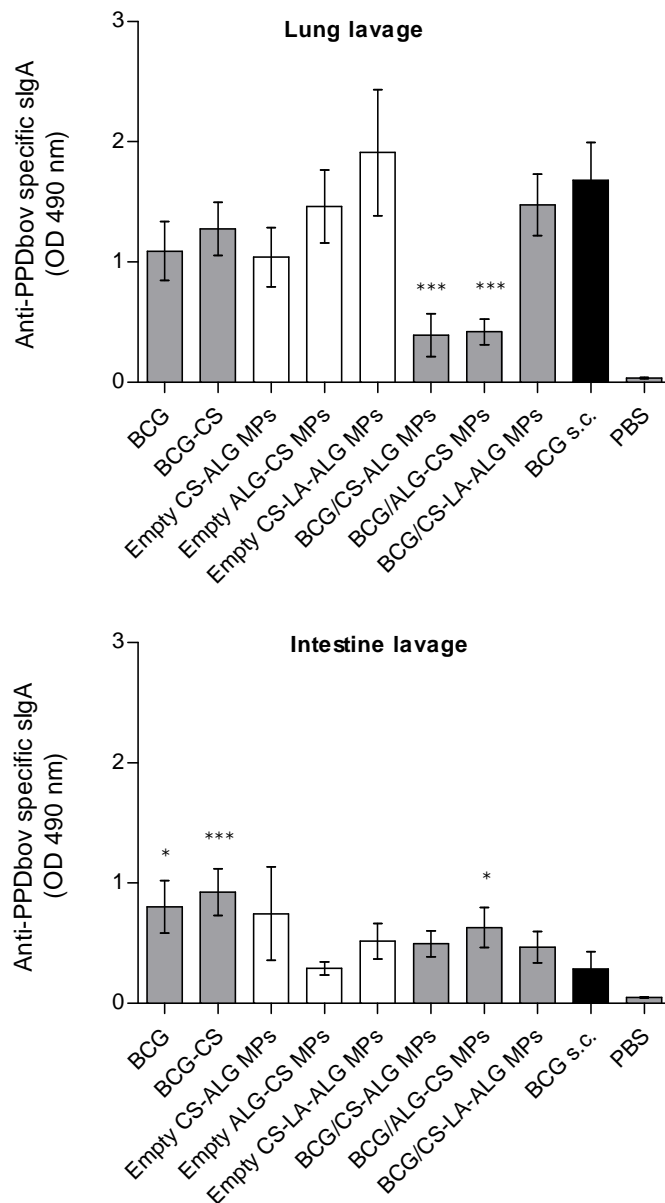


**Figure 8** – Serum anti-PPDbov specific secretory IgA levels in mice lungs and intestines homogenates, 26 weeks after priming immunization of female BALB/c mice with the BCG vaccines (mean  $\pm$  S.D.;  $n \geq 4$ ). Statistical analysis was performed by Dunnett's multiple comparison tests, comparing i.n. vaccines with s.c. BCG. \*  $P < 0.05$ ; \*\*\*  $P < 0.0001$ . CS, chitosan; ALG, sodium alginate; MPs, microparticles; LA, linoleic acid; s.c., subcutaneous.

### 3.5. Cytokine production by splenocytes

Protective immunity against *M. tuberculosis* requires an adequate cellular immune response, which involves potent T-cell responses. The activation and differentiation of lymphocytes lies on the production of specific cytokines by Th cells. The expression profile of IL-2, IFN- $\gamma$ , and tumour necrosis factor- $\alpha$  (TNF- $\alpha$ ) correlates with Th1 response, whereas IL-4 cytokine correlate with Th2 response.<sup>52</sup> In order to evaluate cellular immune response, key cytokines expressed by sensitized splenocytes from immunized animals are currently quantified using enzyme-linked immunosorbent assays (ELISA). In this context, the supernatants of spleen cells from immunized mice were collected to quantify the cytokines produced in response to stimulation with bovine tuberculin. The obtained results are depicted in Fig. 9.

Intranasal immunization with BCG effectively stimulated Th1 and Th2-type cytokines production, substantiating the predominant Th1-type response elicited by intranasal immunization, in opposition to subcutaneous route. There were significant differences in Th1-type cytokine production among vaccine groups (44-67% % of total variation, determined by two-way ANOVA). Interestingly, empty polymeric microparticle formulations also evoked strong immune responses following i.n. immunization.

The data for cytokine secretion indicate that IL-2 levels were substantially elevated following i.n. immunization with microencapsulated BCG when comparing with plain BCG or BCG suspended in chitosan. Significant increases of IL-2 ( $P = 0.006$ ) were obtained with the BCG suspended in chitosan and BCG-loaded polymeric microparticle vaccines compared to those detected in non-stimulated splenocytes (data not shown). Similarly, the group treated with i.n. BCG showed a general increase in all cytokine levels, compared to those detected in non-stimulated splenocytes (data not shown).

Regarding specific cytokine IFN- $\gamma$ , higher concentrations were detected following intranasal immunization with microencapsulated BCG or plain BCG with respect to the group that received BCG by subcutaneous route, with the group immunized with positively charged BCG (suspended in chitosan) by intranasal route revealing also a good response. These results suggest that particle surface charge, more than particle size distribution, may play an important role in the interaction of antigens with APC, by a phenomena that is not completely understood. The levels of TNF- $\alpha$  were significantly higher in all groups immunized by intranasal route, in comparison with the group that received BCG subcutaneously, whereas the elicited IL-4 levels were low for all vaccine groups, being similar to levels elicited by “medium”, which was used as negative control.

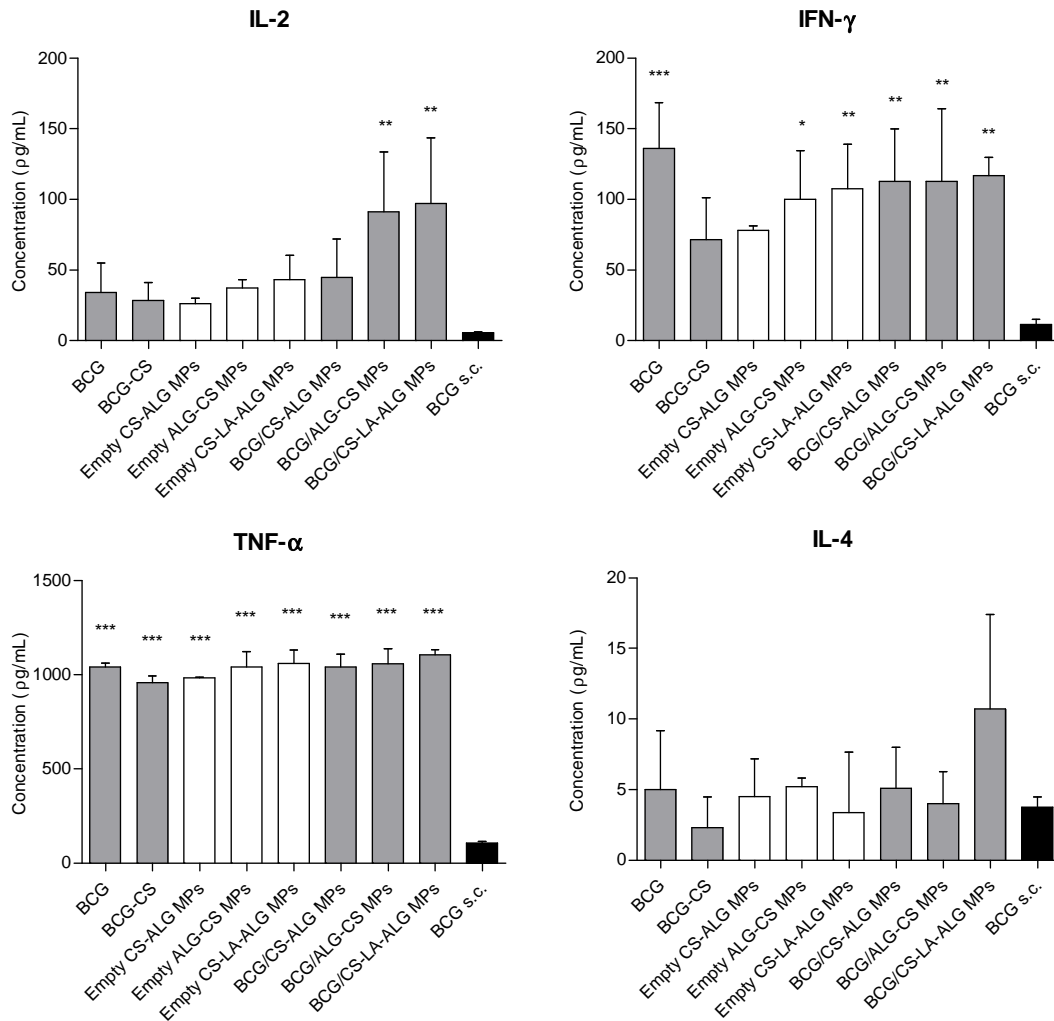


**Figure 9** – Concentration of cytokines IL-2, IFN- $\gamma$ , TNF- $\alpha$ , and IL-4 in supernatants of splenocytes after 72h stimulation with PPD bovine (mean  $\pm$  S.D.;  $n \geq 4$ ). Statistical analysis was performed by Dunnett's multiple comparison tests, comparing i.n. vaccines with s.c. BCG. \*  $P < 0.05$ ; \*\*  $P < 0.001$  \*\*\*  $P < 0.0001$ . CS, chitosan; ALG, sodium alginate; MPs, microparticles; LA, linoleic acid; s.c., subcutaneous.

Overall, intranasal immunization with microencapsulated BCG evoked long-lasting (182 days) Th1 immunity against *M. tuberculosis*, which was superior to that elicited by plain BCG administered by subcutaneous route. The obtained results suggest that both i.n. route and particulate system antigen presentation may play an important role in facilitating antigens' intracellular trafficking, favouring antigen presentation through MHC II pathway, thus, stimulating cellular immune response, meeting the previous results that pointed out a mixed immune response based on the IgG2a/IgG1 ratio.

## 4. Discussion

Limitations of current BCG vaccination strategies to confer protection against tuberculosis in the adulthood are probably related to BCG's inability to elicit long-lasting immunity and to provide sterilizing immunity against primary *Mycobacterium tuberculosis* infection.<sup>2,4,53-58</sup> Since *M. tuberculosis* causes infection mainly via the respiratory mucosa, it is expected that a strong mucosal response will be important for protection.<sup>59-62</sup> Compelling evidence also indicates that an efficient stimulation of Th1-type immune responses is crucial in protection against intracellular pathogens.<sup>63,64</sup> Therefore, we propose a mucosal TB vaccine candidate for intranasal immunization as a prime only approach, without a prior BCG immunization, as recommended by WHO.

In this study, we describe the formulation and *in vivo* testing of a novel microparticulate BCG vaccine candidate that targets the nasal epithelial surface. The direct targeting of BCG microparticles to nasal epithelial cells could potentially enhance the vaccine uptake by APC and increase the specific immune response. We address this by using mucoadhesive polymers in vaccine formulation, such as chitosan and alginate, in order to increase BCG residence time within the NALT, thus, increasing the intracellular uptake of the vaccine by alveolar macrophages, while also modifying BCG's surface properties, thus, modulating the interaction with APC and intracellular processing.

We used the BCG-loaded chitosan-alginate microparticles and the monodispersed BCG in chitosan that have been previously used for mucosal delivery of BCG and were shown to be biocompatible and adjuvant in preliminary *in vivo* studies conducted in mice (Chapter III, section 2.3. and 3.5.). Furthermore, we designed two additional BCG formulations, consisting of BCG-loaded alginate-chitosan microparticles, which differ from the abovementioned ones in the addition order of the polymers, leading to distinct particle size distribution and erosion kinetics, and a fourth formulation consisting of BCG-loaded chitosan-alginate-linoleic acid microparticles, as linoleic acid is described as a polyunsaturated fatty acid with a pro-inflammatory profile. All the prepared BCG vaccine formulations were characterised for their physicochemical properties *in vitro* and were shown to provide a suitable system to microencapsulate BCG bacilli within a wide range of particle size distributions and surface charge, without compromising cell viability.

It has been recently well described that there is a relation between secretion of IFN- $\gamma$ , TNF- $\alpha$  and IL-2 by CD4+ T-cells and protection against *M. tuberculosis* infection.<sup>59,62,65-73</sup> The *in vivo* results show that intranasal administration of microparticulate BCG prompted predominantly Th1-type immune responses in mice, as depicted from the

higher titres of IgG2a over IgG1, and also high levels of IFN- $\gamma$ , TNF- $\alpha$  and IL-2, in opposition to subcutaneous immunization with BCG. Similar results were obtained, regarding the cytokine profile, for i.n. immunization with BCG alone (without microparticles nor chitosan). However, we found that i.n. immunization with BCG alone originated an IgG2a/IgG1 ratio approximately 8-fold higher than the obtained with microparticulate BCG or BCG suspended in chitosan, leading to a not so well-balanced Th1/Th2 profile, which is critical to avoid both immunotolerance and autoimmune reactions. This occurrence showed the importance of microparticulate formulation of BCG for intranasal immunization purposes.

The obtained cytokine profiles suggest that multiple cytokine-producing cells were induced following mice intranasal immunization with BCG. The highest levels of produced cytokines were obtained following intranasal immunization with microparticulate delivery systems, suggesting that microparticles play a major role in inducing cytokines production by CD4<sup>+</sup> T-cells, while pointing out intranasal route as a promising immunization approach for BCG. It is also noteworthy that i.n. immunization with microparticulate BCG or BCG suspended in chitosan was able to elicit a systemic immune response, in agreement with previous studies in our group with encapsulated antigens in chitosan nanoparticles.<sup>33,35</sup>

There is evidence that effective immunity correlates better with the presence of specific antibodies in local secretions, such as secretory immunoglobulin A (SIgA), than with serum antibodies.<sup>59,74–76</sup> Moreover, several vaccine candidates against tuberculosis via non-invasive administration routes (per oral, nasal, or pulmonary) have shown to effectively induce mucosal immunity.<sup>7,19,60,77,78</sup> Additional advantages of nasal vaccine delivery arise from the fact that nasal vaccine delivery can surpass antigen degradation by digestive enzymes, thus, requiring a smaller antigen dose, while it also enables cross-protective immunity in the lung and gut through the common mucosal immune system.<sup>11</sup>

In this study, mucosal responses were 2-4 times higher in the lung when compared with the intestine. Interestingly, “BCG-loaded chitosan-alginate-linoleic acid microparticle” vaccine appeared to be superior to the other two microparticulate BCG vaccines in terms of total IgG titres, Th1-type cytokines concentration, and IgA titres in lung mucosa, although differences in IgA titres were not statistically significant when compared with other vaccination groups. We also found in our experiments that i.n. immunization with positively charged BCG (suspended in chitosan) elicited superior total IgG titres among i.n. BCG vaccines, and higher sIgA titres in both lung and intestine homogenates when compared to i.n. BCG alone, thus, suggesting the important role of chitosan in

modulation of BCG surface charge, leading to adequate humoral and mucosal immune responses.

Overall, “BCG-loaded chitosan-alginate-linoleic acid microparticle” vaccine induced high and well-balanced immune responses, being an important indicator of formulation contribution to vaccine global immunogenicity. The apparent superior immunogenicity of this formulation can potentially be attributed to the specialized recognition of the microparticulate delivery system by APCs although the possibility of intrinsic immunogenicity of chitosan cannot be excluded. It is noteworthy, however, that our experiments didn't specifically analyse the impact of the various components of the induced immune response in protection against *M. tuberculosis*. Therefore, further work is required to fully characterise the role of the immune responses induced by the vaccine in protections against *M. tuberculosis* infection.

## 5. Conclusions

In conclusion, the present data showed that targeting the nasal mucosa is an effective way of inducing mucosal and systemic immune responses, particularly for boosting BCG-induced immunity when compared with current parenteral BCG vaccine. Vaccine preparation by ionotropic gelation allowed the production of polymeric microparticles containing viable BCG. Formulating BCG with microparticles further enhanced the specific immune responses and conferred significantly improved mucosal and cellular immune responses. Further studies with this mucosal vaccine are required, in order to comprise the assessment of conferred protection after challenge with *M. tuberculosis* and understanding of the cellular and molecular mechanisms that are involved.

## 6. Acknowledgements

The authors would like to thank Prof. Elsa Anes (FFUL) and her team (Dr. David Pires, Dr. Nuno Carmo) for BCG Pasteur strain supply and technical support. Work supported by FCT (PEst-OE/SAU/UI4013/2011). The authors thank iMed.Ulisboa for financial support (UID/DTP/04138/2013) from Fundação para a Ciência e Tecnologia (FCT), Portugal, and Escola Superior de Tecnologia da Saúde de Lisboa for financial support from merit scholarship for Ph.D. (ESTeSL-IPL/CGD/2012) granted by Caixa Geral de Depósitos, Portugal.

## 7. References

1. World Health Organization. *Global Tuberculosis Report 2013*. (World Health Organization 2013, 2013). at <[http://apps.who.int/iris/bitstream/10665/91355/1/9789241564656\\_eng.pdf?ua=1](http://apps.who.int/iris/bitstream/10665/91355/1/9789241564656_eng.pdf?ua=1)>
2. Bishai, W., Sullivan, Z., Bloom, B. R. & Andersen, P. Bettering BCG: a tough task for a TB vaccine? *Nat. Med.* **19**, 410–1 (2013).
3. Holmgren, J. & Czerkinsky, C. Mucosal immunity and vaccines. *Nat. Med.* **11**, S45–S53 (2005).
4. Giri, P. K., Verma, I. & Khuller, G. K. Protective efficacy of intranasal vaccination with *Mycobacterium bovis* BCG against airway *Mycobacterium tuberculosis* challenge in mice. *J. Infect.* **53**, 350–6 (2006).
5. Jeyanathan, M., Heriazon, A. & Xing, Z. Airway luminal T cells: a newcomer on the stage of TB vaccination strategies. *Trends Immunol.* **31**, 247–52 (2010).
6. Dietrich, J. *et al.* Mucosal administration of Ag85B-ESAT-6 protects against infection with *Mycobacterium tuberculosis* and boosts prior Bacillus Calmette-Guérin immunity. *J. Immunol.* **177**, 6353–6360 (2010).
7. Rebelatto, M. C., Guimond, P., Bowersock, T. L. & HogenEsch, H. Induction of systemic and mucosal immune response in cattle by intranasal administration of pig serum albumin in alginate microparticles. *Vet. Immunol. Immunopathol.* **83**, 93–105 (2001).
8. Pavot, V., Rochereau, N., Genin, C., Verrier, B. & Paul, S. New insights in mucosal vaccine development. *Vaccine* **30**, 142–54 (2012).
9. Czerkinsky, C. *et al.* Mucosal immunity and tolerance: relevance to vaccine development. *Immunol. Rev.* **170**, 197–222 (1999).
10. Baudner, B. C. & O'Hagan, D. T. Bioadhesive delivery systems for mucosal vaccine delivery. *J. Drug Target.* **18**, 752–770 (2010).
11. Caetano, L. A., Almeida, A. J. & Gonçalves, L. M. D. Approaches to Tuberculosis Mucosal Vaccine Development Using Nanoparticles and Microparticles: A Review. *J. Biomed. Nanotechnol.* **10**, 2295–2316 (2014).
12. Agnihotri, S. a, Mallikarjuna, N. N. & Aminabhavi, T. M. Recent advances on chitosan-based micro- and nanoparticles in drug delivery. *J. Control. Release* **100**, 5–28 (2004).
13. Singh, M., Chakrapani, A. & O'Hagan, D. Nanoparticles and microparticles as vaccine-delivery systems. *Expert Rev. Vaccines* **6**, 797–808 (2007).
14. Kang, M. L., Cho, C. S. & Yoo, H. S. Application of chitosan microspheres for nasal delivery of vaccines. *Biotechnol. Adv.* **27**, 857–65 (2009).
15. Csaba, N., Garcia-Fuentes, M. & Alonso, M. J. Nanoparticles for nasal vaccination. *Adv. Drug Deliv. Rev.* **61**, 140–57 (2009).
16. Almeida, A. J. & Souto, E. Solid lipid nanoparticles as a drug delivery system for peptides and proteins. *Adv. Drug Deliv. Rev.* **59**, 478–90 (2007).
17. Amidi, M., Mastrobattista, E., Jiskoot, W. & Hennink, W. E. Chitosan-based delivery systems for protein therapeutics and antigens. *Adv. Drug Deliv. Rev.* **62**, 59–82 (2010).
18. Look, M., Bandyopadhyay, A., Blum, J. S. & Fahmy, T. M. Application of nanotechnologies for improved immune response against infectious diseases in the developing world. *Adv. Drug Deliv. Rev.* **62**, 378–93 (2010).
19. Borges, O., Lebre, F., Bento, D., Borchard, G. & Junginger, H. E. Mucosal vaccines: recent progress in understanding the natural barriers. *Pharm. Res.* **27**, 211–23 (2010).
20. Chadwick, S., Kriegel, C. & Amiji, M. Nanotechnology solutions for mucosal immunization. *Adv. Drug Deliv. Rev.* **62**, 394–407 (2010).
21. Moon, J. J., Irvine, D. J. & Huang, B. Engineering nano- and micro-particles to tune immunity. *Adv Mater* **24**, 3724–3746 (2012).

22. Bacon, A. *et al.* Carbohydrate biopolymers enhance antibody responses to mucosally delivered vaccine antigens. *Infect. Immun.* **68**, 5764–5770 (2000).
23. McNeela, E. A. *et al.* A mucosal vaccine against diphtheria: formulation of cross reacting material (CRM(197)) of diphtheria toxin with chitosan enhances local and systemic antibody and Th2 responses following nasal delivery. *Vaccine* **19**, 1188–1198 (2000).
24. Dobakhti, F. *et al.* Stabilizing effects of calcium alginate microspheres on *Mycobacterium bovis* BCG intended for oral vaccination. *J. Microencapsul.* **23**, 844–854 (2006).
25. Tønnesen, H. H. & Karlsen, J. Alginate in drug delivery systems. *Drug Dev. Ind. Pharm.* **28**, 621–30 (2002).
26. Borges, O. Alginate coated chitosan nanoparticles as adjuvant for mucosal vaccination with hepatitis B antigen. (Coimbra University, 2007).
27. Florindo, H. F. *et al.* The enhancement of the immune response against *S. equi* antigens through the intranasal administration of poly-epsilon-caprolactone-based nanoparticles. *Biomaterials* **30**, 879–91 (2009).
28. Caetano, L. A., Figueiredo, L., Almeida, A. J. & Gonçalves, L. M. D. Alginate-chitosan particulate delivery systems for mucosal immunization against tuberculosis. in *Bioengineering (ENBENG), 2012 IEEE 2nd Portuguese Meeting in I.I.*, 2 (Xplore, IEEE, 2012). doi:10.1109/ENBENG.2012.6331346
29. Ouyang, W. *et al.* Artificial cell microcapsule for oral delivery of live bacterial cells for therapy: design, preparation, and in-vitro characterization. *J. Pharm. Pharm. Sci.* **7**, 315–24 (2004).
30. Li, X. *et al.* Preparation of alginate coated chitosan microparticles for vaccine delivery. *BMC Biotechnol.* **8**, 89 (2008).
31. Douglas, K. L. & Tabrizian, M. Effect of experimental parameters on the formation of alginate-chitosan nanoparticles and evaluation of their potential application as DNA carrier. *J. Biomater. Sci. Polym. Ed.* **16**, 43–56 (2005).
32. Borges, O. *et al.* Immune response by nasal delivery of hepatitis B surface antigen and codelivery of a CpG ODN in alginate coated chitosan nanoparticles. *Eur. J. Pharm. Biopharm.* **69**, 405–16 (2008).
33. Florindo, H. F., Pandit, S., Goncalves, L., Alpar, H. O. & Almeida, A. J. New approach on the development of a mucosal vaccine against strangles: Systemic and mucosal immune responses in a mouse model. *Vaccine* **27**, 1230–1241 (2009).
34. Cadete, A. *et al.* Development and characterization of a new plasmid delivery system based on chitosan-sodium deoxycholate nanoparticles. *Eur. J. Pharm. Sci.* **45**, 451–8 (2012).
35. Figueiredo, L., Cadete, A. & Gonçalves, L. M. D. Intranasal immunisation of mice against *Streptococcus equi* using positively charged nanoparticulate carrier systems. *Vaccine* **30**, 6551–6558 (2012).
36. Figueiredo, L., Calado, C. C. R., Almeida, A. J. & Gonçalves, L. M. D. Protein and DNA nanoparticulate multiantigenic vaccines against *H. pylori*: in vivo evaluation. in *2nd Portuguese BioEngineering Meeting* (ed. IEEE EMBS Portuguese Chapter) I.I, 1 (2012).
37. Rodrigues, M. A. *et al.* Development of a novel mucosal vaccine against strangles by supercritical enhanced atomization spray-drying of *Streptococcus equi* extracts and evaluation in a mouse model. *Eur. J. Pharm. Biopharm.* **82**, 392–400 (2012).
38. Leithner, K. & Bernkop-schn, A. in *Chitosan-Based Systems for Biopharmaceuticals* (eds. Sarmiento, B. & Neves, J.) 159–180 (2012 John Wiley & Sons, Ltd, 2012).
39. Caetano, L. A., Amaral, R., Figueiredo, L., Almeida, A. J. & Goncalves, L. M. D. Chitosan-alginate microparticulate delivery system for an alternative route of administration of BCG vaccine. in *Bioengineering (ENBENG), 2013 IEEE 3rd Portuguese Meeting in 1–3* (2013). doi:10.1109/ENBENG.2013.6518391

40. Jordao, L. *et al.* Effects of omega-3 and -6 fatty acids on *Mycobacterium tuberculosis* in macrophages and in mice. *Microbes Infect.* **10**, 1379–86 (2008).
41. Vicente, S. *et al.* A polymer/oil based nanovaccine as a single-dose immunization approach. *PLoS One* **8**, e62500 (2013).
42. Bettencourt, P., Pires, D., Carmo, N. & Anes, E. in *Microscopy: Science, Technology, Applications and Education* (eds. Méndez-Vilas, A. & Díaz, J.) 614–621 (2010).
43. Dorer, D. E. *et al.* Lymphatic tracing and T cell responses following oral vaccination with live *Mycobacterium bovis* (BCG). *Cell. Microbiol.* **9**, 544–53 (2007).
44. Clark, S. *et al.* Assessment of different formulations of oral *Mycobacterium bovis* Bacille Calmette-Guérin (BCG) vaccine in rodent models for immunogenicity and protection against aerosol challenge with *M. bovis*. *Vaccine* **26**, 5791–7 (2008).
45. Florindo, H. F. *et al.* Antibody and cytokine-associated immune responses to *S. equi* antigens entrapped in PLA nanospheres. *Biomaterials* **30**, 5161–9 (2009).
46. Sharp, F. a *et al.* Uptake of particulate vaccine adjuvants by dendritic cells activates the NALP3 inflammasome. *Proc. Natl. Acad. Sci. U. S. A.* **106**, 870–875 (2009).
47. Zhang, A., Groves, M. J. & Klegerman, M. E. The surface charge of cells of *Mycobacterium bovis* BCG vaccine, Tice substrain. *Microbios* **53**, 191–195 (1988).
48. Cooper, A. M. Cell-mediated immune responses in tuberculosis. *Annu. Rev. Immunol.* **27**, 393–422 (2009).
49. Abebe, F. & Bjune, G. The protective role of antibody responses during *Mycobacterium tuberculosis* infection. *Clin. Exp. Immunol.* **157**, 235–43 (2009).
50. Fujikuyama, Y. *et al.* Novel vaccine development strategies for inducing mucosal immunity. *Expert Rev. Vaccines* **11**, 367–379 (2012).
51. Slütter, B. *et al.* Nasal vaccination with N-trimethyl chitosan and PLGA based nanoparticles: Nanoparticle characteristics determine quality and strength of the antibody response in mice against the encapsulated antigen. *Vaccine* **28**, 6282–6291 (2010).
52. Flynn, J. Tumor necrosis factor- $\gamma$  is required in the protective immune response against *Mycobacterium tuberculosis* in mice. *Immunity* **2**, 561–572 (1995).
53. Dietrich, G., Viret, J.-F. & Hess, J. *Mycobacterium bovis* BCG-based vaccines against tuberculosis: novel developments. *Vaccine* **21**, 667–70 (2003).
54. Barreto, M. L., Pereira, S. M. & Ferreira, A. a. BCG vaccine: efficacy and indications for vaccination and revaccination. *J. Pediatr. (Rio. J.)* **82**, S45–54 (2006).
55. Franco-Paredes, C., Roupheal, N., Del Rio, C. & Santos-Preciado, J. I. Vaccination strategies to prevent tuberculosis in the new millennium: from BCG to new vaccine candidates. *Int. J. Infect. Dis. IJID Off. Publ. Int. Soc. Infect. Dis.* **10**, 93–102 (2006).
56. Cosgrove, C. A. *et al.* Boosting of cellular immunity against *Mycobacterium tuberculosis* and modulation of skin cytokine responses in healthy human volunteers by *Mycobacterium bovis* BCG substrain Moreau Rio de Janeiro oral vaccine. *Infect. Immun.* **74**, 2449–2452 (2006).
57. Clark, S. O. *et al.* Oral delivery of BCG Moreau Rio de Janeiro gives equivalent protection against tuberculosis but with reduced pathology compared to parenteral BCG Danish vaccination. *Vaccine* **28**, 7109–16 (2010).
58. Romano, M. & Huygen, K. An update on vaccines for tuberculosis - there is more to it than just waning of BCG efficacy with time. *Expert Opin. Biol. Ther.* **12**, 1601–10 (2012).
59. Li, W., Deng, G., Li, M., Liu, X. & Wang, Y. Roles of Mucosal Immunity against *Mycobacterium tuberculosis* Infection. *Tuberc. Res. Treat.* **2012**, 791–728 (2012).
60. Källénus, G., Pawlowski, A., Brandtzaeg, P. & Svenson, S. Should a new

- tuberculosis vaccine be administered intranasally? *Tuberculosis* **87**, 257–66 (2007).
61. Caetano, L. A., Figueiredo, L., Almeida, A. J. & Gonçalves, L. M. D. New delivery strategy to enhance mucosal vaccination against Tuberculosis. in *Tuberculosis symposium\_SPI-SPP* (eds. Sociedade Portuguesa de Imunologia & Sociedade Portuguesa de Pneumologia) 6 (2012).
  62. Stylianou, E. *et al.* Mucosal delivery of antigen-coated nanoparticles to lungs confers protective immunity against tuberculosis infection in mice. *Eur. J. Immunol.* **44**, 440–449 (2014).
  63. Stenger, S. & Modlin, R. L. Control of *Mycobacterium tuberculosis* through mammalian Toll-like receptors. *Curr. Opin. Immunol.* **14**, 452–7 (2002).
  64. Forbes, E. K. *et al.* Multifunctional, high level cytokine producing Th1 cells in the lung, but not spleen, correlate with protection against *Mycobacterium tuberculosis* aerosol challenge in mice. *J. Immunol.* **181**, 4955–4964 (2008).
  65. Kaufmann, S. H. E. Future vaccination strategies against tuberculosis: thinking outside the box. *Immunity* **33**, 567–577 (2010).
  66. Reed, S. G., Bertholet, S., Coler, R. N. & Friede, M. New horizons in adjuvants for vaccine development. *Trends Immunol.* **30**, 23–32 (2009).
  67. Anes, E. in *Understanding Tuberculosis – Analyzing the Origin of Mycobacterium Tuberculosis Pathogenicity* (ed. Cardona, P.) 123–125; 131–133 (InTech, 2012).
  68. Dalmia, N. & Ramsay, A. J. Prime-boost approaches to tuberculosis vaccine development. *Expert Rev. Vaccines* **11**, 1221–33 (2012).
  69. Landesman-Milo, D. & Peer, D. Altering the immune response with lipid-based nanoparticles. *J. Control. Release* **161**, 600–8 (2012).
  70. Abebe, M. *et al.* Modulation of cell death by M. tuberculosis as a strategy for pathogen survival. *Clin. Dev. Immunol.* **2011**, 678570 (2011).
  71. Belkaid, Y. & Tarbell, K. Regulatory T cells in the control of host-microorganism interactions (\*). *Annu. Rev. Immunol.* **27**, 551–89 (2009).
  72. Ballester, M. *et al.* Nanoparticle conjugation and pulmonary delivery enhance the protective efficacy of Ag85B and CpG against tuberculosis. *Vaccine* **29**, 6959–66 (2011).
  73. Kaveh, D. a, Bachy, V. S., Hewinson, R. G. & Hogarth, P. J. Systemic BCG immunization induces persistent lung mucosal multifunctional CD4 T(EM) cells which expand following virulent mycobacterial challenge. *PLoS One* **6**, e21566 (2011).
  74. Brandtzaeg, P. Role of secretory antibodies in the defence against infections. *Int. J. Med. Microbiol.* **293**, 3–15 (2003).
  75. Foxwell, A. R., Kyd, J. M. & Cripps, A. W. Mucosal immunization against respiratory bacterial pathogens. *Expert Rev. Vaccines* **2**, 551–560 (2003).
  76. Corthésy, B. Role of secretory immunoglobulin A and secretory component in the protection of mucosal surfaces. *Future Microbiol.* **5**, 817–829 (2010).
  77. Mutwiri, G. *et al.* Induction of mucosal immune responses following enteric immunization with antigen delivered in alginate microspheres. *Vet. Immunol. Immunopathol.* **87**, 269–276 (2002).
  78. Goonetilleke, N. P. *et al.* Enhanced immunogenicity and protective efficacy against *Mycobacterium tuberculosis* of bacille Calmette-Guerin vaccine using mucosal administration and boosting with a recombinant modified vaccinia virus Ankara. *J. Immunol.* **171**, 1602–1609 (2003).

## ***Chapter V***

---

### ***General conclusions and Future perspectives***



## 1. General conclusions

The development of novel and optimized vaccine delivery systems and adjuvants is becoming as important as the development of novel vaccines. Regarding immunization strategies against infectious agents, especially for those that invade the body through mucosal surfaces, such as *Mycobacterium tuberculosis*, there is increasing evidence on the advantages of targeting the mucosae, as the production of mucosal antibodies following oral, nasal and even pulmonary immunization is related with increased levels of protection. An additional challenge regarding tuberculosis, due to the high prevalence of the disease in underdeveloped countries, relies on the interdependence between successful mass vaccination programmes, and the availability of novel delivery systems suitable for the rapid production of more stable, cheaper and “needle free” vaccines. Taking in consideration the abovementioned, the present work aimed primarily at the design of a novel BCG-loaded chitosan microparticle-based delivery system for mucosal immunization against tuberculosis by intranasal vaccination.

Due to its unique mucoadhesive and immunogenic properties, chitosan was considered of great interest for the encapsulation of BCG into polymeric microparticles. The entrapment and adsorption of BCG bacilli into chitosan microparticles was considered a convenient and safe loading method, with chitosan as mucosal adjuvant. However, for low porous microparticles, the BCG bacilli would be rapidly desorbed and cleared, leading to reduced residence time in the nasal mucosa. Moreover, antimicrobial properties are attributed to chitosan, which could potentially hamper BCG cell viability. Hence, sodium alginate was chosen as second polymer for the microparticle preparation, in order to provide a better protection of the BCG bacilli, with subsequent increase of the residence time in the NALT. Sodium alginate was chosen because of its well described association with chitosan by ionic gelation, leading to the formation of more compact gel matrices (depending on polymers stoichiometric proportion), thus, modifying particle erosion kinetics and sustaining vaccine release, and also because of its mucoadhesive properties. In addition, alginate has been extensively used for cell immobilization and storage purposes, whereas its insolubility in the acidic environment of lysosomal compartments in alveolar macrophages might prompt distinct antigen processing pathways within the cell, thereby, modifying the antigen presentation to the immune system.

Hence, our strategy focused, firstly, on the technological issues of polymeric microparticle preparation and BCG microencapsulation while maintaining vaccine viability; secondly, it focused on the assessment of the interaction of the developed BCG-

loaded polymeric particulate carriers with antigen presenting cells; and, thirdly, it focused on the assessment of the immune responses elicited in mice following pre-exposure intranasal immunization with the developed vaccine delivery systems.

In the second chapter of this thesis, the development of three different preparation methods of chitosan and alginate microparticles by ionic gelation is described. Particle size and size distribution uniformity was considered to be a critical aspect throughout the formulation studies. As stated previously, it may be influenced by several variables, such as the properties of the polymers and agents of ionic complexation used; type, speed and duration of homogenization; polymer/polymer and polymer/vaccine load ratio; pH value of the polymer solutions used; the addition order of the polymers. Plain microparticles were initially prepared, in order to determine the influence of experimental conditions in critical particle features, and, afterwards, BCG-loaded microparticles were prepared and characterized. From the technological perspective, it was possible to optimize the preparation method of BCG-loaded polymeric microparticles with reproducible size distribution, association efficiency (A.E.) and production yield (YP) values, as well as to obtain a complete characterization of the microparticulate carriers in terms of morphology, surface charge, polymer interactions (FT-IR) and *in vitro* biocompatibility.

The methodology developed in this work allowed obtaining polymeric particles below 30 $\mu$ m and adaptable surface charge. It was possible to observe that, for chitosan-alginate microparticles, size distribution was mainly influenced by the molecular weight and type of the used polymer blends. These variables were not, however, equally determinant in particle surface charge, which was mainly influenced by polymer-to-polymer mass ratio and the addition order of the polymers. According to the obtained results, the use of calcium as the crosslinker of alginate (Method I), and the use of TPP as the complexation agent for chitosan (Method III) contributed for the formation of electronegatively charged particles, whereas the partial neutralization of the alginate molecule by pre-gelation with chitosan (Method II) resulted in a positive zeta potential of the particles, an important aspect for efficient interaction with negatively charged mucin in the lung mucosa. Although the encapsulation of BCG did not exert a considerable effect on the particles final properties (i.e. size distribution, surface charge, morphology), the formulation method, namely the addition order of the polymers, as well as the BCG load used, proved to be crucial in achieving high A.E. values. These results were important for considering microparticles effective for whole live bacterial vaccine encapsulation.

Particle surface charge, together with the size of the particles, surface hydrophobicity and particle shape, are believed to be important for efficient particle internalization by alveolar macrophages. Therefore, Method III was chosen to prepare BCG-loaded microparticles with a particle mean diameter below 40  $\mu\text{m}$  in a stable colloidal suspension, while maintaining BCG cell viability. The uptake studies performed in THP-1 cells with the BCG-loaded chitosan-alginate microparticles confirmed the internalisation of the particles (Chapter III). Although there are limitations in these uptake studies, as the performed bidimensional image processing does not allow an accurate quantification of internalized vs. adsorbed particles, nor does it clarify the underlying internalization mechanisms, the obtained results were important to support the decision to continue with vaccination studies in mice (Chapter IV). As future perspectives, more detailed and quantitative uptake studies must be performed, for a better understanding of the interaction of the BCG-loaded chitosan-alginate microparticles with the antigen presenting cells present at the mucosal surfaces. The same hold for the elucidation of the involved intracellular trafficking pathways, as required for the development of a more efficient vaccine delivery system.

The role of the BCG-loaded chitosan-alginate microparticles as pre-exposure vaccine for tuberculosis was evaluated in BALB/c mice model in two independent *in vivo* studies. The data from the first *in vivo* study confirmed an effective stimulation of both humoral and cellular immune responses. Two formulations were evaluated in two independent groups, which were intranasally immunized with BCG suspended in chitosan or BCG-loaded chitosan-alginate microparticles. The elicited immune response was compared with two other mice groups, immunized with BCG suspension by either intranasal or subcutaneous route.

This first *in vivo* study was performed in a reduced number animals, thus, no conclusive information was obtained about the relation between the proposed delivery systems and the elicited immune responses. One important result, though, was that all groups immunized with BCG by intranasal route were responders after a single dose. Hence, the obtained results were important to consolidate our intended immunization strategy, by validating the proposed delivery systems for a prime only immunization regime by intranasal administration route, and the adequacy of the chosen BCG dose. The validation of the BCG dose and immunization route was crucial, in the recent context of global constraints of BCG supply. The standard dose of the BCG vaccine in humans is 0.1 mg in 1 ml, corresponding to  $2-8 \times 10^5$  CFU, though manufacturers of certain strains of BCG, such as the Danish strain (BCG strain Copenhagen 1331, used in Portugal), recommend half dose in infants. The association of BCG with the proposed delivery

systems allowed using a BCG dose of  $1 \times 10^7$  CFU, only 1.4-fold more from the standard dose. In fact, higher antigen concentrations (approximately 10-fold more from the standard dose by subcutaneous route) are usually necessary when intranasal or oral vaccination is performed, due to the presence of multiple biological barriers.

Following intranasal administration of the BCG associated with the chitosan solution, an enhancement of the anti-PPD<sub>bov</sub> IgG and IgG2a serum titers was observed when compared with the suspension of the BCG administered by subcutaneous route. This was an important result, as high levels of IgG2a specific antibodies are known to be related to a Th1 type immune response, thus, confirming chitosan as an effective adjuvant for cellular immunity by intranasal immunization with BCG. The mechanism responsible for that result was not further investigated in detail and should be clarified in the future. In comparison with the BCG suspended in chitosan, BCG-loaded microparticles originated approximately 2-3 fold inferior serum titers of anti-PPD<sub>bov</sub> IgG and IgG2a. These differences in the specific immune response, between BCG suspended in chitosan and BCG-loaded microparticles, are probably related to particle features, namely, the opposite surface charge and different particle size distribution of the two delivery systems. As aforementioned, the BCG associated with the chitosan solution presented highly positive zeta potential values, whereas BCG-loaded microparticles were electronegatively charged. Moreover, the microencapsulation process of BCG led to the upload of multiple bacilli per particle, leading to a decreased available surface area of microencapsulated BCG when compared with the, monodispersed, BCG associated with the chitosan.

Commercial injectable BCG vaccines originate mild adverse effects related to the site of administration. Typically, a mild local reaction occurs at the injection site reaction, characterized by a red papule that may progress to ulcerate, leaving a superficial scar. This local sensitivity to BCG poses an additional challenge for vaccination through mucosal routes. Hence, the association of the BCG vaccine with the herein proposed delivery systems aims at overcoming this challenge, by allowing the vaccine delivery without immune exacerbations, while also avoiding the immune tolerance phenomena, which would lead to hypo-responsiveness to the vaccine.

Regarding mucosal response, at the end of the first *in vivo* study, it was possible to detect mucosal antibodies in the lung homogenates within all mice groups after intranasal vaccination. We have found that, among the intranasally vaccinated mice groups, the anti-PPD<sub>bov</sub> sIgA levels were higher for the BCG associated with the chitosan solution, which were also above the levels detected for the subcutaneously vaccinated mice. In

contrast, the levels of mucosal antibodies in the lung homogenates after intranasal vaccination with the BCG-loaded chitosan-alginate microparticles were inferior to those elicited by subcutaneous BCG. The results were in accordance with previous systemic immunity results, with the BCG associated with chitosan vaccine leading to higher specific immune response, both systemic and mucosal, among the intranasally vaccinated groups, and BCG-loaded chitosan-alginate microparticles performing below subcutaneous BCG. This was probably due to the favorable combination of available surface area, surface charge and mucoadhesive properties of this delivery system. Our observations in this first *in vivo* study stimulated us to think about the possibility to improve the properties of chitosan microparticles.

In Chapter IV, two additional polymeric formulations were developed and evaluated *in vivo*, namely, BCG-loaded alginate-chitosan microparticles, and BCG-loaded chitosan-alginate microparticles containing linoleic acid. The two newly proposed formulations were in the micrometre size range and electronegatively charged. This second *in vivo* evaluation was performed in a much larger number of animals within nine independent vaccination groups. The specific immune responses were compared between groups of mice immunized by intranasal route with the proposed BCG formulations (*BCG associated with chitosan*; *BCG-loaded chitosan/alginate microparticles*; *BCG-loaded alginate/chitosan microparticles*; and *BCG-loaded chitosan/alginate plus linoleic acid microparticles*), and groups of mice immunized with BCG suspension by intranasal or subcutaneous route.

Specific antibodies were detected in mice serum five weeks after vaccination, increasing until the final 26<sup>th</sup> week. The vaccination route is an important aspect to consider regarding the induction of the ideal immune profile of a balanced Th1/Th2 type response. In this study, we found that subcutaneous vaccination with BCG suspension elicited the enhancement of the humoral immune response with a predominance of the Th2 type antibodies, whereas the intranasal vaccination with BCG suspension, BCG-loaded polymeric microparticles, or BCG associated with chitosan, elicited the enhancement of the Th1 type response. Similar results were observed in the first *in vivo* study. The immune response was re-directed to a more balanced mixed Th1/Th2 profile when the BCG entrapped into polymeric microparticles was co-delivered with the linoleic acid, with a specific IgG2a/IgG1 ratio around the unity. In order to evaluate cellular immunity, the production of specific Th1-type cytokines by CD4<sup>+</sup> T-cells was evaluated in mice sensitized splenocytes. Among the proposed formulations, the highest levels of TNF- $\alpha$ , IL-2 and IFN- $\gamma$  were observed in the intranasally vaccinated mice group with the BCG-loaded chitosan/alginate plus linoleic acid microparticle vaccine. The obtained results

are suggestive of the efficiency of this formulation in inducing Th1-type immune responses, while pointing out intranasal route as a promising immunization approach for vaccination with BCG. Hence, this formulation revealed potential for the improvement of the currently licensed BCG vaccine, namely, for the induction of an effective and long lasting pre-exposure immunity, as it is believed that a strong Th1 cellular immune response is required to confer protection against tuberculosis through adulthood. Furthermore, it would be worth to investigate whether the controlled delivery of the BCG bacilli and the linoleic acid from the chitosan-alginate microparticles is able to enhance the longevity of the immune response.

Concerning mucosal immunity, specific sIgA levels were 2-4 fold higher in the lung than in the intestine. These results are in accordance with the expected, as the localized secretion of antigen specific IgA depends on the vaccination route. For instance, intranasal vaccination is described to be more efficient to evoke mucosal antibodies in the upper airway mucosa, and saliva and nasal secretions in humans. Among the intranasally vaccinated mice groups, it was possible to observe that the concentration of anti-PPD<sub>bov</sub> sIgA was higher in lung homogenates with BCG-loaded chitosan/alginate plus linoleic acid microparticles and, interestingly, with plain microparticles. A possible explanation for this unexpected observation is most probably related with the inferior particle size distribution of plain microparticles which results in a higher available concentration of the microparticles to interact with the mucosa. Although the mechanism of interaction with the mucosa was not further explored, the presence of linoleic acid in the formulation is possibly involved in the enhancement of mucosal immunity.

In summary, a new micro-sized chitosan and alginate based delivery system for mucosal vaccination of the BCG is described in this work. Bearing in mind the initial objectives aims of this work, it was possible to successfully encapsulate BCG into microparticulate carriers composed by chitosan and sodium alginate. Vaccine preparation by ionotropic gelation allowed the production of polymeric microparticles containing viable BCG. The appropriateness of the methodology for a high association efficiency of BCG, with a high yield of microparticle production, was demonstrated. It was possible to demonstrate the biocompatibility of these systems and to evaluate their interaction with a human macrophage derived from monocyte cell line, which provided information on the cellular uptake of these carriers by antigen presenting cells. The study of the adjuvant effect of chitosan and alginate microparticles was performed by intranasal vaccination route, and compared to subcutaneous route. Adding linoleic acid to the microparticles formulation further enhanced the specific immune responses and conferred significantly improved

mucosal and cellular immune responses. The immunization studies have shown that chitosan and alginate microparticles have an adjuvant effect for the BCG vaccine when administered by intranasal route. In addition, it was demonstrated that targeting the nasal mucosa is an effective way of inducing mucosal and systemic immune responses, particularly for boosting BCG-induced immunity, when compared with current parenteral BCG vaccine.

## **2. Future perspectives**

Although important results were achieved with the present work, several issues should be investigated in the future.

As previously mentioned, the biocompatibility and toxicological assessment of microparticles and new adjuvants are highly relevant. In our group, research work has been developed on the characterization of the cellular uptake of polymeric carriers, using several cell lines, such as macrophages. In the case of BCG vaccine, it would be also relevant to evaluate the cellular interaction of the developed carriers with dendritic cells. Additional studies have to be performed with the proposed microparticulate delivery systems in order to further understand the molecular mechanisms involved in particle cellular uptake, particle erosion kinetics, and particle trafficking and antigen presentation.

Another aspect that has been a recent focus of attention in our group is the assessment of the interaction between polymeric microparticles and mucin. To design an effective particulate delivery system having mucoadhesive function, several mucoadhesion tests for polymers and the resultant particulate systems can be performed, such as the mucin-particle method using commercial mucin particles to estimate mucoadhesive properties, or even particle diffusion through mucus layers using fluorescence microscopy. In this context, a collaboration is already established with a research group in the Instituto de Medicina Molecular (IMM), Universidade de Lisboa, in AFM techniques, and a future collaboration is envisioned with a research group in the University of Castilla la Vieja, Spain. In addition, to evaluate the mucoadhesive phenomena in the lung, mice lung can be analysed using confocal laser scanning microscopy after intranasal administration of the particulate systems.

Furthermore, with adequate improvement of the delivery system, namely, reduction of particle size, microencapsulation of monodispersed BCG bacilli, and more precise tuning of particle surface charge, the suspension of the microparticles containing the BCG bacilli and the linoleic acid should be investigated in order to have a higher seroconversion

rate. Moreover, as future perspectives, the advantages of the developed chitosan and alginate microparticles over the currently used adjuvant (sodium glutamate) in the commercial formulation of the BCG vaccine should be assessed for the subcutaneous route in terms of long-term protection and local sensitivity at the administration site. The association of linoleic acid to the BCG-loaded chitosan and alginate microparticles should be also evaluated for a new administration route for the vaccine, namely, the oral route, as a more suitable immunization route for *M. tuberculosis* wildlife reservoirs and cattle. The long-term protection should be evaluated in additional studies with a suitable animal model.

Another key issue, considering the ultimate goal of this work to convey a widespread use of a particulate polymeric BCG vaccine, is the need for the optimization of the preparation methods in order to enable the upscale of vaccine production.

As a conclusion, the microencapsulation field has gained increasing attention over the last decades. Although the impact of microencapsulation has been only moderate when it comes to development of vaccines, promising results have been achieved with the important research made in this field. With the results obtained in this thesis, along with the on-going and future projects, we hope to contribute for the further development of novel and innovative live vaccine carriers.

